

MYOCARDIAL INFARCTION

Early diagnosis and cardioprotective strategies

MARISH OERLEMANS



Myocardial infarction
Early diagnosis and cardioprotective strategies

© Marish Oerlemans, 2012

ISBN: 978-90-8891-526-0
Vormgeving en Lay-out: W. Schoneveld, www.wenz iD.nl
Printed by: Proefschriftmaken.nl | Printyourthesis.com
Published by: Uitgeverij BOXPress, 's-Hertogenbosch

MYOCARDIAL INFARCTION

Early diagnosis and cardioprotective strategies

MYOCARDINFARCT

Vroege diagnostiek en cardioprotectieve strategieën

(met een samenvatting in het Nederlands)

PROEFSCHRIFT

ter verkrijging van de graad van doctor aan de Universiteit Utrecht op gezag van de rector magnificus, prof.dr. G.J. van der Zwaan, ingevolge het besluit van het college voor promoties in het openbaar te verdedigen op donderdag 6 december 2012 des middags te 2.30 uur

door

Martinus Ishak Flavius Jan Oerlemans

geboren op 25 september 1983 te Rotterdam

Promotor:

Prof. P.A. Doevendans

Co-promotor:

Dr. J.P.G. Sluijter

Financial support by the Heart & Lung Foundation Utrecht and Dutch Heart Foundation for the publication of this thesis is gratefully acknowledged.

Publication of this thesis was additionally supported by Stichting Cardiovasculaire Biologie, Chipsoft, Boehringer Ingelheim BV, Hartfalen Foundation.

CONTENTS

CHAPTER 1

General Introduction

9

PART ONE | EARLY DIAGNOSIS

CHAPTER 2

Early assessment of acute coronary syndromes in the emergency department:
the potential diagnostic value of circulating microRNAs

17

PART TWO | CARDIOPROTECTIVE STRATEGIES

CHAPTER 3

Inhibition of miR-223 reduces inflammation but not adverse cardiac remodelling
after myocardial ischemia-reperfusion *in vivo*

37

CHAPTER 4

Active Wnt signaling in response to cardiac injury

51

CHAPTER 5

Human *versus* porcine mesenchymal stromal cells: phenotype, differentiation
potential, immunomodulation and cardiac improvement after transplantation

69

CHAPTER 6

Targeting cell death in the reperfused heart: pharmacological approaches for
cardioprotection

93

CHAPTER 7

Inhibition of RIP1-dependent necrosis prevents adverse cardiac remodeling
after myocardial ischemia-reperfusion *in vivo*

125

CHAPTER 8

Necrostatin-1 reduces myocardial ischemia/reperfusion injury in pigs

149

PART THREE | SUMMARY, GENERAL DISCUSSION AND FUTURE PERSPECTIVES

CHAPTER 9

Summary, general discussion and future perspectives 161

CHAPTER 10

Nederlandse samenvatting 173

ADDENDUM

Dankwoord 184

List of Publications 189

Curriculum Vitae 190

1



General introduction

Myocardial infarction

Cardiovascular disease remains one of the leading causes of morbidity and mortality in the western world¹. With increasing aging of the population and the increasing incidence of cardiovascular risk factors like obesity, diabetes, and hypertension, one can expect even a further increase in the near future. With 500.000 ST- Elevation Myocardial Infarction (STEMI) events each year in the United States alone, the impact is evident. STEMI is one of the most important manifestations of cardiovascular disease. Also in the Netherlands, hospital admission due to cardiovascular disease is still increasing².

Currently, reperfusion is the most effective therapy for patients suffering from acute myocardial infarction (MI). During the last decade, technical and pharmacological advances have improved patient outcome and prognosis, especially in terms of infarct-related acute deaths. As a consequence, however, the incidence of heart failure is increasing, as well as its public health burden worldwide. Next to primary prevention and reduction of classical risk factors, the ongoing quest for new diagnostic and therapeutic strategies is essential to deal with this growing problem.

Myocardial infarct healing – from cell death to myocardial wound healing

As infarct size is a major determinant of cardiac remodelling and prognosis after MI, early reperfusion is crucial^{3, 4}. However, within minutes after the restoration of blood flow, reperfusion itself results in additional damage also known as myocardial ischemia-reperfusion (I/R) injury⁵. Based on experimental studies, it has become clear that I/R injury contributes to a significant amount of additional cell death, also referred to as lethal reperfusion injury⁶. Cell death can be classified based on various criteria, but the two most important types in the ischemic heart are apoptosis and necrosis⁷. Where apoptosis was considered as a regulated form of cell death, since the cell starts its suicide program, necrosis was generally seen as a passive and unregulated process resulting from externally-induced cellular injury⁸. This traditional view has changed during the last years, as a growing body of evidence clearly demonstrated that at least some part of necrotic cell death can be regulated⁹⁻¹¹.

Following MI, the process of myocardial wound healing starts with the inflammatory phase, in which granulocytes and other inflammatory cells are recruited to the infarcted area to remove dead cells and their remaining debris^{12, 13}. Furthermore, these cells also release growth factors, cytokines and matrix metalloproteinases (MMPs), leading to degradation of extracellular matrix (ECM). After several days, the acute inflammatory reaction converts to the next phase, which is characterized by the formation of granulation tissue and invasion of myofibroblasts. This transition, mainly regulated by key signalling pathways including transforming growth factor- β (TGF- β) and Wnt/ β -catenin, ensures the production of new ECM by the attracted myofibroblast to strengthen the wound and prevent cardiac rupture^{14, 15}. At the same time, the endogenous repair mechanisms of the heart are activated, including newly formed capillaries that start to grow to provide the area with oxygen and nutrients¹⁶. Except for myofibroblast, cells start to disappear from the infarct and most of the collagen becomes cross-linked. As a result, the infarcted area will become an organized scar.

Endogenous repair

About a decade ago, the first reports provided evidence for the existence of endogenous cardiac progenitor cells in the heart, which could be expanded *in vitro* and contributed to myocardial repair post-MI¹⁷⁻¹⁹. These cells are probably also activated and differentiated by modulation of TGF- β and Wnt pathways^{20, 21}. Although various cardiac-derived progenitor cells were isolated by several laboratories, differentiation towards mature cardiomyocytes was demonstrated for several²². In addition to the role of TGF- β and Wnt, short non-coding small RNAs, microRNAs, that regulate the expression of proteins by translational repression or degradation of messenger RNAs (mRNAs), could enhance differentiation efficacy²³⁻²⁵. Interestingly, several clusters of microRNAs are also reactivated during cardiac wound healing and heart failure^{26, 27}. Both the process of cardiac wound healing and activation of endogenous cardiac progenitor cells could therefore be influenced by these small RNAs, making them potentially interesting therapeutic targets²⁸.

Cell therapy

Either stimulation of the endogenous progenitor cells or therapeutic delivery of progenitor cells by injection might facilitate the generation of *de novo* functional myocardium. However, in addition to the cardiac progenitor cells, many other cell types could be used, all with its own advantages or disadvantages²⁹. After initial research was merely focussed on bone marrow-derived stem cells, the balance shifted towards cells that can actually become cardiac(-like) cells, including adult cardiac stem/progenitor cells and embryonic/induced-pluripotent (iPSC) stem cells²². Currently, stem cell engraftment and the number of newly generated cardiomyocytes in many experimental studies is too low to explain the significant cardiac improvement described, thereby leading to the "paracrine hypothesis"³⁰. Not the transplanted cells themselves, but rather their secretome might facilitate myocardial repair, via activation/recruitment of endogenous progenitor cells, modulation of cardiac wound healing and inflammation, and stimulation of angiogenesis in a paracrine fashion^{31, 32}. From this perspective, as the cell type might be less important for repair than their paracrine factors, mesenchymal stem cells (MSCs) seem to be an attractive source³³. MSCs can be used autologously, expand easily and have been used in the clinical setting for many years already.

Outline of this thesis

Considering the major public health burden worldwide, new ways to reduce the impact of acute MI, and its negative consequences are necessary. The overall aim of this thesis is to provide new solutions to improve patient outcome after MI by improving early diagnosis and by increasing our basic understanding of cardiac wound healing, cell transplantation and cell death, in order to find novel cardioprotective strategies (Figure 1).

Early diagnosis (Part One)

In approximately 5-10% of the patients presenting with acute MI, clear cut ST-elevation is present, providing a straightforward diagnosis and subsequent reason for revascularization within minutes. In most cases, however, diagnosis depends on the elevation of cardiac troponins to identify high-risk patients^{34, 35}. Despite the development of high-sensitive

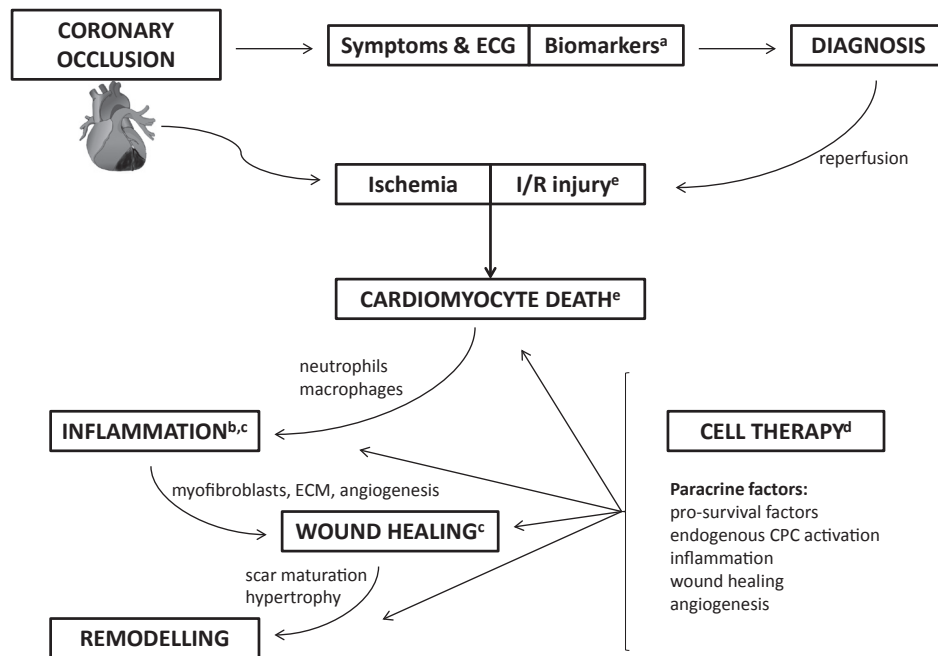


Figure 1 | Overview of events after myocardial infarction and possible diagnostic and cardioprotective strategies.

After coronary occlusion, in the majority of patients diagnosis of acute MI depends on clinical symptoms, ECG and measurement of troponin. Depending on the duration of ischemia as well as the extent of reperfusion injury, irreversible loss of cardiomyocyte takes place, thereby evoking an inflammatory response. After the inflammatory phase, further infarct healing is initiated by myofibroblasts producing new extracellular matrix (ECM) and promoting angiogenesis. The final phase of scar maturation and cardiac remodelling, although merely depending on the earlier events, greatly influences patient prognosis. Aim of this thesis is to provide new solutions to improve patient outcome after MI by improving early diagnosis (a) and by increasing our basic understanding of inflammation (b) and cardiac wound healing (c), cell transplantation (d) and cell death (e), in order to find novel cardioprotective strategies.

troponin assays, still a substantial delay of about 2-3 hours exists before final diagnosis is established³⁶. Among other biomarkers currently under investigation, circulating microRNAs - released into the circulation upon cardiac injury - could be novel candidates³⁷⁻³⁹. Although present in the circulation, it is currently unclear what their biological role is and where they originate from. Several possibilities have been proposed, including passive leakage from necrotic cardiomyocytes as well as extra-cardiac sources like platelets, endothelial cells, or microparticles and exosomes^{38, 39}. Up till now, studies investigating the diagnostic potential of circulating microRNAs typically included patients already known to have coronary artery disease. In **Part One** of this thesis, we address the question whether circulating microRNAs could be used as novel biomarkers to identify patients with acute coronary syndrome (ACS) in a population presenting with chestpain to the emergency department, when diagnostic uncertainty is most evident (**Chapter 2**).

Cardioprotective strategies (Part Two)

Next to their presence in the circulation and their reactivation during cardiac wound healing, miRNAs are also increasingly seen as master regulators of immune cell function and inflammation⁴⁰. Most studies investigating the role of miRNAs after MI focussed on cell survival, remodelling and activation of endogenous stem cells, leaving their role during the inflammatory response rather unexplored²⁸. Interestingly, miRNAs can be modulated *in vivo* using synthetic complementary oligonucleotides of 8–25 nt of length, directed against the seed sequence (i.e. antimirs/antagomirs)^{41, 42}. In **Chapter 3** the role of miR-223, regarded as an inflammatory microRNA⁴³, is explored during cardiac wound healing, followed by its modulation *in vivo*.

Wnt/ β -catenin is regarded as an important regulator of wound healing and endogenous stem cell activation. Very recently, inhibition of Frizzled proteins, one of the receptors involved in Wnt signalling, prevented adverse cardiac remodelling by increasing fibroblast influx in the infarcted area⁴⁴. In addition to its effect on fibroblasts, Wnt molecules have numerous other actions¹⁵. Considering its potency to act as a therapeutic target, fundamental insights on Wnt time-dependency and cell specificity after cardiac injury is necessary, which is explored in **Chapter 4**.

Clinical trials have started aiming to improve cardiac function after MI in patients, although several issues still need to be addressed including proper cell characterization and optimal expansion *in vitro*, arrhythmogenesis and optimal delivery and timing^{45, 46}. To address these questions, pre-clinical MSC studies are needed for which pigs appear to be the species of choice, preferably using autologous porcine cells to prevent immune rejection. To what extent porcine MSCs (pMSC) resemble human MSCs (hMSC) to assure safe extrapolation to the human situation is currently unknown. Therefore, both characteristics and therapeutic efficacy of human *versus* porcine MSC are compared in a mouse model of MI (**Chapter 5**).

Prevention of lethal reperfusion injury (i.e. 'damage control') as adjuvant therapy next to reperfusion, might be a strategy which can be implemented easily into the clinic⁴⁷. After an extensive overview of cell death in the reperfused heart and how this can be targeted pharmacologically (**Chapter 6**), the effect of Necrostatin-1 – a novel inhibitor of necrotic cell death – is presented using a mouse model (**Chapter 7**) and porcine model (**Chapter 8**) of myocardial I/R.

This thesis concludes with **Part Three**, providing a summary and discussion of the previous chapters (**Chapter 9**).

REFERENCES

1. Lloyd-Jones D, Adams RJ, Brown TM, et al. Heart disease and stroke statistics–2010 update: a report from the American Heart Association. *Circulation* 2010;121:e46-e215.
2. Vaartjes I, van Dis I, Visseren FLJ, et al. Hart- en vaatziekten in Nederland 2011, cijfers over leefstijl- en risicofactoren, ziekte en sterfte. Den Haag: Hartstichting; 2011.
3. McKay RG, Pfeffer MA, Pasternak RC, et al. Left ventricular remodeling after myocardial infarction: a corollary to infarct expansion. *Circulation* 1986;74:693-702.
4. Sobel BE, Bresnahan GF, Shell WE, et al. Estimation of infarct size in man and its relation to prognosis. *Circulation* 1972;46:640-648.
5. Yellon DM, Hausenloy DJ. Myocardial reperfusion injury. *N Engl J Med* 2007;357:1121-1135.
6. Prasad A, Stone GW, Holmes DR, et al. Reperfusion injury, microvascular dysfunction, and cardioprotection: the “dark side” of reperfusion. *Circulation* 2009;120:2105-2112.
7. Galluzzi L, Vitale I, Abrams JM, et al. Molecular definitions of cell death subroutines: recommendations of the Nomenclature Committee on Cell Death 2012. *Cell Death Differ* 2012;19:107-120.
8. Oerlemans MI, Koudstaal S, Chamuleau SA, et al. Targeting cell death in the reperfused heart: Pharmacological approaches for cardioprotection. *Int J Cardiol* 2012.
9. Baines CP, Kaiser RA, Purcell NH, et al. Loss of cyclophilin D reveals a critical role for mitochondrial permeability transition in cell death. *Nature* 2005;434:658-662.
10. Nakagawa T, Shimizu S, Watanabe T, et al. Cyclophilin D-dependent mitochondrial permeability transition regulates some necrotic but not apoptotic cell death. *Nature* 2005;434:652-658.
11. Kung G, Konstantinidis K, Kitsis RN. Programmed necrosis, not apoptosis, in the heart. *Circ Res* 2011;108:1017-1036.
12. Cleutjens JP, Blankesteijn WM, Daemen MJ, et al. The infarcted myocardium: simply dead tissue, or a lively target for therapeutic interventions. *Cardiovasc Res* 1999;44:232-241.
13. Frantz S, Bauersachs J, Ertl G. Post-infarct remodelling: contribution of wound healing and inflammation. *Cardiovasc Res* 2009;81:474-481.
14. Dobaczewski M, Chen W, Frangogiannis NG. Transforming growth factor (TGF)-beta signaling in cardiac remodeling. *J Mol Cell Cardiol* 2011;51:600-606.
15. Brade T, Manner J, Kuhl M. The role of Wnt signalling in cardiac development and tissue remodelling in the mature heart. *Cardiovasc Res* 2006;72:198-209.
16. Frangogiannis NG. Regulation of the inflammatory response in cardiac repair. *Circ Res* 2012;110:159-173.
17. Beltrami AP, Barlucchi L, Torella D, et al. Adult cardiac stem cells are multipotent and support myocardial regeneration. *Cell* 2003;114:763-776.
18. Oh H, Bradfute SB, Gallardo TD, et al. Cardiac progenitor cells from adult myocardium: homing, differentiation, and fusion after infarction. *Proc Natl Acad Sci U S A* 2003;100:12313-12318.
19. Bearzi C, Rota M, Hosoda T, et al. Human cardiac stem cells. *Proc Natl Acad Sci U S A* 2007;104:14068-14073.
20. Goumans MJ, de Boer TP, Smits AM, et al. TGF-beta1 induces efficient differentiation of human cardiomyocyte progenitor cells into functional cardiomyocytes *in vitro*. *Stem Cell Res* 2007;1:138-149.
21. Cohen ED, Wang Z, Lepore JJ, et al. Wnt/beta-catenin signaling promotes expansion of Isl-1-positive cardiac progenitor cells through regulation of FGF signaling. *J Clin Invest* 2007;117:1794-1804.
22. Liu J, Sluijter JP, Goumans MJ, et al. Cell therapy for myocardial regeneration. *Curr Mol Med* 2009;9:287-298.
23. Lewis BP, Shih IH, Jones-Rhoades MW, et al. Prediction of mammalian microRNA targets. *Cell* 2003;115:787-798.
24. Sluijter JP, van Mil A, van Vliet P, et al. MicroRNA-1 and -499 regulate differentiation and proliferation in human-derived cardiomyocyte progenitor cells. *Arterioscler Thromb Vasc Biol* 2010;30:859-868.
25. Hosoda T, Zheng H, Cabral-da-Silva M, et al. Human cardiac stem cell differentiation is regulated by a mircrine mechanism. *Circulation* 2011;123:1287-1296.

26. Thum T, Galuppo P, Wolf C, et al. MicroRNAs in the human heart: a clue to fetal gene reprogramming in heart failure. *Circulation* 2007;116:258-267.
27. van Rooij E, Sutherland LB, Liu N, et al. A signature pattern of stress-responsive microRNAs that can evoke cardiac hypertrophy and heart failure. *Proc Natl Acad Sci USA* 2006;103:18255-18260.
28. Thum T. MicroRNA therapeutics in cardiovascular medicine. *EMBO Mol Med* 2012;4:3-14.
29. Mohsin S, Siddiqi S, Collins B, et al. Empowering adult stem cells for myocardial regeneration. *Circ Res* 2011;109:1415-1428.
30. Gnechchi M, He H, Noiseux N, et al. Evidence supporting paracrine hypothesis for Akt-modified mesenchymal stem cell-mediated cardiac protection and functional improvement. *FASEB J* 2006;20:661-669.
31. Gnechchi M, Zhang Z, Ni A, et al. Paracrine mechanisms in adult stem cell signaling and therapy. *Circ Res* 2008;103:1204-1219.
32. Jadczyk T, Faulkner A, Madeddu P. Stem cell therapy for cardiovascular disease: The demise of alchemy and rise of pharmacology. *Br J Pharmacol* 2012.
33. Williams AR, Hare JM. Mesenchymal stem cells: biology, pathophysiology, translational findings, and therapeutic implications for cardiac disease. *Circ Res* 2011;109:923-940.
34. Hamm CW, Bassand JP, Agewall S, et al. ESC Guidelines for the management of acute coronary syndromes in patients presenting without persistent ST-segment elevation: The Task Force for the management of acute coronary syndromes (ACS) in patients presenting without persistent ST-segment elevation of the European Society of Cardiology (ESC). *Eur Heart J* 2011;32:2999-3054.
35. Thygesen K, Alpert JS, White HD, et al. Universal definition of myocardial infarction. *Circulation* 2007;116:2634-2653.
36. Twerenbold R, Jaffe A, Reichlin T, et al. High-sensitive troponin T measurements: what do we gain and what are the challenges? *Eur Heart J* 2012;33:579-586.
37. Mitchell PS, Parkin RK, Kroh EM, et al. Circulating microRNAs as stable blood-based markers for cancer detection. *Proc Natl Acad Sci USA* 2008;105:10513-10518.
38. Gupta SK, Bang C, Thum T. Circulating microRNAs as biomarkers and potential paracrine mediators of cardiovascular disease. *Circ Cardiovasc Genet* 2010;3:484-488.
39. Zampetaki A, Willeit P, Drozdov I, et al. Profiling of circulating microRNAs: from single biomarkers to re-wired networks. *Cardiovasc Res* 2012;93:555-562.
40. O'Connell RM, Zhao JL, Rao DS. MicroRNA function in myeloid biology. *Blood* 2011;118:2960-2969.
41. Krutzfeldt J, Rajewsky N, Braich R, et al. Silencing of microRNAs *in vivo* with 'antagomirs'. *Nature* 2005;438:685-689.
42. Montgomery RL, Hullinger TG, Semus HM, et al. Therapeutic inhibition of miR-208a improves cardiac function and survival during heart failure. *Circulation* 2011;124:1537-1547.
43. Johnnidis JB, Harris MH, Wheeler RT, et al. Regulation of progenitor cell proliferation and granulocyte function by microRNA-223. *Nature* 2008;451:1125-1129.
44. Laeremans H, Hackeng TM, van Zandvoort MA, et al. Blocking of frizzled signaling with a homologous peptide fragment of wnt3a/wnt5a reduces infarct expansion and prevents the development of heart failure after myocardial infarction. *Circulation* 2011;124:1626-1635.
45. Richardson JD, Nelson AJ, Zannettino AC, et al. Optimization of the Cardiovascular Therapeutic Properties of Mesenchymal Stromal/Stem Cells-Taking the Next Step. *Stem Cell Rev* 2012.
46. Ranganath SH, Levy O, Inamdar MS, et al. Harnessing the mesenchymal stem cell secretome for the treatment of cardiovascular disease. *Cell Stem Cell* 2012;10:244-258.
47. Garcia-Dorado D, Ruiz-Meana M, Piper HM. Lethal reperfusion injury in acute myocardial infarction: facts and unresolved issues. *Cardiovascular research* 2009;83:165-168.

2



Martinus I.F.J. Oerlemans¹

Arend Mosterd^{1,2,3}

Marieke S. Dekker^{2,3,4}

Evelyn A. de Vrey³

Alain van Mil^{1,5}

Gerard Pasterkamp¹

Pieter A. Doevendans^{1,5}

Arno W. Hoes²

Joost P.G. Sluijter^{1,5}

¹ Department of Cardiology, University Medical Center Utrecht, the Netherlands

² Julius Center for Health Sciences and Primary Care, University Medical Center, Utrecht, the Netherlands

³ Department of Cardiology, Meander Medical Center, Amersfoort, the Netherlands

⁴ Department of Cardiology, Isala Clinics, Zwolle, the Netherlands

⁵ Interuniversity Cardiology Institute Netherlands (ICIN), Utrecht, the Netherlands

Early assessment of acute coronary syndromes in the emergency department: the potential diagnostic value of circulating microRNAs

EMBO Mol Med 2012, Epub ahead of print

ABSTRACT

Previous studies investigating the role of circulating microRNAs in acute coronary syndrome (ACS) were based on small patient numbers, performed no comparison with established markers of cardiac injury and did not have appropriate controls. We determined the potential diagnostic value of circulating microRNAs as novel early biomarkers in 332 suspected ACS patients on presentation to the emergency department (ED) in a prospective single-center study including cardiac miRNAs (miR-1,-208a and -499), miR-21 and miR-146a. Levels of all miRs studied were significantly increased in 106 patients diagnosed with ACS, even in patients with initially negative high-sensitive troponin or symptom onset <3 hours. MiR-1, miR-499 and miR-21 significantly increased the diagnostic value in all suspected ACS patients when added to high-sensitive troponin T (AUC 0.90). These three miRs were strong predictors of ACS independent of clinical co-variables, including patient history and cardiovascular risk factors. Interestingly, the combination of these three miRs resulted in a significantly higher AUC of 0.94 than hs-troponin T (0.89). Circulating microRNAs hold great potential as novel early biomarkers for the management of suspected ACS patients.

INTRODUCTION

Acute coronary syndrome (ACS) remains one of the leading causes of morbidity and mortality in the Western world. Early diagnosis of ACS is essential because of improvement in prognosis following timely interventions. Currently, the diagnosis of ACS is based on elevation of (high-sensitive) cardiac troponin I or T (cTnI or cTnT), in the context of clinical and electrocardiographic (ECG) findings^{1, 2}. Unfortunately, these biomarkers are not consistently elevated within the first hours after symptom onset, requiring repetitive measurements and hindering early diagnosis³. In the setting of typical symptoms and ST segment elevation on the ECG, the diagnosis and subsequent management is straightforward⁴. In daily clinical practice, however, this scenario only pertains to a minority of patients presenting to the emergency department (ED) with symptoms suggestive of an ACS, making the early diagnosis of ACS a challenge and new diagnostic markers to improve early recognition of ACS are required.

MicroRNAs (miRNAs) are short, non-coding small RNAs that regulate the expression of proteins by translational repression or degradation of messenger RNAs (mRNAs)⁵. Over the last few years it has been established that miRNAs play a crucial role in cardiac development and homeostasis and that miRNA expression is altered in the diseased heart⁶⁻⁸. Interestingly, miRNAs were also found to be present in human serum and plasma and altered expression profiles were observed in cancer and other diseases like diabetes⁹⁻¹¹. This led to the hypothesis that miRNAs might be released upon cardiac injury and that the detection of cell-free miRNAs – including cardiac-related miR-1, miR-499 and miR-208a – could be used for the diagnosis of ACS¹²⁻²². Previous studies investigating miRNAs for detection of cardiac injury have been relatively small (mostly including less than 100 patients) and were not carried out in the clinically relevant patient population (i.e. unselected patients suspected of ACS presenting to the ED), but typically included patients already known to have coronary artery disease (e.g. those undergoing primary percutaneous coronary intervention [PCI]) and compared these with healthy controls^{14, 16, 18, 23}. In addition, several studies used samples taken at the time of reperfusion to determine miRNAs, rather than samples taken upon initial presentation to the ED, when diagnostic uncertainty is most evident.

Our aim was to determine the diagnostic value of circulating miRNAs, in particular cardiac-related miR-1, miR-499 and miR-208a, and stress-related miR-21 and miR-146a²⁴⁻²⁶ in the early assessment of suspected ACS patients presenting at the ED. In addition, we determined the diagnostic value of miRNAs in subgroups of suspected ACS patients with initially negative high-sensitive (hs-) troponin levels and in those presenting within 3 hours of symptom onset, since in these patients the diagnostic accuracy of available biomarkers is limited.

MATERIALS AND METHODS

Study population

The present study a single-center, prospective diagnostic study among patients presenting to the ED within 24 hours of onset of chest pain suggestive of ACS. Patients were enrolled at the ED of the Meander Medical Center (Amersfoort, the Netherlands) between May 2007 and November 2007 ST-elevation myocardial infarction (STEMI) – these patients underwent immediate percutaneous coronary intervention (PCI) – or refusal to provide informed consent were the only exclusion criteria, 470 patients were evaluated. All included patients provided written informed consent, the protocol was approved by the local ethics committee and the study was conducted in accordance with the Declaration of Helsinki. RNA extraction and analysis of stored serum samples was performed in all 470 patients. Despite several attempts to isolate good quality RNA, we had to exclude 138 patients because of poor RNA integrity, mostly due to errors in sample processing at time of collection and/or storage. The current analyses thus included 332 patients with chest pain. Importantly, the mean age (61.7 ± 14.9) and median onset of symptoms (3.2 hours; interquartile range (IQR) 2.0-6.7) in the 138 excluded patients and in the 332 included patients were similar (supporting information Table S5).

Routine clinical assessment

All patients underwent routine clinical assessment, including medical history, physical examination, serial 12 lead ECGs, pulse oxymetry and chest radiography. Immediately upon presentation, venous blood was drawn to determine cardiac Troponin I (cTnI) and other routine laboratory parameters. At the same time, additional samples were taken and stored for future analyses, including serum miRNA analysis (Supporting information Figure S1). cTnI levels were measured by sandwich chemoluminescence immunoassay (Synchron Lxi 725 integrated clinical chemistry, Beckman Coulter). The lower detection limit for cTnI was 0.01ug/L and the cut-off level for positivity was $\geq 0.04 \mu\text{g/L}$. High-sensitive cardiac Troponin T (hs-cTnT) was determined post-hoc in serum stored at -80°C . The lower detecting limit for hs-cTnT was 3pg/mL, measured by the Elecsys troponin T high-sensitive assay fourth generation (Roche Diagnostics) with the 99th-percentage cut-off point of $\geq 14 \text{pg/mL}$.

Blood processing

Blood samples were collected via a venous puncture at the time of presentation at the ED and 5ml of blood was collected in a standard serum tube (BD #368968). Blood was centrifuged for 10 minutes after which serum was aspirated, aliquoted in RNase-free tubes and stored at -80°C until further processing.

RNA isolation

RNA was extracted of fixed volumes of serum (250 μL) using TRIzol LS reagent (Invitrogen 10296-028) as described previously^{10, 20}. Genomic DNA contamination was eliminated using DNase I kit (Ambion) and RNA concentration quantified with a spectrophotometer (NanoDrop ND-1000, Thermo Scientific, Wilmington, DE). The RNA integrity of small RNAs

was determined using small RNA Chip analysis (5067-1548) for an Agilent Bioanalyzer 2100 (Agilent Technologies).

Quantitative RT-PCR

A total of 20ng DNA-free RNA was used as input in the reverse transcription reaction (RT) using the TaqMan miRNA Reverse Transcription Kit and miRNA-specific primers (Applied Biosystems) as described previously³⁷. Real-time PCR (RT-PCR) amplification was performed in duplicate using 1:5 diluted RT products for the following miRNAs: miR-1 (#002222), miR-208a (#000511), miR-499 (#002427), miR-21 (#000397) and miR-146a (#000468). Currently, no consensus exists on the use of an internal control for real-time PCR analysis of circulating miRNAs. All RT-PCR data were standardized to U6, which was used by others before^{31,38}, moreover, U6 levels did not differ between ACS and non-ACS patients. After normalisation for RNU6, relative gene expression was calculated by the $\Delta\Delta C_t$ method^{39,40}.

Outcome

The primary outcome of this study was ACS, including unstable angina (UA) and non ST-elevation myocardial infarction (NSTEMI). Final diagnosis was made by an expert panel of three cardiologists, based on all available clinical information including serial troponin measurements, serial ECG findings, coronary angiography, echocardiography, cardiac exercise tests, and information from hospital discharge letters.

Early invasive coronary angiography was performed in 30 (36.6%) out of 82 NSTEMI-ACS patients. Most important reasons were recurrent or non-resolving symptoms (n=10), dynamic ECG changes (n=8), prior CABG or recent PCI (n=11), and ventricular tachycardia (n=1). From the remaining 52 patients, in 38 (73.1%) patients symptoms resolved upon medicinal treatment. Of the 14 patients with non-resolving symptoms, 4 patients requested conservative therapy, in 5 patients a conservative strategy was chosen considering comorbidity (aged >85 years, renal failure, CVA) and in 5 patients no coronary angiography was performed due to known multivessel disease (>2 coronary arteries) or graft or stent failure requiring CABG surgery.

The presence of ACS was determined according to the universal definition of myocardial infarction¹. NSTEMI was diagnosed when there was evidence of myocardial necrosis together with clinical signs and symptoms of myocardial ischemia, according to the current guidelines^{2,41}. Myocardial necrosis was diagnosed by a rising and/or fall in cardiac troponin with at least one value above the 99th percentile. Unstable angina was diagnosed in the presence of clinical signs and symptoms of myocardial ischemia, including cardiac exercise test, without elevation of cardiac biomarkers.

Statistical analysis

Data are presented as mean \pm SEM unless otherwise indicated. Differences between groups were analyzed by Mann-Whitney U Test or Kruskal-Wallis Test (>2 groups) when appropriate using Bonferroni correction for multiple comparisons. Spearman rank correlation was used to compare patient characteristics with circulating microRNAs. Receiver-operating-characteristic (ROC) curves were constructed to of each miRNA using the Area Under the

ROC Curve (AUC) to assess their ability to diagnose ACS⁴². To compare diagnostic discriminatory ability of miRNAs with cardiac (hs-)troponin, likelihood ratio (LR) tests were performed after logistic regression to assess the additional diagnostic value of miRNA to the information provided by (hs-) troponin. Multivariate logistic regression was used to investigate whether miRNAs were independent predictors of ACS after adjustment for relevant co-variables including patient history (age, sex, previous MI, PCI or surgery) and cardiovascular risk factors (hypertension, hypercholesterolemia, family history, current and former smoking and diabetes mellitus). All tests were two-sided, using a significance level of $P < 0.05$ (SPSS Statistics v17, Chicago, United States).

RESULTS

Patient characteristics

The median onset of chest pain in the 332 suspected ACS patients was 3.2 hours (interquartile range (IQR) 1.8-8.0) prior to presentation (Table 1). ACS was diagnosed in 106 (31.2%) patients, consisting of UA (n=25, 23.6%) and NSTEMI (n=81, 76.4%). Of the ACS-patients, 21.7% (23/106) had a hs-troponin level < 0.14 pg/mL at initial presentation, with a median hs-troponin of 7.25 (IQR 3.1-11.3) whereas in the hs-troponin > 14 pg/mL this was 41.2 (IQR 18.7-108.2).

Table 1 | Patient Characteristics of 332 Patients With Chest Pain

Characteristic	Non-ACS	ACS	All	P
N (%)	226 (68.1)	106 (31.2)	332 (100)	
Age (yrs)	60.2±14.3	68.7±12.6	62.9±14.4	0.00
Male sex (% male)	120 (53.1)	70 (66.0)	190 (57.2)	0.03
Onset of chest pain, median (IQR)	3.2 (1.9-9.0)	3.1 (1.6-8.0)	3.2 (1.8-8.0)	0.64
Risk factors				
Current smoker	62 (27.7)	24 (22.9)	86 (26.1)	0.42
Former smoker	71 (31.8)	32 (30.8)	103 (31.5)	0.90
Hypertension	90 (39.8)	61 (58.7)	151 (45.8)	0.02
Hypercholesterolemia	65 (28.9)	44 (41.9)	109 (33.0)	0.02
Diabetes Mellitus	31 (13.8)	21 (20.0)	52 (15.8)	0.19
Body mass index (kg/m ²)	26.4±6.1	26.0±5.1	26.3±5.8	0.34
Parental CVD	89 (39.7)	44 (42.7)	133 (40.7)	0.63
History of CVD	97 (42.9)	62 (58.5)	159 (47.9)	0.01
Cardiac Troponin I (µg/L)	0.02 (0.01-0.03)	0.07 (0.04-0.21)	0.03 (0.02-0.05)	0.00
Cardiac hs-Troponin T (pg/mL)	3.3 (1.1-8.5)	23.7 (10.6-80.8)	6.0 (2.2-18.7)	0.00

Data presented as mean±SD for age, body mass index and as median (25th – 75th interquartile range) for onset of chest pain and cardiac troponin levels. All other variables are presented as n (%); ACS = acute coronary syndrome; CVD = cardiovascular disease; Mann-Whitney (continuous variables) or χ^2 test (categorical variables), ACS (n=106) vs. non-ACS (n=226).

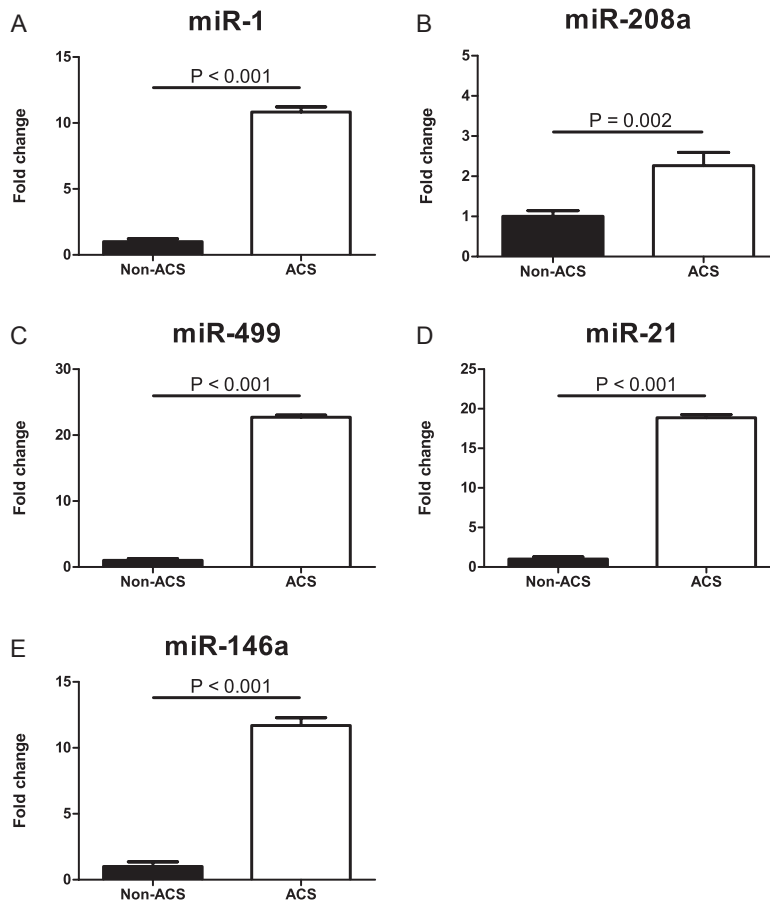


Figure 1 | Expression levels of circulating miRNAs in serum of ACS and non-ACS patients
Cardiac-specific miR-1, miR-208a and miR-499 were significantly increased in ACS patients (A-C). Both levels of miR-21 (D) and miR-146a (E) were markedly elevated in ACS patients compared to non-ACS patients. Data are presented as mean \pm SEM, P values versus non-ACS patients, Mann-Whitney test.

In 226 (68.1%) patients an ACS could be ruled out; in the non-ACS population the following diagnoses were established by the expert-panel: stable angina (n=39), rhythm disorders (n=9), heart failure (n=3), pericarditis (n=2), other cardiac diagnosis (unlisted, n=12) and non-cardiac chest pain (n=161).

Circulating miRNA levels in ACS patients

Compared to the non-ACS population, circulating levels of all cardiac-expressed miRNAs studied were higher (miR-1, miR-499, and miR-208a) in patients with ACS (Figure 1A-C). Furthermore, circulating levels of miR-21 (19-fold) and miR-146a (12-fold) were markedly elevated in ACS patients as well ($P < 0.001$; Figure 1D, E). None of the circulating miRNAs were significantly associated with age, gender or other relevant clinical co-variables (supporting information Table S1). Furthermore, heparin treatment or platelet inhibition

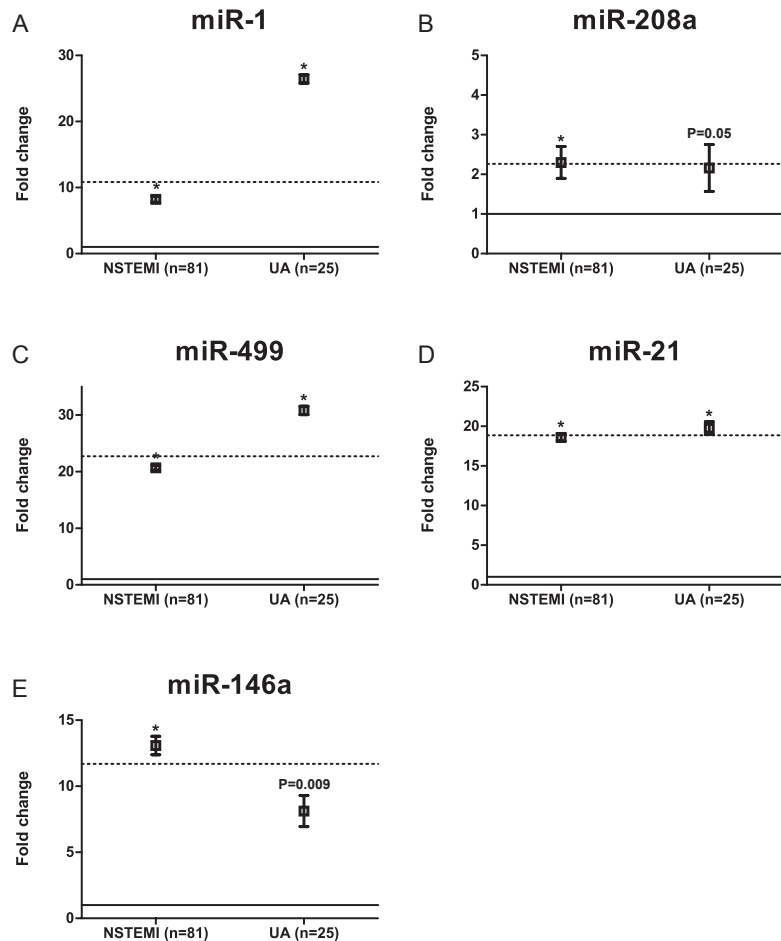


Figure 2 | Expression pattern of circulating miRNAs in STEMI and UA patients

Circulating miRNAs displayed different expression levels within the ACS population. Dotted lines represent fold increase in all ACS patients. While the increase in levels of miR-1 (A) and miR-499 (C) was relatively high in UA patients, miR-208a levels were only increased in NSTEMI patients (B). MiR-21 levels were comparable between NSTEMI and UA patients (D), the increase in levels of miR-146a (E) was most pronounced in NSTEMI patients. Data are presented as mean \pm SEM. P values and *P<0.001 *versus* non-ACS patients, Mann-Whitney test.

(aspirin, clopidogrel) at presentation was not significantly correlated with any of the circulating miRs, as depicted in supporting information Table S2.

Expression pattern of circulating miRNAs in UA and NSTEMI patients

Levels of both miR-1 and miR-499 were elevated in UA and NSTEMI patients when compared to non-ACS patients (P<0.001; Figure 2A, C), while circulating miR-208a levels were significantly increased in NSTEMI patients only (Figure 2B). MiR-21 and miR-146a were significantly increased in both ACS subcategories (Figure 2D, E). For miR-208a and miR-146a, circulating miRNA levels seemed to be the highest in NSTEMI patients, while

miR-21 levels were comparable between patients with unstable angina and NSTEMI patients. Levels of miR-1 and miR-499 were higher in UA patients.

Circulating miRNA levels in suspected ACS patients with a negative hs-troponin at first presentation and in patients presenting within 3 hours of symptom onset.

In 194 suspected ACS patients (53.6% men, mean age 58.4±12.7 years) initial hs-troponin levels were negative (<0.14pg/mL). Of these, 23 (11.9%) were subsequently classified as having an ACS (median hs-troponin level 2.81 (IQR 1.0-6.1) pg/mL, including 18 UA and 5 NSTEMI patients. In this troponin-negative subgroup of suspected ACS patients, cardiac-related miRNAs were considerably higher in patients with ACS (Table 2). Circulating levels of miR-21 and miR-146a were also elevated.

In 152 suspected ACS patients (55.3% men, mean age 62.9±14.5 years), the onset of chest pain was less than three hours prior to presentation. In this subgroup, circulating levels of miR-1, miR-499 and miR-208a were also higher in ACS patients than non-ACS patients (Table 3). Mir-21 and miR-146a were markedly elevated in ACS patients as well.

Additional diagnostic value of circulating microRNAs in ACS patients

The area under the ROC curve (AUC) of both cardiac troponin I (0.85; 95% Confidence Interval (CI) 0.80-0.90) and hs-troponin T (0.86; 95%CI 0.82-0.91) was higher than that of any of the miRs (Table 3). Of the miRs, miR-1, miR-499 and miR-21 had the highest AUC. When combining these miRs, the diagnostic value became significantly higher than that of hs-troponin T in the total suspected ACS patients and in the subgroup of suspected ACS patients with initially negative troponin levels (Table 3). Furthermore, combining miR-1, miR-499 or miR-21 with hs-troponin T significantly improved the diagnostic value by increasing the AUC to 0.90 (P<0.001; Table 3).

As expected, the AUC of hs-troponin was low (0.61; 95% CI 0.47-0.75) in the subgroup of suspected ACS patients with initially negative hs-troponin levels (Table 3). Interestingly, the AUC of miR-1 and miR-499 were higher than any of the other miRs or cardiac (hs-) troponin. The AUC of miR-21 was comparable with hs-troponin (0.75; 95% CI 0.65-0.85).

Table 2 | Relative expression of circulating miRNAs in serum of suspected ACS patients with a negative hs-troponin (n=194) or with onset of symptoms <3 hours (n=152) compared to non-ACS patients (n=226)

MicroRNA	Non-ACS	ACS patients with negative hs-troponin	P	ACS patients with symptom onset <3 hours	P
miR-1	1.0±0.2	14.9±0.8	0.00	6.0±0.6	0.00
miR-208a	1.0±0.2	2.8±0.7	0.03	2.4±0.5	0.01
miR-499	1.0±0.3	34.2±0.7	0.00	24.0±0.5	0.00
miR-21	1.0±0.3	15.5±0.8	0.00	11.0±0.5	0.00
miR-146a	1.0±0.4	6.2±1.3	0.04	11.9±0.8	0.00

Data are presented as mean±SEM. P versus non-ACS patients.

Addition of miR-1, miR-499 or miR-21 further increased the diagnostic discriminatory value significantly compared to hs-troponin alone (Table 3). Combining miR-1, miR-499 and miR-21 with hs-troponin T significantly improved the diagnostic value by increasing the AUC to 0.88 (95% CI 0.83-0.94). In patients with symptoms <3hours, a similar increase in AUC was observed, with the addition of miR-1, miR-499 and miR-21 (Table 3).

Circulating miRNAs are independent predictors for ACS

The clinical model with age, sex and cardiovascular risk factors resulted in an AUC of 0.72 (95% CI 0.66-0.78) for all suspected ACS patients (Table 4), which increased to 0.89 after addition hs-troponin T. Addition of miR-1, miR-499, or miR-21 to the clinical model with hs-troponin T significantly increased the AUC to 0.92 ($P<0.001$). Importantly, after correction for the clinical model and (hs-)troponin, miR-1, miR-499 and miR-21 were still strong predictors for ACS as illustrated by their odds ratio (Table 4). Interestingly, the combination of the three miRs resulted in an even higher AUC of 0.94 (95% CI 0.92 - 0.97).

In patients with negative hs-troponin at presentation, addition of miR-1, miR-499 and miR-21 also resulted in a significant increase in AUC to 0.92 (Table 5), whereas miR-208a and miR-146a showed no additional effect. Despite negative hs-troponin levels at presentation, the combination of three miRs (miR-1, miR-499, miR-21) resulted in a very high AUC value of 0.96 (95% CI 0.93-0.99), again independent of other clinical risk factors (Table 5).

Table 3 | Diagnostic value of cardiac troponin and circulating microRNAs in suspected ACS patients

Marker	All patients (n=332)		Hs-troponin negative patients (n=194)		Patients with symptoms <3 hours (n=152)	
	AUC	95% CI	AUC	95% CI	AUC	95% CI
Cardiac troponin I	0.85	0.80-0.90	0.61	0.47-0.75	0.82	0.75-0.90
Cardiac hs-troponin T	0.86	0.82-0.91	0.74	0.62-0.85	0.86	0.80-0.92
miR-1	0.75	0.70-0.81	0.79 ^b	0.69-0.89	0.67	0.28-0.77
miR-208 ^a	0.61	0.54-0.67	0.64	0.52-0.77	0.62	0.53-0.72
miR-499	0.79	0.74-0.84	0.83 ^c	0.76-0.90	0.79	0.71-0.86
miR-21	0.76	0.71-0.82	0.75	0.65-0.85	0.72	0.64-0.80
miR-146 ^a	0.68	0.62-0.74	0.64	0.52-0.75	0.70	0.61-0.78
miR-1 + miR-499 + miR-21	0.89 ^a	0.85-0.94	0.88 ^a	0.83-0.94	0.82	0.76-0.89
Cardiac hs-troponin T with:						
miR-1	0.90 ^a	0.86-0.93	0.86 ^a	0.79-0.92	0.88 ^c	0.83-0.94
miR-208 ^a	0.86	0.82-0.91	0.78	0.68-0.89	0.86	0.81-0.92
miR-499	0.90 ^a	0.86-0.93	0.89 ^a	0.83-0.94	0.90 ^a	0.84-0.94
miR-21	0.89 ^a	0.86-0.93	0.84 ^a	0.77-0.91	0.89 ^b	0.83-0.94
miR-146 ^a	0.87	0.83-0.91	0.79	0.70-0.88	0.86	0.80-0.92

AUC = Area under the ROC Curve; 95% CI = 95% Confidence Interval; ^a $P<0.001$, ^b $P=0.03$, ^c $P=0.003$ versus hs-troponin T.

In patients with symptom onset <3 hours, these three miRs were the strongest predictors for ACS, increasing the AUC significantly as well (supporting information Table S3 en S4). As a final step, we compared the combination of miR-1, miR-499 and miR-21 with the combination of three established markers of myocardial necrosis (hs-troponin, myoglobin and CK-MB) in the model with clinical risk factors (supporting information Table S4).

Table 4 | AUCs and Odds Ratios of miRNAs in suspected ACS patients in a clinical model (n=332)

	AUC	95% CI	OR†	95% CI
Marker	0.72	0.66-0.78	NA	NA
Clinical model (CM)	0.88	0.85-0.92	NA	NA
CM + Cardiac troponin	0.89	0.85-0.92	NA	NA
CM + Cardiac hs-troponin T				
CM + Cardiac hs-troponin T with:				
miR-1	0.92 ^a	0.90-0.95	1.30	1.17-1.42
miR-208 ^a	0.89	0.85-0.93	1.16	1.03-1.30
miR-499	0.92 ^a	0.89-0.95	1.28	1.18-1.40
miR-21	0.92 ^a	0.89-0.95	1.28	1.18-1.39
miR-146 ^a	0.90	0.87-0.94	1.14	1.08-1.21
miR-1 + miR-499 + miR-21	0.94 ^a	0.92-0.97	NA	NA

CM = Clinical model (age, sex, hypertension, hypercholesterolemia, family history, current and former smoking, diabetes mellitus, and history of myocardial infarction, PCI or coronary bypass surgery); AUC = Area under the ROC Curve; 95% CI = 95% Confidence Interval; ^aP<0.001 *versus* hs-troponin T. NA = not applicable; † Adjusted for clinical model and cardiac hs-troponin T.

Table 5 | AUCs and Odds Ratios of miRNAs in suspected ACS patients with a negative hs-troponin in a clinical model (n=194)

Marker	AUC	95% CI	OR†	95% CI
Clinical model (CM)	0.84	0.76-0.93	NA	NA
CM + Cardiac troponin	0.85	0.77-0.94	NA	NA
CM + Cardiac hs-troponin T	0.86	0.79-0.93	NA	NA
CM + Cardiac hs-troponin T with:				
miR-1	0.92 ^a	0.87-0.96	1.44	1.19-1.73
miR-208 ^a	0.87	0.78-0.95	1.12	0.95-1.35
miR-499	0.93 ^a	0.87-0.99	1.38	1.19-1.61
miR-21	0.92 ^a	0.88-0.97	1.34	1.15-1.55
miR-146 ^a	0.86	0.78-0.93	1.06	0.97-1.15
miR-1 + miR-499 + miR-21	0.96 ^a	0.93-0.99	NA	NA

CM = Clinical model (age, sex, hypertension, hypercholesterolemia, family history, current and former smoking, diabetes mellitus, and history of myocardial infarction, PCI or coronary bypass surgery); AUC = Area under the ROC Curve; 95% CI = 95% Confidence Interval; ^aP<0.001 *versus* hs-troponin T; NA = not applicable; † Adjusted for clinical model and cardiac hs-troponin T.

In the total population, hs-troponin negative patients and early presenting patients, the combination of miRs performed better than the combination of these three necrosis markers. However, only in the hs-troponin negative population, this led to a statistically significant difference in AUC.

DISCUSSION

Circulating miRNAs have been proposed as potentially useful novel biomarkers for detecting cardiac injury. We selected three miRNAs – miR-1, miR-499 and miR-208 – because of their known high expression in cardiac tissue to determine their diagnostic value in suspected ACS patients upon first presentation in the ED. Our results demonstrate that the levels of miR-1 and miR-499 are markedly elevated in patients with ACS compared to non-ACS patients (Figure 1A and 1C). These data confirm and extend previous reports showing high levels in patients with myocardial damage^{13, 13-18, 20}. The increase in miR-1 levels was less pronounced than that of miR-499. This might explain why a previous study failed to demonstrate a significant increase in miR-1 levels compared to miR-499, which was markedly elevated in patients suffering from acute MI¹⁶. MiR-208a only increased slightly in the ACS group (Figure 1B). This is probably explained by the fact that miR-208a was undetectable in 86% of our samples (286/332), supported by an earlier study²⁰. Also because of known difficulties in detecting miR-208a (and miR-208b) levels^{17, 18, 21}, miR-208(a/b) appears to be the least suitable of the selected cardiac-expressed candidates.

In addition, we investigated the expression of miR-21 and miR-146a in ACS –suspected patients based on reports showing that these miRNAs were clearly related to cardiac injury or myocyte cell death and in patients suffering from ACS^{25, 27}. Although further research is necessary to identify why these two miRNAs are upregulated, their involvement in cardiac disease has been established. Inhibition of miR-21 (depending on the anti-miR used) inhibited extensive fibrosis in the failing heart, mainly by decreasing fibroblast survival^{28, 29}. Additionally, miR-21 exerted cardioprotective effects as overexpression reduced myocardial cell death^{25, 30} and miR-146a was reported to be upregulated in Doxorubicin-induced cardiotoxicity²⁶. Circulating levels of miR-21 (diastolic dysfunction) and miR-146a (diastolic dysfunction and viral myocarditis) showed no changes compared to control patients¹⁶. In line with our data, two recent studies reported increased miR-21 levels post-MI^{22, 31}.

Analysis of miRNA levels in ACS subcategories revealed an increase of all miRNAs studied in UA and NSTEMI patients, except for miR-208a (only in NSTEMI patients). Interestingly, UA patients had relatively high levels of both miR-1 and miR-499, although this was not statistically different from NSTEMI patients. MiR-146a levels were the highest in NSTEMI patients; miR-21 levels were comparable between UA and NSTEMI patients. It is not unlikely that both miR-21 and miR-146a are subjected to more dynamic changes in the ischemic heart. This is supported by the fact that different profiling studies reported an increase in miR-21 and miR-146a after MI while miR-1 and miR-499 levels (already highly expressed) showed a more stable expression over time^{24, 32}. Furthermore, levels of miR-146a in UA patients were below the mean level of all ACS patients, which might suggest that miR-146a could be helpful in discriminating NSTEMI from UA patients. Larger diagnostic

studies will be necessary to validate these observations. These differences raise the question whether miRNAs are released on a regular base (i.e. intercellular communication upon stress signals) or simply reflect myocardial damage leading to uncontrolled leakage from damaged myocardium³³.

It was previously reported that miRNAs in serum can be found in exosomes and microvesicular bodies^{34,35}. As their release can be affected by any form of cellular stress, cardiac necrosis is not necessary to evoke this response. This could explain why we observed elevated miRNA levels in patients found to have an ACS whose troponin was negative on initial presentation (i.e. patients with unstable angina pectoris - in whom troponin remains negative by definition - and MI patients presenting too early after symptom onset for troponin to be positive). These observations suggest that miRNAs holds potential to improve the prognosis of both NSTEMI and UA patients who are known to benefit from swift initiation of treatment.

A recent study with a final diagnosis of ACS suggested that circulating miRs provide rather poor prognostic and diagnostic information²¹. However, as this was designed as a prognostic study, a control group consisting of suspected ACS patients, but ultimately not having an ACS, was absent. A very recent study elegantly demonstrated that the transcoronary concentration of several miRs, including miR-499, are increased in patients undergoing catheterization²³. Importantly, our data further extend these reports, as we included non-ACS patients and analyzed blood collected at first presentation. The increase in AUC when adding miRNAs to the current ACS biomarker high-sensitive troponin, the fact that a combination of miRNAs resulted in a higher AUC than high-sensitive troponin, and the AUC of single miRs in the troponin-negative population, underscore the potential diagnostic value of these novel biomarkers in clinical practice. Finally, in a clinical model with important co-variables including age, sex and cardiovascular risk factors, miRNAs were shown to be strong independent predictors of ACS. Importantly, circulating miRs were not significantly correlated with age, hypertension, and cholesterol levels.

Especially three of the investigated miRs (miR-1, miR-499 and miR-21) seem very promising, as their combined diagnostic performance is statistically better than hs-troponin. Furthermore, this miR-combination also led to higher AUC values than the combination of three myocardial necrosis markers (hs-troponin, myoglobin, CK-MB).

Strengths and limitations

The main strength of our study is the evaluation of miRNAs isolated from serum collected immediately upon presentation to the ED in a large group (n=332) of patients, in a clinically relevant setting: i.e. patients suspected of an ACS in whom clinical and ECG findings are inconclusive. Apart from comparing miRNA levels in patients with and without an ACS, we also evaluated the added diagnostic value of miRNA compared to high-sensitive troponin and in a clinical model with relevant co-variables. Importantly, a combination of three miRNAs showed better diagnostic performance than hs-troponin T alone.

Several limitations have to be taken into account. From the original 470 patients, 138 were excluded because of poor RNA integrity indicating that the starting material was not optimal for our analysis; but importantly, the patient characteristic of these 138 patients and the 332 included patients were similar, indicating that this is very unlikely to have changed our

findings. The material was collected in 2007 when optimal methods for processing and storage of serum for miRNAs isolation was largely unknown. Measurement of circulating miRNAs requires RT-PCR, which is currently the limiting factor in terms of rapid detection. However, as miRNAs have clear diagnostic potential, newer and less expensive techniques to detect serum miRNA levels more rapidly can be expected in the near future. This would also facilitate additional research investigating the incremental value of circulating miRs when added to a clinical risk score of ACS like the GRACE Risk Score or HEART score, which might be clinically very relevant³⁶.

Given the inherent limitations of our study, they remain to be confirmed in a larger, prospective, multicenter diagnostic study and in a large independent population of hs-troponin negative patients.

Conclusion

In patients suspected of ACS presenting to the ED within 24 hours of symptom onset, circulating microRNA levels (miR-1, miR-208a, miR-499, miR-21 and miR-146a) are higher in those with an ACS and are already increased in suspected ACS patients with initially negative troponin levels and in those presenting within 3 hours of symptom onset. Addition of miR-1, miR-499 or miR-21 significantly increased the diagnostic value compared to hs-troponin T and these three miRs were independent predictors of ACS. Interestingly, the combination of these three miRs resulted in a higher AUC than hs-troponin T, including the hs-troponin negative patients. These findings demonstrate that circulating miRNAs hold great potential as novel early biomarkers of cardiac injury. MiRNAs might be useful for better management of suspected ACS patients, in particular those with unstable angina pectoris and NSTEMI in whom diagnostic uncertainty is high.

Acknowledgements

We thank Sridevi Jaksani, Sebastian Baars and Krijn Vrijssen (all at the University Medical Center Utrecht, the Netherlands) and Peter Zuithoff (Julius Center for Health Sciences and Primary Care, University Medical Center, Utrecht) for their excellent technical assistance. This work was supported by the Novartis Foundation for Cardiovascular Excellence (JS), a Bekalis price (PD) and "Stichting Swaeneborgh" (MO).

Author contributions

MO, AM, AvM, PD, AH and JS designed, analysed and interpreted and were responsible for drafting the article. MO, AM, MD and EV were responsible data acquisition. All authors critically revised the article and finally approved the manuscript prior to publication.

Supporting Information is available at EMBO Molecular Medicine online.

REFERENCES

1. Thygesen K, Alpert JS, White HD, et al. Universal definition of myocardial infarction. *Circulation* 2007;116:2634-2653.
2. Anderson JL, Adams CD, Antman EM, et al. 2011 ACCF/AHA Focused Update Incorporated Into the ACC/AHA 2007 Guidelines for the Management of Patients With Unstable Angina/Non-ST-Elevation Myocardial Infarction: a report of the American College of Cardiology Foundation/American Heart Association Task Force on Practice Guidelines. *Circulation* 2011;123:e426-e579.
3. Dekker MS, Mosterd A, van 't Hof AW, et al. Novel biochemical markers in suspected acute coronary syndrome: systematic review and critical appraisal. *Heart* 2010;96:1001-1010.
4. Kushner FG, Hand M, Smith SC, Jr., et al. 2009 Focused Updates: ACC/AHA Guidelines for the Management of Patients With ST-Elevation Myocardial Infarction (updating the 2004 Guideline and 2007 Focused Update) and ACC/AHA/SCAI Guidelines on Percutaneous Coronary Intervention (updating the 2005 Guideline and 2007 Focused Update): a report of the American College of Cardiology Foundation/American Heart Association Task Force on Practice Guidelines. *Circulation* 2009;120:2271-2306.
5. Lewis BP, Shih IH, Jones-Rhoades MW, et al. Prediction of mammalian microRNA targets. *Cell* 2003;115:787-798.
6. Sluijter JP, van Mil A, van Vliet P, et al. MicroRNA-1 and -499 regulate differentiation and proliferation in human-derived cardiomyocyte progenitor cells. *Arterioscler Thromb Vasc Biol* 2010;30:859-868.
7. Thum T, Galuppo P, Wolf C, et al. MicroRNAs in the human heart: a clue to fetal gene reprogramming in heart failure. *Circulation* 2007;116:258-267.
8. van Rooij E, Sutherland LB, Liu N, et al. A signature pattern of stress-responsive microRNAs that can evoke cardiac hypertrophy and heart failure. *Proc Natl Acad Sci USA* 2006;103:18255-18260.
9. Mitchell PS, Parkin RK, Kroh EM, et al. Circulating microRNAs as stable blood-based markers for cancer detection. *Proc Natl Acad Sci USA* 2008;105:10513-10518.
10. Chen X, Ba Y, Ma L, et al. Characterization of microRNAs in serum: a novel class of biomarkers for diagnosis of cancer and other diseases. *Cell Res* 2008;18:997-1006.
11. Zampetaki A, Kiechl S, Drozdov I, et al. Plasma microRNA profiling reveals loss of endothelial miR-126 and other microRNAs in type 2 diabetes. *Circ Res* 2010;107:810-817.
12. Ji X, Takahashi R, Hiura Y, et al. Plasma miR-208 as a biomarker of myocardial injury. *Clin Chem* 2009;55:1944-1949.
13. Ai J, Zhang R, Li Y, et al. Circulating microRNA-1 as a potential novel biomarker for acute myocardial infarction. *Biochem Biophys Res Commun* 2010;391:73-77.
14. Wang GK, Zhu JQ, Zhang JT, et al. Circulating microRNA: a novel potential biomarker for early diagnosis of acute myocardial infarction in humans. *Eur Heart J* 2010;31:659-666.
15. Cheng Y, Tan N, Yang J, et al. A translational study of circulating cell-free microRNA-1 in acute myocardial infarction. *Clin Sci (Lond)* 2010;119:87-95.
16. Corsten MF, Dennert R, Jochems S, et al. Circulating MicroRNA-208b and MicroRNA-499 reflect myocardial damage in cardiovascular disease. *Circ Cardiovasc Genet* 2010;3:499-506.
17. Adachi T, Nakanishi M, Otsuka Y, et al. Plasma microRNA 499 as a biomarker of acute myocardial infarction. *Clin Chem* 2010;56:1183-1185.
18. D'Alessandra Y, Devanna P, Limana F, et al. Circulating microRNAs are new and sensitive biomarkers of myocardial infarction. *Eur Heart J* 2010;31:2765-2773.
19. Gidlof O, Andersson P, van der PJ, et al. Cardiospecific microRNA Plasma Levels Correlate with Troponin and Cardiac Function in Patients with ST Elevation Myocardial Infarction, Are Selectively Dependent on Renal Elimination, and Can Be Detected in Urine Samples. *Cardiology* 2011;118:217-226.
20. Kuwabara Y, Ono K, Horie T, et al. Increased MicroRNA-1 and MicroRNA-133a Levels in Serum of Patients With Cardiovascular Disease Indicate Myocardial Damage. *Circ Cardiovasc Genet* 2011;4:446-454.
21. Widera C, Gupta SK, Lorenzen JM, et al. Diagnostic and prognostic impact of six circulating microRNAs in acute coronary syndrome. *J Mol Cell Cardiol* 2011;51:872-875.

22. Olivieri F, Antonicelli R, Lorenzi M, et al. Diagnostic potential of circulating miR-499-5p in elderly patients with acute non ST-elevation myocardial infarction. *Int J Cardiol* 2012.
23. De Rosa S, Fichtlscherer S, Lehmann R, et al. Transcoronary Concentration Gradients of Circulating MicroRNAs. *Circulation* 2011;124:1936-1944.
24. van Rooij E, Sutherland LB, Thatcher JE, et al. Dysregulation of microRNAs after myocardial infarction reveals a role of miR-29 in cardiac fibrosis. *Proc Natl Acad Sci USA* 2008;105:13027-13032.
25. Dong S, Cheng Y, Yang J, et al. MicroRNA expression signature and the role of microRNA-21 in the early phase of acute myocardial infarction. *J Biol Chem* 2009;284:29514-29525.
26. Horie T, Ono K, Nishi H, et al. Acute doxorubicin cardiotoxicity is associated with miR-146a-induced inhibition of the neuregulin-ErbB pathway. *Cardiovasc Res* 2010;87:656-664.
27. Guo M, Mao X, Ji Q, et al. miR-146a in PBMCs modulates Th1 function in patients with acute coronary syndrome. *Immunol Cell Biol* 2010;88:555-564.
28. Patrick DM, Montgomery RL, Qi X, et al. Stress-dependent cardiac remodeling occurs in the absence of microRNA-21 in mice. *J Clin Invest* 2010;120:3912-3916.
29. Thum T, Chau N, Bhat B, et al. Comparison of different miR-21 inhibitor chemistries in a cardiac disease model. *J Clin Invest* 2011;121:461-462.
30. Cheng Y, Liu X, Zhang S, et al. MicroRNA-21 protects against the H(2)O(2)-induced injury on cardiac myocytes via its target gene PDCD4. *J Mol Cell Cardiol* 2009;47:5-14.
31. Zile MR, Mehurg SM, Arroyo JE, et al. Relationship Between The Temporal Profile of Plasma microRNA and Left Ventricular Remodeling In Patients Following Myocardial Infarction. *Circ Cardiovasc Genet* 2011;4:614-619.
32. Roy S, Khanna S, Hussain SR, et al. MicroRNA expression in response to murine myocardial infarction: miR-21 regulates fibroblast metalloprotease-2 via phosphatase and tensin homologue. *Cardiovasc Res* 2009;82:21-29.
33. Gupta SK, Bang C, Thum T. Circulating microRNAs as biomarkers and potential paracrine mediators of cardiovascular disease. *Circ Cardiovasc Genet* 2010;3:484-488.
34. Wang K, Zhang S, Weber J, et al. Export of microRNAs and microRNA-protective protein by mammalian cells. *Nucleic Acids Res* 2010;38:7248-7259.
35. Zampetaki A, Willeit P, Drozdov I, et al. Profiling of circulating microRNAs: from single biomarkers to re-wired networks. *Cardiovasc Res* 2012;93:555-562.
36. Backus BE, Six AJ, Kelder JH, et al. Risk scores for patients with chest pain: evaluation in the emergency department. *Curr Cardiol Rev* 2011;7:2-8.
37. Kroh EM, Parkin RK, Mitchell PS, et al. Analysis of circulating microRNA biomarkers in plasma and serum using quantitative reverse transcription-PCR (qRT-PCR). *Methods* 2010;50:298-301.
38. Tijssen AJ, Creemers EE, Moerland PD, et al. MiR423-5p As a Circulating Biomarker for Heart Failure. *Circulation Research* 2010.
39. Oerlemans MI, Goumans MJ, van Middelaar B, et al. Active Wnt signaling in response to cardiac injury. *Basic Res Cardiol* 2010;105:631-641.
40. Noort WA, Oerlemans MI, Rozemuller H, et al. Human versus porcine mesenchymal stromal cells: phenotype, differentiation potential, immunomodulation and cardiac improvement after transplantation. *J Cell Mol Med* 2011;. In press.
41. Hamm CW, Bassand JP, Agewall S, et al. ESC Guidelines for the management of acute coronary syndromes in patients presenting without persistent ST-segment elevation: The Task Force for the management of acute coronary syndromes (ACS) in patients presenting without persistent ST-segment elevation of the European Society of Cardiology (ESC). *Eur Heart J* 2011;32:2999-3054.
42. Reichlin T, Hochholzer W, Bassetti S, et al. Early diagnosis of myocardial infarction with sensitive cardiac troponin assays. *N Engl J Med* 2009;361:858-867.

SUPPORTING INFORMATION

Table S1 | Correlation of patient characteristics with circulating microRNAs in ACS-suspected patients (n=332)

Characteristic	miR-1		miR-208a		miR-499		miR-21		miR-146a	
	R	P	R	P	R	P	R	P	R	P
Age	0.154	0.12	-0.026	0.63	0.139	0.07	0.071	0.19	0.013	0.82
Gender	0.032	0.55	-0.063	0.25	0.088	0.10	0.032	0.55	-0.026	0.64
Onset of chest pain	0.001	0.99	0.017	0.76	0.034	0.54	-0.051	0.37	-0.073	0.20
Current smoker	0.078	0.15	-0.026	0.63	0.058	0.29	-0.022	0.69	0.050	0.36
Former smoker	0.071	0.19	-0.080	0.15	0.113	0.07	0.045	0.41	-0.055	0.32
Hypertension	-0.003	0.95	-0.080	0.11	-0.129	0.07	0.026	0.64	-0.012	0.83
Hypercholesterolemia	-0.086	0.12	-0.011	0.85	-0.093	0.09	-0.110	0.09	-0.080	0.14
Diabetes Mellitus	0.004	0.94	-0.009	0.87	-0.114	0.07	-0.071	0.19	-0.019	0.73
Body mass index (kg/m ²)	0.013	0.84	-0.013	0.84	-0.019	0.77	0.009	0.89	-0.103	0.11
Family history of CVD	0.124	0.09	0.136	0.07	0.028	0.61	0.011	0.84	-0.077	0.16
History of CVD	0.020	0.72	-0.035	0.52	-0.067	0.21	0.028	0.60	0.004	0.94

Correlation given as Spearman's correlation coefficient (R), CVD = cardiovascular disease;

Table S2 | Correlation of antiplatelet or heparin therapy with circulating microRNAs in ACS-suspected patients (n=332)

Therapy	miR-1		miR-208a		miR-499		miR-21		miR-146a	
	R	P	R	P	R	P	R	P	R	P
Aspirin	0.16	0.11	-0.03	0.79	0.08	0.41	-0.18	0.08	-0.10	0.06
Clopidogrel	0.11	0.27	-0.19	0.06	-0.06	0.57	-0.14	0.17	-0.11	0.26
Heparin	0.04	0.69	0.09	0.39	-0.10	0.34	-0.05	0.60	0.03	0.78

Correlation given as Spearman's correlation coefficient (R);

Table S3 | AUCs and Odds Ratios of miRNAs in suspected ACS patients with symptom onset <3 hours in a clinical model (n=152)

Marker	AUC	95% CI	OR†	95% CI
Clinical model (CM)	0.78	0.71-0.85	NA	NA
CM + Cardiac troponin	0.88	0.83-0.94	NA	NA
CM + Cardiac hs-troponin T	0.89	0.84-0.94	NA	NA
CM + Cardiac hs-troponin T with:				
miR-1	0.92 ^a	0.88-0.96	1.27	1.10-1.47
miR-208a	0.90	0.86-0.95	1.28	1.07-1.54
miR-499	0.92 ^b	0.88-0.96	1.32	1.15-1.52
miR-21	0.92 ^b	0.88-0.96	1.27	1.13-1.44
miR-146a	0.90	0.85-0.95	1.12	1.00-1.21
miR-1 + miR-499 + miR-21	0.94 ^b	0.90-0.98	NA	NA

CM = Clinical model (age, sex, hypertension, hypercholesterolemia, family history, current and former smoking, diabetes mellitus, and history of myocardial infarction, PCI or coronary bypass surgery); AUC = Area AUC = Area under the ROC Curve; 95% CI = 95% Confidence Interval; ^aP=0.004, ^bP<0.001 *versus* hs-troponin T; NA = not applicable; † Adjusted for clinical model and cardiac hs-troponin T.

Table S4 | Diagnostic value the combined miRs and myocardial necrosis markers in suspected ACS patients (n=332)

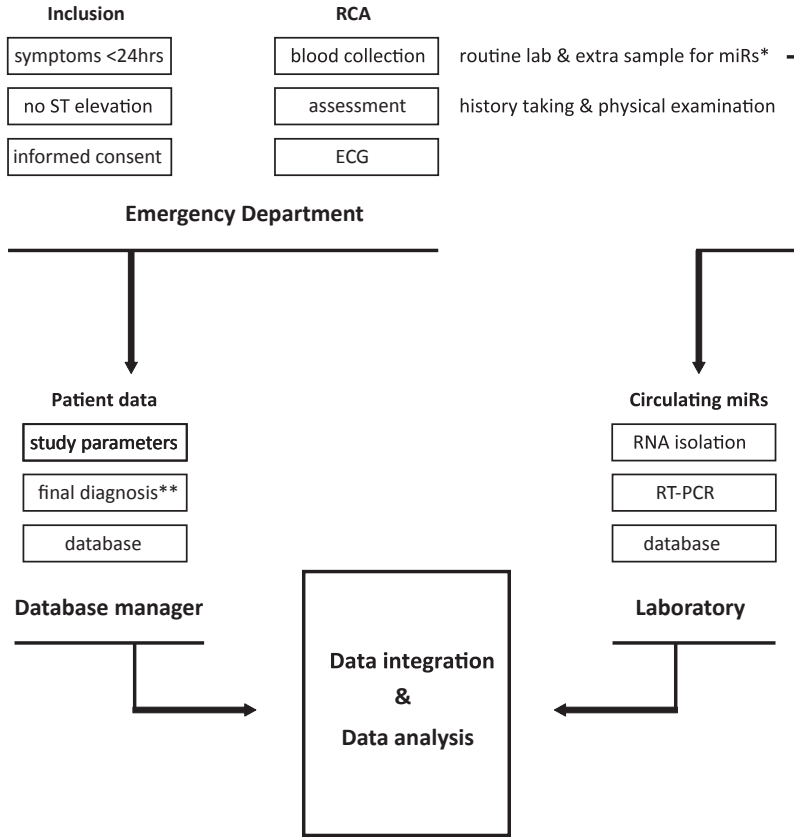
Marker	All patients (n=332)		Hs-troponin negative patients (n=194)		Patients with symptoms <3 hours (n=152)	
	AUC	95% CI	AUC	95% CI	AUC	95% CI
Myoglobin/CK-MB/hs-troponin T	0.87	0.83-0.92	0.87	0.81-0.94	0.89	0.84-0.95
miR-1/ miR-499/miR-21	0.89	0.86-0.93	0.94	0.90-0.99	0.92	0.88-0.97
P	0.41		0.001		0.07	

AUC = Area under the ROC Curve; CK-MB = MB fraction of creatine kinase; 95% CI = 95% Confidence Interval; P value *versus* myoglobin/CK-MB/hs-troponin T.

Table S5 | Patient Characteristics of included *versus* excluded Patients With Chest Pain

Characteristic	Excluded (n=138)	Included (n=332)	P
N (%)	138 (29.4)	332 (70.6)	
Age (yrs)	61.7±14.9	62.9±14.4	0.42
Male sex (% male)	73 (53.5)	190 (57.2)	0.44
Onset of chest pain, median (IQR)	3.2 (2.0-6.7)	3.2 (1.8-8.0)	0.89
Risk factors			
Current smoker	39 (28.2%)	86 (26.1)	0.45
Former smoker	34 (24.6%)	103 (31.5)	0.11
Hypertension	57 (41.3)	151 (45.8)	0.25
Hypercholesterolemia	42 (30.4%)	109 (33.0)	0.42
Diabetes Mellitus	22 (15.9%)	52 (15.8)	0.90
Body mass index (kg/m ²)	26.7±4.8	26.3±5.8	0.69
Parental CVD	50 (36.2%)	133 (40.7)	0.24
History of CVD	67 (48.6%)	159 (47.9)	0.91
Cardiac Troponin I (µg/L)	0.03 (0.02-0.04)	0.03 (0.02-0.05)	0.83
Cardiac hs-Troponin T (pg/mL)	5.3 (2.8-18.2)	6.0 (2.2-18.7)	0.77

Data presented as mean±SD for age, body mass index and as median (25th – 75th interquartile range) for onset of chest pain and cardiac troponin levels. All other variables are presented as n (%); ACS = acute coronary syndrome; CVD = cardiovascular disease; P value excluded *versus* included patients with chest pain, based on RNA quality. Mann-Whitney (continuous variables) or χ^2 test (categorical variables).



RCA = routine clinical assessment
 *collected at presentation; **by expert panel based on all available clinical data

Figure S1 | Overview of patient inclusion, blood collection and quantification of circulating miRs

2

3



Martinus I.F.J. Oerlemans¹

Alain van Mil^{1,2}

Jia Liu^{1,3}

Esther van Eeuwijk¹

Krista den Ouden¹

Pieter A. Doevendans^{1,2}

Joost P.G. Sluijter^{1,2}

¹ Department of Cardiology, University Medical Center Utrecht, the Netherlands.

² ICIN Netherlands Heart Institute, Utrecht, the Netherlands.

³ Department of Endocrinology, Provincial Hospital Affiliated to Shandong University, Jinan, China

Inhibition of miR-223 reduces inflammation but not adverse cardiac remodelling after myocardial ischemia-reperfusion *in vivo*

Accepted for publication in Discovery Biology and Medicine

ABSTRACT

Background

Coronary artery occlusion results in ischemic heart tissue and subsequent death of cardiomyocytes, followed by an inflammatory response to clear the infarcted area from dead cells. Invading inflammatory cells are suggested to contribute to myocardial ischemia-reperfusion (I/R) injury and adverse remodelling. Given the importance of the inflammatory phase during cardiac wound healing, better understanding is needed to develop novel interventions. In the present study, we investigated the role of the inflammatory-related miR-223 in the ischemic heart. Furthermore, we determined the effect of miR-223 modulation on inflammation and cardiac remodelling in a mouse model of myocardial I/R.

Methods and Results

Mice underwent 30 minutes of ischemia and received, 5 minutes before reperfusion, 8mg/kg antagomiR-223 or mismatch-miR treatment, and consecutive injections at day 1 and 2 post-I/R. MiR-223 expression significantly increased 1 and 3 days after I/R, corresponding with the inflammatory phase upon cardiac injury. MiR-223 expression mainly increased in myocytes, as confirmed by *in situ* hybridization and *in vitro* stimulation of isolated cardiomyocytes. Inhibition of miR-223 by antagomir treatment significantly reduced total leukocyte (CD45+ cells) and macrophages (Mac-3+ cells) influx at 3 days of reperfusion, as quantified by immunohistochemistry. By using magnetic resonance imaging (MRI), cardiac dimensions and function were assessed before and 28 days after surgery. End-diastolic volume (EDV) and end-systolic volume (ESV) showed a similar increase in both treatment groups, as well as a comparable decline in ejection fraction (EF) post-I/R.

Conclusion

Although inhibition of miR-223 resulted in less inflammatory influx after reperfusion, this did not lead to less adverse cardiac remodelling. More research on the complex temporal and spatial role of miR-223 during the process of myocardial wound healing is necessary in order to understand the role of miR-223 upon I/R injury and whether it can be used as a novel therapeutic strategy.

INTRODUCTION

Acute myocardial infarction (MI) remains one of the leading causes of morbidity and mortality in the western world¹. Coronary artery occlusion results in ischemic heart tissue and subsequent death of cardiomyocytes, followed by an inflammatory response to clear the infarct from dead cells^{2, 3}. Currently, the most effective therapy to salvage dying myocytes is early reperfusion, although reperfusion itself also leads to additional damage known as myocardial ischemia-reperfusion (I/R) injury⁴. Although the exact mechanism still remains to be established, generation of reactive oxygen species (ROS) by local endogenous cells and a rapid influx of inflammatory cells and cytokines seems to play an important role⁵. Consequently, the role of inflammatory cells and its cytokine production in infarct healing has been investigated thoroughly during the last decades as extensively reviewed elsewhere⁶. Unfortunately, therapeutic interventions did not lead to desirable results, mostly due to the complex spatial and temporal role of inflammation during the process of myocardial wound healing⁷. Given the importance of the inflammatory phase during cardiac wound healing, better understanding as well as novel interventions still need to be explored.

MicroRNAs (miRNAs) are short, non-coding small RNAs that regulate the expression of proteins by translational repression or degradation of messenger RNAs (mRNAs)⁸. Over the last few years it has become clear that miRNAs play a crucial role in cardiac development and homeostasis and that miRNA expression is altered in the diseased heart⁹⁻¹¹. Not surprisingly, miRNAs are increasingly seen as master regulators of many processes, including immune cell function and inflammation¹².

To examine the role of miRNAs during wound healing in the heart, we profiled the expression of several miRNAs after I/R injury. One interesting candidate was miR-223. Interestingly, this miRNA is considered to play a role in insulin metabolism¹³, coronary artery disease¹⁴, hypercholesterolemia¹⁵, and importantly, in the regulation of neutrophil and macrophage response to inflammatory stimuli¹⁶.

In the present study, we demonstrate that miR-223 is differentially expressed during the inflammatory phase after cardiac ischemia. Furthermore, we determined the effect of miR-223 inhibition on inflammation and cardiac remodelling in a mouse model of myocardial I/R.

METHODS

This study was approved by the Animal Ethical Experimentation Committee (Utrecht University) and was carried out in accordance with the *Guide for the Care and Use of Laboratory Animals*.

Murine Model of Myocardial Ischemia-Reperfusion

Male C57Bl/6 mice (10-12 weeks, Harlan Laboratories) underwent left coronary artery (LCA) ligation as previously described^{17, 18}, followed by reperfusion. Briefly, mice were anesthetized with fentanyl (0.05 mg/kg), midazolam (5 mg/kg), and medetomidine (0.5 mg/kg) through an intraperitoneal (ip) injection, and the adequacy of anaesthesia was monitored by

disappearance of the pedal withdrawal reflex. Mice were ventilated with 100% oxygen, maintaining a core body temperature of 37°C. The LCA was ligated just below the left atrial appendage for 30 minutes with an 8-0 Ethilon monofil suture, including a piece of soft tubing. Reperfusion was initiated by releasing the ligature and removal of the tubing, leaving a piece of suture in place. The chest wall was closed in layers and the animals received atipamezole (2.5 mg/kg ip), flumazenil (0.5 mg/kg ip), and temgesic (0.1 mg/kg ip) for pain killing. After detubation, mice were kept warm until fully recovered. At different times, mice were sacrificed using a cocktail of ketamine (100mg/kg ip) and medetomidine (8mg/ml), followed by cardiac explantation.

Micro-Array

After myocardial ischemia-reperfusion, total RNA was isolated with the mirVana RNA Isolation Kit (Ambion). MiRNA expression profile was determined by microarray using the Paraflo microfluidic chip (MiHuman_8.2, LC Sciences), according to the manufacturer, and validated with Taqman MicroRNA Assays (Applied Biosystems).

Quantitative RT-PCR of miRNAs

Total RNA was isolated from cells, total left ventricle (LV), or other organs using TriPure Isolation Reagent (Roche Applied Science, Penzberg, Germany). Ten nanogram DNA-free RNA was used for miRNA-specific (miR-223; assay ID 002295, Applied Biosystems) reverse transcription and subsequent amplification and detection in a MyIQ single-colour quantitative real time polymerase chain reaction (qRT-PCR) system (Bio-Rad, Hercules, CA) as described previously¹⁹. After normalization against the small nuclear RNA RNU19 (assay ID 001003, Applied Biosystems), the relative difference in expression levels was calculated and presented as fold induction ($2^{\Delta\Delta Ct}$).

Isolation of Neonatal Mouse Cardiomyocytes

Neonatal mouse cardiomyocytes were isolated and cultured as reported previously²⁰. Briefly, after termination by decapitation, five 1-3 days old mouse hearts were cut into small pieces and digested by 0.5% trypsin to form a single cell suspension. This suspension was incubated another 5 minutes in a stirring water bath at 37°C, which was repeated three times after washing in Dulbecco's modified Eagle's medium (DMEM) (Gibco, Carlsbad), supplemented with 20% fetal calf serum (FCS) (Gibco). After resuspending the cell pellet in culture medium of DMEM with 20% FCS, 5% horse serum (Gibco), penicillin (100 U/ml), and streptomycin (100 mg/ml), cells were pre-plated in an uncoated dish for 2.5 hours, replated in 1% gelatine at a density of 1.5×10^5 cells/cm² and left to attach over night at 37°C before any experiment was started.

Cardiomyocyte Viability Assay

Neonatal mouse cardiomyocytes were pre-incubated with culture medium (DMEM with penicillin and streptomycin) without serum for one hour and challenged with 50 μ M H₂O₂ or DMSO (control) for 18 hours, after which the cells were washed and dissolved in TriPure Isolation Reagent (Roche Applied Science, Penzberg, Germany) and stored at -80°C.

Antagomirs

Antagomirs were designed as previously described and custom synthesized (VBC Biotech, Vienna, Austria)²¹. Antagomir sequences used were: antagomir-223 (5'-ugggguauuugacaaacugaca-3'), and antagomir-mismatch-ctrl (5'-uggcguaucugucauacagaaa-3'). The mismatch control antagomir (ctrl-antagomir) contained 6 mismatches, all antagomirs were 3' cholesterol-modificated, 2'O-methylated, and contained PTO-linkages at the first two and last four nucleotides. The mismatch control antagomir did not target any other known miRNAs.

Antagomir Treatment

Mice underwent intravenous (tail vein) injections of 8 mg/kg body weight antagomir 5 min prior to reperfusion and 1 and 2 days later. The efficiency of miRNA knockdown was confirmed by TaqMan MicroRNA Assay either 3 (short term follow-up) or 28 days (long term follow-up) after initial injection.

Magnetic Resonance Imaging

Mice underwent serial assessment of cardiac dimensions and function by magnetic resonance imaging (9.4T MRI; Bruker, Germany) under isoflurane anaesthesia before and 28 days after surgery (n=7/group) as described previously²². LV function and geometry was assessed by a blinded observer. All MRI data were analyzed with Qmass digital imaging software (Medis, Leiden, the Netherlands).

In Situ Hybridization

In situ hybridization was performed to determine hsa-miR-223 localization as described previously¹⁹. Briefly, ten μm thick cryosections were hybridized O/N at 46 °C with 5 nM LNA DIG-labelled probes (Scramble-miR, Exiqon, 99001-01 and hsa-miR-499, Exiqon, 38500-01) in denaturizing hybridization buffer, incubated with an anti-DIG-alkaline phosphatase antibody (1:1500, Roche 11093274910), an anti-troponin antibody (Sigma) at RT for 2 hours. After washing, sections were incubated with fluorescent-labelled secondary antibodies, exposed to Fast-Red Substrate-Chromogen (DAKO, K0597) O/N at RT and mounted in VectaShield (Molecular Probes, Amsterdam).

Immunohistochemistry and Histology

After termination at 3 days post-IR, hearts were flushed with 0.9% saline, explanted and snap-frozen in liquid nitrogen. Frozen heart sections of 7 μm were stained for neutrophils (rat anti-mouse Ly6G, BD Pharmingen 551459) and macrophages (rat anti-mouse Mac-3, BD Pharmingen 553322). Secondary antibody used was goat anti-rat IgG (Southern Biotech, 3052-08) followed by HRPO-coupled streptavidine (Southern Biotech, 7100-05), using 3-Amino-9-ethyl carbazole (AEC) for visualisation.

Statistical analysis

Data are presented as mean \pm SEM. Differences between groups were analyzed using ANOVA with Bonferroni correction or Mann-Whitney U test when appropriate. All tests were two-sided, using a significance level of $P < 0.05$ (SPSS Statistics v17 Chicago, United States).

RESULTS

MiR-223 expression is increased after ischemia-reperfusion *in vivo*

To examine the role of miRNAs during wound healing in the heart, we performed a micro-array on several miRNAs after cardiac I/R injury (data not shown). Interestingly, miR-223 showed increased levels after 1 and 3 days post I/R compared to baseline (Figure 1A). At 10 days, miR-223 levels were almost returned to basal levels. Micro-array data on miR-223 was validated using RT-PCR, showing a significant increase after 1 and 3 days, corresponding with the inflammatory phase after cardiac injury³ (Figure 1B).

Furthermore, we determined the tissue expression of miR-223 in the heart compared to other mouse organs. MiR-223 expression was most obvious in spleen and lung tissue, which contain large numbers of monocytes and alveolar macrophages, respectively (Figure 1C). MiR-223 levels were the lowest in brain tissue and moderately expressed in skeletal muscle and liver.

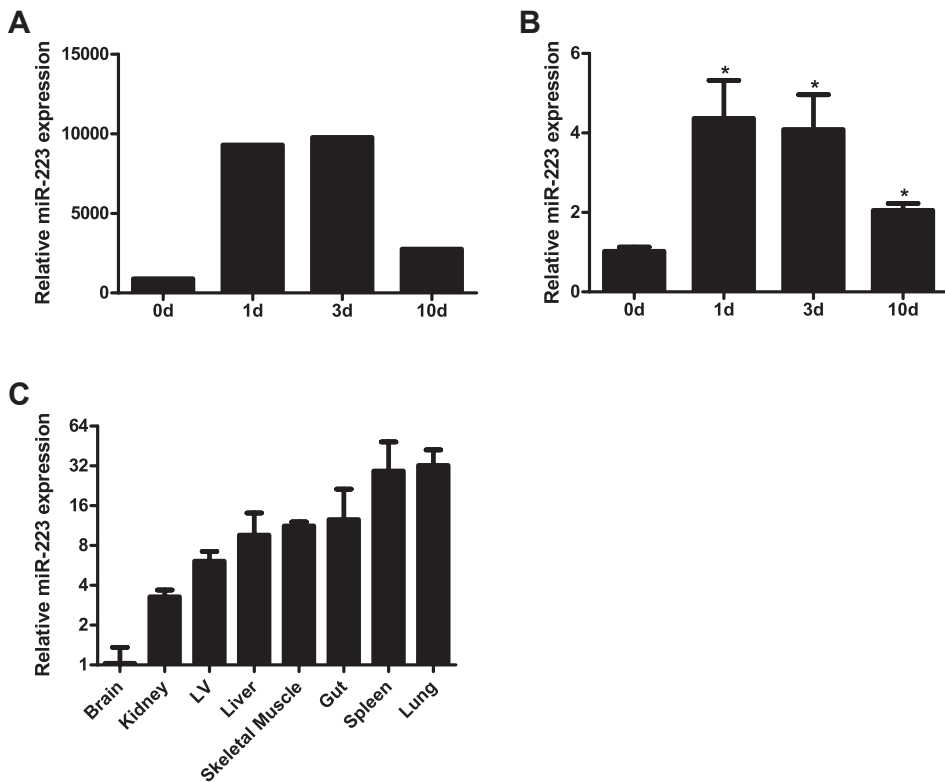


Figure 1 | MiR-223 expression is increased after ischemia-reperfusion *in vivo*

Micro-array data showing miR-223 expression after ischemia-reperfusion (A). MiR-223 levels increased significantly at 1 and 3 days after ischemia-reperfusion ($n=3/\text{group}$, $*P<0.05$ compared to baseline), as validated by RT-PCR (B). When compared to the heart, miR-223 levels are highly expressed in lung and spleen (C).

Mir-223 is highly expressed in cardiomyocytes after ischemia-reperfusion *in vivo*

We performed *in situ* hybridization to determine in which cells miR-223 was localized. At baseline, only a small number of cells showed peri-nuclear staining for miR-223 (Figure 2A), which was comparable with the remote area three days post-I/R (Figure 2B). However, miR-223 staining was markedly increased in the border zone (Figure 2C) in cardiomyocytes predominantly and to a lesser extent in non-myocytes. *In situ* hybridization of the negative control (scramble-miR) did not result in any staining of the border zone (Figure 2D).

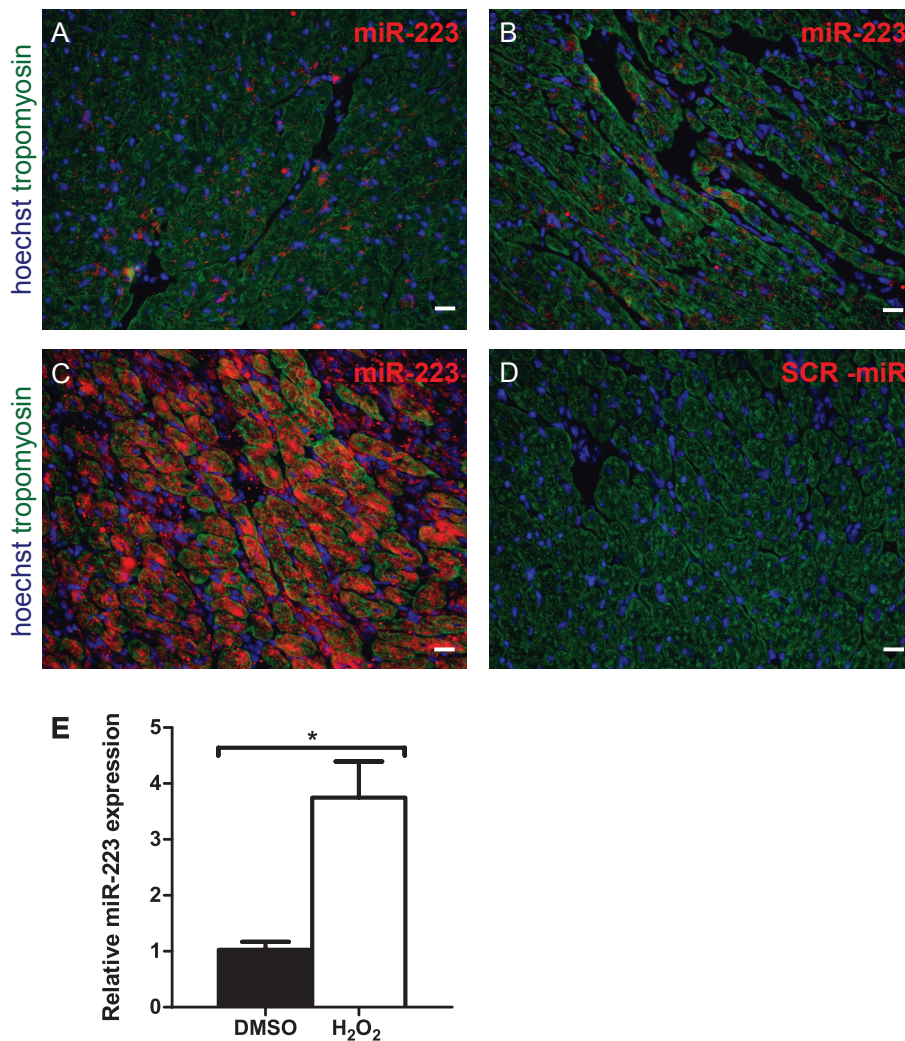


Figure 2 | Mir-223 is highly expressed in cardiomyocytes after ischemia-reperfusion *in vivo*

Representative *in situ* hybridization pictures of myocardial miR-223 (red) at baseline combined with tropomyosin (green) and nuclear (Hoechst, blue) staining (A). Remote area (B), border zone (C) and Scramble (SCR) – miR negative control (D) after 3 days of reperfusion (scale bar 20µm). (E) Quantification of miR-223 expression in neonatal mouse cardiomyocytes under oxidative stress after stimulation with H₂O₂ (n=4/group, *P<0.05).

To verify whether the increased expression of miR-223 could result from stressed cardiomyocytes rather than from invading inflammatory cells, freshly isolated neonatal mouse cardiomyocytes were challenged by H₂O₂ stimulation to assess the effect of oxidative stress. Compared to normal conditions, oxidative stress resulted in a 3.75 fold increase of miR-223 expression, as quantified by RT-PCR (Figure 2E, P<0.05).

Inhibition of miR-223 reduced inflammatory cell influx after myocardial I/R *in vivo*

Considering the increased miR-223 expression after I/R, we investigated the effect of its modulation *in vivo* using an antagomir or a mismatch (scramble-miR) control. As a first step, we determined miR-223 levels, by RT-PCR after a three day inhibition protocol in several organs, including the heart. Mice treated with antagomir-223 displayed a significant reduction of miR-223 expression after 3 days of the initial injection of almost 100% (Figure 3A).

As our previous results showed that miR-223 mainly increased during the inflammatory phase after I/R, we studied whether its inhibition influenced the influx of inflammatory cells. Antagomir-treated animals showed a reduction of leukocyte influx compared to mismatch treatment as quantified by CD45 staining (Figure 3B-C, P<0.05). In accordance with a reduction of total inflammatory influx, antagomir treatment significantly reduced macrophage influx at 3 days of reperfusion as well (Figure 3D-E).

Inhibition of miR-223 does not influence adverse remodelling after myocardial I/R *in vivo*

Invading leukocytes contribute to myocardial I/R injury and adverse remodelling^{23, 24}. Since inhibition of miR-223 inhibited the inflammatory influx into the myocardium, we assessed the effect of antagomir treatment on cardiac function and remodelling. End-diastolic volume (EDV) and end-systolic volume (ESV) of both treatment groups increased significantly after myocardial I/R at 28 days (Figure 4A-B). Antagomir administration did not preserve LV volumes compared to mismatch treatment. As a consequence, the decline in ejection fraction (EF) post-I/R was similar in both the treatment groups (Figure 4C). PCR revealed that miR-223 knockdown was still achieved at 28 days after the antagomir injections (Figure 4D).

DISCUSSION

In this study, we have demonstrated that miR-223 increased after myocardial I/R *in vivo*, particularly in cardiomyocytes during day 1 and 3, which was confirmed by *in situ* hybridization and mimicked in *in vitro* experiments. Furthermore, we were able to inhibit miR-223 using an antagomir resulting in an ~ 99% knockdown *in vivo*. Inhibition of miR-223 reduced the influx of inflammatory cells and macrophages in the myocardium after I/R, but did not lead to a long term functional benefit in terms of cardiac function.

Initial reports on miR-223 function were mostly related to a role in granulocyte and monocyte maturation and differentiation^{25, 26}. Yu et al. were one of the first suggesting a role for miR-223 in ischemic disease, reporting an increase if miR-223 expression after

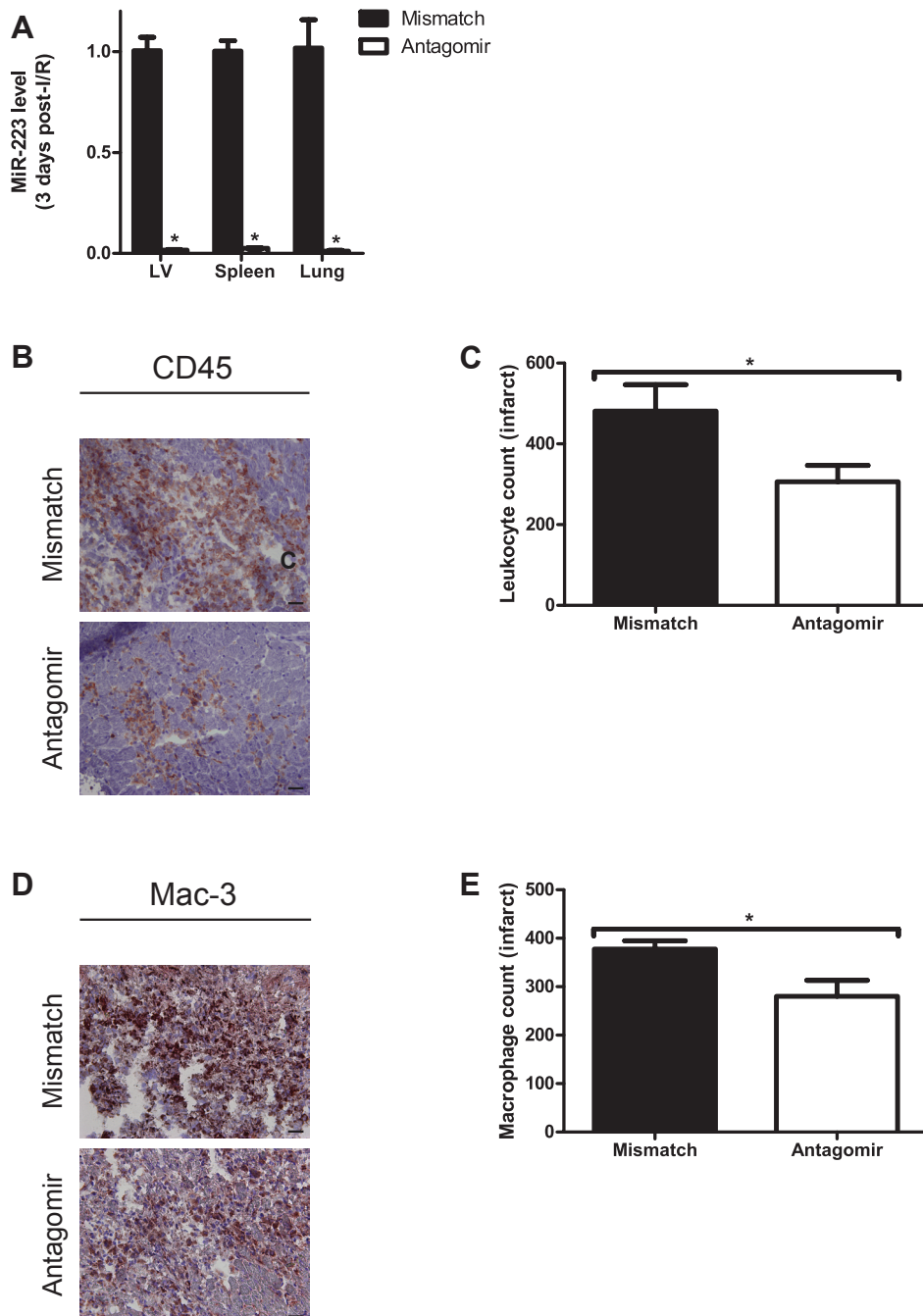


Figure 3 | Effect of miR-223 inhibition on inflammatory cell influx

(A) Antagomir treatment resulted in a 99% reduction of miR-223 at 3 days after the initial injection. Representative pictures (B) and quantification (C) of total inflammatory cell influx (CD45 staining, brown) 3 days after I/R (n=6/group, *P<0.05; scale bar 20µm). Representative pictures (D) and quantification (E) of macrophages (Mac-3 staining, brown) 3 days after I/R (n=6/group, *P<0.05; scale bar 20µm).

hepatic I/R injury²⁷, which was followed by reports showing increased miR-223 expression in Duchenne muscle dystrophy and spinal cord injury, including co-expression on invading neutrophils²⁸⁻³⁰. Cardiac miR-223 levels were previously shown to be increased in left ventricle biopsies of patients with type 2 diabetes, positively regulating Glut4 expression on cardiomyocytes¹³.

In line with a previous report investigating miRNA changes in a mouse model of permanent coronary artery occlusion³¹, we report increased levels of miR-223 after cardiac I/R. Interestingly, this was most obvious in the cardiomyocytes themselves. During myocardial infarction and cardiac ischemia, it was suggested that increased glucose uptake could lead to the activation of Akt leading to BAD-phosphorylation and subsequently to an increase in cell survival³². As miR-223 was suggested to increase GLUT4 expression¹³, increased myocardial miR-223 levels might lead to increased glucose uptake, thereby promoting cell survival.

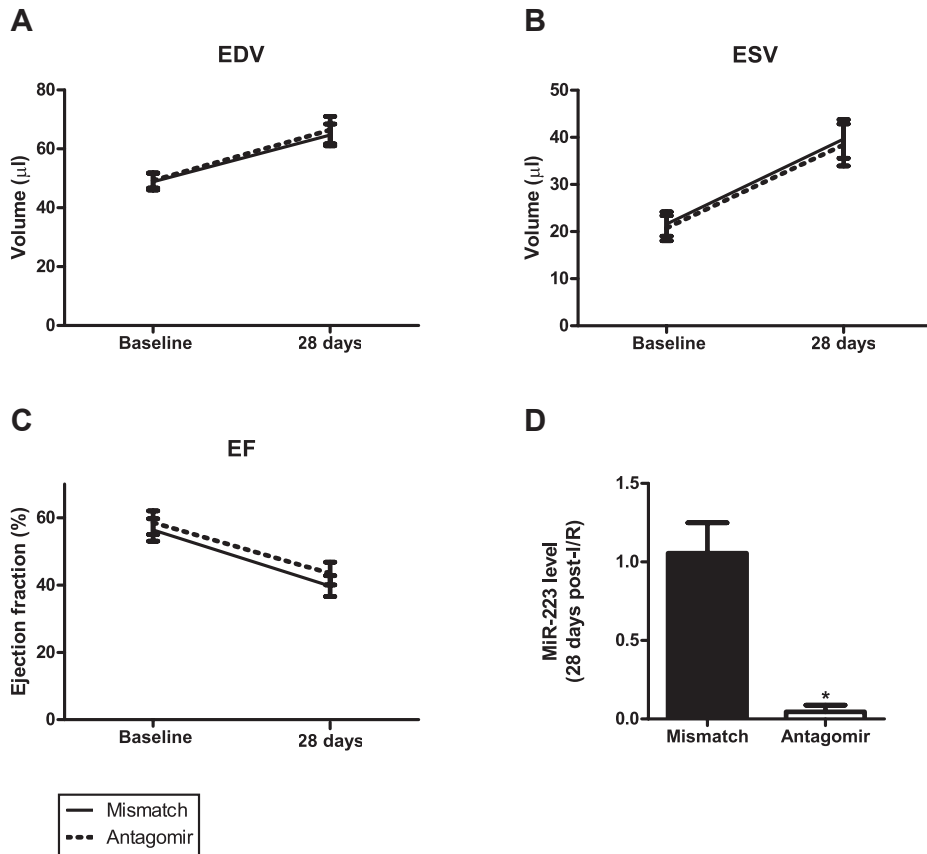


Figure 4 | Cardiac geometry and function

Antagomir and mismatch treatment resulted in a similar increase in EDV (A) and ESV (B), as well as a decline in ejection fraction (C) after I/R (n=7/group). After antagomir treatment, miR-223 levels were still significantly lower at 28 days post-I/R (D), (n=5/group, *P<0.05).

It was shown previously that neutrophils lacking miR-223 have an increased oxidative burst making them more effective against hostile pathogens, showing that miR-223 negatively regulates their activation²⁵. Very recently, it was reported that mice with a total miR-223 knock-out developed a more pro-inflammatory macrophage programme, increasing M1 subtype macrophages and leading to an increased inflammatory response³³. Although we used a model of cardiac ischemia, our results demonstrate that miR-223 inhibition leads to decreased levels of leukocytes and especially macrophages. Although we did not further characterize the subtype of macrophages, miR-223 modulation neither improved nor led to a further decline in long-term cardiac performance compared to control animals. One explanation could be that the inhibitory effect was long-lasting where temporal inhibition in the early inflammatory phase could be beneficial.

It remains to be seen whether miR-223 modulation can lead to functional improvements after cardiac I/R as several questions need to be addressed first. As with previous attempts to modulate the process of inflammation after myocardial I/R, close attention must be paid to the spatial and temporal role of miR-223 during the process of myocardial wound healing. It could well be that the effect of miR-223 modulation on cardiomyocytes (i.e. inhibition leading to increased survival) is opposite to the effect on inflammatory cells (i.e. inhibition leading to a more pro-inflammatory subset). Although preliminary, the results from the above study suggest that general miR-223 inhibition after ischemia-reperfusion, involving many cell types in a period that exceeds the inflammatory phase, will not lead to a net beneficial effect in the ischemic heart. More in depth studies on the complex temporal and spatial role of miR-223 during the process of myocardial wound healing seems necessary in order to translate this interesting concept into a novel therapeutic strategy.

Funding

This work was supported by the Novartis Foundation for Cardiovascular Excellence (JS), a Bekalis price (PD), and "Stichting Swaeneborgh" (MO).

Acknowledgements

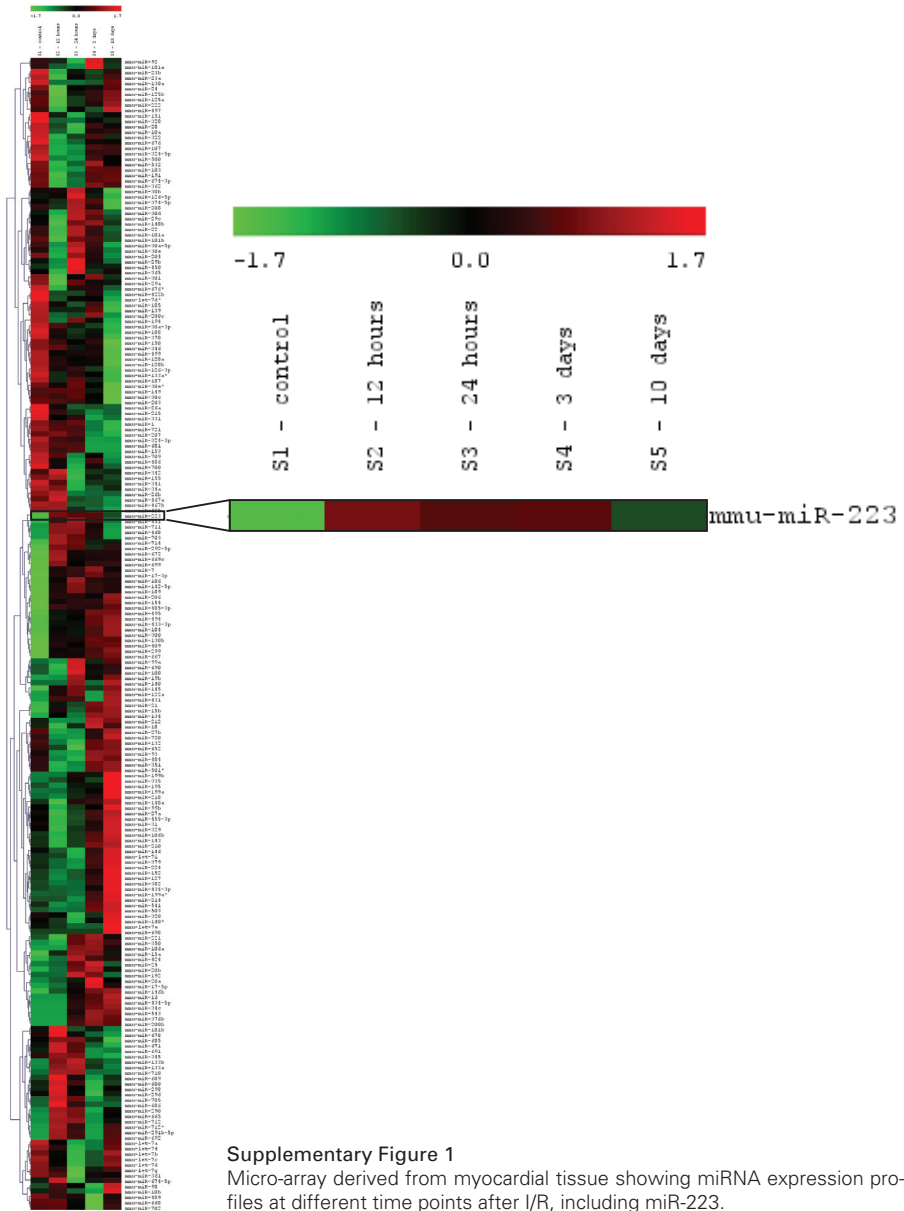
We thank the following persons for their excellent assistance: Esther van Eeuwijk, Corina Metz and Arjan Schoneveld (all at the University Medical Center Utrecht, the Netherlands).

REFERENCES

1. Lloyd-Jones D, Adams RJ, Brown TM, et al. Heart disease and stroke statistics--2010 update: a report from the American Heart Association. *Circulation* 2010;121:e46-e215.
2. Frantz S, Bauersachs J, Ertl G. Post-infarct remodelling: contribution of wound healing and inflammation. *Cardiovasc Res* 2009;81:474-481.
3. Cleutjens JP, Blankesteyn WM, Daemen MJ, et al. The infarcted myocardium: simply dead tissue, or a lively target for therapeutic interventions. *Cardiovasc Res* 1999;44:232-241.
4. Oerlemans MI, Koudstaal S, Chamuleau SA, et al. Targeting cell death in the reperfused heart: Pharmacological approaches for cardioprotection. *Int J Cardiol* 2012.
5. Yellon DM, Hausenloy DJ. Myocardial reperfusion injury. *N Engl J Med* 2007;357:1121-1135.
6. Frangogiannis NG. Regulation of the inflammatory response in cardiac repair. *Circ Res* 2012;110:159-173.
7. Frangogiannis NG. Targeting the inflammatory response in healing myocardial infarcts. *Curr Med Chem* 2006;13:1877-1893.
8. Lewis BP, Shih IH, Jones-Rhoades MW, et al. Prediction of mammalian microRNA targets. *Cell* 2003;115:787-798.
9. Sluijter JP, van Mil A, van Vliet P, et al. MicroRNA-1 and -499 regulate differentiation and proliferation in human-derived cardiomyocyte progenitor cells. *Arterioscler Thromb Vasc Biol* 2010;30:859-868.
10. Thum T, Galuppo P, Wolf C, et al. MicroRNAs in the human heart: a clue to fetal gene reprogramming in heart failure. *Circulation* 2007;116:258-267.
11. van Rooij E, Sutherland LB, Liu N, et al. A signature pattern of stress-responsive microRNAs that can evoke cardiac hypertrophy and heart failure. *Proc Natl Acad Sci USA* 2006;103:18255-18260.
12. O'Connell RM, Zhao JL, Rao DS. MicroRNA function in myeloid biology. *Blood* 2011;118:2960-2969.
13. Lu H, Buchan RJ, Cook SA. MicroRNA-223 regulates Glut4 expression and cardiomyocyte glucose metabolism. *Cardiovasc Res* 2010;86:410-420.
14. Zampetaki A, Kiechl S, Drozdov I, et al. Plasma microRNA profiling reveals loss of endothelial miR-126 and other microRNAs in type 2 diabetes. *Circ Res* 2010;107:810-817.
15. Vickers KC, Palmisano BT, Shoucri BM, et al. MicroRNAs are transported in plasma and delivered to recipient cells by high-density lipoproteins. *Nat Cell Biol* 2011;13:423-433.
16. Schroen B, Heymans S. Small but smart--microRNAs in the centre of inflammatory processes during cardiovascular diseases, the metabolic syndrome, and ageing. *Cardiovasc Res* 2012;93:605-613.
17. Oerlemans MI, Goumans MJ, van Middelaar BJ, et al. Active Wnt signaling in response to cardiac injury. *Basic Res Cardiol* 2010;105:631-641.
18. Oerlemans MI, Liu J, Arslan F, et al. Inhibition of RIP1-dependent necrosis prevents adverse cardiac remodeling after myocardial ischemia-reperfusion in vivo. *Basic Res Cardiol* 2012;270-282.
19. van Mil A, Grundmann S, Goumans MJ, et al. MicroRNA-214 inhibits angiogenesis by targeting Quaking and reducing angiogenic growth factor release. *Cardiovasc Res* 2012;93:655-665.
20. Sreejit P, Kumar S, Verma RS. An improved protocol for primary culture of cardiomyocyte from neonatal mice. *In Vitro Cell Dev Biol Anim* 2008;44:45-50.
21. Krutzfeldt J, Rajewsky N, Braich R, et al. Silencing of microRNAs in vivo with 'antagomirs'. *Nature* 2005;438:685-689.
22. Noort WA, Oerlemans MI, Rozemuller H, et al. Human versus porcine mesenchymal stromal cells: phenotype, differentiation potential, immunomodulation and cardiac improvement after transplantation. *J Cell Mol Med* 2011.
23. Yellon DM, Hausenloy DJ. Myocardial reperfusion injury. *N Engl J Med* 2007;357:1121-1135.
24. Oerlemans MI, Koudstaal S, Chamuleau SA, et al. Targeting cell death in the reperfused heart: Pharmacological approaches for cardioprotection. *Int J Cardiol* 2012; Epub ahead of print..
25. Johnnidis JB, Harris MH, Wheeler RT, et al. Regulation of progenitor cell proliferation and granulocyte function by microRNA-223. *Nature* 2008;451:1125-1129.

26. Fazi F, Rosa A, Fatica A, et al. A minicircuitry comprised of microRNA-223 and transcription factors NFIA and C/EBPalpha regulates human granulopoiesis. *Cell* 2005;123:819-831.
27. Yu CH, Xu CF, Li YM. Association of MicroRNA-223 expression with hepatic ischemia/reperfusion injury in mice. *Dig Dis Sci* 2009;54:2362-2366.
28. Greco S, De SM, Colussi C, et al. Common micro-RNA signature in skeletal muscle damage and regeneration induced by Duchenne muscular dystrophy and acute ischemia. *FASEB J* 2009;23:3335-3346.
29. Nakanishi K, Nakasa T, Tanaka N, et al. Responses of microRNAs 124a and 223 following spinal cord injury in mice. *Spinal Cord* 2010;48:192-196.
30. Izumi B, Nakasa T, Tanaka N, et al. MicroRNA-223 expression in neutrophils in the early phase of secondary damage after spinal cord injury. *Neurosci Lett* 2011;492:114-118.
31. van Rooij E, Sutherland LB, Thatcher JE, et al. Dysregulation of microRNAs after myocardial infarction reveals a role of miR-29 in cardiac fibrosis. *Proc Natl Acad Sci USA* 2008;105:13027-13032.
32. Kalra BS, Roy V. Efficacy of metabolic modulators in ischemic heart disease: an overview. *J Clin Pharmacol* 2012;52:292-305.
33. Zhuang G, Meng C, Guo X, et al. A Novel Regulator of Macrophage Activation: miR-223 in Obesity Associated Adipose Tissue Inflammation. *Circulation* 2012.

SUPPLEMENTAL



Supplementary Figure 1

Micro-array derived from myocardial tissue showing miRNA expression profiles at different time points after I/R, including miR-223.

4



Martinus I.F.J. Oerlemans¹

Marie-José Goumans²

Ben J. van Middelaar³

Hans Clevers⁴

Pieter A. Doevendans^{1,4}

Joost P.G. Sluijter^{1,4}

¹ Department of Cardiology, University Medical Centre Utrecht, Utrecht, the Netherlands.

² Department of Molecular Cell Biology, Leiden University Medical Centre, Leiden, the Netherlands

³ Hubrecht Laboratory, Institute for Developmental Biology, Utrecht, the Netherlands

⁴ Interuniversity Cardiology Institute Netherlands (ICIN)

Active Wnt signaling in response to cardiac injury

Basic Res Cardiol 2010; 105: 631-641

ABSTRACT

Background

Although the contribution of Wnt signaling in infarct healing is suggested, its exact role after myocardial infarction (MI) still needs to be unraveled. We evaluated the cardiac presence of active Wnt signaling *in vivo* following MI and investigated in which cell types active Wnt signaling was present by determining Axin2 promoter driven LacZ expression.

Methods

C57BL/6 Axin2-LacZ reporter mice were sacrificed at day 0, 1, 3, 7, 14 and 21 after LAD ligation. Hearts were snap-frozen for immunohistochemistry (IHC) or enzymatically digested to obtain a single cell suspension for flow cytometric analysis. For both FACS and IHC, samples were stained for β -galactosidase and antibodies against Sca-1, CD31, c-kit and CD45.

Results

Active Wnt signaling increased markedly in the myocardium, from 7 days post-MI onwards. Using Sca-1 and CD31, to identify progenitor and endothelial cells, a significant increase in LacZ⁺ cells was found at 7 and 14 days post-MI. LacZ⁺ cells also increased in the ckit⁺ and CD45⁺ cell population. IHC revealed LacZ⁺ cells co-expressing Sca, CD31, CD45, vWF and α SMA in the border zone and the infarcted area.

Conclusion

Wnt signaling increased significantly after MI in Sca⁺ and CD31⁺ expressing cells, suggesting involvement of Wnt signaling in resident Sca⁺ progenitor cells, as well as endothelial cells. Moreover, active Wnt signaling was present in ckit⁺ cells, leukocytes and fibroblast. Given its broad role during the healing phase after cardiac injury, additional research seems warranted before a therapeutic approach on Wnt to enhance cardiac regeneration can be carried out safely.

INTRODUCTION

Cardiovascular disease is one of the leading causes of morbidity and mortality in the western world¹. Following myocardial infarction (MI), damaged myocardium is replaced by scar tissue, which may result in heart failure for which limited therapeutic options are available. One potential important signal transduction pathway involved in regulating cardiac repair and potentially stem cell maintenance and differentiation is the Wnt pathway, which plays an essential role in normal cardiac development². Wnt signaling has been shown to be a key regulator of stem cell growth, differentiation and proliferation in both normal homeostasis and diseased state^{3,4}. Wnt proteins form a family of highly conserved secreted signaling molecules in which the canonical Wnt/ β -catenin pathway is mostly studied. Upon binding of Wnt to the seven-transmembrane domain spanning frizzled (Fzd) receptor and the co-receptor lipoprotein receptor related 5/6 (Lrp5/6) proteins GSK3 β is inactivated, thereby preventing the breakdown of β -catenin. After stabilization and accumulation, β -catenin enters the nucleus where it binds to LEF/TCF transcription factors to activate the transcription of Wnt target genes.

Although extensively studied in cardiac development, the exact role of Wnt signaling after MI still needs to be unraveled. Infarct size reduction was achieved by both stimulation and inhibition of Wnt/ β -catenin signaling^{5,6} and both downregulation⁷ and upregulation⁸ of β -catenin gene levels were observed in cardiac hypertrophy. Moreover, epicardium-derived progenitor cells lacking β -catenin displayed impaired coronary artery formation⁹ while β -catenin depletion in cardiac progenitor cells enhanced differentiation during cardiac remodeling¹⁰. Recent data demonstrates that β -catenin is involved in expansion of resident cardiac progenitor cells, but its role in differentiation of these cells remains controversial¹⁰⁻¹³. Most studies investigating Wnt signaling during pathological conditions (e.g. myocardial infarction) focused on proteins participating in Wnt signal transduction such as Dishevelled-1^{14,15} and β -catenin^{16,17}. However, this not necessarily means that active Wnt/ β -catenin signaling including transcription of Wnt target genes is present.

Considering its potency to act as a therapeutic target, fundamental insights on Wnt time-dependency and cell specificity upon injury in the adult injured myocardium is necessary. Therefore, we evaluated the presence of active Wnt signaling *in vivo* in the heart following MI. Moreover, we investigated in which cell types active Wnt signaling was present during different phases following MI.

After binding of β -catenin to LEF/TCF transcription factors in the nucleus, several Wnt target genes are activated including the Axin2 gene¹⁸. Axin2 is able to downregulate β -catenin and acts as a negative regulator of Wnt signaling¹⁹. We used Axin2^{+/LacZ} reporter mice in which the LacZ gene is under the control of the Axin2 promoter, providing a reliable way to detect Wnt activity by visualizing LacZ-reporter positive cells²⁰.

MATERIALS AND METHODS

Animals

Male and female C57BL/6 Axin2^{+LacZ} reporter mice were bred and used at 8-10 weeks of age. For generation of the Axin2-lacZ mouse²⁰, the β -galactosidase (NLS-lacZ) gene was introduced in frame to the endogenous Axin2 promoter by homologous recombination, thereby replacing most of exon 2 (MGI Ref ID J:74286) but leaving the Axin2 promoter intact. All experiments were approved by the Animal Experimentation Committee of the Utrecht University and were in accordance with the *Guide for the Care and Use of Laboratory Animals* of the Institute of Laboratory Animal Resources. The investigation conforms with the Guide for the Care and Use of Laboratory Animals published by the US National Institutes of Health (NIH Publication No. 85-23, revised 1996).

Myocardial infarction

MI was induced by ligation of the left anterior descending (LAD) coronary artery under isoflurane anesthesia, as described previously²¹. Briefly, mice were anesthetized with isoflurane, orally intubated and ventilated. A left thoracotomy was performed at the 3rd intercostal space, muscles and pericardium were dissected. LAD ligation was performed with an 8-0 non-absorbable ethilon suture. After verification that coronary occlusion had occurred by the change of color and kinesis of the apex and anterior-lateral wall, the thorax was closed in layers. After detubation, mice were kept warm until fully recovered. Mice were sacrificed at baseline (0d) and at 1, 3, 7, 14 and 21 days after MI. The hearts were flushed with phosphate-buffered saline (PBS) and dissected. The left ventricle was cut in two halves through the center of the infarct along the longitudinal axis. One half was snap-frozen in liquid nitrogen and stored at -80°C , the other half was kept in PBS for further processing. Remote area was defined as the non-infarcted part of the interventricular septum.

Cell isolation and flow cytometry analysis

Freshly dissected hearts, containing the infarcted and non-infarcted area, were perfused with PBS and washed, minced into 1-2 mm² pieces, digested for 45 minutes at 37°C with 10mg/ml collagenase A (Roche) and passed through a 70- μm filter. Remaining cells were plated on a 12-wells plate DMEM with 10% fetal bovine serum (FBS) as described previously²² or aliquoted after centrifugation for flow cytometric analysis. After centrifugation, cells were resuspended in PBS containing 4% FBS and aliquots containing 1.0×10^6 cells were stained. Single cell suspensions were stained with FDG (Fluoreporter[®] LacZ Kit F-1930, Molecular Probes) to detect β -galactosidase activity. Next, isolated cells were labeled with antibodies against Sca-1 (BD Pharmingen 553108, PE conjugated), isotype control (BD Pharmingen, 553930), CD31 (Biolegend 102417, Pe-Cy7 conjugated), isotype control (Biolegend, 400521), c-kit (Abcam 46790, APC-Cy5.5 conjugated), isotype control (Abcam 46745) and CD45 (Abcam 51482, PE-Texas Red conjugated). To exclude dead cells from analysis (including cardiomyocytes), 7-AAD (BD 559925) was used. Samples were analyzed by flow cytometry (Beckman Coulter Cytomics FC500 FACS), collecting 15,000 to 50,000 events per sample.

Histology and immunohistochemistry/immunocytochemistry

Frozen sections of 5 to 7- μ m were cut in a cryostat (Microm HM560, Cryo-Star) and mounted on silane-BSA coated slides. Histological analysis of MI was performed by H&E staining. Sections were fixed in acetone, blocked with 10% normal goat serum (NGS) and incubated overnight with primary antibody. After incubation with secondary antibody for 1 hour, sections were washed in PBS and mounted in Fluoromount (Southern Biotech). For immunocytochemistry, coverslips with cultured cells were fixed in 4% paraformaldehyde at room temperature and permeabilized with 0.2% Triton X-100 in PBS. Cells were blocked with 2% bovine serum albumin (BSA) for 15 minutes and incubated overnight at 4 °C with primary antibody with 10% NGS. The coverslips were then incubated with secondary antibody in PBS with 10% NGS for one hour and subsequently mounted. For both IHC and ICC, Hoechst dye was used to visualize nuclei. Primary antibodies for Sca-1 (BD Pharmingen, 57403), CD31 (BD Pharmingen, 550274), CD45 (BD Pharmingen 553774), tropomyosin (Sigma, T9283), β -galactosidase (Abcam ab616) and von Willebrand Factor (Dako, M0616) were used with matching isotypes and a FITC-conjugated antibody against alpha-smooth muscle actin (Sigma, A2547). Secondary antibodies were conjugated with AF555 (Invitrogen A21429), AF488 (Invitrogen A11001) and AF647 (Invitrogen A21247). Slides and coverslips were examined with a Nikon light microscope equipped for epifluorescence or Zeiss LSM 510 Meta confocal microscope for high magnification capturing. All images illustrated are representative of least three independent experiments.

β -galactosidase (LacZ) staining on cultured cells

Cells were fixed in 0.2% paraformaldehyde for 10 minutes, followed by a 10-minutes wash in PBS with 2mM MgCl₂ on ice. Cells were then placed in Xgal staining solution (2 mM MgCl₂, 0.1% sodium deoxycholate and 0.02% NP-40, 5mM K₃Fe(CN)₆, 5mM K₄Fe(CN)₆ and 1 mg/ml X-gal (Invitrogen) in PBS) at 37°C for 30 minutes. Thereafter, cells were washed twice in PBS with 2mM MgCl₂ at room temperature and covered with coverslips and examined by light microscopy.

Statistics

Data (mean \pm s.e.m.) were analyzed by Mann-Whitney U test, using a significance level of $P < 0.05$ (SPSS for Windows, v15.0).

RESULTS

Increased number of cells display active Wnt signaling in the heart after myocardial infarction

To identify Wnt signaling in the adult mouse heart, we used the Axin2-LacZ reporter mouse which will result in LacZ expression in those cells that have active canonical Wnt signaling. To demonstrate specificity of β -galactosidase activity only in cells having active Wnt signaling, a single cell suspension was made from Axin2 reporter hearts and put into culture. Immunocytochemistry revealed the presence of LacZ expressing cells (and thus canonical Wnt signaling) in the culture, while cell cultures from wild type hearts did not

show any positive staining (Supplementary Figure 1a-d). Moreover, Wnt reporter positive staining increased upon stimulation with Lithium chloride, a strong chemical inducer of Wnt signaling (Supplementary Figure 1e, f). In order to quantify the number of Wnt reporter expressing cells (LacZ⁺ cells), we fluorescently labeled single cell suspensions with FDG. Flow cytometry analysis revealed that in the heart of adult Axin2-reporter mice, a LacZ expressing cell population of $9.55 \pm 0.78\%$ is present (Figure 1a), while no β -galactosidase activity could be observed in non-transgenic hearts (Figure 1a, right panel). Next we analyzed whether Wnt signaling increased following myocardial infarction (MI). At 7 days post-MI, the number of LacZ⁺ cells had increased significantly ($14.47 \pm 0.75\%$) compared to basal levels of non-operated mice (Figure 1b). Since the number/percentage of LacZ⁺ cells at day 3 post-MI was still comparable with basal levels ($9.44 \pm 0.30\%$), the increase in active Wnt signaling started between day 3 and 7 post MI.

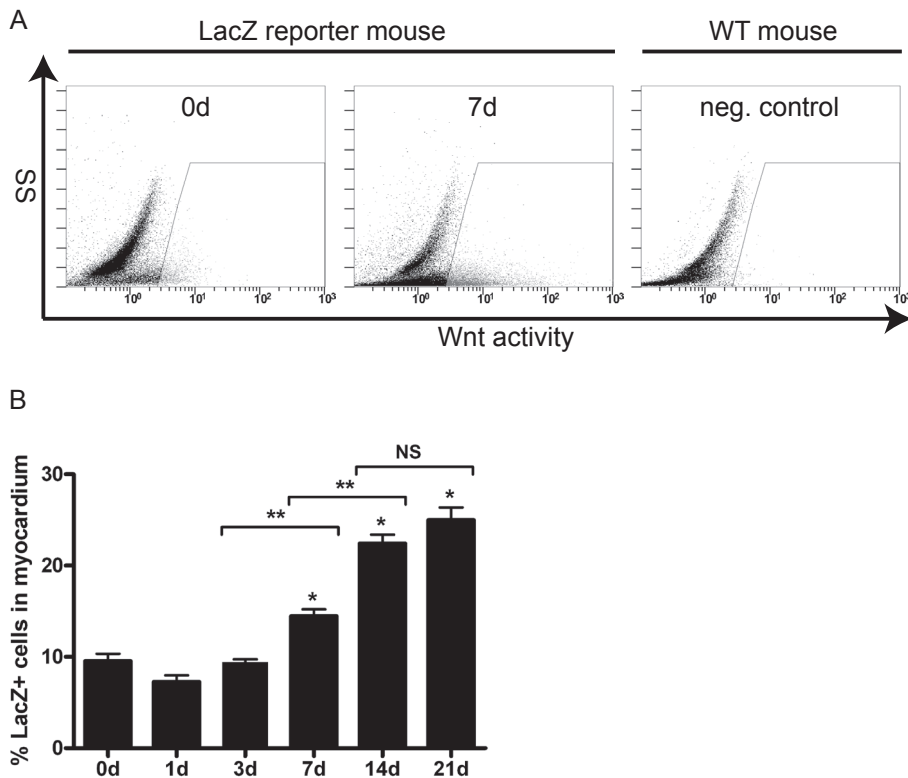


Figure 1 | Increased Wnt signaling after myocardial infarction

Freshly dissected hearts were digested into a single cell suspension and stained with FDG to detect β -galactosidase activity. (A) Representative flow cytometric scatter plots of a control heart (0 days, left window) together with a sample 7 days (middle window) of the LacZ-reporter mouse after myocardial infarction (MI). Wnt⁺ cell population increased in response to MI, while wild type samples showed no Wnt activity (right window). (B) Flow cytometric analysis showed a significant increase in LacZ⁺ cells on day 7, 14 and 21 after MI compared to baseline levels of a non-operated mouse. A significant difference in the LacZ⁺ cells was observed between day 3 – 7 and day 7 – 14. After 14 days the amount of Wnt⁺ cells started to stabilize. * $P < 0.01$ compared to control and ** $P < 0.01$ between groups, $n = 5-10$ per group.

LacZ⁺ cells increased further on 14 days ($22.42 \pm 0.97\%$) and 21 days ($24.98 \pm 1.37\%$). Although there was a significant increase in LacZ⁺ cells between day 7 and 14, the number of LacZ⁻ expressing cells stabilized between day 14 and 21 post-MI. Real time RT-PCR on temporal Axin2 expression confirmed the Axin2 promoter driven β -galactosidase activity after myocardial infarction.

LacZ-expressing cells increase significantly throughout the whole myocardium

To localize active Wnt signaling in the injured heart, we analyzed β -galactosidase expression by staining cardiac sections from different time points post-MI. In all sections stained,

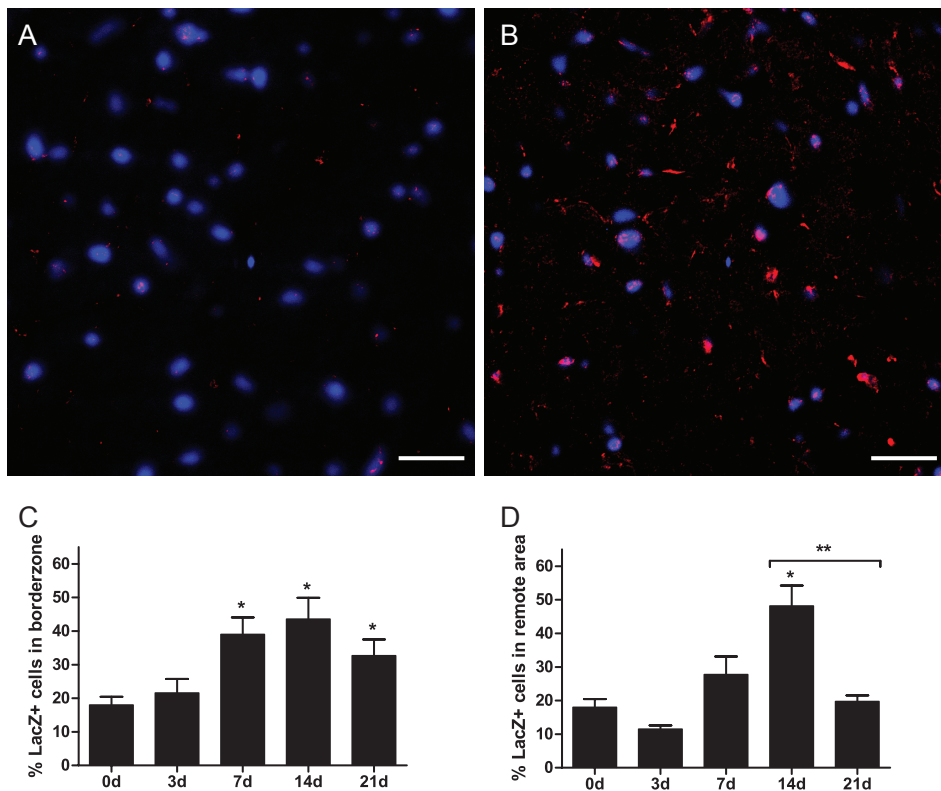


Figure 2 | LacZ⁺ cells increase significantly throughout the whole myocardium

Frozen sections of mouse hearts from different time points after MI were fluorescently stained for β -galactosidase (red) and Hoechst (nuclei, blue) to localize LacZ⁺ cells. (A) Representative section of a control heart showing some LacZ⁺ nuclei (purple spots). (B) Representative section of a mouse heart 14 days after MI, showing an increase in LacZ⁺ nuclei (purple) as well as more active Wnt signaling in the surrounding tissue in the border zone. Scale bar represents 20 μ m, 630x magnification. (C and D) Quantification of LacZ⁺ cells based on LacZ⁺ positive nuclei compared to total nuclei in border zone and remote area. The number of LacZ⁺ cells increased significantly after MI in both the remote area and the border zone. *P < 0.05 compared to control and **P < 0.05 between groups, n = 6–8 per group.

we observed LacZ-positive cells throughout the whole myocardium, including border zone and remote area. LacZ+ cells were also found in the infarcted area, although not as much as in the border zone. The number of LacZ+ nuclei increased compared to control sections (Figure 2a, b). LacZ+ nuclei were counted and compared with the total number of nuclei in both the border zone and the remote area, to see whether the increase of LacZ+ cells was restricted to a particular area. Active Wnt signaling increased significantly in both remote area and the border zone (Figure 2c, d). The increase in LacZ+ cells showed a peak around 14 days post MI and started to normalize between 14 and 21 days. Although to a large extent upregulated in the border zone, active Wnt reporter cells can be found throughout the whole myocardium, showing a significant increase in response to myocardial injury.

LacZ+ cells increase significantly in the progenitor, endothelial and leukocyte cell population

To characterize the composition of the LacZ+ positive cell population in the myocardium, we used Sca-1 and c-kit (CD117) to identify progenitor populations, CD31 to detect endothelial cells and CD45 was used as a common leukocyte marker, using flow cytometry. LacZ+ cells displayed expression of both Sca-1 and CD31 on their cell surface (Figure 3a). Active Wnt-reporter cells were also found to express c-kit and CD45, the latter only at 3 and 7 days post-MI. Immuno labeling on different sections after MI confirmed the flow cytometric analysis, demonstrating co-localization of LacZ+ nuclei with Sca-1, CD31 and CD45 (Figure 3b-d). Since CD31 can be expressed on non-endothelial cells as well, we confirmed that LacZ+ nuclei were present in vessels in the border zone by using von Willebrand factor (vWF) (Supplementary Figure 2a). Furthermore, using alpha-smooth muscle actin (α SMA) we found fibroblast (Supplementary Figure 2b) and vascular smooth muscle cells (Supplementary Figure 2c) with LacZ+ nuclei in the border zone and infarct, respectively. Cytoplasmic LacZ-positive staining was also observed, mainly in the infarcted area where clusters of cardiomyocytes were still present. This was probably caused by either nuclear leakage from dying cardiomyocytes or senescence-associated β -galactosidase activity²³. Therefore, not only cardiac progenitor cells and endothelial cells demonstrated LacZ positivity but also leukocytes, fibroblasts and myocytes.

Subsequently, we analyzed whether changes in active Wnt signaling was present in specific cell populations, exploring the role of Wnt signaling in different cell types that play an important role after MI. Flow cytometric analysis indeed displayed a significant increase of LacZ+ cells in both Sca-1+ and CD31+ cell populations, parallel with an increase in total Sca+ and CD31+ cell numbers (Figure 4a-d). The total number of Sca+ cells increased significantly between 3 and 7 days post-MI, but started to decrease again after 14 days (Figure 4a). A similar pattern was found for CD31+ cells, although the number of cells at 7, 14 and 21 days remained significantly higher compared to baseline levels (Figure 4c). LacZ+ cells increased significantly in Sca+ and CD31+ cell populations, starting from day 7 post-MI. Ckit+ cells also increased significantly after MI, showing a peak at 14 days post-MI. This increase started between day 7 and 14, still having higher levels at 21 days then compared to baseline (Figure 4e). LacZ+ cells in the ckit+ population increased gradually after MI with highest level at 3 days (Figure 4f). The CD45+ cell population increased after MI, showing a significant increase at 3, 7 and 14 days post-MI, followed by a gradual

decrease towards basal levels at 21 days (Figure 4g). Interestingly, the number of LacZ+ cells in CD45+ cell population increased significantly as well, following almost the same trend as total CD45+ population with peaks at 3 and 7 days post-MI (Figure 4h). Additionally, we tested whether different subsets of LacZ-positive cells changed during time following MI. Since it has been suggested that cardiac progenitor cells express Sca-1, we tested LacZ expression in Sca+/CD31- cells. Wnt signaling increased significantly in Sca+/CD31- cell population, showing a peak at 7 days after MI (Figure 5a). The endothelial cell population (Sca-/CD31+ cells), displayed a significant increase in Wnt signaling at 7 and 14 days after MI (Figure 5b).

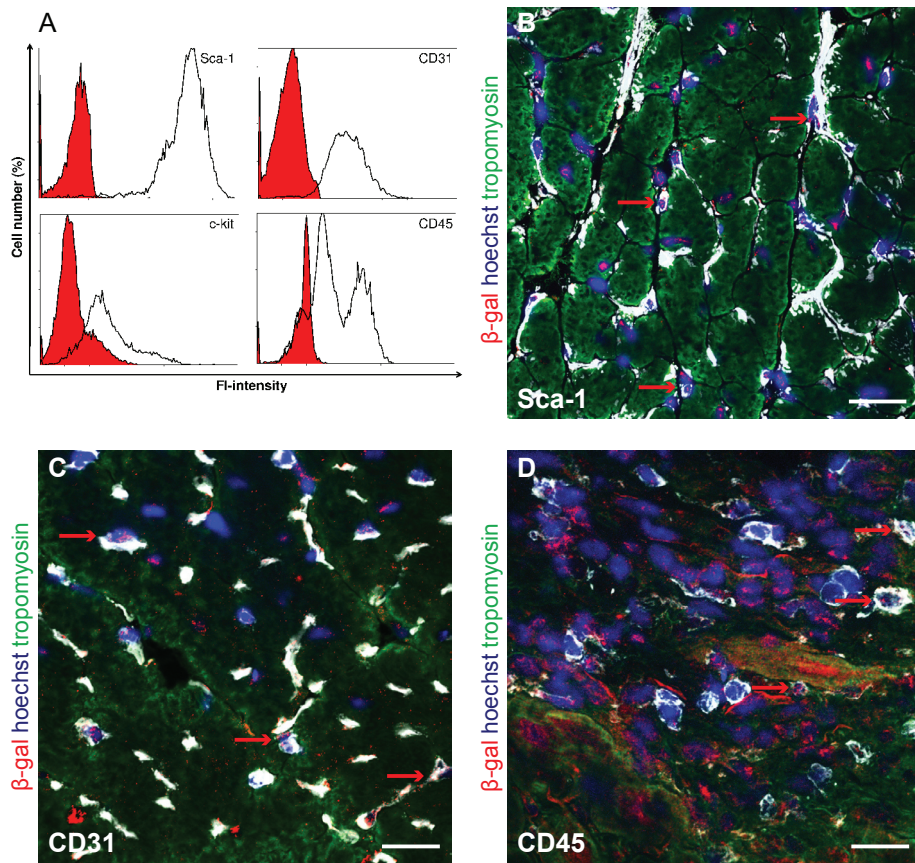


Figure 3 | LacZ+ cells are present in the progenitor, endothelial and leukocyte cell population (A) Characterization of LacZ+ cells by co-expression of Sca-1, CD31, c-kit and CD45 using flow cytometry. Solid histograms represent isotype control antibodies. All markers studied were present within the LacZ+ cell population. Using immunohistochemistry to reveal co-localization, frozen sections were fluorescently stained for β -galactosidase (red), Hoechst (nuclei, blue), tropomyosin (green) and for Sca-1 (B), CD31 (C) and CD45 (D). Confocal microscopy showed that LacZ+ cells co-localize with progenitor, endothelial and leukocyte cell populations (red arrows), confirming flow cytometric analysis. Scale bar represents 20 μ m, 630x magnification.

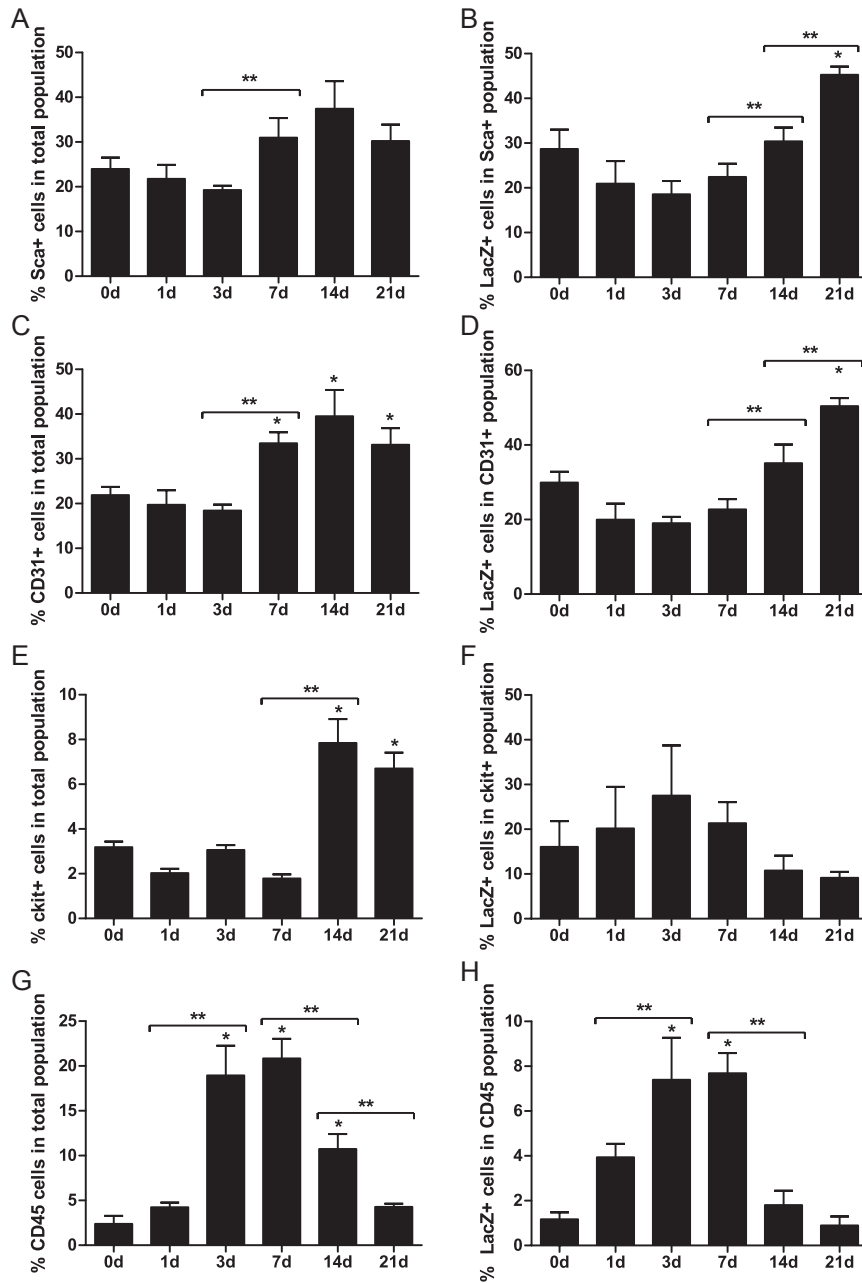


Figure 4 | LacZ⁺ cells increase significantly in the progenitor, endothelial and leukocyte cell population

Flow cytometric analysis showing a significant increase of LacZ⁺ cells in both Sca1⁺ (B) and CD31⁺ (D) cell populations, parallel with an increase in total Sca1⁺ (A) and CD31⁺ (C) cell numbers. Total ckit⁺ (E) and CD45⁺ (G) cell populations increased significantly as well. LacZ⁺ cells in ckit⁺ cell population increased with a peak at day 3 post-MI (F). Within the CD45⁺ leukocyte cell population, LacZ⁺ cells showed a significant increase at day 3, 7 and 14 days post-MI (H). *P<0.05 compared to control and **P<0.05 between groups, (A-D) n=5-10 per group, (E-H) n=3-5 per group.

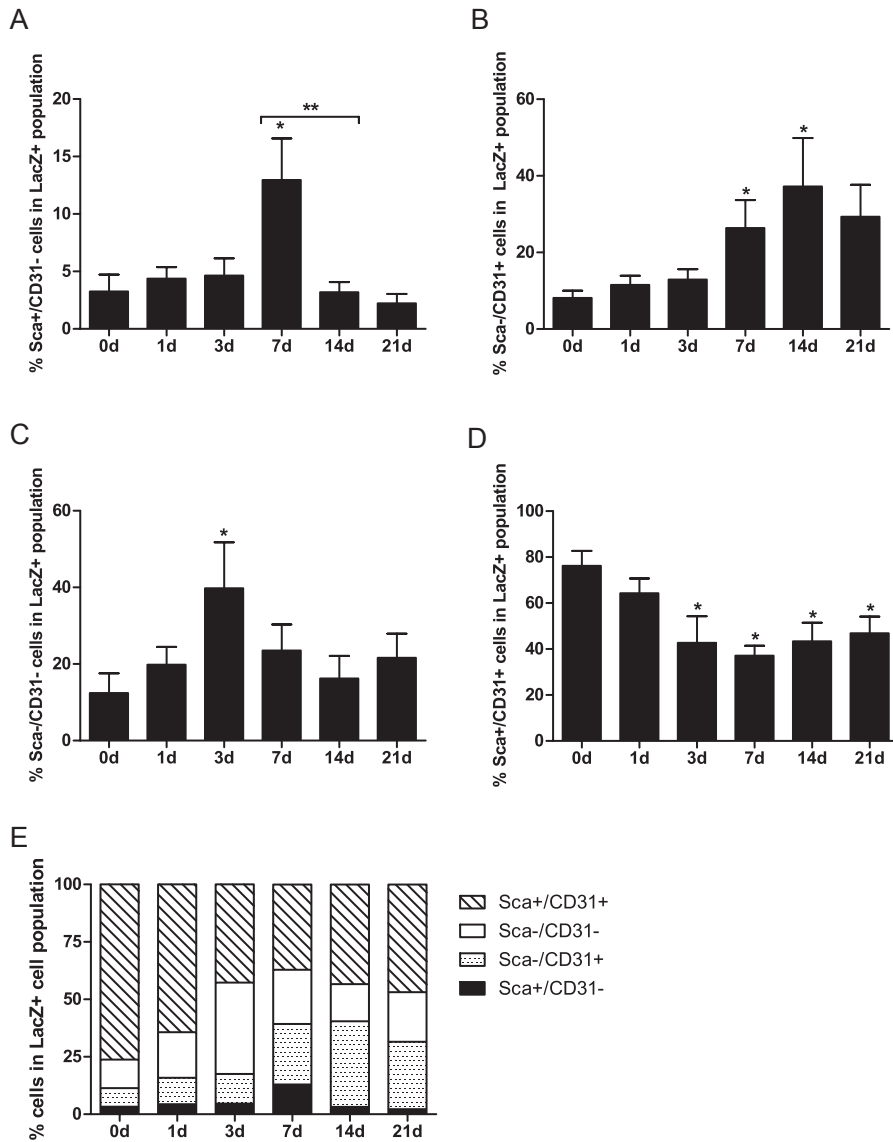


Figure 5 | Sca+/CD31- and Sca-/CD31+ cells increase significantly in LacZ+ cell population

Flow cytometric analysis of specific subsets of LacZ+ cells, based on the co-expression of Sca-1 and CD31 to distinguish between progenitor (Sca+/CD31-) and endothelial (Sca-/CD31+) cell populations. (A) The amount of Sca+/CD31- progenitor cells increased significantly within the LacZ+ cell population 7 days post-MI. (B) The amount of Sca-/CD31+ endothelial cells increased significantly within the LacZ+ cell population after infarction. (C) The amount of Sca-/CD31- progenitor cells increased significantly within the LacZ+ cell population 3 days post-MI. (D) Sca+/CD31+ cell population formed the largest population of LacZ+ cells, but decreased significantly starting from 3 days after infarction. * $P < 0.05$ compared to control and ** $P < 0.05$ between groups, $n = 5-10$ per group. (E) Cumulative overview of changes in Wnt+ cell population during time, based on the co-expression of Sca-1 and CD31. Sca+/CD31+ cells, although decreasing in time, formed the majority within the LacZ+ cell population. An early increase in the Sca-/CD31- cell fraction, probably CD45+ cells, can be appreciated. Both Sca+/CD31- and Sca-/CD31+ cell fractions increased significantly starting at day 7 after MI.

Furthermore when looking at the Sca-/CD31- cell population, probably representing inflammatory (e.g. CD45+) and other circulating cell populations, an increase was found at 3 days post-MI (Figure 5c). At all studied time points Sca+/CD31+ cell population formed the largest population of LacZ+ cells (Figure 5d). However, this subpopulation decreased significantly starting from day 3, reaching the lowest levels at 7 days post-MI (Figure 5d). When looking at the changes in cells showing active Wnt signaling during time, more than 50% of the LacZ+ cells were either Sca+/CD31+ or Sca-/CD31- at all time points (Figure 5e). Although a significant increase in Sca+/CD31- progenitor cells and Sca-/CD31+ endothelial cells was observed, these two subsets of cells together did not exceed 40% of the LacZ+ cell population.

DISCUSSION

4

Wnt signaling is an important regulatory pathway in biology and behavior of stem cells^{3, 4} and is required for normal cardiac development^{2, 24}. In response to cardiac stress and injury, reactivation of Wnt/ β -catenin signaling takes place, probably being part of a fetal gene reprogramming required for tissue repair^{25, 26}. Considering its potency to be used as a therapeutic target, it is of great interest to gain more information on the function of Wnt signaling in the adult heart, especially in the context of cardiac tissue repair. However, during the last few years contradictory results were reported upon inhibition and stimulation of Wnt with respect to the adaptive response on hypertrophic and ischemic stimuli^{5-7, 15, 27}. It is becoming clear that Wnt-molecules do not simply drive proliferation or differentiation but rather regulate and fine tune these processes in a cell-type and time-dependant manner. There are 19 Wnt proteins, 10 Fzd receptors and two Lrp co-receptors in mammals, representing a complex regulatory family.

In our study, cell specific Wnt signaling and its localization was visualized in response to cardiac injury using Axin2^{+LacZ} reporter mice. Although an indirect measurement of the active Wnt cascade, the not cell-specific role of Axin-2 in the Wnt response³ makes it a reliable way to detect canonical Wnt activity. We demonstrate that active Wnt signaling is significantly upregulated in those cell populations that are considered to play a role in cardiac wound healing after MI and in cardiomyocytes. Active Wnt signaling was significantly increased in the border zone and remote area after cardiac injury. Together with an increase in total progenitor, endothelial and leukocyte cell populations, the number of LacZ+ cells in these populations increased significantly. Also, a significant increase in Sca+/CD31- progenitor and Sca-/CD31+ endothelial cell number was found within the population that showed active Wnt signaling. Moreover, we observed active Wnt signaling in fibroblasts, vWF-positive endothelial cells, vascular smooth muscle cells (α SMA+), fibroblasts (α SMA+) and in the cytoplasm of cardiomyocytes.

Since active Wnt signaling was present in all cell populations studied, one question is whether we can enhance cardiac repair by modulating Wnt. Different compounds are available already that can interfere with Wnt signaling, but up till now Wnt modulation after myocardial infarction did not result in consistent results. Frizzled or secreted Frizzled-related proteins (sFRPs) can compete for Wnt binding, thereby antagonizing Wnt signaling.

Transgenic mice overexpressing Frizzled-A, a member of the frizzled family, displayed less apoptosis and a higher capillary density resulting in reduced infarct size as compared to wild-type animals⁶. Others reported that mesenchymal stem cells (MSCs) overexpressing sFRPs showed better survival after injection into the peri-infarct region. This resulted in increased engraftment and vascularized granulation tissue after MI^{28, 29}, probably by antagonizing Wnt3a which resulted in less apoptosis³⁰. In contrary, direct β -catenin injection in the border zone of rats after coronary artery ligation decreased infarct size and promoted cell survival in both cardiomyocytes and cardiac fibroblasts⁵. Also cardioprotection by ischemic preconditioning was shown after GSK3 β inhibition³¹, due to induction of neovascularization and inhibition of apoptosis. The opposite effect was demonstrated by sFRP1 overexpression²⁷. Recently, fibrosis was shown to be limited in sFRP1 null mice after myocardial infarction³², although regulated via mechanisms independently of Wnt signaling. As indicated, different Wnt dependent- and independent stimuli seem to interact with GSK3 β and sFRPs with respect to cell survival and repair^{33, 34}.

In our study, both Sca+ progenitor as endothelial cells and cardiomyocytes showed increased LacZ expression and these LacZ+ cells increased in number. This increase in number suggests that increased Wnt signaling might influence survival or proliferation of these cells in response to cardiac injury. Furthermore, ckit+ and CD45+ cell populations showed increased LacZ expression as well. Although this association was observed, our study is purely descriptive and do not allow to conclude any causal relationship between an increased presence of LacZ and the different cell numbers. Interestingly, studies aiming at wound healing after MI reported an upregulation of β -catenin in vascular endothelial cells during neovascularization^{14, 35} and in proliferating and migrating myofibroblasts¹⁴ after MI. Consistent with these studies, our findings indirectly suggest that Wnt signaling drives expansion of different cell types, including Sca+/CD31- progenitor and Sca-/CD31+ endothelial cells as well as in ckit+ and CD45 cell populations in response to cardiac injury. The upregulation of β -catenin observed in these studies does not necessarily mean that a higher promoter activity is present though. Whether increased Wnt signaling directly influences cardiac wound healing or cell survival remains unanswered.

A second question is whether Wnt signaling modulates differentiation after cardiac injury. Several studies reported that canonical and non-canonical Wnt signaling are required for differentiation of cardiac progenitor cells¹³ and enhances cardiomyogenic potential of bone marrow cells³⁶. Different progenitor cell populations, resident in the adult heart, have been shown to differentiate into cardiomyocytes or vascular structures both *in vitro* and *in vivo*³⁷⁻³⁹. Although stimulation of endogenous regeneration capacity might offer a new treatment modality, activation of resident cardiac progenitor cells to repair the injured myocardium still remains a matter of debate. From this point, it is at least striking that we observed a significant increase in Sca+/CD31- progenitor cells and Sca-/CD31+ endothelial cells within the LacZ+ population. LacZ+ cells expressing both Sca+ and CD31+ decreased after MI. These shifts within the LacZ+ populations might suggest involvement of Wnt signaling in the process of differentiation in response to MI. Several other reports have been published supporting a role for Wnt signaling in expansion and proliferation of cardiac progenitor cells during development^{12, 24, 40}. Canonical and non-canonical Wnt signaling has been shown to stimulate cell growth and survival in isolated endothelial cells *in vitro*^{17, 41, 42}. Also β -catenin

stabilization via lithium stimulation and administration of different Wnt-molecules induced muscle regeneration via differentiation of Sca+/CD45+ cells, which was reduced upon sFRP2/3 injection⁴³. In contrast, cardiac specific β -catenin depletion was shown to attenuate cardiac remodeling, mainly through enhanced differentiation of Sca+ progenitor cells¹⁰. In conclusion, the present study demonstrates a temporal upregulation of active Wnt signaling after MI which is not restricted to a particular area of the heart. LacZ+ cells were shown to co-express progenitor, endothelial, leukocyte and fibroblast markers, suggesting a broad role of Wnt in reaction to cardiac injury. Interestingly, different cell populations displayed a distinct LacZ response in time, suggesting a time and cell specific activation of Wnt after MI. When considering Wnt reactivation as a therapeutic approach to enhance cardiac regeneration, one should consider this time and cell specific expression window. Based on the significant upregulation of the progenitor and endothelial cell populations that show active Wnt signaling, it is possible that Wnt modulates cardiac regeneration and neovascularization during the healing phase after MI. However, as more populations are involved, this also illustrates its complexity.

Acknowledgements

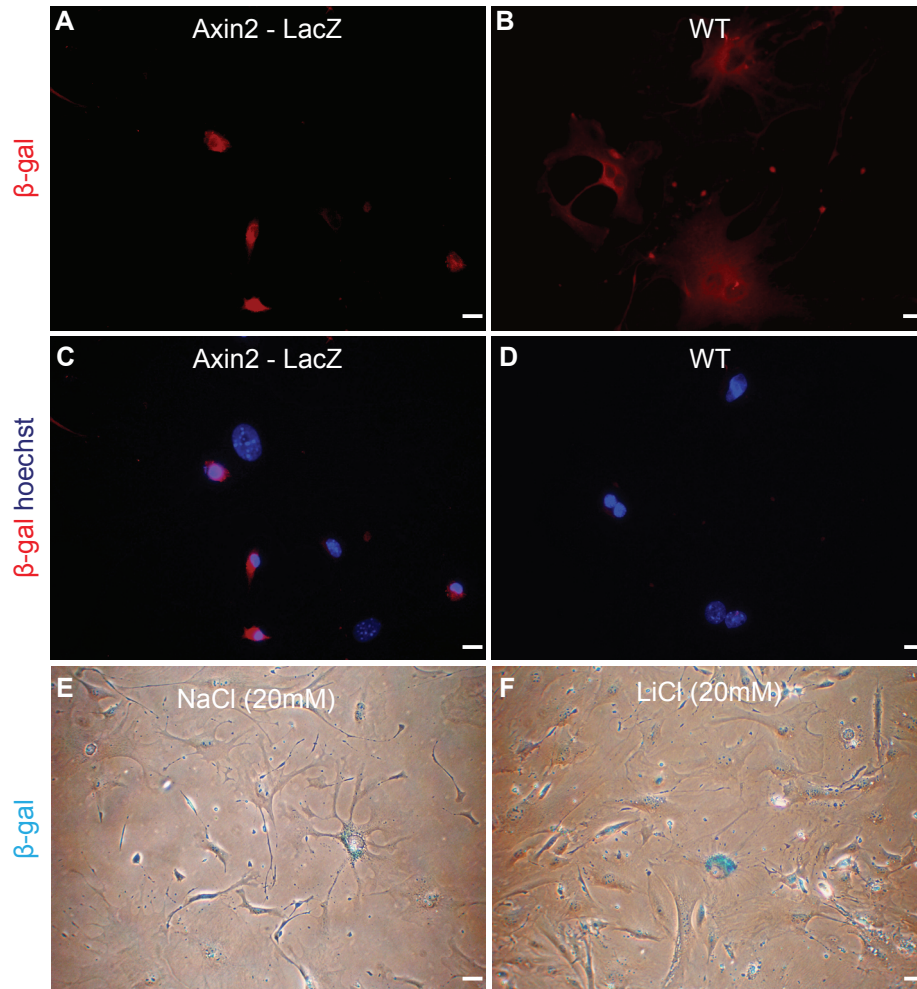
This work was supported by a VIDI grant (016.056.319) from the Netherlands Organization for Scientific Research (NWO), the Netherlands Heart Foundation (2003B07304), BSIK program "Dutch Program for Tissue Engineering", grants 6746, Bekalis price (PD) and "Stichting Swaeneborgh" (MO).

REFERENCES

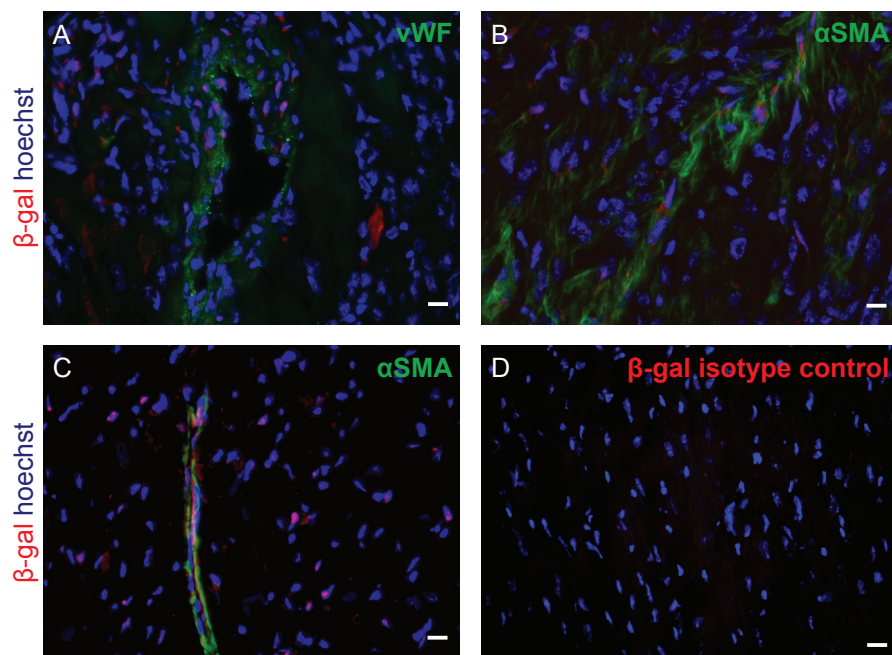
1. Lloyd-Jones D, Adams RJ, Brown TM, et al. Heart disease and stroke statistics–2010 update: a report from the American Heart Association. *Circulation* 2010;121:e46-e215.
2. Brade T, Manner J, Kuhl M. The role of Wnt signalling in cardiac development and tissue remodelling in the mature heart. *Cardiovasc Res* 2006;72:198-209.
3. Clevers H. Wnt/beta-catenin signaling in development and disease. *Cell* 2006;127:469-480.
4. Reya T, Clevers H. Wnt signalling in stem cells and cancer. *Nature* 2005;434:843-850.
5. Hahn JY, Cho HJ, Bae JW, et al. Beta-catenin overexpression reduces myocardial infarct size through differential effects on cardiomyocytes and cardiac fibroblasts. *J Biol Chem* 2006;281:30979-30989.
6. Barandon L, Couffignal T, Ezan J, et al. Reduction of infarct size and prevention of cardiac rupture in transgenic mice overexpressing FrzA. *Circulation* 2003;108:2282-2289.
7. Baurand A, Zelarayan L, Betney R, et al. Beta-catenin downregulation is required for adaptive cardiac remodeling. *Circ Res* 2007;100:1353-1362.
8. Qu J, Zhou J, Yi XP, et al. Cardiac-specific haploinsufficiency of beta-catenin attenuates cardiac hypertrophy but enhances fetal gene expression in response to aortic constriction. *J Mol Cell Cardiol* 2007;43:319-326.
9. Zamora M, Manner J, Ruiz-Lozano P. Epicardium-derived progenitor cells require beta-catenin for coronary artery formation. *Proc Natl Acad Sci U S A* 2007;104:18109-18114.
10. Zelarayan LC, Noack C, Sekkali B, et al. Beta-Catenin downregulation attenuates ischemic cardiac remodeling through enhanced resident precursor cell differentiation. *Proc Natl Acad Sci U S A* 2008;105:19762-19767.
11. Qyang Y, Martin-Puig S, Chiravuri M, et al. The renewal and differentiation of Isl1+ cardiovascular progenitors are controlled by a Wnt/beta-catenin pathway. *Cell Stem Cell* 2007;1:165-179.
12. Lin L, Cui L, Zhou W, et al. Beta-catenin directly regulates Islet1 expression in cardiovascular progenitors and is required for multiple aspects of cardiogenesis. *Proc Natl Acad Sci U S A* 2007;104:9313-9318.
13. Kwon C, Arnold J, Hsiao EC, et al. Canonical Wnt signaling is a positive regulator of mammalian cardiac progenitors. *Proc Natl Acad Sci U S A* 2007;104:10894-10899.
14. Chen L, Wu Q, Guo F, et al. Expression of Dishevelled-1 in wound healing after acute myocardial infarction: possible involvement in myofibroblast proliferation and migration. *J Cell Mol Med* 2004;8:257-264.
15. van de Schans V, van den Borne SW, Strzelecka AE, et al. Interruption of Wnt signaling attenuates the onset of pressure overload-induced cardiac hypertrophy. *Hypertension* 2007;49:473-480.
16. Blankesteijn WM, van Gijn ME, Essers-Janssen YP, et al. Beta-catenin, an inducer of uncontrolled cell proliferation and migration in malignancies, is localized in the cytoplasm of vascular endothelium during neovascularization after myocardial infarction. *Am J Pathol* 2000;157:877-883.
17. Wang X, Xiao Y, Mou Y, et al. A role for the beta-catenin/T-cell factor signaling cascade in vascular remodeling. *Circ Res* 2002;90:340-347.
18. Leung JY, Kolligs FT, Wu R, et al. Activation of AXIN2 expression by beta-catenin-T cell factor. A feedback repressor pathway regulating Wnt signaling. *J Biol Chem* 2002;277:21657-21665.
19. Jho EH, Zhang T, Domon C, et al. Wnt/beta-catenin/Tcf signaling induces the transcription of Axin2, a negative regulator of the signaling pathway. *Mol Cell Biol* 2002;22:1172-1183.
20. Lustig B, Jerchow B, Sachs M, et al. Negative feedback loop of Wnt signaling through upregulation of conductin/axin2 in colorectal and liver tumors. *Mol Cell Biol* 2002;22:1184-1193.
21. van Laake LW, Passier R, Monshouwer-Kloots J, et al. Monitoring of cell therapy and assessment of cardiac function using magnetic resonance imaging in a mouse model of myocardial infarction. *Nat Protoc* 2007;2:2551-2567.
22. Tiede K, Melchior-Becker A, Fischer JW. Transcriptional and posttranscriptional regulators of biglycan in cardiac fibroblasts. *Basic Res Cardiol* 2010;105:99-108.

23. Maejima Y, Adachi S, Ito H, et al. Induction of premature senescence in cardiomyocytes by doxorubicin as a novel mechanism of myocardial damage. *Aging cell* 2008;7:125-136.
24. Cohen ED, Tian Y, Morrisey EE. Wnt signaling: an essential regulator of cardiovascular differentiation, morphogenesis and progenitor self-renewal. *Development* 2008;135:789-798.
25. Kim Y, Phan D, van RE, et al. The MEF2D transcription factor mediates stress-dependent cardiac remodeling in mice. *J Clin Invest* 2008;118:124-132.
26. Oka T, Xu J, Molkenin JD. Re-employment of developmental transcription factors in adult heart disease. *Semin Cell Dev Biol* 2007;18:117-131.
27. Barandon L, Dufourcq P, Costet P, et al. Involvement of FrzA/sFRP-1 and the Wnt/frizzled pathway in ischemic preconditioning. *Circ Res* 2005;96:1299-1306.
28. Alfaro MP, Pagni M, Vincent A, et al. The Wnt modulator sFRP2 enhances mesenchymal stem cell engraftment, granulation tissue formation and myocardial repair. *Proc Natl Acad Sci U S A* 2008;105:18366-18371.
29. Mirotsoou M, Zhang Z, Deb A, et al. Secreted frizzled related protein 2 (Sfrp2) is the key Akt-mesenchymal stem cell-released paracrine factor mediating myocardial survival and repair. *Proc Natl Acad Sci U S A* 2007;104:1643-1648.
30. Zhang Z, Deb A, Zhang Z, et al. Secreted frizzled related protein 2 protects cells from apoptosis by blocking the effect of canonical Wnt3a. *J Mol Cell Cardiol* 2009;46:370-377.
31. Kaga S, Zhan L, Altaf E, et al. Glycogen synthase kinase-3beta/beta-catenin promotes angiogenic and anti-apoptotic signaling through the induction of VEGF, Bcl-2 and survivin expression in rat ischemic preconditioned myocardium. *J Mol Cell Cardiol* 2006;40:138-147.
32. Kobayashi K, Luo M, Zhang Y, et al. Secreted Frizzled-related protein 2 is a procollagen C proteinase enhancer with a role in fibrosis associated with myocardial infarction. *Nat Cell Biol* 2009;11:46-55.
33. Miura T, Miki T. Limitation of myocardial infarct size in the clinical setting: current status and challenges in translating animal experiments into clinical therapy. *Basic Res Cardiol* 2008;103:501-513.
34. Heusch G, Boengler K, Schulz R. Inhibition of mitochondrial permeability transition pore opening: the Holy Grail of cardioprotection. *Basic Res Cardiol* 2010;105:151-154.
35. Blankesteyn WM, van Gijn ME, Essers-Janssen YP, et al. Beta-catenin, an inducer of uncontrolled cell proliferation and migration in malignancies, is localized in the cytoplasm of vascular endothelium during neovascularization after myocardial infarction. *Am J Pathol* 2000;157:877-883.
36. Flaherty MP, bde-Latif A, Li Q, et al. Noncanonical Wnt11 signaling is sufficient to induce cardiomyogenic differentiation in unfractionated bone marrow mononuclear cells. *Circulation* 2008;117:2241-2252.
37. Beltrami AP, Barlucchi L, Torella D, et al. Adult cardiac stem cells are multipotent and support myocardial regeneration. *Cell* 2003;114:763-776.
38. Oh H, Bradfute SB, Gallardo TD, et al. Cardiac progenitor cells from adult myocardium: homing, differentiation, and fusion after infarction. *Proc Natl Acad Sci U S A* 2003;100:12313-12318.
39. Bearzi C, Rota M, Hosoda T, et al. Human cardiac stem cells. *Proc Natl Acad Sci U S A* 2007;104:14068-14073.
40. Cohen ED, Wang Z, Lepore JJ, et al. Wnt/beta-catenin signaling promotes expansion of Isl-1-positive cardiac progenitor cells through regulation of FGF signaling. *J Clin Invest* 2007;117:1794-1804.
41. Masckauchan TN, Agalliu D, Vorontchikhina M, et al. Wnt5a signaling induces proliferation and survival of endothelial cells *in vitro* and expression of MMP-1 and Tie-2. *Mol Biol Cell* 2006;17:5163-5172.
42. Samarzija I, Sini P, Schlange T, et al. Wnt3a regulates proliferation and migration of HUVEC via canonical and non-canonical Wnt signaling pathways. *Biochem Biophys Res Commun* 2009.
43. Poleskaya A, Seale P, Rudnicki MA. Wnt signaling induces the myogenic specification of resident CD45+ adult stem cells during muscle regeneration. *Cell* 2003;113:841-852.

SUPPLEMENTAL

**Supplementary Figure 1**

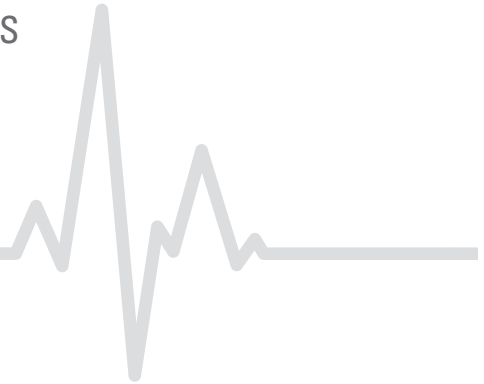
Cells were isolated as was done for flow cytometric analysis. Axin2^{+LacZ} and wild type (WT) isolated cells were cultured in DMEM with 10% fetal bovine serum (FBS) and fluorescently stained for β-galactosidase (red) and Hoechst (nuclei, blue) to detect active Wnt signaling. (A, C) LacZ expressing cells (and thus canonical Wnt signaling) are present in the culture, while cell cultures from wild type hearts did not show any positive staining (B, D). Cells of LacZ⁺ reporter hearts were isolated and cultured in DMEM with 10% fetal bovine serum (FBS). Wnt reporter positive staining increased upon stimulation with Lithium chloride, a strong chemical inducer of Wnt signaling. (E) Xgal staining on control treatment with 20mM NaCl showing some blue spots. (F) Upon stimulation with 20mM LiCl, Xgal staining increased in intensity and number of cells staining positively. Scale bar represents 20μm, 400x magnification.



Supplementary Figure 2

Using immunohistochemistry to reveal co-localization, frozen sections were fluorescently stained for β -galactosidase (red) and Hoechst (nuclei, blue). (A) vWF+ endothelial cells (green) expressing LacZ surrounding a vessel. (B) α SMA+ fibroblast and vascular smooth muscle cells (C) with LacZ+ nuclei were present after myocardial infarction. (D) Isotype control for β -galactosidase (red) showing unstained nuclei only. Scale bar represents 20 μ m, 400x magnification.

5



Martinus I.F.J. Oerlemans^{1,*}

Willy A. Noort^{1,2,4,*}

Henk Rozemuller³

Dries Feyen¹

Sridevi Jaksani^{1,2}

David Stecher¹

Benno Naaijken³

Anton C. Martens^{3,4}

Hans-Jörg Bühring⁵

Pieter A. Doevendans^{1,2}

Joost P.G. Sluijter^{1,2}

¹ Department of Cardiology, University Medical Center Utrecht, Utrecht, The Netherlands

² Interuniversity Cardiology Institute of the Netherlands (ICIN), Utrecht, The Netherlands

³ Department of Immunology, University Medical Center Utrecht, Utrecht, The Netherlands

⁴ Department of Cell Biology, University Medical Center Utrecht, Utrecht, The Netherlands

⁵ University Clinic of Tübingen, Department of Internal Medicine II, Division of Hematology, Oncology and Immunology, Tübingen, Germany

** authors contributed equally*

Human *versus* Porcine Mesenchymal Stromal Cells: Phenotype, Differentiation Potential, Immunomodulation and Cardiac Improvement after Transplantation

J Cell Mol Med 2012; 16: 1827-1839

ABSTRACT

Although Mesenchymal Stromal Cells (MSC) have been applied clinically to treat cardiac diseases, it is unclear how and to which extent transplanted MSC exert their beneficial effects. To address these questions, pre-clinical MSC administrations are needed for which pigs appear to be the species of choice. This requires the use of porcine cells to prevent immune rejection. However, it is currently unknown to what extent porcine MSC (pMSC) resemble human MSC (hMSC). Aim of this study was to compare MSC from porcine bone marrow (BM) with human cells for phenotype, multi-lineage differentiation potential, immune-modulatory capacity and the effect on cardiac function after transplantation in a mouse model of myocardial infarction.

Flow cytometric analysis revealed that pMSC expressed surface antigens also found on hMSC, including CD90, MSCA-1 (TNAP/ W8B2 antigen), CD44, CD29, and SLA class I. Clonogenic outgrowth was significantly enriched following selection of CD271+ cells from BM of human and pig (129±29 and 1,961±485 fold, respectively). hMSC and pMSC differentiated comparably into the adipogenic, osteogenic or chondrogenic lineages, although pMSC formed fat much faster than hMSC. Immuno-modulation, an important feature of hMSC, was clearly demonstrated for pMSC when co-cultured with porcine peripheral blood cells stimulated with PMA and pIL-2. Finally, pMSC transplantation after myocardial infarction attenuated adverse remodeling to a similar extent as hMSC when compared to control saline injection. These findings demonstrate that pMSC have comparable characteristics and functionality with hMSC, making reliable extrapolation of pre-clinical pMSC studies into a clinical setting very well possible.

INTRODUCTION

Studies on bone marrow (BM) cell transplantation after acute myocardial infarction (MI) or for chronic myocardial ischemia are accumulating¹⁻⁵. Most studies showed significant improvement in cardiac function, however, these were only modest when compared with control patients^{6,7}. Two main mechanisms have been put forward to be responsible for the observed improvement in myocardial perfusion. First, BM cells might differentiate into endothelial cells, smooth muscle cells or cardiomyocytes. However, an active participation of these transplanted cells in regeneration of tissue has not been convincingly demonstrated. Second, transplanted BM cells secrete paracrine factors, which promote angiogenesis, exert cytoprotective effects, recruit resident cardiac stem cells, reduce inflammatory responses, and decrease fibrosis and stiffness of the scar⁸⁻¹³. BM comprises a heterogeneous population of cells, however, many of the beneficial activities have been ascribed to the Mesenchymal Stromal Cell (MSC).

For better understanding and improvement of cellular therapy, extended pre-clinical studies are most important. The porcine heart shows close similarities with the human heart in terms of size, structure and function. In recent years, pre-clinical studies in pigs focussed on issues such as differences in number of MSCs injected, autologous versus allogeneic cells injected, time of delivery of cells after myocardial infarction (MI), and route of delivery¹⁴⁻¹⁶. Although culture-expanded porcine MSCs (pMSC) were used in these studies, the characterization and knowledge on their functional potential has lagged behind, and no direct comparison between hMSC and pMSC was made. Reliable extrapolation of pre-clinical data to the clinical situation highly depends on similarities between human and porcine MSC.

In 2006, the International Society of Cell Therapy (ISCT) formulated an international definition of MSC to standardize isolation and characterization of MSC¹⁷. The minimal criteria include; 1) adherence to plastic under standard culture conditions, 2) expression of CD105, CD73, CD90 and a lack in expression of CD45, CD34, CD14 or CD11b, CD79 or CD19 and HLA-DR, 3) differentiation *in vitro* towards osteoblasts, adipocytes and chondrocytes. Additional features are the immunosuppressive potential *in vitro* and *in vivo*¹⁸⁻²¹, and the possibility to enrich MSC by selecting CD271+ cells. The immune-modulatory potential of MSC is applied in clinical trials to prevent and treat graft-versus-host disease and prevent graft rejection²²⁻²⁴. This capacity further intensifies the interest for MSC in cellular therapy. Upon selecting CD271+ cells from fresh BM, an enrichment in MSC frequency can be obtained, which therefore can be used as a marker for MSC²⁵⁻²⁷.

Aim of our study was to compare porcine versus human MSC (pMSC versus hMSC) in terms of phenotyping, multi-lineage differentiation potential and CD271+ and CD271-enrichment of MSC. Furthermore, we compared the immune-modulatory capacity of pMSC and hMSC *in vitro* after co-culturing with peripheral blood mononuclear cells (PBMC). Finally, we compared the effect of pMSC *versus* hMSC transplantation on cardiac function after myocardial infarction.

MATERIALS AND METHODS

Isolation, expansion and determination of frequency of MSC from bone marrow

pMSC

Mononuclear cells (MNC) were obtained after ficoll separation (1.077 g/ml, GE Healthcare, Uppsala, Sweden) from BM of pigs (\pm six month old landrace pigs, 55-85 kg). Animal experiments were performed according to the '*Guide for Care and Use of Laboratory Animals*', and were approved by the Animal Ethical Experimentation Committee, Utrecht University. MNC were plated in 0.1% gelatin-coated 6-wells plates (5×10^5 MNC/cm²) as previously described²⁸ and cultured in medium 199 (Lonza, Verviers, Belgium) supplemented with 10% heat inactivated fetal bovine serum (HI FBS) (HyClone, Logan, UT, USA), 100 Units/ml penicillin and 100 μ g/ml streptomycin (P/S) (PAA laboratories GmbH, Cölbe, Germany), 20 μ g/ml Endothelial Cell Growth Factor (Roche diagnostics, Indianapolis, USA) and 8 IU/ml heparin (Leo Pharma, Breda, The Netherlands) at 37°C under 5% CO₂/95% air atmosphere. Additional medium for expansion: α -MEM (Gibco, Paisley, UK) with HI FBS, P/S, L-ascorbic acid-2-phosphate (0.2 mM) and bFGF (1ng/ml). After 48-72 hrs, non-adherent cells were removed and adherent cells refreshed with medium.

hMSC

hMSC were obtained from healthy BM donors after informed consent and expanded at the GMP facility of the Stem Cell Laboratory of the UMC Utrecht.

CFU-F assays

0.5, 1.0, 2.5, 5 or 10×10^6 cells were plated in T25, either after ficoll separation or after lysing red blood cells (RBC) from the BM (lysing buffer 8.818g NH₄Cl, 1.062g KHCO₃, 0.03952g Na₂EDTA, for 10 min on ice), and cultured for an additional 10 days (Friedenstein et al., 1976). Subsequently, adherent cells were washed twice with PBS and fixed with ice-cold methanol for 15 minutes at 4°C. To visualise colonies, cells were stained with Giemsa (Sigma-Aldrich, Zwijndrecht, The Netherlands) diluted 1:8 with H₂O for 15 minutes at RT and washed twice with H₂O. CFU-F colonies containing at least 50 cells were scored using an inverted microscope (Zeiss, Munich, Germany).

Antibodies for flow cytometric analysis and sorting

For the screening of cultured MSC from human and pig a panel of more than 50 antibodies (Abs) was used that contained the following commercially available Abs against human CD3, CD13, CD14, CD19, CD29, CD31, CD34, CD44, CD45, CD49e, CD55, CD71, CD73, CD90, CD117, CD133, CD146, HLA-ABC, HLA-DR (Becton Dickinson (BD), Franklin Lakes, NJ, USA), CD49b (Biolegend, San Diego, CA), CD105 (Ansell Corp, Bayport, MN, USA), CD166 (clone 3A6, RDI Concord MA), CD235a (Dako, Glostrup, Denmark), CD271 (Clone 20.4 against Low-affinity NGFR, Miltenyi Biotec, Bergisch Gladbach, Germany), Sca-1 (BD), ALP (clone B4-78-c, Hybridoma Bank, Iowa city, Iowa, USA), KDR (R&D Systems, Minneapolis, MN, USA), SSEA-4 (clone MC-813-70, Hybridoma Bank), W8B2 (human mesenchymal stem cell antigen-1 (MSCA-1), Biolegend), W4A5B5 (Biolegend). Additionally, a series of Abs showing reactivity with the CD271 positive subpopulation in human BM

with putative MSC specificity was used; W3C4E11 (CD349; frizzled-9), W5C4, and 39D5 (CD56 epitope expressed on MSC but not on NK cells) or MY31 (CD56 on MSC and NK cells), W1C3, W6B3H10 (CD133), 24D2E2 (CD340), W5C5A8, 58B1A3, CH3A4A7AR (CD340), 67D2 (CD164), W7C5 (CD109), 67A4 (CD324), 28D4D0 (CD140b), HEK-3D6C9, W3D5A9 and CUB1 (CD318)²⁹. Binding of the non-conjugated Ab was detected using isotype (IgG, IgG1, IgM or IgG3) PE-conjugated goat anti-mouse antisera (Southern Biotechnology Associates, Inc, Birmingham, USA). Additional antibodies which specifically recognizing porcine cells (Ab Serotec, Düsseldorf, Germany) were directed against CD45 (clone K252-1E4), CD31 (clone LCI-4), SLA class I (clone JM1E3), or SLA class II DR (clone 2E9/13). The antibodies against CD49d (Thermo Scientific, Rockford, IL, USA), and CD49f (GoH3, Becton Dickinson) had been reported to show cross reactivity with porcine protein. Flow cytometric analysis was performed on a FACS Calibur (Becton Dickinson, Biosciences, San Jose, CA), or a Cytomics FC 500 (Beckman Coulter, Fullerton, CA, USA), while for cell sorting the FACS Aria (Becton Dickinson) was used. At least 3 different MSC donors were analyzed, and sorting of CD271+ cells was performed at least three times from different BM samples. 1×10^6 per BM sample and 1×10^4 cells per MSC culture were measured within a "live cell" gate based on light scatter properties. To calculate the enrichment factors for the CFU-F after single or double Ab labelling, we divided the frequency of CFU-F in the sorted fraction by the frequency of CFU-F in the starting material, i.e. the MNC fraction after ficoll separation of the BM aspirates.

Osteogenic and adipogenic differentiation potential

Three different protocols were used for induction towards osteogenesis and adipogenesis; protocol A (21 days, previously used for murine MSC as well as hMSC^{30, 31}; protocol B (18 days, previously used for hMSC³²; and protocol C (10 days, for hMSC, developed by Miltenyi Biotec, Bergisch Gladbach, Germany). All differentiations were performed in triplicate in 24 wells plates (2.5×10^4 cells/cm²), using MSC of passage ≥ 4 .

Protocol A

Osteogenic differentiation

MSC were differentiated in basic medium (α -MEM (Gibco, Paisley, UK) supplemented with L-ascorbic acid-2-phosphate (280 μ M), dexamethasone (10^{-7} M), and 5 mM β -glycerophosphate (from day 7 onwards).

Adipogenic differentiation

Similar as for osteogenic differentiation, but medium was additionally supplemented with indomethacin (50 μ M), insulin (10ug/ml), and 1-methyl-3-isobutylxanthine (IBMX, 5 μ M).

Protocol B

Osteogenic differentiation

MSC were cultured in DMEM (Gibco, Paisley, UK) supplemented with L-ascorbic acid-2-phosphate (50 μ M), dexamethasone (0.1 μ M), and β -glycerol phosphate (10 mM).

Adipogenic differentiation

MSC were cultured for 48-72hrs in induction medium (DMEM supplemented with dexamethasone (1 μ M), indomethacin (100 μ M), insulin (10 μ g/ml) and IBMX (500 μ M)),

followed by a 24hrs culturing in maintenance medium. This alternate culturing in induction and maintenance medium was repeated two times, accomplished by a culturing period of 1 week in maintenance medium.

Protocol C

MSC were cultured in media manufactured by Miltenyi (Nonhematopoetic (NH) stem cell media) for osteogenic and adipogenic differentiation.

Microscopic observations during osteogenic and adipogenic induction

To determine the extent of differentiation, cells were checked twice a week and classified as indicated in Table 2 for adipogenic or osteogenic differentiation.

Histochemical staining and quantification

After differentiation, cells were washed with PBS, fixed with 4% formalin for 10 minutes, and alkaline phosphatase expression was determined with a substrate solution of naphtholphosphate AS-MX (0.2mg/ml) and Fast Blue RR Salt (0.6mg/ml) in TRIS buffer (0.1 M pH 8.9) with MgSO₄ (0.3 mg/ml). After washing with PBS, cells were decolorized with ethanol/sodium hydroxide, and its supernatant was measured spectrophotometrically (550nm, Bio-Rad microplate reader model 550). To detect calcium deposition, the fixated cells were stained with Alizarin Red S (2% in distilled water, pH of 5.5 with ammonium hydroxide) for 2-5 minutes, rinsed with PBS, and quantified by extracting Alizerin Red S from the cells with a 10% Cetylpyridinium ClPO₄ buffer and measurement at 550nm. Adipocytes were fixed, stained with Oil-Red-O (30mg Oil-Red-O/ml 60% isopropanol) for 10 minutes, decolorized with ethanol, and extracts were measured spectrophotometrically at 550nm.

Quantitative polymerase chain reaction for detecting osteogenic and adipogenic genes

Total RNA was isolated using TriPure (Roche, Indianapolis, USA), according to the instructions of the manufacturer. From 500ng RNA, free of genomic DNA, cDNA was generated (iScript™ cDNA Synthesis Kit; Bio Rad, Hercules, California, USA). For quantitative RT-PCR (qPCR) (Bio-Rad, MyiQ™ System), cDNA was mixed with iQ™ SYBR® Green Supermix (Bio-Rad) and specific forward and reverse primers (Invitrogen Ltd, Paisley, UK). Primers used for pig; for β-actin as a housekeeping gene, forward ATC CAC GAG ACC ACC TTC AA, reversed TGA TCT CCT TCT GCA TCC TG, for the adipogenic genes, aP2, forward AAC CCA ACC TGA TCA TCA CTG, reversed TCT TTC CAT CCC ACT TCT GC, and PPARγ2, forward AGG AGC AGA GCA AAG AGG, reversed AGA GTT ACT TGG TCA TTC AGG. For the osteogenic genes; osteocalcin, forward CAG GAG GGA GGT GTG TGA G, reversed TGC GAG GTC TAG GCT ATG C, alkaline phosphatase, forward CCA AAG GCT TCT TCT TGC TG, reversed TGT ACC CGC CAA AGG TAA AG, and osteopontin, forward AAG GAC AGT CAG GAG ACG AG, reversed TCA ATC ACA TTG GAA TGC TC. After normalisation for β-actin (housekeeping), relative gene expression was calculated by ΔΔCt as previously described.

Chondrogenic differentiation potential

2.5x10⁵ MSC were pelleted into 15 ml tubes via centrifugation (800 x g for 5 minutes), and cultured in chondrogenic medium (high glucose (4.5 g/l) DMEM with 6.25 μg/ml insulin, 6.25 μg/ml transferrin, 6.25 μg/ml selenous acid, 5.33 μg/ml linoleic acid, 1.25 mg/ml bovine

serum albumin (ITS+, Collaborative Research, Cambridge, MA), 0.1 μ M dexamethasone, 10 ng/ml TGF- β 1, 50 μ g/ml ascorbate 2-phosphate, 2 mM pyruvate, and P/S) [24]. At harvest, the pellets were fixed in 4% formaldehyde, paraffin embedded, sectioned and analyzed after staining with hematoxylin, fast green and safranin-O to visualize collagen accumulation and proteoglycans.

Immunomodulatory effect of MSC on peripheral blood (PB)

MNC were obtained after ficoll separation from porcine and human peripheral blood (pPBMC and hPBMC, respectively), and stained with carboxyfluorescein diacetate succinimidyl ester (CFSE; 0.6 μ M/ml, 10min 37° C, Molecular Probes, Invitrogen Ltd). In 96 wells plates, 2×10^4 pPBMC or hPBMC were maximally stimulated with phorbol-12-myristate-13-acetate (PMA; 50ng/ml) in combination with pIL-2 or hIL-2 (150 IU/ml), respectively, or with OKT3 (anti-CD3 antibody; 2 μ g/ml) in case of hPBMC. Stimulation was performed in the presence or absence of MSC (2×10^4). After 6 days of culture CFSE expression of PBMC was measured by flow cytometry^{33, 34}.

Myocardial infarction and MSC injection

All animal procedures were approved in accordance with the Guide for the Care and Use of Laboratory Animals, with prior approval of the Animal Ethical Experimentation Committee, Utrecht University. In NOD/SCID mice (male, aged 9–12 weeks), myocardial infarction was induced by LAD occlusion as described previously³⁵. Human or porcine MSCs were injected (500.000 cells per animal) in the border zone by two injections of 5μ l³⁶. Cardiac parameters were determined at baseline and at 28 days post-MI. End-diastolic volume (EDV), end-systolic volume (ESV) and ejection fraction were determined 4 weeks post-MI by high resolution MRI (9.4T, Bruker Biospin) as described³⁷. Analysis was performed using Q-mass for mice digital imaging software (Medis) by a blinded investigator. Heart sections of mice at 28 days post-MI were used to quantify the fibrotic scar using picrosirius red staining with circularly polarized light microscopy³⁸.

Characterization of transplanted cells

Characterization of transplanted cells by immunofluorescence was performed on 7 μ m cryosections. Mouse anti-integrin-b1 (1:50; SC-53711, SantaCruz) and rabbit anti-troponin-I (1:100, ab47003, Abcam) were used as primary antibodies, followed by Alexa-labeled (Invitrogen) secondary antibodies against mouse and rabbit. Sections were fixed in acetone, blocked with 2% bovine serum albumin (BSA) and incubated overnight with primary antibody. After incubation with secondary antibody for 1 hour, sections were washed in PBS and mounted in Fluoromount (Southern Biotech) after counterstaining with DAPI (Invitrogen).

Statistical analysis

Data are presented as mean \pm SEM. Differences between groups were analyzed by Mann-Whitney U, using a significance level of $P < 0.05$ (SPSS Statistics v17 Chicago, United States).

RESULTS

Isolation, expansion and frequency of MSC derived from porcine bone marrow

Colonies were found 7 to 12 days after plating MNC suspension from porcine BM (Figure 1A). After expansion of both human and pig MSC, pMSC (P>3, pMSC (Figure 1B) seemed to be less elongated and spindle-shaped than hMSC (Figure 1C). No differences in growth potential were observed between hMSC and pMSC during a period of 3 weeks (Figure 1D, population doubling times of 2.5, and 2.4 days, respectively). To determine pMSC frequency, CFU-F assays were performed (Figure 1E). Together with a higher starting amount of porcine BM cells, an increasing number of colonies was formed. Moreover, outgrowth of ficolled BM cells resulted in a 2-fold higher number of colonies compared to that of lysed BM cells at a dose of 1 and 2.5×10^6 cells. However, after correction for the original number of fresh BM cells used, both isolation methods resulted in equal numbers of CFU-F (Figure 1F).

Selection of CD271+ cells from human as well as porcine BM enrich for MSC frequency

Selection of CD271+ cells from human BM resulted in a significant increase in hMSC frequency following culture in a CFU-F assay (data not shown), as described before for hMSC^{39, 40}. Also from porcine BM, the outgrowth of CD271+ cells resulted in a significant higher number of colonies, as compared to unsorted BM cells (Supplementary Figure 1). Although not statistically different, the number of colonies cultured from the CD271- fraction of porcine bone marrow was less than the non-manipulated porcine BM.

Immunophenotypic characterization by flow cytometry

Culture-expanded pBM cells expressed several markers that are characteristic for hMSC (Table 1). The pMSC were positive for CD90, CD44, CD29, CD49d, CD49f, SLA class I, and negative for hematopoietic markers such as CD45, CD34, CD14. In addition, pMSC were negative for the endothelial marker CD31, positive for CD146, and had no expression of SLA class II and CD166. Unfortunately, no cross-reactivity was found on peripheral blood of pig for CD105, CD73, CD19, CD49b, ALP and SSEA4 antibodies. CD271 and W8B2, antigens used to enrich primary MSC from fresh bone marrow, were equally expressed on culture-expanded pMSC and hMSC. Other candidates, which have been used in the past to select primary MSC, like W4A5 and Stro-1^{41, 42}, were also expressed on culture-expanded MSC, however in lower percentages on pMSC than on hMSC.

Adipogenic differentiation potential

Several differentiation protocols are used for hMSC differentiation, but optimal conditions for differentiation of pMSC are currently not known. Therefore we included 3 different protocols and determined its effect on MSC differentiation. As for hMSC, diversity in differentiation potential was also observed for pMSC. Differentiation efficiency depended on the protocol used, but was also donor dependent (Table 2). Protocol A showed the largest potential for inducing adipogenic differentiation for both human and porcine MSC. Adipocytes were clearly formed in pMSC cultures during induction with protocol A, B or C as indicated by the accumulation of fat droplets. Interestingly, differentiating pMSC also

started to excrete fat (Figure 2A arrow and right panel), which did not occur in hMSC (Figure 2B; intracellular accumulation). The optimal differentiation for pMSC was already reached at 7-10 days (Figure 2C), while an additional period of 10-14 days was needed for hMSC (Figure 2E). Protocol A, B or C did not show significant differentiation differences for pMSC or hMSC, confirming microscopic observations (Table 2). Due to fat excretion after the

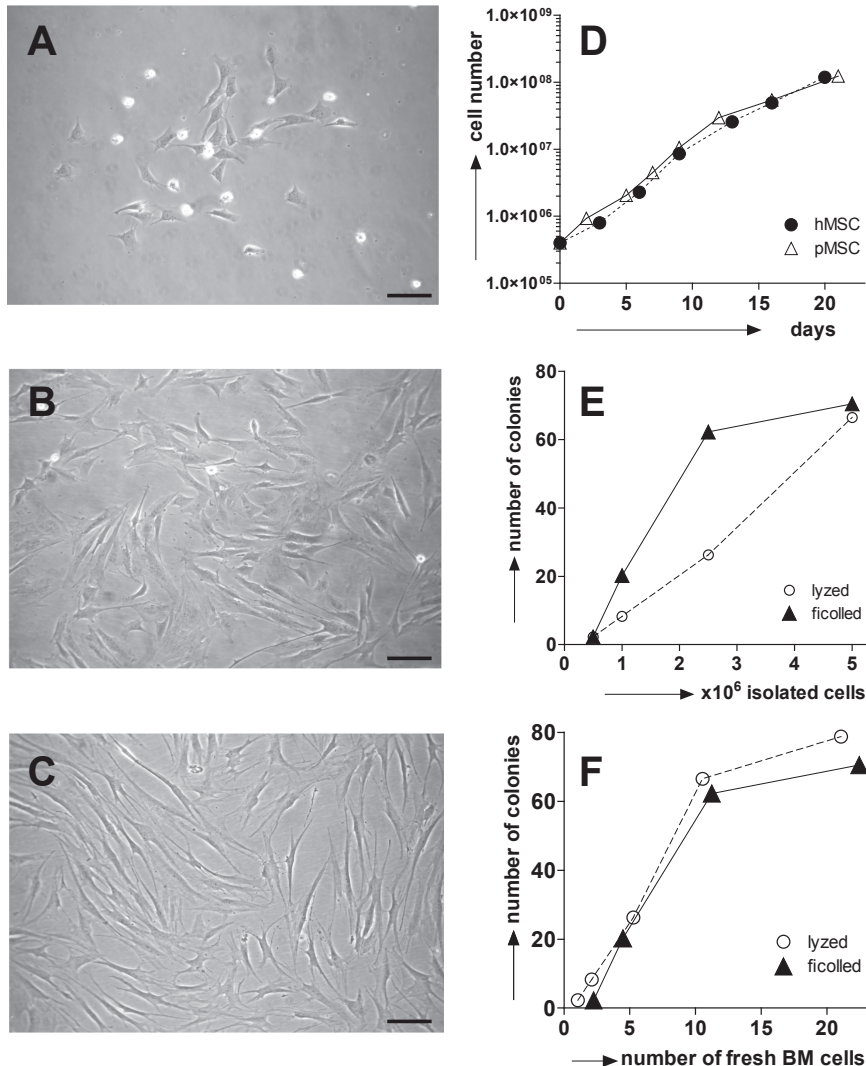


Figure 1 | Isolation and expansion of pMSC and hMSC

Colonies of different size appeared after plating porcine BM (A). At passage >3 pMSC (B) showed to be less elongated and spindle-shaped than hMSC (C). Growth potential of hMSC and pMSC (D). CFU-F assays of pMSC showing more colony outgrowth in ficolled BM than lysed BM after plating 1.0 and 2.5x10⁶ cells (E). Normalized number of colonies to the original amount of fresh BM cells showing equal numbers of CFU-F between both isolation methods (F). Scale bar 50µm.

optimal differentiation period, intracellular lipid accumulation within pMSC had decreased at week 3 as compared to hMSC differentiation. Therefore, quantitative measurements following decolorization of Oil-Red-O-stained adipocytes are an underestimation of the actual fat that was formed by pMSC (Figure 2D, F). Undifferentiated hMSC (data not shown) and adipogenic-induced human fibroblasts (Figure 2G) did not show any positive staining.

Table 1 | Surface antigens expression on hMSC and pMSC

	Surface antigen	Human	Pig
Minimal definition of hMSC	CD73	+++	nc
	CD90	+++	+++
	CD105	+++	nc
	CD34	-	-
	hCD45/pCD45	-	-
	CD14	-	-
	CD19	-	nc
Additional positive markers on hMSC	CD44	+++	+++
	CD166	+++	-
	CD29	+++	+++
	CD49b	+	nc
	CD49d	+	++
	CD49f	+	+
	CD49-e	+++	- CND
	HLA/SLA class I	+++	+++
HLA/SLA class II	-	-	
Candidate markers to enrich for primary MSC and "Bühning antibodies"	NGFR or CD271	±	±
	Stro-1	++	±
	W4A5B5	+	±
	W8B2B10	+	+
	58B1	++	++
	W5C4	++	++
Endothelial markers	hCD31/pCD31	-	-
	CD146	+++	+
Other stem cell markers	SSEA-4	++	nc
	SSEA-1	-	-
	c-kit	-	-
	Sca-1	-	-

human (h) or pig (p) specific antibody, nc = no cross reactivity, CND = cross reactivity not determined; +++ almost all cells are positive; ++ between 50-90% of cells are positive; + between 10-50% positive cells; ± 1-9% of cells are positive; - less than 1 % positive cells.

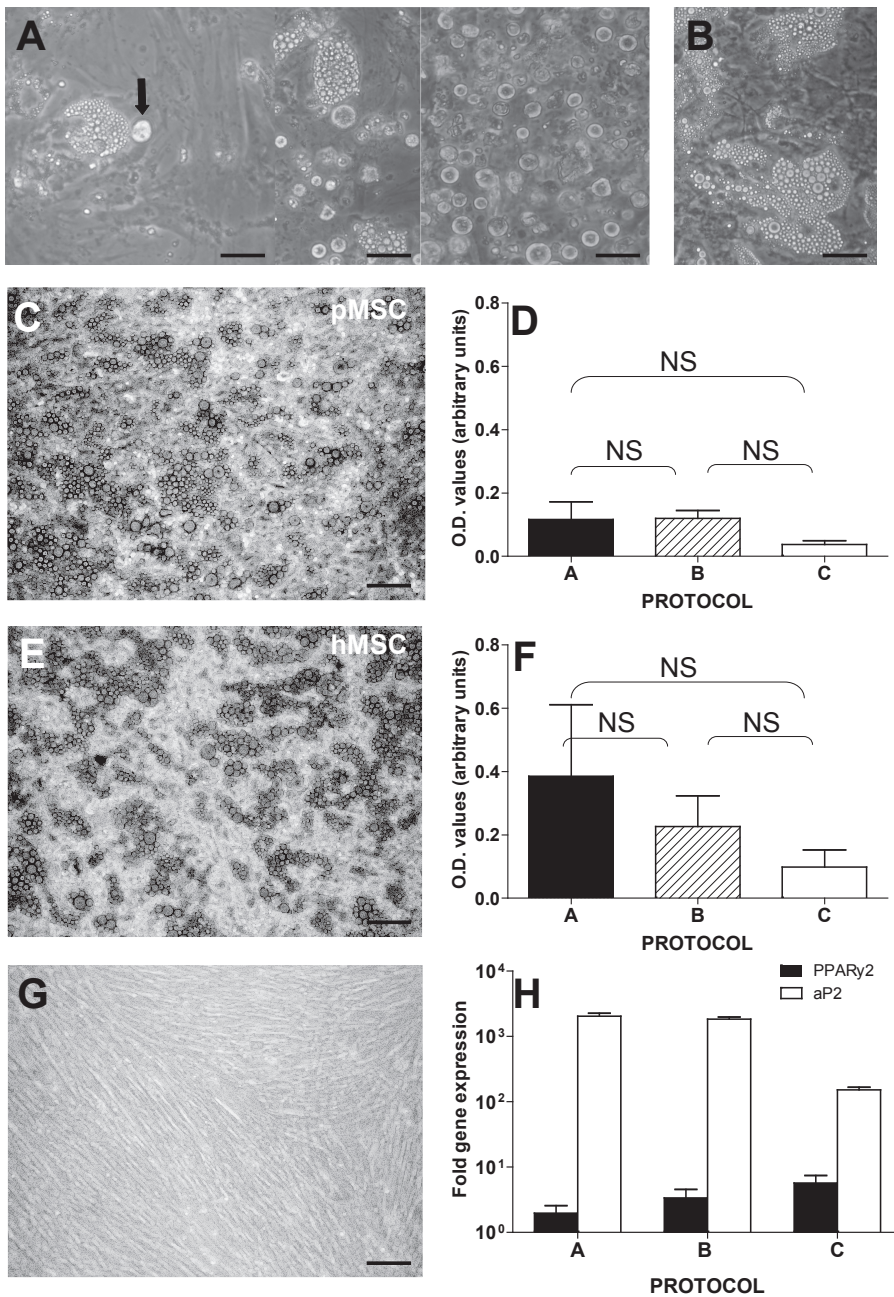


Figure 2 | Differentiation of pMSC and hMSC towards adipocytes

Representative porcine donor showing fat accumulation (A) and large amounts of fat excretion during differentiation (arrow and right part of A). During hMSC differentiation, fat was accumulated but not excreted (B). Consequently, fat accumulation during pMSC differentiation had decreased at week 3 as compared to hMSC differentiation (C and E). Quantitative measurements of Oil-Red-O-stained adipocytes (n=3-5) by pMSC and hMSC (D versus F). Human fibroblasts were not able to differentiate into adipocytes (G). mRNA levels of PPAR γ 2 and aP2 (n=4) are increased upon adipogenic differentiation in pMSC (H). Scale bars 25 μ m (A, B) and 50 μ m (C, E, G).

PPAR γ 2 and aP2 mRNA expression, indicative of adipogenic differentiation, were increased in all three protocols (Figure 2H). Based on aP2 mRNA expression, protocol A and B displayed the highest induction. PPAR 2 expression levels were not statistically significant between the three protocols.

Osteogenic differentiation potential

By combining the results of all differentiated donors, protocol A and C showed a trend for optimal osteogenic differentiation in hMSC (Figure 3C and D), and protocol C for pMSC (Figure 3A and B), confirming the observed microscopic data (Table 2). This was further confirmed by Alkaline Phosphatase (ALP) staining (data not shown). Osteogenic differentiation of human fibroblasts did not result in the formation of osteoblasts (Figure 3E). Osteopontin and ALP mRNA expression after osteogenic induction of pMSC were highly increased (Figure 3F), in favour of protocol B. Osteocalcin expression was enhanced after induction with protocol C, but not after induction with protocol A or B.

Table 2 | Diversity in adipogenic or osteogenic differentiation for human and pig MSC

hMSC	adipogenic differentiation			osteogenic differentiation		
	A	B	C	A	B	C
Protocol	A	B	C	A	B	C
donor 1: P4	+++	ND	ND	-	ND	ND
donor 2: P3	++++	+++	(+)	++	+	(+)
donor 3: P3	++++	+++	++	++	-	+++
donor 4: P7	+++	++	ND	+++	-	ND
donor 5: P4	+	++	(+)	(+)	+	+++
donor 6: P6	+++	++++	++	++	(+)	(+)
donor 7: P5	++++	++	(+)	+++	++	++
pMSC	adipogenic differentiation			osteogenic differentiation		
	A	B	C	A	B	C
Protocol	A	B	C	A	B	C
donor 1: P3	+++	ND	ND	-	ND	ND
donor 2: P6	++++	++	++++	-	-	ND
donor 3: P17	++	+++	+	+	-	+++
donor 5: P9	(+)	+	+	(+)	+	+++
donor 6: P4	++++	+++	+++	++	+++	(+)
donor 7: P6	+++	+	(+)	++++	+++	+++
donor 8: P3	+	++	(+)	++	++	(+)

Large variations were found within one protocol (donor variation), as well as within one particular donor when differentiated with protocol A, B or C (protocol variation). - = no differentiation observed. (+) = very less differentiation. + = some differentiation. ++ = obvious differentiation. +++ = strong differentiation. ND = Not Determined

Chondrogenic differentiation potential

After three weeks of induction, chondrogenic differentiation of pMSC resulted in pellets that were larger than those from hMSC (Figure 4). Since cell proliferation does not further occur during these culture conditions, the increase in pellet size is due to the formation of

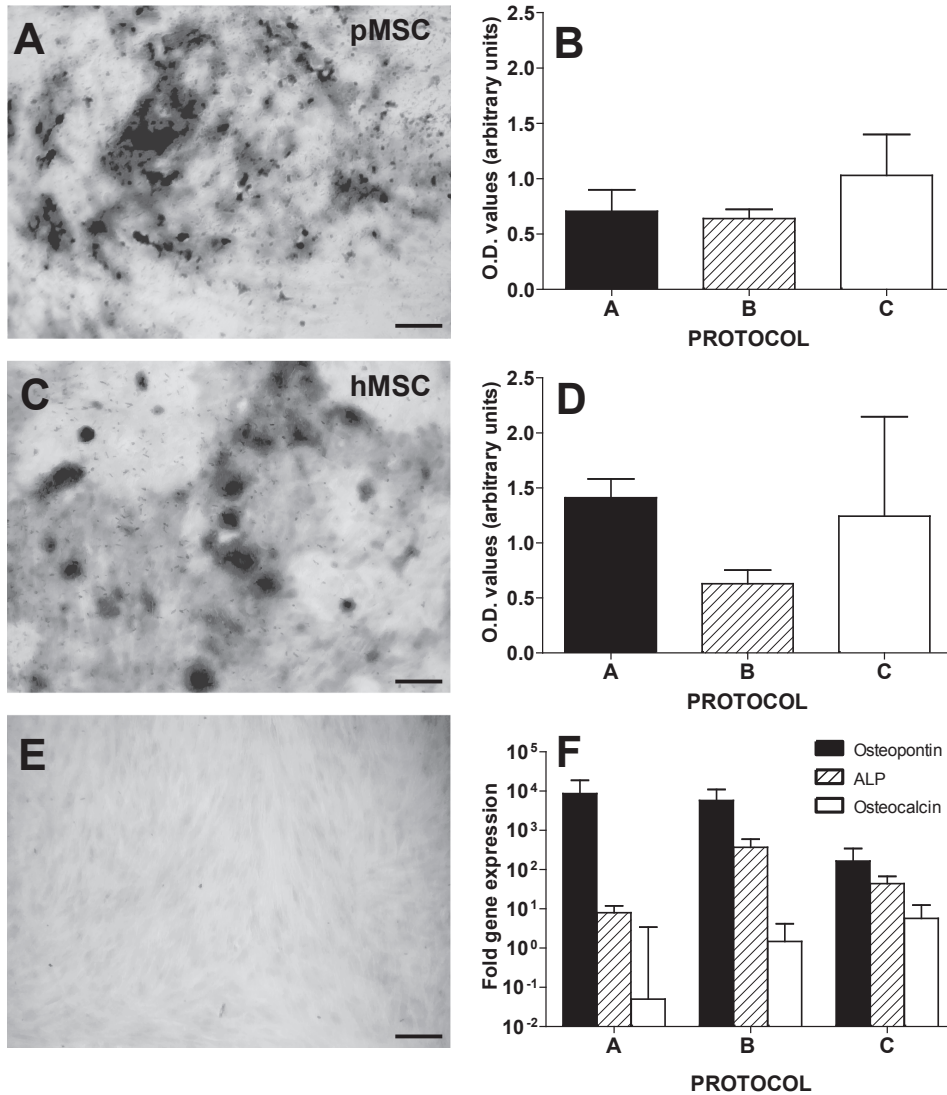


Figure 3 | Differentiation of pMSC and hMSC towards osteoblasts

Representative pictures of Alizarin Red S staining of pMSC and hMSC differentiation towards osteoblasts (A,C). After induction of differentiation ($n=3-5$ per protocol) large differences were observed within one protocol (donor variation), but also among the protocols as illustrated by the variation in quantitative measurements of the different protocols (B, pMSC; D, hMSC). Human fibroblasts were not able to differentiate into osteoblasts (E). mRNA levels of osteopontin, alkaline phosphatase (ALP) and osteocalcin ($n=4$) upon osteogenic differentiation in pMSC (F). Scale bar 50 μ m.

additional extracellular matrix or hypertrophic cell growth. Fast green staining, indicating collagen accumulation, was found for both human (left in Figure 4A and B) and pig MSC (Figure 4C-F). One particular pMSC donor showed massive chondrogenic differentiation, with clear lacunes formed (Figure 4 C and D).

Immunomodulatory effect on stimulated peripheral blood

Stimulation of human peripheral blood (PB) with OKT3 resulted in blast-like cells with a significant increase in size and granularity as compared to the non-stimulated cells (Figure 5A-D) and showed several cell divisions at day 6 of stimulation (Figure 5D, gates a-e). Non-stimulated cells were small, with no proliferation induced and a high CFSE staining (Figure 5A and B). Combined stimulation of human and porcine PB with PMA and IL-2 (human and pig) resulted in a significant number of dividing cells (Figure 5F and H, respectively); 52% hPBMNC divided 4 times, and 72% pPBMNC divided 5 times. In the presence of hMSC (10%) or pMSC (13%), division rates were significantly lower than in absence of MSC (Figure 5G and I).

Cardiac function and remodeling after MSC transplantation

Myocardial infarction was induced and mice received injections of either PBS (n=5), pMSC (n=4) or hMSC (n=4) in the border zone of the infarct. In all groups, both end-diastolic volume (EDV) and end-systolic volume (ESV) increased significantly post-MI when compared to baseline (Figure 6A and B). However, pMSC- and hMSC-injected animals exhibited less cardiac remodeling, demonstrated by a significantly smaller EDV ($132.4 \pm 18.0 \mu\text{l}$ pMSC; $137.6 \pm 18.3 \mu\text{l}$ hMSC; $P < 0.05$) and ESV ($105.8 \pm 19.7 \mu\text{l}$ pMSC; $115.9 \pm 18.1 \mu\text{l}$ hMSC; $P < 0.05$).

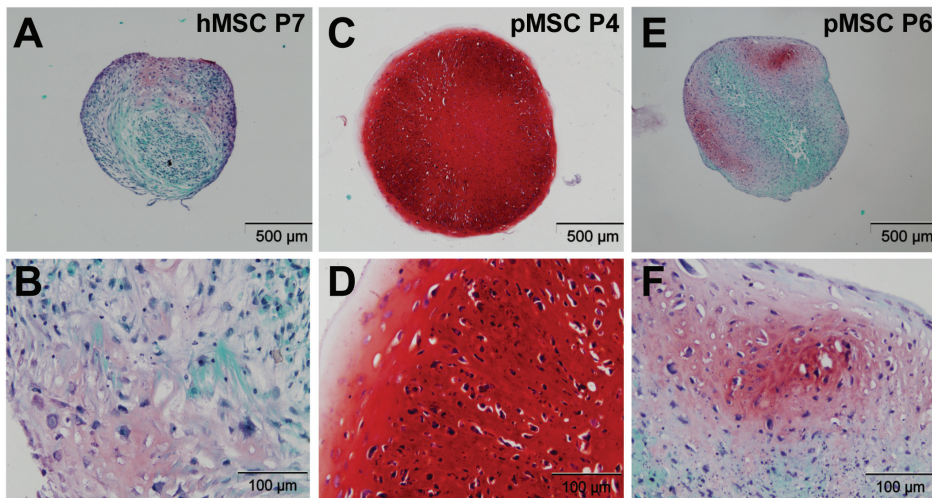


Figure 4 | Differentiation of pMSC and hMSC towards chondrocytes
pMSC show impressive differentiation towards chondrocytes (C-F), forming larger pellets than differentiated hMSC (A, B) and more extracellular matrix formation (B, D, F) illustrated by intense collagen staining (fast green staining) and proteoglycans (safranin-O).

Cardiac function significantly declined in all groups (Figure 4C), which was most pronounced in PBS-injected animals (EF $11.7 \pm 1.0\%$). Compared to PBS, pMSC transplantation significantly conserved EF ($21.4 \pm 4.8\%$; $P < 0.05$). Although borderline significant, this was similar in hMSC-injected animals ($16.4 \pm 2.6\%$; $P = 0.05$). Surviving MSCs were very low at 28 days post-MI and mainly resided in the infarcted area (Supplementary Figure 2). In accordance with less adverse remodeling, area of myocardial fibrosis (scar area) was less in MSC-transplanted animals (Supplementary Figure 3).

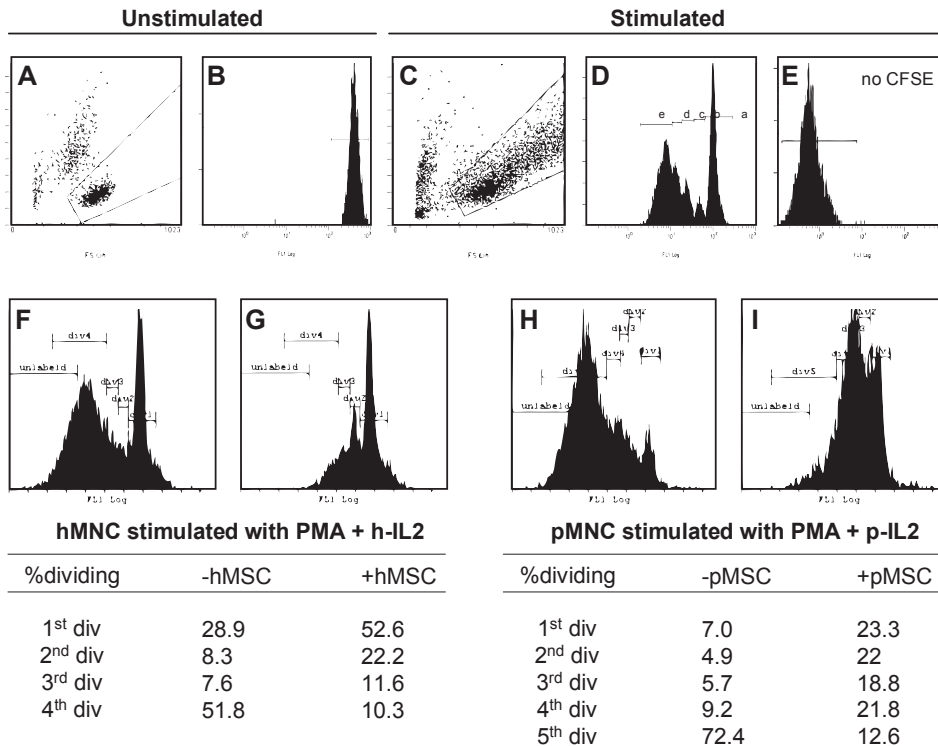


Figure 5 | pMSC suppress proliferation of T cells from pig

Unstimulated human PBMNC were small and CFSE staining was high (A, B). Stimulation resulted in an increase in size and proliferation (C, D). Unstimulated stimulated cells showed no CFSE staining (E). Combinational stimulation (PMA and IL-2) of hPBMNC (F) and pPBMNC (H) resulted in significant numbers of cells in 4th or 5th division after 6 days, which was markedly decreased in the presence of hPBMNC or pPBMNC (G, I).

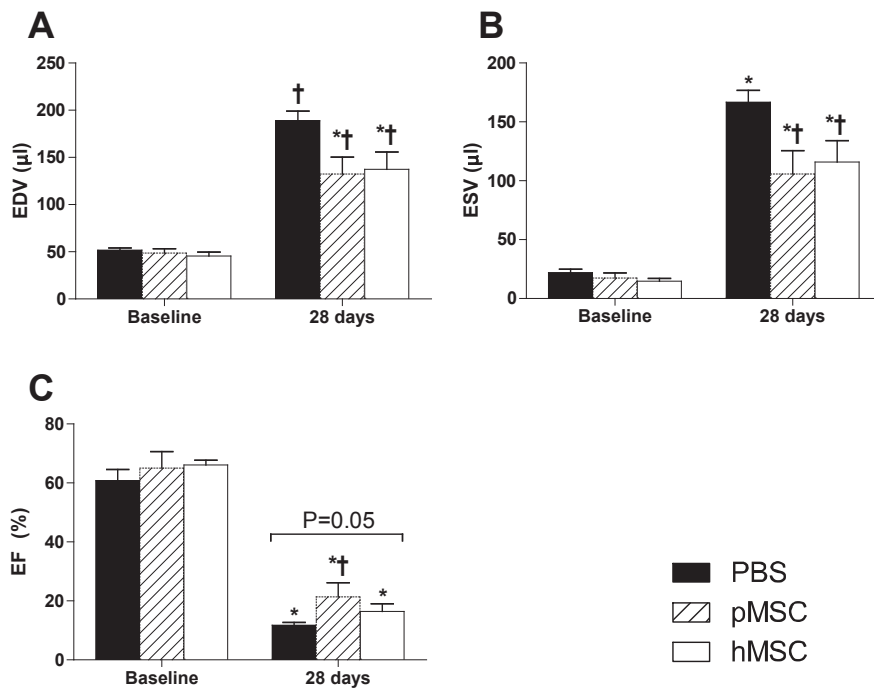


Figure 6 | Cardiac geometry and function after MSC transplantation

Animals injected with pMSC and hMSC exhibited less cardiac remodeling as indicated by significantly smaller EDV (A) and ESV (B) when compared to PBS-injected animals 28 days post-MI. pMSC transplantation improved EF when compared to PBS (C), with hMSC showing borderline significant improvements (n=4-5/group, *P<0.05 vs. baseline, †P<0.05 vs. PBS).

DISCUSSION

Although pre-clinical studies in pigs have been performed to improve our understanding of the effects of MSC therapy⁴³⁻⁴⁶, the characterization of pMSC has lagged behind. The comparison of pMSC with hMSC is necessary to reliably extrapolate pre-clinical data on pMSC therapy, which highly depends on similarities between porcine and human MSC. This is illustrated by the fact that clear differences in murine MSC were found depending on mice strains, required growth media, growth rates and presence of surface epitopes⁴⁷. The expression of markers on pig MSC, and differentiation to osteoblasts, adipocytes and chondrocytes have been described before⁴⁸⁻⁵⁰. However, a direct comparison of pMSC with hMSC for all the described MSC features is still lacking.

In our study, we therefore compared the immune-phenotype of pMSC and hMSC, as well as their multi-lineage differentiation potential using various differentiation protocols. Moreover, we demonstrated for the first time that isolation of CD271 (NGFR)+ cells from fresh porcine bone marrow enrich for MSC outgrowth, and that both pMSC and hMSC have immunosuppressive properties. Finally, we showed that pMSC transplantation improved cardiac function and attenuated remodeling to similar extent as hMSC after myocardial infarction in mice.

Small morphological differences were observed in culture; pMSC seemed to be less elongated and spindle-shaped than hMSC. Both cell types exhibited similar growth expansion potential following culture. Concerning the surface markers studied, hMSC and pMSC showed similar expression for most of them. However, for several markers we did not find cross-reactivity (CD105, CD73, CD19, CD49b, ALP and SSEA4), since most of the antibodies are directed to human. Unfortunately, we could not find porcine-reactive antibodies for most of these epitopes.

It is known that a significant enrichment in MSC can be obtained by selecting CD271+ cells from fresh human BM. We show for the first time that selecting CD271+ cells from porcine BM resulted in enrichment of MSC. This surface antigen seems to represent a true MSC marker present on primary MSC, which is well conserved among species and decreases in expression following culture-expansion⁵¹. In the same report, cross-reactivity on MSC for other antibodies was shown, including CD271, W8B2, W4A5, CD56, W3C4 (CD349), W5C4 and 58B1. In line with our findings, this might suggest that the minimal criteria for MSC as defined in 2006 need further adjustments¹⁷.

We used 3 different protocols for adipocytes and osteoblast differentiation, since a general consensus on the optimal differentiation conditions for these cells was not known. Therefore, three culture media were selected, which are commonly used for both porcine and human MSC differentiations to make a fair comparison possible. We showed that pMSC were able to differentiate to the osteogenic, adipogenic and chondrogenic lineages. Adipogenic differentiation kinetics of pMSC were faster than that of hMSC, and fat accumulated initially in the adipocytes itself, but was subsequently secreted. This secretion of fat was not observed in hMSC differentiation. From our results we can conclude that pMSC do not need other induction-stimuli for osteoblast/adipocyte differentiation than those used for hMSC. Nevertheless, variations in differentiation potential for pMSC as well as for hMSC donors were observed among and within protocols.

Diversities in differentiation potential are already known for human MSC as well as for mice MSC⁵², depending on the heterogeneity of the starting population and their subsequent expansion. Attempts to define the starting population more precisely with limited differentiation potential for specific applications, thereby enriching for naïve MSC or a population of choice, have been described previously⁵³⁻⁵⁸. Recently, human BM cells were selected, expressing CD271 and W8B2, with no expression for CD56, which differentiated preferentially to adipocytes in contrast to CD271+W8B2+CD56+ cells, showing primarily chondrocytic differentiation⁵⁹.

In the present study, we demonstrate that pMSC, like hMSC, also have potent immunosuppressive capacities. The immunosuppressive effect of MSC has been ascribed to a non-specific anti-proliferative effect⁶⁰. However, if host MSC and allogeneic donor BM cells were combined for transplantation, engraftment of transplanted cells was enhanced⁶¹. When transplanted MSC and BM cells were both of an allogeneic donor, engraftment was not significantly improved, suggesting that MSC are not intrinsically immuno-privileged and trigger immune responses *in vivo*. This underlines the need for autologous pMSC in pre-clinical models in order to prevent an immune response, thereby enhancing engraftment of donor cells.

We also compared the effect of pMSC with hMSC transplantation on functional improvement after myocardial infarction *in vivo*, another important feature of MSC. Transplantation of pMSC significantly improved cardiac function and attenuated adverse remodeling to a similar extent as hMSC transplantation, accompanied by less myocardial fibrosis. Since we could hardly see transplanted cells connecting with viable myocardial cells, we do not think that physical and electronic integration is the explanation of the observed effects, rather a paracrine benefit for the endogenous cells. Although the exact mechanism (paracrine effects or differentiation) remains a matter of debate^{62, 63}, pMSC performed equally well as hMSC. Therefore, we indirectly assumed that pMSC and hMSC might produce the same (cocktail of) growth factors.

In conclusion, we found that pMSC were similar in phenotype and multi-lineage differentiation which did not require different osteoblast/adipocyte differentiation protocols when compared to hMSC, although some phenotypical differences do exist between the MSC populations. We demonstrated for the first time that isolation of CD271+ (NGFR+) cells from fresh porcine bone marrow enrich for MSC and that pMSC have comparable immunosuppressive properties *in vitro*. Finally, we showed that pMSC transplantation after MI exhibited a similar cardiac improvement as hMSC *in vivo*.

These findings demonstrate that pMSC are comparable with hMSC, making reliable functional and safety extrapolation of future porcine pre-clinical studies on cellular therapy to the clinical situation possible.

Acknowledgements

Cees Verlaan and Hans Vosmeer are acknowledged for collecting porcine BM and PB. Dr I. Slaper and Dr D. Gawlitta kindly provided us with hMSC. Dr I. Hoefer helped with obtaining flow cytometric data. Alain van Mil supported in the qPCR work. Mattie van Rijen is acknowledged for chondrogenic staining of differentiated MSC. Dr T. Guichelaar advised in the immune-modulation assay. Krista den Ouden is acknowledged for mouse MRI measurement and analysis.

Author Contributions

WN, MO, HR, DF, SJ, DS and BN performed the research; WN, PD and JS designed the research study; WN, MO, DF, SJ, DS and JS analyzed the data; WN, MO, HR, HB and JS wrote the manuscript; AM, HB, PD and JS approved the final manuscript.

Sources of Funding

The work was supported by the Netherlands Heart Foundation (2003B07304), BSIK program "Dutch Program for Tissue Engineering" grant 6746 and grant 6729, a Bekalis price, SMARTCARE project (BioMedical Materials, BMM), a grant from the Deutsche Forschungsgemeinschaft, project BU 516/2-1 and "Stichting Swaeneborgh".

Conflict of Interests

The authors confirm that there are no conflicts of interest.

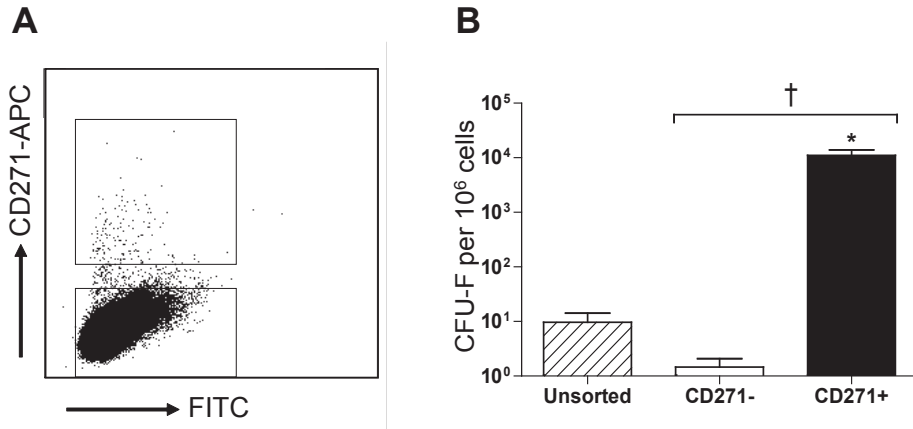
REFERENCES

1. Segers VF, Lee RT. Stem-cell therapy for cardiac disease. *Nature* 2008;451:937-942.
2. van Ramshorst J., Bax JJ, Beeres SL, et al. Intramyocardial bone marrow cell injection for chronic myocardial ischemia: a randomized controlled trial. *JAMA* 2009;301:1997-2004.
3. Chen SL, Fang WW, Ye F, et al. Effect on left ventricular function of intracoronary transplantation of autologous bone marrow mesenchymal stem cell in patients with acute myocardial infarction. *Am J Cardiol* 2004;94:92-95.
4. Chen S, Liu Z, Tian N, et al. Intracoronary transplantation of autologous bone marrow mesenchymal stem cells for ischemic cardiomyopathy due to isolated chronic occluded left anterior descending artery. *J Invasive Cardiol* 2006;18:552-556.
5. Katritsis DG, Sotiropoulou PA, Karvouni E, et al. Transcoronary transplantation of autologous mesenchymal stem cells and endothelial progenitors into infarcted human myocardium. *Catheter Cardiovasc Interv* 2005;65:321-329.
6. Abdel-Latif A, Bolli R, Tleyjeh IM, et al. Adult bone marrow-derived cells for cardiac repair: a systematic review and meta-analysis. *Arch Intern Med* 2007;167:989-997.
7. van der Spoel TI, Jansen Of Lorkeers SJ, Agostoni P, et al. Human relevance of pre-clinical studies in stem cell therapy: systematic review and meta-analysis of large animal models of ischaemic heart disease. *Cardiovasc Res* 2011.
8. Burchfield JS, Dimmeler S. Role of paracrine factors in stem and progenitor cell mediated cardiac repair and tissue fibrosis. *Fibrogenesis Tissue Repair* 2008;1:4.
9. Benvenuto F, Ferrari S, Gerdoni E, et al. Human mesenchymal stem cells promote survival of T cells in a quiescent state. *Stem Cells* 2007;25:1753-1760.
10. Nesselmann C, Ma N, Bieback K, et al. Mesenchymal stem cells and cardiac repair. *J Cell Mol Med* 2008;12:1795-1810.
11. Satija NK, Singh VK, Verma YK, et al. Mesenchymal stem cell-based therapy: a new paradigm in regenerative medicine. *J Cell Mol Med* 2009;13:4385-4402.
12. Wen Z, Zheng S, Zhou C, et al. Repair mechanisms of bone marrow mesenchymal stem cells in myocardial infarction. *J Cell Mol Med* 2011;15:1032-1043.
13. Vrijisen KR, Sluijter JP, Schuchardt MW, et al. Cardiomyocyte progenitor cell-derived exosomes stimulate migration of endothelial cells. *J Cell Mol Med* 2010;14:1064-1070.
14. Shake JG, Gruber PJ, Baumgartner WA, et al. Mesenchymal stem cell implantation in a swine myocardial infarct model: engraftment and functional effects. *Ann Thorac Surg* 2002;73:1919-1925.
15. Amado LC, Schuleri KH, Saliaris AP, et al. Multimodality noninvasive imaging demonstrates *in vivo* cardiac regeneration after mesenchymal stem cell therapy. *J Am Coll Cardiol* 2006;48:2116-2124.
16. Halkos ME, Zhao ZQ, Kerendi F, et al. Intravenous infusion of mesenchymal stem cells enhances regional perfusion and improves ventricular function in a porcine model of myocardial infarction. *Basic Res Cardiol* 2008;103:525-536.
17. Dominici M, Le BK, Mueller I, et al. Minimal criteria for defining multipotent mesenchymal stromal cells. The International Society for Cellular Therapy position statement. *Cytotherapy* 2006;8:315-317.
18. Di Nicola M, Carlo-Stella C, Magni M, et al. Human bone marrow stromal cells suppress T-lymphocyte proliferation induced by cellular or nonspecific mitogenic stimuli. *Blood* 2002;99:3838-3843.
19. Le Blanc K, Frassoni F, Ball L, et al. Mesenchymal stem cells for treatment of steroid-resistant, severe, acute graft-versus-host disease: a phase II study. *Lancet* 2008;371:1579-1586.
20. Le Blanc K, Rasmusson I, Sundberg B, et al. Treatment of severe acute graft-versus-host disease with third party haploidentical mesenchymal stem cells. *Lancet* 2004;363:1439-1441.
21. Ball LM, Bernardo ME, Roelofs H, et al. Cotransplantation of ex vivo expanded mesenchymal stem cells accelerates lymphocyte recovery and may reduce the risk of graft failure in haploidentical hematopoietic stem-cell transplantation. *Blood* 2007;110:2764-2767.
22. Le Blanc K, Frassoni F, Ball L, et al. Mesenchymal stem cells for treatment of steroid-resistant, severe, acute graft-versus-host disease: a phase II study. *Lancet* 2008;371:1579-1586.

23. Le Blanc K, Rasmusson I, Sundberg B, et al. Treatment of severe acute graft-versus-host disease with third party haploidentical mesenchymal stem cells. *Lancet* 2004;363:1439-1441.
24. Ball LM, Bernardo ME, Roelofs H, et al. Cotransplantation of ex vivo expanded mesenchymal stem cells accelerates lymphocyte recovery and may reduce the risk of graft failure in haploidentical hematopoietic stem-cell transplantation. *Blood* 2007;110:2764-2767.
25. Quirici N, Soligo D, Bossolasco P, et al. Isolation of bone marrow mesenchymal stem cells by anti-nerve growth factor receptor antibodies. *Exp Hematol* 2002;30:783-791.
26. Battula VL, Trembl S, Bareiss PM, et al. Isolation of functionally distinct mesenchymal stem cell subsets using antibodies against CD56, CD271, and mesenchymal stem cell antigen-1. *Haematologica* 2009;94:173-184.
27. Bühring HJ, Battula VL, Trembl S, et al. Novel markers for the prospective isolation of human MSC. *Ann N Y Acad Sci* 2007;1106:262-271.
28. Noort WA, Kruisselbrink AB, in't Anker PS, et al. Mesenchymal stem cells promote engraftment of human umbilical cord blood-derived CD34(+) cells in NOD/SCID mice. *Exp Hematol* 2002;30:870-878.
29. Bühring HJ, Battula VL, Trembl S, et al. Novel markers for the prospective isolation of human MSC. *Ann N Y Acad Sci* 2007;1106:262-271.
30. Noort WA, Kruisselbrink AB, in't Anker PS, et al. Mesenchymal stem cells promote engraftment of human umbilical cord blood-derived CD34(+) cells in NOD/SCID mice. *Exp Hematol* 2002;30:870-878.
31. Dang ZC, van Bezooijen RL, Karperien M, et al. Exposure of KS483 cells to estrogen enhances osteogenesis and inhibits adipogenesis. *J Bone Miner Res* 2002;17:394-405.
32. Pittenger MF, Mackay AM, Beck SC, et al. Multilineage potential of adult human mesenchymal stem cells. *Science* 1999;284:143-147.
33. Di Nicola M, Carlo-Stella C, Magni M, et al. Human bone marrow stromal cells suppress T-lymphocyte proliferation induced by cellular or nonspecific mitogenic stimuli. *Blood* 2002;99:3838-3843.
34. Quah BJ, Warren HS, Parish CR. Monitoring lymphocyte proliferation *in vitro* and *in vivo* with the intracellular fluorescent dye carboxyfluorescein diacetate succinimidyl ester. *Nat Protoc* 2007;2:2049-2056.
35. Oerlemans MI, Goumans MJ, van MB, et al. Active Wnt signaling in response to cardiac injury. *Basic Res Cardiol* 2010;105:631-641.
36. Smits AM, van Laake LW, den OK, et al. Human cardiomyocyte progenitor cell transplantation preserves long-term function of the infarcted mouse myocardium. *Cardiovasc Res* 2009;83:527-535.
37. van Laake LW, Passier R, Monshouwer-Kloots J, et al. Monitoring of cell therapy and assessment of cardiac function using magnetic resonance imaging in a mouse model of myocardial infarction. *Nat Protoc* 2007;2:2551-2567.
38. Arslan F, Smeets MB, O'Neill LA, et al. Myocardial ischemia/reperfusion injury is mediated by leukocytic toll-like receptor-2 and reduced by systemic administration of a novel anti-toll-like receptor-2 antibody. *Circulation* 2010;121:80-90.
39. Bühring HJ, Battula VL, Trembl S, et al. Novel markers for the prospective isolation of human MSC. *Ann N Y Acad Sci* 2007;1106:262-271.
40. Quirici N, Soligo D, Bossolasco P, et al. Isolation of bone marrow mesenchymal stem cells by anti-nerve growth factor receptor antibodies. *Exp Hematol* 2002;30:783-791.
41. Simmons PJ, Torok-Storb B. Identification of stromal cell precursors in human bone marrow by a novel monoclonal antibody, STRO-1. *Blood* 1991;78:55-62.
42. Battula VL, Bareiss PM, Trembl S, et al. Human placenta and bone marrow derived MSC cultured in serum-free, b-FGF-containing medium express cell surface frizzled-9 and SSEA-4 and give rise to multilineage differentiation. *Differentiation* 2007;75:279-291.
43. Krause U, Harter C, Seckinger A, et al. Intravenous delivery of autologous mesenchymal stem cells limits infarct size and improves left ventricular function in the infarcted porcine heart. *Stem Cells Dev* 2007;16:31-37.
44. Halkos ME, Zhao ZQ, Kerendi F, et al. Intravenous infusion of mesenchymal stem cells enhances regional perfusion and improves ventricular function in a porcine model of myocardial infarction. *Basic Res Cardiol* 2008;103:525-536.
45. Groggaard HK, Sigurjonsson OE, Brekke M, et al. Cardiac accumulation of bone marrow mononuclear

- progenitor cells after intracoronary or intravenous injection in pigs subjected to acute myocardial infarction with subsequent reperfusion. *Cardiovasc Revasc Med* 2007;8:21-27.
46. Amado LC, Schuleri KH, Saliaris AP, et al. Multimodality noninvasive imaging demonstrates *in vivo* cardiac regeneration after mesenchymal stem cell therapy. *J Am Coll Cardiol* 2006;48:2116-2124.
 47. Peister A, Mellad JA, Larson BL, et al. Adult stem cells from bone marrow (MSCs) isolated from different strains of inbred mice vary in surface epitopes, rates of proliferation, and differentiation potential. *Blood* 2004;103:1662-1668.
 48. Moscoso I, Centeno A, Lopez E, et al. Differentiation "*in vitro*" of primary and immortalized porcine mesenchymal stem cells into cardiomyocytes for cell transplantation. *Transplant Proc* 2005;37:481-482.
 49. Thomson BM, Bennett J, Dean V, et al. Preliminary characterization of porcine bone marrow stromal cells: skeletogenic potential, colony-forming activity, and response to dexamethasone, transforming growth factor beta, and basic fibroblast growth factor. *J Bone Miner Res* 1993;8:1173-1183.
 50. Ringe J, Kaps C, Schmitt B, et al. Porcine mesenchymal stem cells. Induction of distinct mesenchymal cell lineages. *Cell Tissue Res* 2002;307:321-327.
 51. Rozemuller H, Prins HJ, Naaijken B, et al. Prospective isolation of mesenchymal stem cells from multiple mammalian species using cross-reacting anti-human monoclonal antibodies. *Stem Cells Dev* 2010;19:1911-1921.
 52. Post S, Abdallah BM, Bentzon JF, et al. Demonstration of the presence of independent pre-osteoblastic and pre-adipocytic cell populations in bone marrow-derived mesenchymal stem cells. *Bone* 2008;43:32-39.
 53. Simmons PJ, Torok-Storb B. Identification of stromal cell precursors in human bone marrow by a novel monoclonal antibody, STRO-1. *Blood* 1991;78:55-62.
 54. Simmons PJ, Torok-Storb B. CD34 expression by stromal precursors in normal human adult bone marrow. *Blood* 1991;78:2848-2853.
 55. Gronthos S, Zannettino AC, Hay SJ, et al. Molecular and cellular characterisation of highly purified stromal stem cells derived from human bone marrow. *J Cell Sci* 2003;116:1827-1835.
 56. Jones EA, Kinsey SE, English A, et al. Isolation and characterization of bone marrow multipotential mesenchymal progenitor cells. *Arthritis Rheum* 2002;46:3349-3360.
 57. Boiret N, Rapatel C, Veyrat-Masson R, et al. Characterization of nonexpanded mesenchymal progenitor cells from normal adult human bone marrow. *Exp Hematol* 2005;33:219-225.
 58. Battula VL, Trembl S, Bareiss PM, et al. Isolation of functionally distinct mesenchymal stem cell subsets using antibodies against CD56, CD271, and mesenchymal stem cell antigen-1. *Haematologica* 2009;94:173-184.
 59. Battula VL, Trembl S, Bareiss PM, et al. Isolation of functionally distinct mesenchymal stem cell subsets using antibodies against CD56, CD271, and mesenchymal stem cell antigen-1. *Haematologica* 2009;94:173-184.
 60. Ramasamy R, Lam EW, Soeiro I, et al. Mesenchymal stem cells inhibit proliferation and apoptosis of tumor cells: impact on *in vivo* tumor growth. *Leukemia* 2007;21:304-310.
 61. Poncelet AJ, Vercruyse J, Saliez A, et al. Although pig allogeneic mesenchymal stem cells are not immunogenic *in vitro*, intracardiac injection elicits an immune response *in vivo*. *Transplantation* 2007;83:783-790.
 62. Makino S, Fukuda K, Miyoshi S, et al. Cardiomyocytes can be generated from marrow stromal cells *in vitro*. *J Clin Invest* 1999;103:697-705.
 63. Toma C, Pittenger MF, Cahill KS, et al. Human mesenchymal stem cells differentiate to a cardiomyocyte phenotype in the adult murine heart. *Circulation* 2002;105:93-98.

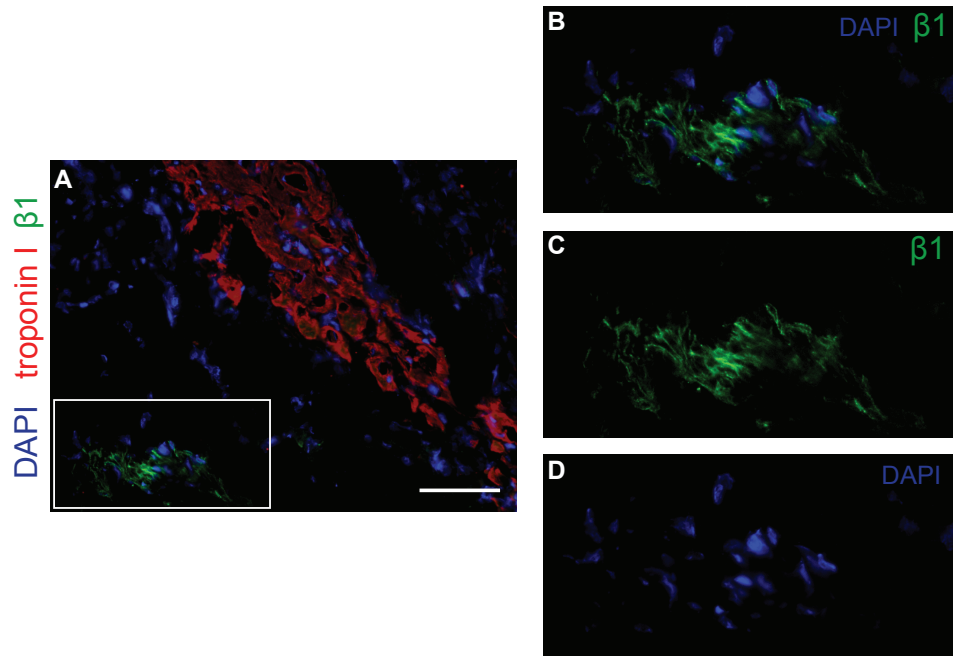
SUPPLEMENTAL



Supplementary Figure 1 | Selection of CD271+ cells enrich for MSC

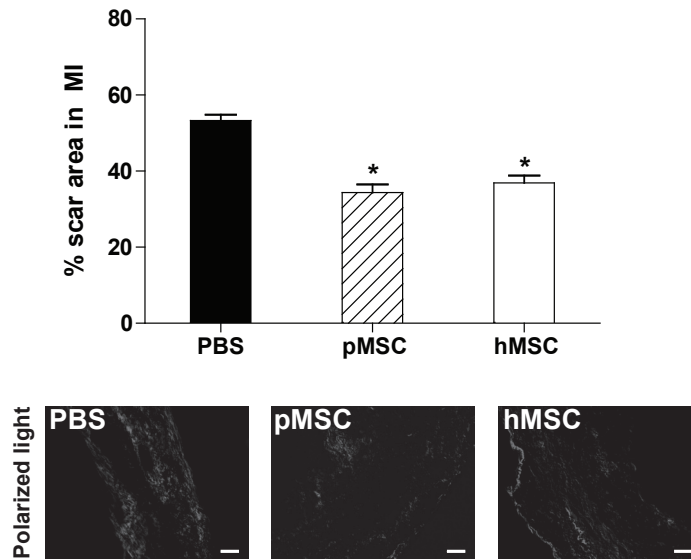
CD271+ cells were selected from porcine bone marrow using flow cytometry (A). CFU-F assay showing more colonies (B) after selection for CD271 compared to both unselected and CD271- negative bone marrow (n=6-10, *P<0.05 vs. baseline, †P<0.05 vs. CD271- cells).

5



Supplementary Figure 2 | Surviving MSCs at 28 days after transplantation

Representative immunofluorescent picture at 28 days post-MI, showing very few surviving human MSCs after transplantation (A) and at higher magnifications (B-D). MSCs (β1-integrin, green) showed no troponin I (red) staining and a connection with surviving myocytes was not observed. Scalebar 20μm.



Supplementary Figure 3 | Cardiac fibrosis

Picrosirius red staining (n=4-5/group) showed a significant smaller scar size in the infarct of MSC-treated animals compared to PBS-treated animals at 28 days post-MI ($P < 0.05$). Scalebar 20 μ m.

6



Martinus I.F.J. Oerlemans¹
Stefan Koudstaal^{1,2}
Steven A. Chamuleau^{1,2}
Dominique P. de Kleijn^{1,2}
Pieter A. Doevendans^{1,2}
Joost P.G. Sluijter^{1,2}

¹ Department of Cardiology, University Medical Center Utrecht, the Netherlands

² Interuniversity Cardiology Institute Netherlands (ICIN), Utrecht, the Netherlands

Targeting Cell Death in the Reperfused Heart: Pharmacological Approaches for Cardioprotection

Int J Cardiol 2012, Epub ahead of print

ABSTRACT

During acute myocardial infarction and in the reperfused heart, loss of cardiomyocytes is mostly caused by apoptosis and necrosis. As apoptosis was considered as the only form of regulated cell death for many years, initial studies investigating cardiomyocyte cell death mainly focused on direct inhibition of apoptosis. However, it has become clear that ischemic conditioning protocols - the application of alternating periods of non-lethal ischemia and reperfusion - can reduce necrotic cell death in the reperfused heart. Research on the signal-transduction pathways responsible for this phenomenon resulted in the discovery of many pharmacological targets to limit cell death after reperfusion, in which the activation of survival kinases and inhibition of mitochondrial permeability transition pore (MPTP) play an important role. Very recently, a regulated form of necrotic cell death (called 'necroptosis') was identified together with potential pharmacological inhibitors, which may also protect the myocardium from lethal reperfusion injury. This review highlights the role of apoptosis and necrosis in the reperfused hearts, including its execution and regulation and the emerging role of programmed necrosis (necroptosis). Furthermore, we will focus on the results of pharmacological interventions in experimental studies as well as relevant proof-of-concept clinical trials trying to limit apoptosis, necrosis and necroptosis in the reperfused heart. Although the list of cardioprotective compounds is promising, large multi-center clinical trials, with enough statistical power, will be necessary to determine whether they can improve clinical outcome and can be applied in patients as adjuvant therapy next to reperfusion.

INTRODUCTION

Acute myocardial infarction (MI) remains one of the leading causes of morbidity and mortality in the western world as this leads to irreversible loss of cardiomyocytes¹. Myocyte cell death during ischemia-reperfusion (I/R) is mainly caused by apoptosis and necrosis. Currently, the most effective therapy is early reperfusion, as infarct size is a major determinant of cardiac remodelling and prognosis after MI^{2,3}. However, within minutes after the restoration of blood flow, reperfusion itself results in additional damage also known as myocardial ischemia-reperfusion (I/R) injury⁴. Based on experimental studies it has become clear that I/R injury contributes to a significant amount of cell death taking place after the onset of reperfusion, also referred to as lethal reperfusion injury^{5,6}. Although numerous experimental studies have shown that both pharmacological postconditioning and ischemic postconditioning can lead to infarct size reduction, translation of these cardioprotective approaches has largely failed in the clinical setting⁷⁻⁹. Pharmacological approaches that target programmed cell death and especially the role of programmed necrosis, a relatively new level of cell death regulation, may offer novel therapeutic opportunities to limit cell death in the ischemic heart^{10,11}.

Cell death in the reperfused heart

Cell death can be classified based on various criteria, but the major types are apoptosis, autophagy and necrosis¹². Where apoptosis was considered as a regulated form of cell death (i.e. the cell starts its suicide program), necrosis was generally seen as a passive and unregulated process resulting from externally-induced cellular injury. Autophagy on the other hand is mainly considered to be a survival mechanism by which cells recycle their proteins, lipids and organelles under energy and nutrient-deprived conditions, which may become detrimental¹³. This process is induced in the ischemic heart and seems to be cardioprotective rather than being responsible for myocyte death and therefore beyond the scope of this review. The reader is referred to a comprehensive review on the role of autophagy in cardiac disease elsewhere¹⁴.

Apoptosis was reported to be detectable from approximately 4 hours after coronary artery occlusion and involves cardiomyocytes as well as non-cardiomyocytes¹⁵⁻¹⁸. Real-time imaging of apoptotic cell death in mice even showed that apoptosis occurs within minutes after ischemia when using Annexin-V labelling^{19,20}. Ischemia-reperfusion was suggested to be a stronger stimulus for acute apoptosis than permanent occlusion^{21,22}, which could even be visualized in patients suffering from myocardial infarction²³. Necrosis, in contrast, appeared at 2 hours and continued to increase until 24 hours after MI¹⁵. Therefore, the process of necrosis-induced myocardial cell death mainly takes place within the first 24 hours, after which the inflammatory phase begins^{24,25}.

During the last decades, our view and understanding on cell death in the ischemic heart has changed markedly. As apoptosis was seen as the only regulated form of cell death for many years, genetic and pharmacological approaches targeting necrosis are relatively rare²⁶. During the last two decades, a growing body of evidence clearly demonstrated that oxidative stress and its effect on mitochondria are very important in lethal reperfusion injury and ischemic cell death^{27,28}. It has become clear that at least some part of this necrotic cell

death can be regulated, in which opening of the mitochondrial permeability transition pore (MPTP) plays an important role^{29, 30}. Moreover, emerging evidence has demonstrated that the serine/threonine kinase activity of receptor-interacting protein 1 (RIP1) and its interaction with RIP3 after death receptor stimulation are necessary for programmed necrosis^{31, 32}. Necrostatin-1 (Nec-1), a small molecule capable of inhibiting the kinase activity of receptor interacting protein-1 (RIP1), was shown to inhibit programmed necrosis without affecting other RIP1-mediated processes and efficiently prevented necrotic cell death^{33, 34}.

Next to irreversible loss of cardiomyocytes, another important aspect of post-MI recovery is inflammation^{25, 35}. Apoptosis is characterized by cell shrinkage and the formation of apoptotic bodies in order to avoid inflammation (as plasma integrity is generally maintained). In contrast, necrosis is accompanied by a gain in cell volume, rupture of the plasma membrane and loss of intracellular contents leading to a profound immune response. The possibility to target (programmed) necrosis in the ischemic heart can therefore exert beneficial effects in terms of cardioprotection and may indirectly influence the inflammatory response^{36, 37}. This is particularly important as inflammation-induced ROS can lead to necrotic cell death as well³⁸, which could explain why modulation of pro-inflammatory signals that are re-expressed post-MI can attenuate cardiac remodelling accordingly³⁹⁻⁴².

APOPTOSIS

Apoptosis is a well-defined process by which the cell undergoes cell death following a variety of different stimuli, finally resulting in the activation of a special family of death proteases known as caspases^{43, 44}. Over 14 different caspases have been identified, of which many are involved in regulating apoptosis. One type of caspases (i.e. initiator caspases) act upstream thereby initiating the apoptotic cascade, including caspase-2, -8, -9 and -10. On the other hand, caspase-3 and -7 were found to be involved in downstream signalling in the apoptosis pathway and are therefore called effector caspases.

Like in non-cardiac cells and tissues, caspases are the central players in myocardial apoptosis during pathological conditions such as myocardial infarction and heart failure^{45, 46}. Caspases are synthesized in an inactive form and remain present in the cytosol as pro-caspases. Once activated, initiator (upstream) caspases cleave and activate the effector caspases, caspase-3 and caspase-7. These downstream caspases then inactivate the enzyme poly ADP-ribose polymerase (PARP), cleave structural nuclear proteins and induce DNA fragmentation via endonucleases including caspase-activated DNase (CAD)⁴⁷. Apoptosis can be separated into two distinct pathways - the extrinsic pathway and the intrinsic pathway -, both leading to the activation of downstream effector caspase-3 and -7 (Figure 1).

The extrinsic pathway

The extrinsic pathway is initiated by binding of extracellular death ligands, tumor necrosis factor- α (TNF- α) and Fas-ligand, to their transmembrane death receptors present on the cell surface⁴⁸. After binding to the death receptor, several death adaptor molecules are recruited originating from the cytoplasmic side, including TNF-receptor-associated death

domain (TRADD), TNF-receptor-associated factor (TRAF)⁴⁹. This multiprotein complex, known as the death inducing signalling complex (DISC) or Complex I, then starts binding initiator (pro)caspase-8. As more procaspase-8 will be recruited, autoactivation leads to formation of active caspase-8, thereby causing activation of effector caspases such as caspase-3 more downstream.

The intrinsic pathway

The intrinsic (mitochondrial) pathway is induced by a variety of extracellular and intracellular stimuli such as physical stress or oxidative stress and DNA damage. The balance between pro-apoptotic (Bid, Bax, Bak) and anti-apoptotic (Bcl-2, Bcl-xL) members of the Bcl-2 protein family are crucial for the initiation of this pathway⁵⁰. Upon stimulation, Bax translocates to the mitochondria to form a complex with Bak on the outer mitochondrial membrane (OMM). The OMM then becomes permeabilized, leading to the release of cytochrome *c* and other pro-apoptotic proteins (apoptogens)⁵¹. Once in the cytosol, cytochrome *c* interacts with apoptotic protease activating factor-1 (Apaf-1), forming a complex known as the apoptosome. This complex then activates caspase-9, enabling further activation of effector caspases-3/7 and thus the execution of apoptotic cell death⁵². Other apoptogens that are released upon OMM permeabilization include SMAC (second mitochondria-derived activator of caspase, also known as DIABLO) and apoptosis-inducing factor (AIF)⁵³. Caspase-8 activation (extrinsic apoptosis pathway) can also activate the mitochondrial pathway by

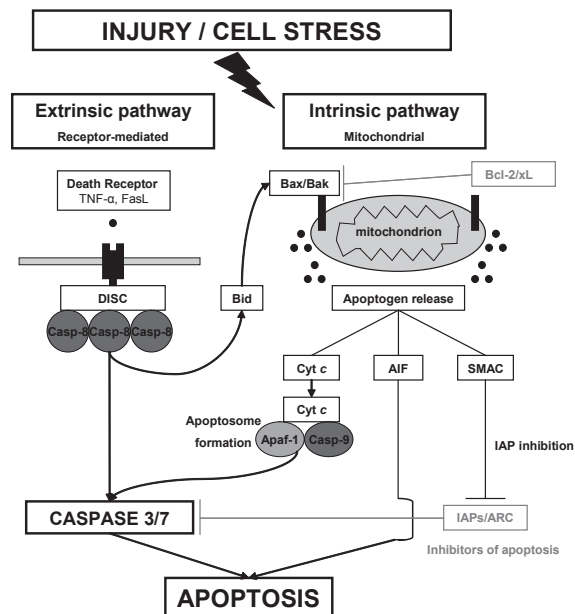


Figure 1
Schematic overview of both the extrinsic (death receptor-mediated) and intrinsic (mitochondrial) pathway leading to apoptosis, as well as the cross-talk between extrinsic apoptosis via Bid cleavage by caspase-8 resulting in Bax/Bak translocation.

cleavage of Bid (BH3-interacting domain death agonist), also resulting in Bax/Bak translocation and apoptogens release⁵⁴.

Regulators of apoptosis

Activation of apoptosis generally occurs upon binding of death ligands to their death receptors (extrinsic pathway) or after specific death-inducing stimuli (intrinsic pathway). Next to the Bcl-2 proteins family, several other proteins are present in the cell that modulate effector caspases, also known as IAPs (inhibitor of apoptosis proteins)⁵⁵. The action of IAPs, including the well-studied XIAP (X-chromosome linked IAP), is mainly to inhibit caspase-3 and to prevent the cell from extensive apoptosis. However, upon activation of the intrinsic pathway and their release from the mitochondria, SMAC^{56, 57} and a protein known as Omi/ HtrA2^{58, 59}, both inhibit IAPs, favouring apoptosis (see Figure 1).

ARC (apoptosis repressor with a caspase recruitment domain) is another apoptosis suppressor which interacts with caspase-2 and caspase-8 via its caspase recruitment domain (CARD)⁶⁰. Interestingly, ARC can regulate both the extrinsic and intrinsic pathway by inhibiting formation of the DISC complex ("caspase-independent") and inhibition of Bax activation, both via its CARD⁶¹. Furthermore, nuclear ARC also negatively regulates p53, which normally induces apoptosis^{62, 63}. More recently it was suggested that ubiquitylation (and consecutive breakdown) of anti-apoptotic proteins and caspases might play an important regulatory role in apoptosis as well⁶⁴, including the cardiovascular system^{65, 66}.

NECROSIS

Necrosis is characterized by a gain in cell volume, swelling of organelles, rupture of the plasma membrane and loss of intracellular contents, which is traditionally seen as a passive and unregulated process. Although necrosis plays a major role after myocardial infarction, most studies investigating cell death mainly focused on apoptosis. However, it became clear that a considerable amount of caspase-independent cell death with necrotic characteristics seemed to be occurring during different models of cardiovascular disease^{29, 30, 67}. In this type of necrotic cell death, the opening of the MPTP in the inner mitochondrial membrane (IMM) plays an important role. Furthermore, it was shown that stimulation of the death receptors in the presence of caspase inhibitors resulted in cell death with necrotic characteristics⁶⁸⁻⁷⁰. Although current knowledge is still in its infancy, at least two different events can be distinguished which lead to necrosis: mitochondrial MPTP opening and stimulation of the death receptors resulting in necroptosis (Figure 2).

MPTP opening

It has become clear that MPTP opening plays a central role during necrotic cell death and is an interesting target for cardioprotection (reviewed⁷¹). In the normal mitochondrion, electron transport by the respiratory chain results in a transmembrane proton gradient between the IMM and OMM. This mitochondrial transmembrane potential (known as the $\Delta\Psi_m$) is essential to generate ATP from ADP and phosphates⁷², providing the necessary amount of energy for the cell. Therefore, IMM integrity is crucial and opening of the MPTP

during reperfusion has two major consequences: redistribution of solutes and ions accompanied by entry of water and swelling of the mitochondrion (osmotic gradient change) and decline of intracellular ATP due to loss of the $\Delta\Psi_m$ ⁷³. Mitochondrial swelling can also lead to OMM rupture, causing the release of apoptogens like cytochrome c, followed by caspase activation²⁹.

However, ATP depletion and loss of plasma membrane integrity due to activation of proteases are thought to be primarily responsible for necrotic cell death following MPTP opening. MPTP opening itself is mainly triggered by Ca^{2+} , but opening can also occur without a dramatic rise in intracellular calcium levels as many factors (including oxidative stress) influence MPTP sensitivity towards the available amount of Ca^{2+} ^{74, 75}. Although the exact molecular mechanism remains unclear, it was suggested that a number of proteins in some way regulate MPTP structure and function^{71, 76}. Of special interest is Cyclophilin D (CypD), which interacts with other components of the MPTP and can be inhibited by the drug cyclosporin A^{77, 78}. Deletion of *ppif*, the gene encoding for CypD, prevented MPTP opening while overexpression strongly induced MPTP opening leading to necrotic cell death^{29, 30}.

Death receptor-induced necrosis (necroptosis)

Stimulation of the death receptor family members (Fas and TNF receptor) by their ligands (Fas-ligand, TNF- α) normally leads to the activation of the extrinsic apoptotic pathway. Surprisingly, death receptor stimulation under apoptosis deficient conditions (i.e. caspase

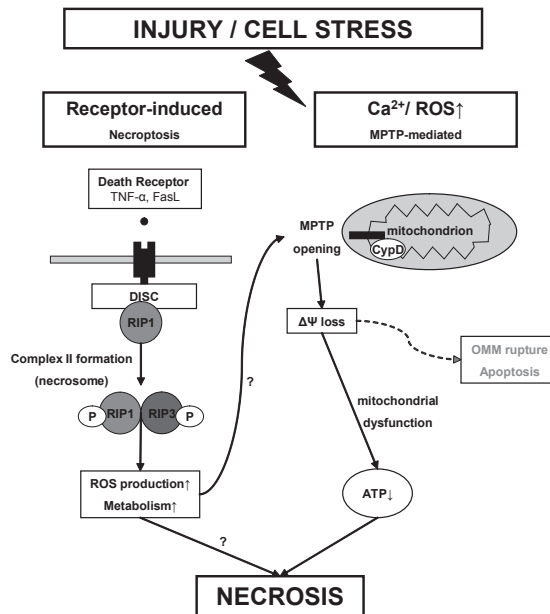


Figure 2

Schematic overview of both necroptosis (receptor-induced) and MPTP-mediated (mitochondrial) necrosis, as well as the cross-talk between MPTP opening and intrinsic apoptosis via rupture of the OMM resulting in release of apoptogens from the mitochondria.

inhibition) could still induce cell death with morphological features of necrosis in certain cell types, supporting the existence of regulated necrosis^{68, 79, 80}. This type of necrotic cell death was later referred to as “necroptosis” by Degterev et al³³, in which the serine/threonine kinase activity of RIP1 plays an essential role^{69, 70}. Since then, research on necroptosis quickly expanded with the aid of Necrostatin-1 (Nec-1), a small molecule capable of inhibiting the kinase activity of RIP1 without affecting other RIP1-mediated processes³⁴, and other necrostatin family members. Necroptosis is induced by different extracellular death ligands including TNF- α and Fas-ligand, in which the role of TNF receptor-1 is most extensively studied^{32, 49, 81}.

Upon ligand binding, a multiprotein complex associates with the TNF receptor at the intracellular side (complex I). This complex includes TRADD, TRAF, the inhibitor of apoptosis 1/2 (cIAP1/2) and RIP1⁴⁹. Interestingly, cIAP1/2 are also known to function as RIP1-ubiquitylating enzymes, thereby promoting nuclear factor- κ B (NF- κ B) survival pathways^{82, 83}. Removal of K63-ubiquitination of RIP1 by deubiquitylating enzymes A20 and cylindromatosis (CYLD) is necessary to recruit RIP1 to complex II^{84, 85}, providing the first switch between life or death. Like in apoptosis, complex II formation highly depends on ubiquitylation status of RIP1, suggesting that this system might regulate both apoptotic and necrotic cell death⁸⁶.

A second switch will then determine if the cell dies from apoptosis or necrosis. RIP1 will assemble with the Fas-associated death domain (FADD), caspase-8, RIP3 and in some cases with TRADD, forming pro-necrotic complex II. Active caspase-8 will cleave RIP1 and induce apoptosis⁸⁷. Furthermore, in the presence of SMAC mimetics (counteracting IAPs), an alternative complex II is formed independently of TRADD, which also leads to caspase-8 activation⁸⁸. When caspase-8 is pharmacologically (or genetically) inhibited, apoptosis cannot be initiated thereby leading to programmed necrosis as an alternative form of cell death^{70, 79}. Nec-1 inhibits this type of cell death, suggesting that RIP1 kinase activity is required for RIP1/3 complex formation, although RIP3 can also phosphorylate RIP1⁸⁹. Altogether, complex II can promote necroptosis (“necrosome complex” in the presence of RIP1 and RIP3) or apoptosis in the presence of caspase-8⁹⁰.

Current understanding of necroptosis is limited, although several mechanisms are thought to contribute to its execution, including ROS production, metabolic changes, and changes in cellular energetics⁸⁹⁻⁹². Interestingly, one of the ideas is that due to cellular stress and in an attempt to survive, the cell increases its energy metabolism turnover thereby facilitating the production of large amounts of ROS, leading to necrotic cell death^{32, 93}.

PHARMACOLOGICAL APPROACHES TO LIMIT CELL DEATH IN THE REPERFUSED HEART

In the context of myocardial infarction, much effort has been put in the modulation of cell death as infarct size is the major determinant of prognosis after MI². In order to find the most optimal strategy for limiting cell death in the ischemic heart, we must critically evaluate experimental studies targeting cell death after myocardial infarction to avoid future problems in a clinical setting^{9, 94}. Ranging from genetic to pharmacological approaches, apoptosis inhibition has been studied extensively^{95, 96}. Most studies, targeting apoptotic

and necrotic cell death, used either caspase inhibitors (and other related compounds) or aimed at the prevention of MPTP opening, including pre- and postconditioning protocols⁷. However, influencing (programmed) necrosis directly has gained considerable scientific attraction over the last few years as this interesting field may lead to new therapeutic approaches^{27, 97}. An overview of the most promising compounds that influence cell death can be found in Figure 3.

Drugs targeting myocardial apoptosis

Genetic approaches clearly showed that inhibition of myocyte apoptosis reduces myocardial infarct size after cardiac I/R (reviewed²⁶). This mainly occurred via interference in the signal transduction of the extrinsic and intrinsic pathway (i.e. death receptor interference) as well as via genetic modification of anti- and pro-apoptotic genes (Bcl-2, Bid, Bax, IAPs). Although these studies provided important mechanistical insights on anti-apoptotic strategies, pharmacological studies have been rather inconclusive in a variety of experimental animal models as discussed below.

Caspase inhibition

Caspases play a pivotal role in the initiation and activation of apoptosis, providing a convincing rationale to use caspase inhibition to limit infarct size post-MI. During the last

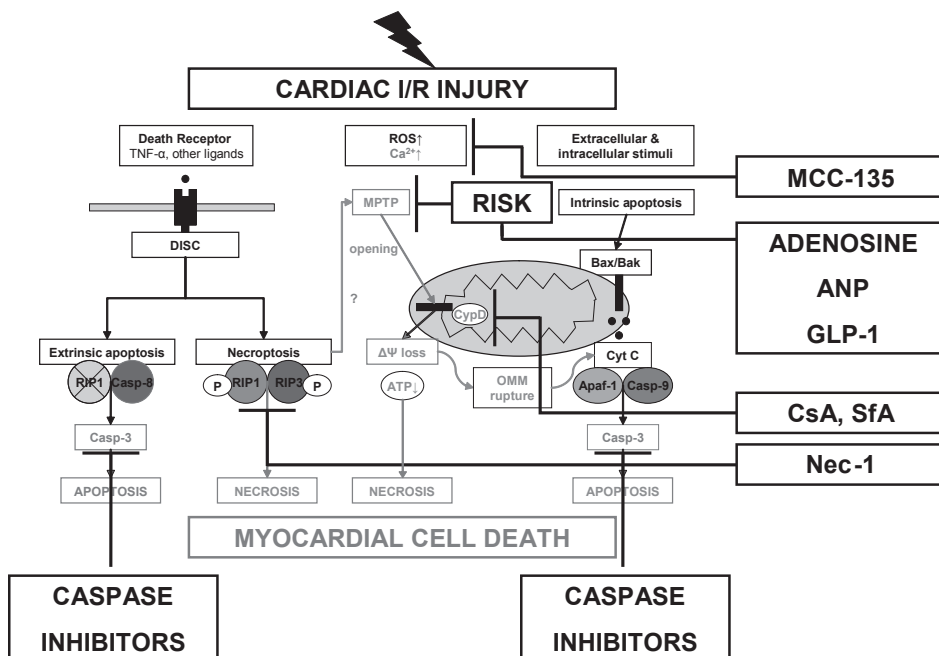


Figure 3

Schematic overview of pharmacological interventions to prevent cell death in the ischemic heart, including the most promising candidates with proven efficacy from both experimental (caspase inhibitors, SfA and Nec-1) and proof-of-concept clinical studies (MCC-135, ANP, adenosine, GLP-1 and CsA).

two decades, several studies investigated the effect of caspase inhibition in various models of myocardial I/R with conflicting results (Table 1)⁹⁸⁻¹¹¹.

Several studies have shown that the application of the pan-caspase inhibitor ZVAD after myocardial I/R limited infarct size (IS) in both rats and rabbits by ~15%^{98, 101, 102, 106, 110}. However, mice subjected to a similar protocol and treatment, as well as Langendorff-perfused rabbit hearts, did not show any effect^{105, 110}. YVAD, a selective caspase-1/4 inhibitor exerted cardioprotection in rabbits and rats^{99, 103}, but failed in two other studies using the same species^{100, 106}. DEVD, a selective caspase-3/7 inhibitor was even less successful in limiting IS – one positive study¹⁰⁶ compared to three negative studies^{100, 101, 103}. Interestingly, DEVD seemed to improve contractile function independent (or even without) inhibition of myocyte apoptosis, although the exact mechanism is still unclear^{104, 109}. Caspase-9 inhibition using Z-LEHD in rats resulted in both positive and negative results^{101, 103}, caspase-8 inhibition (Z-IETD) prior to reperfusion did not show any effects¹⁰³. Neither MMPSI (considered as a more potent non-peptide selective caspase-3/7 inhibitor) nor IDN6734 and Z-Asp-DCB (two other pan-caspase inhibitors) were able to reduce IS compared to control animals¹⁰⁶⁻¹⁰⁸.

Although caspase inhibition did not seem to reduce IS in all cases, several studies did observe a reduction of TUNEL-positive cardiomyocytes, reduced caspase activity or increased functional recovery^{100, 104, 105, 107, 108, 111}. This raises the question whether the beneficial effects solely depend on cardiomyocytes, as non-myocyte cell death (i.e. fibroblasts) and caspase-dependent cleavage of intracellular substrates (i.e. contractile proteins) may influence cardiac remodelling as well. Therefore, clinical application is currently too far away as evidence on apoptosis-dependent cell death and other caspase-dependent processes remains controversial. Moreover, only a minority of these studies investigated the use of caspase inhibitors in a clinically relevant animal model of *in vivo* ischemia-reperfusion.

Other compounds targeting apoptosis

Next to the administration of readily available caspase inhibitors, compounds targeting other components of the apoptotic pathway are very limited. One possible option is the mitochondrial serine protease Omi/ HtrA2, a regulator of apoptosis by inducing caspase activation and which is activated during myocardial I/R¹¹². UCF-101 is a specific inhibitor of Omi/HtrA2, which was shown to prevent inactivation of IAPs via direct binding and cleavage, thereby inhibiting its proteolytic capacity with very little aspecific activity for other serine proteases¹¹³. Two independent reports showed that UCF-101 administration reduced IS by limiting XIAP inactivation and caspase-3/9 activity^{114, 115}. Next to ZVAD, Minatoguchi et al. also investigated whether serine protease inhibition influenced IS¹⁰⁵. Although less TUNEL-positive cardiomyocytes were present, no IS reduction was observed. A more recent paper failed to show reduced caspase-3 activity upon UCF-101 treatment in diabetic mice¹¹⁶. Rather than anti-apoptotic, UCF-101 was suggested to downregulate several enzymes responsible for the degradation of AMP-activated protein kinase (AMPK), thereby preventing cardiac dysfunction during diabetes. Follow-up studies investigating UCF-101 in pre-clinical large-animal models and additional knowledge on its exact mechanism are needed.

Table 1 | Caspase inhibition in heart disease models

Type of inhibitor	Study	Animal	I/R model	Dose & Timing	Effect
Pan-caspase inhibitor	Yaoita et al. 1998 ⁸⁸	Rat	30min / 1day <i>in vivo</i>	3.3mg/kg ZVAD.fmk; bolus prior to ischemia followed by every 6 hours	IS↓ TUNEL+ CM↓
	Mocanu et al. 2000 ⁰¹	Rat	35min / 2hrs Langendorff	0.1μM ZVAD.fmk in perfusate; 5 minutes prior to reperfusion for 15 minutes	IS↓
	Huang et al. 2000 ⁰²	Rat	45min / 3hrs <i>in vivo</i>	500μg/rat ZVAD.fmk or BOCD.fmk; prior to ischemia or 10min prior to reperfusion	IS↓; ZVAD.fmk (both proto-cols) BocD.fmk (protocol 1)
	Minatoguchi et al. 2001 ⁰⁵	Rabbit	30min / 2days <i>in vivo</i>	0.8mg/kg ZVAD.fmk; 20 minutes prior to ischemia	IS unaffected TUNEL+ CM ↓
	Chapman et al. 2002 ⁰⁶	Rabbit	30min / 2hrs Langendorff	10μM ZVAD.fmk; 15 min prior to ischemia	IS↓ TUNEL+ CM↓
	Yarbrough et al. 2003 ⁰⁷	Pig	60min / 7days <i>in vivo</i>	2mg/kg IDN6734; bolus at reperfusion, followed by 2mg/kg for 24 hrs	IS unaffected (at 7 days post-MI) LV dimension change↓
	Chandrasekhar et al. 2004 ⁰⁸	Rat	permanent ligation <i>in vivo</i>	2mg/kg Z-Asp-DCB.mk prior to surgery, followed by 2mg/day for 28 days	LV function↑ (28 days) Caspase-3 activity↓
	Mersman et al. 2008 ¹⁰	Mouse	20min / 4days <i>in vivo</i>	1.5mg/kg Q-VD-Oph or ZVAD.fmk 1.5mg/kg; prior to ischemia, followed by 1.5mg/kg twice a day	IS unaffected
	Mersman et al. 2008 ¹⁰	Rat	25min / 7days <i>in vivo</i>	1.5mg/kg Q-VD-Oph; prior to ischemia, followed by 1.5mg/kg injections twice a day	IS↓ LV function↑
	Yarbrough et al. 2010 ¹¹	Pig	60min / 7days <i>in vivo</i>	6mg/kg IDN6734; bolus at reperfusion, followed by 6mg/kg for 24 hrs	IS unaffected LV function↑
Caspase-1/4 inhibitor	Holly et al. 1999 ⁹⁹	Rabbit	30min / 3hrs <i>in vivo</i>	1.5mg/kg YVAD cmk; prior to ischemia, followed by a bolus at reperfusion	IS↓ TUNEL+ CM↓
	Okamura et al. 2000 ⁰⁰	Rat	30min / 6hrs <i>in vivo</i>	3.5mg/kg YVAD cho; 5 min prior to ischemia	IS unaffected, but TUNEL+ CM↓ Caspase activity↓
	Kovacs et al. 2001 ¹⁰³	Rat	30min / 2hrs Langendorff	0.5μM YVAD.cmk; at reperfusion	IS↓ TUNEL+ CM↓
	Chapman et al. 2002 ⁰⁶	Rabbit	30min / 2hrs Langendorff	20μM YVAD.cmk and MIMPSI (non-peptide inhibitor); 15 min prior to ischemia	IS unaffected (YVAD) IS↓ (MIMPSI)

follow-up table 1

Caspase-3/7 inhibitor	Okamura et al. 2000 ¹⁰⁰	Rat	30min / 6hrs <i>in vivo</i>	3.5mg/kg DEVD.cho; 5 min prior to ischemia	IS unaffected, but CM↓ Caspase activity↓	TUNEL+
	Mocanu et al. 2000 ⁰¹	Rat	35min / 2hrs <i>Langendorff</i>	0.07μM Ac-DEVD.cmk in perfusate; 5 minutes prior to reperfusion for 15 minutes	IS↓	
	Kovacs et al. 2001 ¹⁰³	Rat	30min / 2hrs <i>Langendorff</i>	0.2μM Ac-DEVD.cmk; at reperfusion	IS unaffected	
	Ruetten et al. 2003 ⁰⁴	Rat	30min / 30min <i>Langendorff</i>	1μM Ac-DEVD.cmk; prior to ischemia or at reperfusion	TUNEL+ CM unaffected Caspase-3 activity↓	
	Chapman et al. 2002 ¹⁰⁶	Rabbit	30min / 2hrs <i>Langendorff</i>	20μM DEVD.fmk; 15 min prior to ischemia	IS↓	
	Balsam et al. 2005 ⁰⁹	Mouse	permanent ligatio	1.6mg/kg DEVD.cho; started prior to surgery, continued twice a day	TUNEL+ CM↓ (1 day) LV function↑ (28 days)	
Caspase-8 inhibitor	Mocanu et al. 2000 ⁰¹	Rat	35min / 2hrs <i>Langendorff</i>	0.07μM Z-IETD.fmk in perfusate; 5 minutes prior to reperfusion for 15 minutes	IS↓	
Caspase-9 inhibitor	Mocanu et al. 2000 ⁰¹	Rat	35min / 2hrs <i>Langendorff</i>	0.07μM Z-LEHD.fmk in perfusate; 5 minutes prior to reperfusion for 15 minutes	IS↓	
	Kovacs et al. 2001 ¹⁰³	Rat	30min / 2hrs <i>Langendorff</i>	0.2μM Z-LEHD.fmk; at reperfusion	IS unaffected	
Serine-protease inhibitor	Minatoguchi et al. 2001 ¹⁰⁵	Rabbit	30min / 2days <i>in vivo</i>	2mg/kg DCI; 20 minutes prior to ischemia	IS unaffected TUNEL+ CM ↓	

IS = infarct size; TUNEL = Terminal deoxynucleotidyl transferase dUTP nick end labelling; CM = cardiomyocytes; iv. = intravenously; LV = left ventricle/ventricular; MMPSI = (S)-(+)-5-1-(2-methoxymethylpyrrolidinyl)sulfonylisatin (non-peptide selective caspase-3/7 inhibitor);

Drugs targeting myocardial necrosis

MPTP opening results in myocyte necrosis, characterized by mitochondrial swelling, ATP depletion and cardiomyocyte cell death^{28, 117}. Although the exact molecular composition of the MPTP remains controversial, this has been a challenging area in research involving myocardial I/R injury^{73, 118, 119}. Via pre- and post-conditioning protocols, delayed MPTP opening seems to be mediated through CypD and activation of the Reperfusion Injury Salvage Kinase (RISK) pathway^{120, 121}.

Next to CypD, several other proteins have been proposed in regulating MPTP opening, including voltage- dependent anion channel (VDAC) and adenine nucleotide translocase (ANT). Therefore, most studies aiming for MPTP inhibition targeted these specific proteins (Table 2). Additionally, evidence from both neuronal and myocardial disease models firmly suggested that necroptosis could be an interesting candidate to limit cell death in cardiovascular and many other diseases⁹⁷.

Drugs targeting MPTP opening

As soon as several groups reported that Cyclosporin A (CsA) could inhibit mitochondrial MPTP opening after I/R^{77, 122-124}, Weinbrenner et al. were the first to report IS reduction following CsA treatment. They reached a similar level of inhibition as ischemic preconditioning¹²⁵, which was reported by many others afterwards (Table 2, only studies pharmacologically targeting MPTP during I/R are shown)¹²⁶⁻¹³². Interestingly, hyperglycaemia during ischemia was found to inhibit the protective action of CsA¹³³. Furthermore, CsA was shown to interact with cyclophilin A as well, thereby inhibiting calcineurin signalling and providing cardioprotection via different pathways^{134, 135}. A few years later though, Leshnower et al. showed that calcineurin inhibitor FK506 did not affect infarct size (although administered prior to ischemia), in favour of calcineurin-independent cardioprotection by CsA¹³⁶.

Nevertheless, this controversy led to the development of several CsA analogs including NIM811¹³⁷, which was shown to reduce IS significantly *in vivo*¹³⁸. Similarly, sanglifhrin A (SfA), another inhibitor of MPTP opening and independent of calcineurin signalling, was shown to protect against myocardial I/R injury by lowering LDH levels¹³⁹ and reducing IS¹⁴⁰. Interestingly, Javadov et al. reported a reduced LDH release upon CsA and SfA treatment in Langendorff-perfused rat hearts, which was less effective than ischemic preconditioning¹⁴¹. Importantly, Lim et al. elegantly demonstrated¹⁴² that the protective effect of both CsA and SfA is at least partly mediated via MPTP opening *in vivo* since the observed IS reduction was absent in CypD knockout mice¹³¹. Furthermore, Debio-025 (alisporivir), another cyclophilin inhibitor, exerted cardioprotective effects similar to postconditioning protocols¹⁴².

Piot et al. showed for the first time that CsA administration prior to percutaneous coronary intervention (PCI) reduced infarct size in STEMI patients at 5 days measured by MRI ($P=0.04$)¹⁴³, without any effect on LV function¹⁴⁴, although patient numbers were rather low ($n=58$), as illustrated by non-significant changes in troponin I levels ($P=0.15$). Recently, CsA reduced IS in pigs, again demonstrating its cardioprotective properties¹⁴⁵. Therefore, it remains unclear why three other reports failed to demonstrate a cardioprotective of CsA in pre-clinical models of I/R¹⁴⁶⁻¹⁴⁸, although Lie et al. reported a significantly larger area-at-

risk in the CsA-treated animals¹⁴⁶.

Although the reported pig studies are not consistent, CsA could still be considered as a therapeutic approach, considering the available cardiac and non-cardiac experimental and clinical data^{143, 144, 149}. A recently published meta-analysis on CsA appeared to be rather negative, but also included (negative) studies with administration of CsA prior to ischemia and studies primarily investigating other mechanisms than CsA-induced cardioprotection¹⁵⁰. Furthermore, the success of CsA in large-animal models seems to be related to the time of ischemia applied to the animal (Table 2; 90 vs. 45 minutes ischemia followed by reperfusion), which is in line with recent findings¹⁵¹. Interestingly, several clinical CsA-studies are currently ongoing, including a study investigating the effect of CsA administration on markers of cardiac injury after bypass surgery (clinicaltrials.gov, NCT01002859). Although promising, both knowledge on the molecular identity of MPTP and follow-up studies will be needed to investigate to what extent CypD-mediated MPTP opening can salvage damaged myocardium in a clinically relevant setting, requiring particular attention to the model (i.e. duration of ischemia), application (i.e. relevant concentration in the early phase of reperfusion) and hard end-points.

Drugs targeting necroptosis

In contrast to the role of MPTP opening in cardioprotection, necroptosis is a relatively new and exciting field with clinical relevance in a variety of diseases^{32, 97}. After discovery of Nec-1, a small molecule capable of inhibiting the kinase activity of RIP1^{33, 34}, the group of Yuan focused on the development of Nec-1 and other chemical variants of necrostatins (i.e. Nec-3, Nec-4, Nec-5 and Nec-7)¹⁵²⁻¹⁵⁵. Until now, experimental studies investigating necroptosis mainly used Nec-1. Interestingly, Nec-7 was found to inhibit TNF- α – induced necroptosis in human Jurkat cells without inhibiting RIP1 kinase¹⁵⁵. Recently, both RIP1-dependent and independent protection from cell death upon Nec-1 treatment were reported¹⁵⁶, pointing towards the existence of additional targets that can regulate this complex pathway.

Degtarev et al. were the first to show that Nec-1 administration after 2 hours occlusion of the mid-cerebral artery followed by reperfusion resulted in a significant reduction of infarct size³³. Furthermore, a follow-up study also showed that Nec-1 decreased brain damage in a model of traumatic brain injury, accompanied by improved cerebral function and less inflammation¹⁵⁷. Recently, several others showed that Nec-1 exerted neuroprotective effects in models of retinal ischemia^{158, 159} and after hypoxia in neonatal mice by blocking necrosome formation¹⁶⁰. Xu et al. were even able to show a synergistic effect when Nec-1 was administered in combination with humanin, an apoptosis inhibitor, upon cerebral I/R¹⁶¹. Altogether, these data strongly suggest that necrosis is an important form of cell death after ischemic injury *in vivo* which can be inhibited by Nec-1.

The possibility to inhibit necrotic cell death has important implications for cardiovascular disease, particularly in the context of myocardial ischemia-reperfusion. Until now, both *in vitro* and *in vivo* data on the use of Nec-1 in models of cardiac injury is limited (summarized in Table 3). Smith et al. provided the first indication that Nec-1 protects against myocardial injury¹⁶². Nec-1 administration resulted in less necrotic cell death under oxidative stress (measured by propidium iodide uptake) *in vitro* and treatment with 100 μ M (but not 30 μ M) Nec-1 delayed MPTP opening in isolated rat ventricular myocytes.

Table 2 | Targeting MPTP opening in heart disease models

Type of inhibitor	Study	Animal/Human	I/R model	Dose & Timing	Effect
Cyclosporin A	Weinbrenner et al. 1998 ¹²⁵	Rabbit	30 min / 2 hrs Langendorff	750nM CsA in perfusate; pre-ischemia or 10 minutes post-ischemia	IS↓*
	Squadrito et al. 1999 ¹²⁶	Rat	30 min / 48 hrs <i>in vivo</i>	0.25, 0.5 or 1mg/kg CsA; 5 min after ischemia	IS↓
	Minners et al. 2000 ¹²⁷	Rat	35 min / 2 hrs Langendorff	0.2μM CsA in perfusate; 5 min pre-ischemia	IS↓
	Hausenloy et al. 2002 ¹²⁸	Rat	35 min / 2 hrs Langendorff	200 nM CsA; 5 min prior to reperfusion for 15 minutes	IS↓
	Argaud et al. 2004 ¹²⁹	Rabbit	30 min / 4 hrs <i>in vivo</i>	10mg/kg CsA; 15 min prior to ischemia	IS↓
	Argaud et al. 2005 ¹³⁰	Rabbit	30 min / 4 hrs <i>in vivo</i>	10 mg/kg CsA or NIM811 (analogue); at reperfusion	IS↓
	Krolkowski et al. 2005 ¹³⁰	Rabbit	30 min / 3 hrs <i>in vivo</i>	5 and 10 mg/kg CsA; at reperfusion	IS↓ (only in case of 10mg/kg CsA)
	Lim et al. 2007 ¹³¹	Mouse WT and CypD KO	45 min / 2 hrs <i>in vivo</i>	10mg/kg CsA; at reperfusion	IS↓
	Gomez et al. 2008 ¹³²	Mouse	60 min/24 hrs <i>in vivo</i>	10mg/kg CsA; 5 min prior to reperfusion	IS↓†
	Piot et al. 2008 ¹⁴³	Human	28 patients with STEMI in need for reperfusion therapy	2.5mg/kg CsA; 5 min prior to reperfusion	IS↓ (measured by MRI)
	Skyschally et al. 2010 ¹⁴⁵	Pig	90 min / 2 hrs <i>in vivo</i>	5mg/kg CsA; 5 min prior to reperfusion	IS↓

follow up table 2

Lie et al. 2010 ¹⁴⁶	Pig	40 min / 3 hrs <i>in vivo</i>	10mg/kg CsA; 5 min prior to reperfusion	IS unaffected
Karlsson et al. 2010 ¹⁴⁷	Pig	45 min / 2 hrs <i>in vivo</i>	10mg/kg CsA; 3 min prior to reperfusion	IS unaffected
Karlsson et al. 2011 ¹⁴⁸	Pig	45 min / 4 hrs <i>in vivo</i>	2.5mg/kg CsA; 7 min prior to reperfusion	IS unaffected
Sanglifehrin A				
Hausenloy et al. 2003 ¹⁴⁰	Rat	35 min / 2 hrs <i>Langendorff</i>	1µM CsA; at reperfusion or after 15 min of reperfusion	IS↓ (only when given at reperfusion)
Lim et al. 2007 ¹³¹	Mouse WT and CypD KO	45 min / 2 hrs <i>in vivo</i>	10mg/kg CsA; at reperfusion	IS↓
Debio-025 (alispovir)				
Gomez et al. 2007 ¹⁴²	Mouse	25 min / 1 day <i>in vivo</i>	10mg/kg Debio-025; at reperfusion	IS↓

MPTP = mitochondrial permeability transition pore; CsA = cyclosporin A; SFA = sanglifehrin A (does not inhibit calcineurin); *effect was gone when given 20 minutes after onset of ischemia; †effect was independent of GSK3 activity;

Table 3 | Targeting necroptosis in heart disease models

Type of inhibitor	Study	Cells/Animal	I/R model	Dose & Timing	Effect
Cells	Smith et al. 2007 ¹⁶²	C2C12 myoblasts (mouse)	Oxidative stress for 5.5 hrs; stimulation with peroxide	30µM and 100µM Nec-1; together with stimulus	50% reduction of cell death (30 and 100µM)
	Smith et al. 2007 ¹⁶²	H9c2 cardiac cells (rat)	Oxidative stress for 4 hrs; stimulation with peroxide	30µM and 100µM Nec-1; together with stimulus	20-30% reduction of cell death (30 and 100µM)
	Smith et al. 2007 ¹⁶²	Isolated rat cardiomyocytes	Laser illumination to stimulate ROS generation	30µM and 100µM Nec-1; 10 minutes pre-treatment before stimulus	Delayed MPTP opening* (only in case of 100µM)
Animals	Liu et al. 2010 ¹⁶⁵	CMPCs (human)	Oxidative stress for 16 hrs; stimulation with peroxide	30µM Nec-1; 30 minutes pre-treatment before stimulus	40% reduction of necrosis measured flow cytometry
	Smith et al. 2007 ¹⁶²	Mouse	35 min / 35 min Langendorff	30µM and 100µM Nec-1; at reperfusion	IS↓ (30µM)* IS↑ (100µM)
	Smith et al. 2007 ¹⁶²	Mouse	30 min / 2 hrs in vivo	1.65mg/kg Nec-1; ip-injection prior to reperfusion	IS↓ with 40%
	Lim et al. 2007 ¹⁶³	Mouse WT vs. CypD ^{-/-}	30min/120min, in vivo, open chest model	1.65mg/kg Nec-1; tail vein injection at reperfusion	IS↓ with 70%; no additional IS↓ in CypD ^{-/-}

Nec-1 = Necrostatin-1; ROS = reactive oxygen species; MPTP = mitochondrial permeability transition pore; CMPC = cardiomyocyte progenitor cell; ip = intraperitoneal; CypD^{-/-} = Cyclophilin D knockout mice; * similar effect seen with Nec-1 (inactive form);

However, 100µM Nec-1 (inactive analogue) also delayed MPTP opening and reduced infarct size to a similar extent as Nec-1 after I/R in a Langendorff model. As a final experiment, the authors performed an open-chest model of 30 minutes ischemia, followed by 2 hours reperfusion in C57BL/6J mice demonstrating an infarct size reduction upon Nec-1 treatment only. Using the same approach, this laboratory later showed that the cardioprotective effect of Nec-1 was lost in CypD knockout animals¹⁶³, which could suggest that the activation of the RISK pathway is involved in the protective mechanism following RIP1 inhibition^{131, 164}.

On the other hand, the absolute infarct size reduction in wild-type animals was much more than in the CypD knockout mice (70% vs. 40%), suggesting that Nec-1 could also exert cardioprotective effects independent of CypD. While investigating the role of microRNA-155 (which targets RIP1) in cardiomyocyte progenitor cells *in vitro*, our laboratory for the first time showed that Nec-1 exerts cardioprotective effects against oxidative stress in human cells¹⁶⁵, suggesting that Nec-1 could also be used to improve cell survival during cell transplantation. This implicates that Nec-1, next to limiting reperfusion injury, could also be used in cell transplantation studies in an attempt to improve cardiac recovery by increasing cell retention after infarction¹⁶⁶.

Especially in combination with the data obtained from models of cerebral injury (as mentioned earlier), Nec-1 seems to be promising a cardioprotective compound. However, these data were obtained from a limited number of animals, the protocol was limited to 2 hours of reperfusion only and no functional follow-up was performed. Many interventions aiming at infarct size reduction, although successful in experimental studies, failed in clinical settings⁹. Furthermore, it is unclear whether Nec-1 directly targets necrotic cell death after cardiac I/R *in vivo*, whether apoptosis is involved and if RIP1 and ROS are affected. More importantly, long-term efficiency needs to be established, including large-animal studies. We therefore believe that additional research is warranted before further steps towards a clinical setting can be made.

Compounds reducing infarct size via the activation of survival kinases

The Reperfusion Injury Salvage Kinase (RISK) pathway plays an important role in cardioprotection, which can be activated mechanically (pre- and postconditioning protocols) and with pharmacological compounds⁴. In experimental models, several compounds were identified that could activate these survival kinases, thereby inhibiting MPTP opening¹⁶⁷, which may be useful in the clinic as adjunctive therapy in addition to reperfusion. Unfortunately, translation of these compounds in clinical trials has proven to be difficult, as infarct size reduction was not observed in all clinical studies (Table 4; randomized clinical studies reporting IS (or enzyme release) and LV function only).

Already about twenty years ago, several groups reported that pre-treatment with adenosine (or a selective adenosine A1-receptor agonist) could reduce infarct size to a similar extent as pre-conditioning, which was not effective when administered prior to reperfusion^{168, 169}. Many others confirmed this type of cardioprotection in different animal models (extensively reviewed in¹⁷⁰). Interestingly, Norton et al. were the first to report that stimulation of the A2-receptor at the onset of reperfusion exerted cardioprotective effects¹⁷¹. Activation of adenosine receptors either during ischemia (A1 and A3 subtype) or at reperfusion (A2

subtype) can be effective, as illustrated by a considerable amount of evidence¹⁷⁰. Although the adenosine-mediated cardioprotection might be mediated through K_{ATP} channels, protein kinase C signalling and Akt (RISK activation), the exact mechanism remains unclear¹⁷⁰. As shown in Table 4, clinical studies were less consistent. Although the Acute Myocardial Infarction Study of Adenosine (AMISTAD) trial in patients undergoing thrombolysis reported an infarct size reduction (especially in anterior infarct patients), a positive trend towards more adverse events was observed as well¹⁷². Marzilli et al. reported significantly less adverse events and lower creatine kinase (CK) levels after adenosine treatment prior to reperfusion¹⁷³, while another randomized study did not observe functional improvements when adenosine was given at onset of thrombolysis¹⁷⁴. Although infarct size was comparable between all adenosine-treated patients vs. placebo, the AMISTAD-II trial did show beneficial effects in patients receiving a high dose of adenosine which was correlated with less adverse events¹⁷⁵. In contrast, a bolus injection after thrombus aspiration followed by another injection after stenting failed to show any beneficial effects¹⁷⁶. Overall, adenosine might provide myocardial protection, but larger studies with enough statistical power will be necessary to establish the observed beneficial effects.

Atrial Natriuretic Peptide (ANP), a circulating hormone with profound effects on blood pressure and the neuro-hormonal response upon cardiac injury, has also been considered as promising cardioprotective agent¹⁷⁷. Several small animal studies reported beneficial effects on functional recovery (rat) and infarct size reduction (dog, rabbit) upon ANP administration which might activate the RISK pathway¹⁷⁸⁻¹⁸⁰, as well as less ischemia-induced arrhythmias¹⁸¹, and infarct size reduction in ANP knockout mice after permanent ligation¹⁸². In AMI patients, ANP infusion after reperfusion reduced LV remodelling compared to nitroglycerine or isosorbide dinitrate and reduced the incidence of arrhythmias¹⁸³⁻¹⁸⁵. Major limitations of these studies are the lack of a proper control population and the way LV function (i.e. angiography) and other clinical parameters were measured. More convincing evidence was provided by a clinical trial comparing ANP with a placebo (J-WIND-ANP) given at onset of reperfusion, which resulted in a significant infarct size reduction (measured by CK), preserved long-term ejection fraction and reduced cardiac death¹⁸⁶. Clearly, ANP holds a great potential, but larger multi-center trials are necessary to establish its clinical benefit.

Very recently, compelling evidence was reported on the clinical application of exenatide (Byetta) after thrombolysis (n=105), although its exact mechanism still remains to be elucidated¹⁸⁷. Glucagon-like peptide-1 (GLP-1; exenatide is a synthetic GLP-1 analogue), is a hormone which stimulates insulin secretion and is released into the gastrointestinal tract^{188, 189}. Unlike GLP-1, exenatide and other analogues are resistant for the enzyme dipeptidyl peptidase-IV (DPP-IV), normally responsible for its rapid breakdown. In an attempt to restore normal glucose uptake, the group of Shannon et al. demonstrated that GLP-1 infusion improved LV function in patients after primary angioplasty (n=21) and with chronic heart failure (n=21), as well as in different dog models of cardiomyopathy, suggestive of both metabolic and inotropic effects¹⁹⁰⁻¹⁹⁴. Bose and Yellon were the first to use GLP-1 upon reperfusion, showing that the cardioprotective effect of GLP-1 (combined with a DPP-IV inhibitor) on infarct size was blunted when PI3K-Akt signalling (part of the RISK pathway) was blocked in rat¹⁹⁵⁻¹⁹⁷. Sonne et al. showed similar effects using exendin-4, a peptide

Table 4 | Experimental versus clinical use of several potential cardioprotective agents

Agent (mechanism)	Experimental use	Effect	Clinical use	N	Effect
Adenosine (RISK-mediated)	Summarized in ¹⁷⁰	IS↓	Mahaffy et al. 1999 ¹⁷² prior to thrombolysis	236	IS↓*
	Both during ischemia and prior to reperfusion		Marzilli et al. 2000 ¹⁷³ prior to reperfusion	54	CK↓ ACE↓
			Quintana et al. 2003 ¹⁷⁴ at onset of thrombolysis	608	LV function unaffected
			Ross et al. 2005 ¹⁷⁵ prior to intervention	2218	IS↓† (high dose only)
		Fokkema et al. 2009 ¹⁷⁶ 2x bolus after intervention	448	IS (by CK) unaffected	
ANP (RISK-mediated)	Takagi et al. 2000 ¹⁷⁸ <i>in vivo</i> , at reperfusion	IS↓	Hayashi et al. 2001 ¹⁸³ after reperfusion	65	LV remodeling↓ vs. NTG
	Sangawa et al. 2004 ¹⁷⁹ <i>Langendorff</i> , at reperfusion	LV function↑	Kuga et al 2003 ¹⁸⁴ after reperfusion	37	LV function ↑ (angiography)
	Yang et al. 2006 ¹⁸⁰ <i>Langendorff</i> , at reperfusion	IS↓	Kasama et al. 2007 ¹⁸⁵ upon presentation	50	LV remodeling↓ vs. nitrate
			Kitakaze et al. 2007 ¹⁸⁶ after reperfusion for 3 days	535	IS↓ (by CK), LV function ↑ ACE↓
GLP-1 (or analogues) (RISK-mediated)	Bose et al. 2005 ¹⁹⁵ <i>Langendorff</i> <i>in vivo</i> , pre-ischemia	IS↓	Nikolaidis et al. 2004 ¹⁹⁰ after reperfusion, for 72hrs	21	LV function↑
	Bose et al. 2005 ¹⁹⁶ <i>Langendorff</i> , at reperfusion	IS↓	Lønborg et al. ¹⁸⁷ 15 min before reperfusion	105	IS↓# salvage index↑ #
	Bose et al. 2007 ¹⁹⁷ <i>Langendorff</i> , pre-ischemia	IS↓			
	Sonne et al. ¹⁹⁸ <i>in vivo</i> , at reperfusion	IS↓§			
	Timmers et al. ¹⁹⁹ <i>in vivo</i> , 5 min prior to reperfusion	IS↓#			
MCC-135 (Reducing Ca ²⁺)	Yarbrough et al. 2003 ²⁰⁸ <i>in vivo</i> , at reperfusion	LV fuction↑‡	Bär et al. 2006 ²¹¹ prior to reperfusion	387	no beneficial effects
	Satoh et al. 2004 ²⁰⁹ <i>Langendorff</i> , at reperfusion	LV fuction↑	Jang et al. 2008 ²¹² prior to reperfusion	486	no beneficial effects
	Kawasumi et al. 2007 ²¹⁰ <i>in vivo</i> , prior to reperfusion	IS↓			

AR-agonist = adenosine receptor agonist; IS = infarct size; CK = creatine kinase; ACE = adverse cardiac events; ANP = atrial natriuretic peptide; vs. = versus; NTG = nitroglycerine; * in case of anterior infarcts; † when treated 70µg/kg per minute adenosine (high dose); ‡ measured by regional contractility; § using exendin-4; # using exenatide (Byetta);

constituent of the venom of *H. suspectum* lizard, which also acts as a GLP-1 receptor agonist¹⁹⁸. Timmers et al. elegantly showed that exenatide administration 5 minutes prior to reperfusion reduced infarct size and preserved systolic function after 3 days of reperfusion in a clinically relevant porcine model, which was associated with increased p-Akt levels and reduction of caspase-3 activity¹⁹⁹. Finally, with the use of GLP-1 receptor knockout mice, Ban et al. showed that the cardioprotective effects of GLP-1 and its isoform were receptor-dependent, but that of its metabolite GLP-1(9-36) receptor-independent^{200, 201}. As administration of exenatide (started 15 minutes prior to reperfusion) resulted in a significantly larger salvage index ([AAR-IS]/AAR) and corresponding decrease in myocardial infarct size (cardiac MRI), this can certainly be considered as a promising cardioprotective compound¹⁸⁷. Interestingly, a large safety trial using exenatide in patients suffering from myocardial infarction is currently ongoing²⁰². Next to these initial studies, large multi-center clinical trials will be necessary to answer the question whether exenatide can improve clinical outcomes as well.

Other compounds capable of limiting infarct size

Many mediators of I/R injury not only cause damage by itself, but may lead to a chain reaction of lethal injury when ROS levels reach a certain threshold²⁰³. Not surprisingly, several compounds have been identified capable of reducing cardiac reperfusion injury, mainly by limiting ROS levels or, more indirectly, by influencing pH, calcium levels and via clinically available drugs^{204, 205} (a complete list can be found in⁸). One particular compound that has been investigated in the clinical setting is MCC-135 (or Caldaret; Mitsubishi Pharma Corporation, Osaka, Japan)^{206, 207}. MCC-135 is thought to reduce intracellular calcium overload by enhancing uptake by the sarcoplasmic reticulum, which might reduce MPTP opening. Yarbrough et al. were the first to demonstrate that MCC-135 attenuated contractile dysfunction in an *in vivo* porcine model of ischemia-reperfusion²⁰⁸, which was confirmed by others²⁰⁹. MCC-135 decreased both heart rate and CK-MB release, troponin levels were comparable with the control group though. Although experimental data on infarct size was very limited²¹⁰, Bär et al. performed the first study in patients receiving MCC-135 prior to revascularisation²¹¹. Both in this safety study as in a later study, MCC-135 failed to demonstrate any beneficial effects²¹², except for a sub-study reporting a significant decrease in the incidence of patients with an ejection fraction <30% (P=0.03)²¹³. Based on two relatively large clinical studies and very limited experimental data on infarct size, it remains to be seen whether MCC-135 truly has cardioprotective properties in the acute setting of MI.

More recently, Toll-Like Receptor (TLR) 2 on the circulating cells (but not on cardiomyocyte) was identified as the mediator of TLR2-dependent myocardial I/R injury. Anti-TLR2 therapy using a monoclonal antibody blocking this TLR2 exerts its action by reducing leukocyte influx, cytokine production and pro-apoptotic signalling²¹⁴. In addition, exosomes were identified as the cardioprotective factor in MSC conditioned media²¹⁵. Interestingly, very low concentrations of exosomes resulted in an impressive reduction of infarct size, mainly by delivery of cardioprotective substances (proteins, miRNA) to endangered cardiomyocytes (paracrine effect). As with all experimental compounds, follow-up studies will be necessary to evaluate the protective effects these compounds in large-animal models and in patients in a later stage.

CONCLUDING REMARKS

Cardioprotection has been extensively investigated in the last three decades, but many therapeutic strategies with proven efficacy in experimental studies have failed in the clinical setting. This might be attributed to the use of non-clinically applicable cell- and animal models, wrong timing of compound administration (i.e. during early ischemia) and the lack of functional follow-up and clinically relevant end points (infarct size, cardiac function, mortality). However, a number of pharmacological strategies, mainly focusing on the MPTP (Table 2) or mimicking pre/postconditioning by activation of pro-survival kinases (Table 4), have been able to reduce infarct size when given at time of reperfusion (Figure 3). The discovery of a regulated form of necrotic cell death (necroptosis) and its pharmacological inhibitor (Necrostatin-1) may be another opportunity to limit cell death in the ischemic heart, although additional research is warranted before further steps towards a clinical setting can be made (Table 3).

As therapeutic interventions administered at the time myocardial reperfusion have been proven to reduce infarct size in both experimental and clinical models, the existence of lethal reperfusion injury and its contribution to ischemic cell death can no longer be ignored. Patients presenting with an acute ST-segment elevation myocardial infarction (STEMI) will therefore benefit from therapy aiming for 1) timely reperfusion most likely via primary percutaneous coronary intervention, and 2) prevention of lethal reperfusion injury. Only this dual approach will make sure that patients can benefit completely from the myocardial salvage obtained by reperfusion therapy.

In conclusion, the list of cardioprotective agents that can be used as adjuvant therapy next to reperfusion is promising. Large multi-center clinical trials with enough statistical power will be necessary to establish observed beneficial effects and to answer the question whether they can improve clinical outcomes as well. To prevent translational failure, particular attention must be paid to proper selection of patients (who will benefit the most), application (relevant concentration in the early phase of reperfusion) and hard end-points.

Conflict of Interest

None

Acknowledgements

This work was supported by the Novartis Foundation for Cardiovascular Excellence (JS), a Bekalis price (PD) and "Stichting Swaeneborgh" (MO).

REFERENCES

1. Lloyd-Jones D, Adams RJ, Brown TM, et al. Heart disease and stroke statistics—2010 update: a report from the American Heart Association. *Circulation* 2010;121:e46-e215.
2. McKay RG, Pfeffer MA, Pasternak RC, et al. Left ventricular remodeling after myocardial infarction: a corollary to infarct expansion. *Circulation* 1986;74:693-702.
3. Sobel BE, Bresnahan GF, Shell WE, et al. Estimation of infarct size in man and its relation to prognosis. *Circulation* 1972;46:640-648.
4. Yellon DM, Hausenloy DJ. Myocardial reperfusion injury. *N Engl J Med* 2007;357:1121-1135.
5. Garcia-Dorado D, Ruiz-Meana M, Piper HM. Lethal reperfusion injury in acute myocardial infarction: facts and unresolved issues. *Cardiovascular research* 2009;83:165-168.
6. Prasad A, Stone GW, Holmes DR, et al. Reperfusion injury, microvascular dysfunction, and cardioprotection: the “dark side” of reperfusion. *Circulation* 2009;120:2105-2112.
7. Ovize M, Baxter GF, Di LF, et al. Postconditioning and protection from reperfusion injury: where do we stand? Position paper from the Working Group of Cellular Biology of the Heart of the European Society of Cardiology. *Cardiovasc Res* 2010;87:406-423.
8. Schwartz Longacre L, Kloner RA, Arai AE, et al. New horizons in cardioprotection: recommendations from the 2010 national heart, lung, and blood institute workshop. *Circulation* 2011;124:1172-1179.
9. Hausenloy DJ, Baxter G, Bell R, et al. Translating novel strategies for cardioprotection: the Hatter Workshop Recommendations. *Basic Res Cardiol* 2010;105:677-686.
10. Miura T, Miki T. Limitation of myocardial infarct size in the clinical setting: current status and challenges in translating animal experiments into clinical therapy. *Basic Res Cardiol* 2008;103:501-513.
11. Murphy E, Steenbergen C. Mechanisms underlying acute protection from cardiac ischemia-reperfusion injury. *Physiol Rev* 2008;88:581-609.
12. Kroemer G, Galluzzi L, Vandenabeele P, et al. Classification of cell death: recommendations of the Nomenclature Committee on Cell Death Differ 2009;16:3-11.
13. Levine B, Kroemer G. Autophagy in the pathogenesis of disease. *Cell* 2008;132:27-42.
14. Gottlieb RA, Mentzer RM. Autophagy during cardiac stress: joys and frustrations of autophagy. *Annu Rev Physiol* 2010;72:45-59.
15. Kajstura J, Cheng W, Reiss K, et al. Apoptotic and necrotic myocyte cell deaths are independent contributing variables of infarct size in rats. *Lab Invest* 1996;74:86-107.
16. Bialik S, Geenen DL, Sasson IE, et al. Myocyte apoptosis during acute myocardial infarction in the mouse localizes to hypoxic regions but occurs independently of p53. *J Clin Invest* 1997;100:1363-1372.
17. Scarabelli T, Stephanou A, Rayment N, et al. Apoptosis of endothelial cells precedes myocyte cell apoptosis in ischemia/reperfusion injury. *Circulation* 2001;104:253-256.
18. Palojoki E, Saraste A, Eriksson A, et al. Cardiomyocyte apoptosis and ventricular remodeling after myocardial infarction in rats. *Am J Physiol Heart Circ Physiol* 2001;280:H2726-H2731.
19. Dumont EA, Hofstra L, van Heerde WL, et al. Cardiomyocyte death induced by myocardial ischemia and reperfusion: measurement with recombinant human annexin-V in a mouse model. *Circulation* 2000;102:1564-1568.
20. Dumont EA, Reutelingsperger CP, Smits JF, et al. Real-time imaging of apoptotic cell-membrane changes at the single-cell level in the beating murine heart. *Nat Med* 2001;7:1352-1355.
21. Gottlieb RA, Burleson KO, Kloner RA, et al. Reperfusion injury induces apoptosis in rabbit cardiomyocytes. *J Clin Invest* 1994;94:1621-1628.
22. Fliiss H, Gattinger D. Apoptosis in ischemic and reperfused rat myocardium. *Circ Res* 1996;79:949-956.
23. Hofstra L, Liem IH, Dumont EA, et al. Visualisation of cell death *in vivo* in patients with acute myocardial infarction. *Lancet* 2000;356:209-212.
24. Cleutjens JP, Blankesteyn WM, Daemen MJ, et al. The infarcted myocardium: simply dead tissue, or a lively target for therapeutic interventions. *Cardiovasc Res* 1999;44:232-241

25. Frangogiannis NG. The mechanistic basis of infarct healing. *Antioxid Redox Signal* 2006;8:1907-1939
26. Whelan RS, Kaplinskiy V, Kitsis RN. Cell death in the pathogenesis of heart disease: mechanisms and significance. *Annu Rev Physiol* 2010;72:19-44
27. Kung G, Konstantinidis K, Kitsis RN. Programmed necrosis, not apoptosis, in the heart. *Circ Res* 2011;108:1017-1036
28. Di Lisa F, Carpi A, Giorgio V, et al. The mitochondrial permeability transition pore and cyclophilin D in cardioprotection. *Biochim Biophys Acta* 2011;1813:1316-1322
29. Baines CP, Kaiser RA, Purcell NH, et al. Loss of cyclophilin D reveals a critical role for mitochondrial permeability transition in cell death. *Nature* 2005;434:658-662
30. Nakagawa T, Shimizu S, Watanabe T, et al. Cyclophilin D-dependent mitochondrial permeability transition regulates some necrotic but not apoptotic cell death. *Nature* 2005;434:652-658
31. Vanlangenakker N, Vanden BT, Krysko DV, et al. Molecular mechanisms and pathophysiology of necrotic cell death. *Curr Mol Med* 2008;8:207-220
32. Vandenabeele P, Galluzzi L, Vanden Berghe T, et al. Molecular mechanisms of necroptosis: an ordered cellular explosion. *Nat Rev Mol Cell Biol* 2010;11:700-714
33. Degterev A, Huang Z, Boyce M, et al. Chemical inhibitor of nonapoptotic cell death with therapeutic potential for ischemic brain injury. *Nat Chem Biol* 2005;1:112-119
34. Degterev A, Hitomi J, Germscheid M, et al. Identification of RIP1 kinase as a specific cellular target of necrostatins. *Nat Chem Biol* 2008;4:313-321
35. Frantz S, Bauersachs J, Ertl G. Post-infarct remodelling: contribution of wound healing and inflammation. *Cardiovasc Res* 2009;81:474-481
36. Diwan A, Tran T, Misra A, et al. Inflammatory mediators and the failing heart: a translational approach. *Curr Mol Med* 2003;3:161-182
37. Frangogiannis NG. The immune system and cardiac repair. *Pharmacol Res* 2008;58:88-111
38. Hori M, Nishida K. Oxidative stress and left ventricular remodelling after myocardial infarction. *Cardiovasc Res* 2009;81:457-464
39. Oka T, Xu J, Molkentin JD. Re-employment of developmental transcription factors in adult heart disease. *Semin Cell Dev Biol* 2007;18:117-131
40. Bujak M, Frangogiannis NG. The role of TGF-beta signaling in myocardial infarction and cardiac remodeling. *Cardiovasc Res* 2007;74:184-195
41. Oerlemans MI, Goumans MJ, van MB, et al. Active Wnt signaling in response to cardiac injury. *Basic Res Cardiol* 2010;105:631-641
42. Barandon L, Casassus F, Leroux L, et al. Secreted frizzled-related protein-1 improves postinfarction scar formation through a modulation of inflammatory response. *Arterioscler Thromb Vasc Biol* 2011;30:e80-e87
43. Earnshaw WC, Martins LM, Kaufmann SH. Mammalian caspases: structure, activation, substrates, and functions during apoptosis. *Annu Rev Biochem* 1999;68:383-424
44. Hengartner MO. The biochemistry of apoptosis. *Nature* 2000;407:770-776
45. Regula KM, Kirshenbaum LA. Apoptosis of ventricular myocytes: a means to an end. *J Mol Cell Cardiol* 2005;38:3-13
46. Crow MT, Mani K, Nam YJ, et al. The mitochondrial death pathway and cardiac myocyte apoptosis. *Circ Res* 2004;95:957-970
47. van Gurp M, Festjens N, van LG, et al. Mitochondrial intermembrane proteins in cell death. *Biochem Biophys Res Commun* 2003;304:487-497
48. Peter ME, Krammer PH. The CD95(APO-1/Fas) DISC and beyond. *Cell Death Differ* 2003;10:26-35
49. Hsu H, Huang J, Shu HB, et al. TNF-dependent recruitment of the protein kinase RIP to the TNF receptor-1 signaling complex. *Immunity* 1996;4:387-396
50. Youle RJ, Strasser A. The BCL-2 protein family: opposing activities that mediate cell death. *Nat Rev Mol Cell Biol* 2008;9:47-59
51. Zou H, Li Y, Liu X, et al. An APAF-1, cytochrome c multimeric complex is a functional apoptosome that activates procaspase-9. *J Biol Chem* 1999;274:11549-11556.

52. Boatright KM, Salvesen GS. Mechanisms of caspase activation. *Curr Opin Cell Biol* 2003;15:725-731.
53. Zamzami N, Kroemer G. The mitochondrion in apoptosis: how Pandora's box opens. *Nat Rev Mol Cell Biol* 2001;2:67-71.
54. Li H, Zhu H, Xu CJ, et al. Cleavage of BID by caspase 8 mediates the mitochondrial damage in the Fas pathway of apoptosis. *Cell* 1998;94:491-501.
55. Deveraux QL, Roy N, Stennicke HR, et al. IAPs block apoptotic events induced by caspase-8 and cytochrome c by direct inhibition of distinct caspases. *EMBO J* 1998;17:2215-2223.
56. Verhagen AM, Ekert PG, Pakusch M, et al. Identification of DIABLO, a mammalian protein that promotes apoptosis by binding to and antagonizing IAP proteins. *Cell* 2000;102:43-53.
57. Du C, Fang M, Li Y, et al. Smac, a mitochondrial protein that promotes cytochrome c-dependent caspase activation by eliminating IAP inhibition. *Cell* 2000;102:33-42.
58. Suzuki Y, Imai Y, Nakayama H, et al. A serine protease, HtrA2, is released from the mitochondria and interacts with XIAP, inducing cell death. *Mol Cell* 2001;8:613-621.
59. Yang QH, Church-Hajduk R, Ren J, et al. Omi/HtrA2 catalytic cleavage of inhibitor of apoptosis (IAP) irreversibly inactivates IAPs and facilitates caspase activity in apoptosis. *Genes Dev* 2003;17:1487-1496.
60. Koseki T, Inohara N, Chen S, et al. ARC, an inhibitor of apoptosis expressed in skeletal muscle and heart that interacts selectively with caspases. *Proc Natl Acad Sci U S A* 1998;95:5156-5160.
61. Nam YJ, Mani K, Ashton AW, et al. Inhibition of both the extrinsic and intrinsic death pathways through nonhomotypic death-fold interactions. *Mol Cell* 2004;15:901-912.
62. Foo RS, Nam YJ, Ostreicher MJ, et al. Regulation of p53 tetramerization and nuclear export by ARC. *Proc Natl Acad Sci U S A* 2007;104:20826-20831.
63. Li YZ, Lu DY, Tan WQ, et al. p53 initiates apoptosis by transcriptionally targeting the antiapoptotic protein ARC. *Mol Cell Biol* 2008;28:564-574.
64. Bernassola F, Ciechanover A, Melino G. The ubiquitin proteasome system and its involvement in cell death pathways. *Cell Death Differ* 2010;17:1-3.
65. Sohns W, van Veen TA, van der Heyden MA. Regulatory roles of the ubiquitin-proteasome system in cardiomyocyte apoptosis. *Curr Mol Med* 2010;10:1-13.
66. Willis MS, Townley-Tilson WH, Kang EY, et al. Sent to destroy: the ubiquitin proteasome system regulates cell signaling and protein quality control in cardiovascular development and disease. *Circ Res* 2010;106:463-478.
67. Nakayama H, Chen X, Baines CP, et al. Ca²⁺- and mitochondrial-dependent cardiomyocyte necrosis as a primary mediator of heart failure. *J Clin Invest* 2007;117:2431-2444.
68. Kitanaka C, Kuchino Y. Caspase-independent programmed cell death with necrotic morphology. *Cell Death Differ* 1999;6:508-515.
69. Matsumura H, Shimizu Y, Ohsawa Y, et al. Necrotic death pathway in Fas receptor signaling. *J Cell Biol* 2000;151:1247-1256.
70. Holler N, Zaru R, Micheau O, et al. Fas triggers an alternative, caspase-8-independent cell death pathway using the kinase RIP as effector molecule. *Nat Immunol* 2000;1:489-495.
71. Halestrap AP. What is the mitochondrial permeability transition pore? *J Mol Cell Cardiol* 2009;46:821-831.
72. Dahout-Gonzalez C, Nury H, Trezeguet V, et al. Molecular, functional, and pathological aspects of the mitochondrial ADP/ATP carrier. *Physiology (Bethesda)* 2006;21:242-249.
73. Halestrap AP, Clarke SJ, Javadov SA. Mitochondrial permeability transition pore opening during myocardial reperfusion—a target for cardioprotection. *Cardiovasc Res* 2004;61:372-385.
74. Crompton M, Costi A, Hayat L. Evidence for the presence of a reversible Ca²⁺-dependent pore activated by oxidative stress in heart mitochondria. *Biochem J* 1987;245:915-918.
75. Halestrap AP, Woodfield KY, Connern CP. Oxidative stress, thiol reagents, and membrane potential modulate the mitochondrial permeability transition by affecting nucleotide binding to the adenine nucleotide translocase. *J Biol Chem* 1997;272:3346-3354.
76. Crompton M. The mitochondrial permeability transition pore and its role in cell death. *Biochem J* 1999;341 (Pt 2):233-249.

77. Crompton M, Ellinger H, Costi A. Inhibition by cyclosporin A of a Ca²⁺-dependent pore in heart mitochondria activated by inorganic phosphate and oxidative stress. *Biochem J* 1988;255:357-360
78. Griffiths EJ, Halestrap AP. Further evidence that cyclosporin A protects mitochondria from calcium overload by inhibiting a matrix peptidyl-prolyl cis-trans isomerase. Implications for the immunosuppressive and toxic effects of cyclosporin. *Biochem J* 1991;274 (Pt 2):611-614
79. Vercammen D, Beyaert R, Denecker G, et al. Inhibition of caspases increases the sensitivity of L929 cells to necrosis mediated by tumor necrosis factor. *J Exp Med* 1998;187:1477-1485
80. Kawahara A, Ohsawa Y, Matsumura H, et al. Caspase-independent cell killing by Fas-associated protein with death domain. *J Cell Biol* 1998;143:1353-1360
81. Declercq W, Vanden Berghe T, Vandenabeele P. RIP kinases at the crossroads of cell death and survival. *Cell* 2009;138:229-232
82. Mahoney DJ, Cheung HH, Mrad RL, et al. Both cIAP1 and cIAP2 regulate TNFalpha-mediated NF-kappaB activation. *Proc Natl Acad Sci U S A* 2008;105:11778-11783
83. Hacker H, Karin M. Regulation and function of IKK and IKK-related kinases. *Sci STKE* 2006;2006:re13
84. Wang L, Du F, Wang X. TNF-alpha induces two distinct caspase-8 activation pathways. *Cell* 2008;133:693-703
85. Hitomi J, Christofferson DE, Ng A, et al. Identification of a molecular signaling network that regulates a cellular necrotic cell death pathway. *Cell* 2008;135:1311-1323
86. Vucic D, Dixit VM, Wertz IE. Ubiquitylation in apoptosis: a post-translational modification at the edge of life and death. *Nat Rev Mol Cell Biol* 2011;12:439-452
87. Lin Y, Devin A, Rodriguez Y, et al. Cleavage of the death domain kinase RIP by caspase-8 prompts TNF-induced apoptosis. *Genes Dev* 1999;13:2514-2526
88. Vanlangenakker N, Bertrand MJ, Bogaert P, et al. TNF-induced necroptosis in L929 cells is tightly regulated by multiple TNFR1 complex I and II members. *Cell Death Dis* 2011;2:e230
89. Cho YS, Challa S, Moquin D, et al. Phosphorylation-driven assembly of the RIP1-RIP3 complex regulates programmed necrosis and virus-induced inflammation. *Cell* 2009;137:1112-1123
90. Vandenabeele P, Declercq W, Van Herreweghe F, et al. The role of the kinases RIP1 and RIP3 in TNF-induced necrosis. *Sci Signal* 2010;3:re4
91. Zhang DW, Shao J, Lin J, et al. RIP3, an energy metabolism regulator that switches TNF-induced cell death from apoptosis to necrosis. *Science* 2009;325:332-336
92. Galluzzi L, Kepp O, Kroemer G. RIP kinases initiate programmed necrosis. *J Mol Cell Biol* 2009;1:8-10
93. Van Herreweghe F, Festjens N, Declercq W, et al. Tumor necrosis factor-mediated cell death: to break or to burst, that's the question. *Cell Mol Life Sci* 2010;67:1567-1579
94. Kloner RA, Schwartz Longacre L. State of the Science of Cardioprotection: Challenges and Opportunities— Proceedings of the 2010 NHLBI Workshop on Cardioprotection. *J Cardiovasc Pharmacol Ther* 2011;16:223-232
95. Lee Y, Gustafsson AB. Role of apoptosis in cardiovascular disease. *Apoptosis* 2009;14:536-548
96. Eefting F, Rensing B, Wigman J, et al. Role of apoptosis in reperfusion injury. *Cardiovasc Res* 2004;61:414-426
97. Smith CC, Yellon DM. Necroptosis, necrostatins and tissue injury. *J Cell Mol Med* 2011;15:1797-1806
98. Yaoita H, Ogawa K, Maehara K, et al. Attenuation of ischemia/reperfusion injury in rats by a caspase inhibitor. *Circulation* 1998;97:276-281
99. Holly TA, Drincic A, Byun Y, et al. Caspase inhibition reduces myocyte cell death induced by myocardial ischemia and reperfusion *in vivo*. *J Mol Cell Cardiol* 1999;31:1709-1715
100. Okamura T, Miura T, Takemura G, et al. Effect of caspase inhibitors on myocardial infarct size and myocyte DNA fragmentation in the ischemia-reperfused rat heart. *Cardiovasc Res* 2000;45:642-650
101. Mocanu MM, Baxter GF, Yellon DM. Caspase inhibition and limitation of myocardial infarct size: protection against lethal reperfusion injury. *Br J Pharmacol* 2000;130:197-200
102. Huang JQ, Radinovic S, Rezaiefar P, et al. *In vivo* myocardial infarct size reduction by a caspase inhibitor administered after the onset of ischemia. *Eur J Pharmacol* 2000;402:139-142

103. Kovacs P, Bak I, Szendrei L, et al. Non-specific caspase inhibition reduces infarct size and improves post-ischaemic recovery in isolated ischaemic/reperfused rat hearts. *Naunyn Schmiedeberg's Arch Pharmacol* 2001;364:501-507
104. Ruetten H, Badorff C, Ihling C, et al. Inhibition of caspase-3 improves contractile recovery of stunned myocardium, independent of apoptosis-inhibitory effects. *J Am Coll Cardiol* 2001;38:2063-2070
105. Minatoguchi S, Kariya T, Uno Y, et al. Caspase-dependent and serine protease-dependent DNA fragmentation of myocytes in the ischemia-reperfused rabbit heart: these inhibitors do not reduce infarct size. *Jpn Circ J* 2001;65:907-911
106. Chapman JG, Magee WP, Stukenbrok HA, et al. A novel nonpeptidic caspase-3/7 inhibitor, (S)-(+)-5-[1-(2-methoxymethylpyrrolidinyl)sulfonyl]isatin reduces myocardial ischemic injury. *Eur J Pharmacol* 2002;456:59-68
107. Yarbrough WM, Mukherjee R, Escobar GP, et al. Pharmacologic inhibition of intracellular caspases after myocardial infarction attenuates left ventricular remodeling: a potentially novel pathway. *J Thorac Cardiovasc Surg* 2003;126:1892-1899
108. Chandrashekhar Y, Sen S, Anway R, et al. Long-term caspase inhibition ameliorates apoptosis, reduces myocardial troponin-I cleavage, protects left ventricular function, and attenuates remodeling in rats with myocardial infarction. *J Am Coll Cardiol* 2004;43:295-301
109. Balsam LB, Kofidis T, Robbins RC. Caspase-3 inhibition preserves myocardial geometry and long-term function after infarction. *J Surg Res* 2005;124:194-200
110. Mersmann J, Zacharowski PA, Schmitz I, et al. Caspase inhibitor zVAD.fmk reduces infarct size after myocardial ischaemia and reperfusion in rats but not in mice. *Resuscitation* 2008;79:468-474
111. Yarbrough WM, Mukherjee R, Stroud RE, et al. Caspase inhibition modulates left ventricular remodeling following myocardial infarction through cellular and extracellular mechanisms. *J Cardiovasc Pharmacol* 2010;55:408-416
112. Bhuiyan MS, Fukunaga K. Activation of HtrA2, a mitochondrial serine protease mediates apoptosis: current knowledge on HtrA2 mediated myocardial ischemia/reperfusion injury. *Cardiovasc Ther* 2008;26:224-232
113. Cilenti L, Lee Y, Hess S, et al. Characterization of a novel and specific inhibitor for the pro-apoptotic protease Omi/HtrA2. *J Biol Chem* 2003;278:11489-11494
114. Liu HR, Gao E, Hu A, et al. Role of Omi/HtrA2 in apoptotic cell death after myocardial ischemia and reperfusion. *Circulation* 2005;111:90-96
115. Bhuiyan MS, Fukunaga K. Inhibition of HtrA2/Omi ameliorates heart dysfunction following ischemia/reperfusion injury in rat heart *in vivo*. *Eur J Pharmacol* 2007;557:168-177
116. Li Q, Li J, Ren J. UCF-101 mitigates streptozotocin-induced cardiomyocyte dysfunction: role of AMPK. *Am J Physiol Endocrinol Metab* 2009;297:E965-E973
117. Di Lisa F, Bernardi P. Mitochondria and ischemia-reperfusion injury of the heart: fixing a hole. *Cardiovasc Res* 2006;70:191-199
118. Hausenloy DJ, Yellon DM. The mitochondrial permeability transition pore: its fundamental role in mediating cell death during ischaemia and reperfusion. *J Mol Cell Cardiol* 2003;35:339-341
119. Heusch G, Boengler K, Schulz R. Inhibition of mitochondrial permeability transition pore opening: the Holy Grail of cardioprotection. *Basic Res Cardiol* 2010;105:151-154
120. Hausenloy DJ, Ong SB, Yellon DM. The mitochondrial permeability transition pore as a target for preconditioning and postconditioning. *Basic Res Cardiol* 2009;104:189-202
121. Miura T, Tanno M, Sato T. Mitochondrial kinase signalling pathways in myocardial protection from ischaemia/reperfusion-induced necrosis. *Cardiovasc Res* 2010;88:7-15
122. Nazareth W, Yafei N, Crompton M. Inhibition of anoxia-induced injury in heart myocytes by cyclosporin A. *J Mol Cell Cardiol* 1991;23:1351-1354
123. Griffiths EJ, Halestrap AP. Protection by Cyclosporin A of ischemia/reperfusion-induced damage in isolated rat hearts. *J Mol Cell Cardiol* 1993;25:1461-1469
124. Griffiths EJ, Halestrap AP. Mitochondrial non-specific pores remain closed during cardiac ischaemia, but open upon reperfusion. *Biochem J* 1995;307 (Pt 1):93-98

125. Weinbrenner C, Liu GS, Downey JM, et al. Cyclosporine A limits myocardial infarct size even when administered after onset of ischemia. *Cardiovasc Res* 1998;38:678-684
126. Squadrito F, Altavilla D, Squadrito G, et al. Cyclosporin-A reduces leukocyte accumulation and protects against myocardial ischaemia reperfusion injury in rats. *Eur J Pharmacol* 1999;364:159-168
127. Minners J, van den Bos EJ, Yellon DM, et al. Dinitrophenol, cyclosporin A, and trimetazidine modulate preconditioning in the isolated rat heart: support for a mitochondrial role in cardioprotection. *Cardiovasc Res* 2000;47:68-73
128. Hausenloy DJ, Maddock HL, Baxter GF, et al. Inhibiting mitochondrial permeability transition pore opening: a new paradigm for myocardial preconditioning? *Cardiovasc Res* 2002;55:534-543
129. Argaud L, Gateau-Roesch O, Chalabreysse L, et al. Preconditioning delays Ca²⁺-induced mitochondrial permeability transition. *Cardiovasc Res* 2004;61:115-122
130. Krolkowski JG, Bienengraeber M, Weihsrauch D, et al. Inhibition of mitochondrial permeability transition enhances isoflurane-induced cardioprotection during early reperfusion: the role of mitochondrial KATP channels. *Anesth Analg* 2005;101:1590-1596
131. Lim SY, Davidson SM, Hausenloy DJ, et al. Preconditioning and postconditioning: the essential role of the mitochondrial permeability transition pore. *Cardiovasc Res* 2007;75:530-535
132. Gomez L, Paillard M, Thibault H, et al. Inhibition of GSK3 β by postconditioning is required to prevent opening of the mitochondrial permeability transition pore during reperfusion. *Circulation* 2008;117:2761-2768
133. Huhn R, Heinen A, Weber NC, et al. Hyperglycaemia blocks sevoflurane-induced postconditioning in the rat heart *in vivo*: cardioprotection can be restored by blocking the mitochondrial permeability transition pore. *Br J Anaesth* 2008;100:465-471
134. Wang HG, Pathan N, Ethell IM, et al. Ca²⁺-induced apoptosis through calcineurin dephosphorylation of BAD. *Science* 1999;284:339-343
135. Ikeda Y, Miura T, Sakamoto J, et al. Activation of ERK and suppression of calcineurin are interacting mechanisms of cardioprotection afforded by delta-opioid receptor activation. *Basic Res Cardiol* 2006;101:418-426
136. Leshnower BG, Kanemoto S, Matsubara M, et al. Cyclosporine preserves mitochondrial morphology after myocardial ischemia/reperfusion independent of calcineurin inhibition. *Ann Thorac Surg* 2008;86:1286-1292
137. Waldmeier PC, Feldtrauer JJ, Qian T, et al. Inhibition of the mitochondrial permeability transition by the nonimmunosuppressive cyclosporin derivative NIM811. *Mol Pharmacol* 2002;62:22-29
138. Argaud L, Gateau-Roesch O, Muntean D, et al. Specific inhibition of the mitochondrial permeability transition prevents lethal reperfusion injury. *J Mol Cell Cardiol* 2005;38:367-374
139. Clarke SJ, McStay GP, Halestrap AP. Sangliferin A acts as a potent inhibitor of the mitochondrial permeability transition and reperfusion injury of the heart by binding to cyclophilin-D at a different site from cyclosporin A. *J Biol Chem* 2002;277:34793-34799
140. Hausenloy DJ, Duchon MR, Yellon DM. Inhibiting mitochondrial permeability transition pore opening at reperfusion protects against ischaemia-reperfusion injury. *Cardiovasc Res* 2003;60:617-625
141. Javadov SA, Clarke S, Das M, et al. Ischaemic preconditioning inhibits opening of mitochondrial permeability transition pores in the reperfused rat heart. *J Physiol* 2003;549:513-524
142. Gomez L, Thibault H, Gharib A, et al. Inhibition of mitochondrial permeability transition improves functional recovery and reduces mortality following acute myocardial infarction in mice. *Am J Physiol Heart Circ Physiol* 2007;293:H1654-H1661
143. Piot C, Croisille P, Staat P, et al. Effect of cyclosporine on reperfusion injury in acute myocardial infarction. *N Engl J Med* 2008;359:473-481
144. Mewton N, Croisille P, Gahide G, et al. Effect of cyclosporine on left ventricular remodeling after reperfused myocardial infarction. *J Am Coll Cardiol* 2010;55:1200-1205
145. Skyschally A, Schulz R, Heusch G. Cyclosporine A at reperfusion reduces infarct size in pigs. *Cardiovasc Drugs Ther* 2010;24:85-87
146. Lie RH, Stoettrup N, Sloth E, et al. Post-conditioning with cyclosporine A fails to reduce the infarct size in an *in vivo* porcine model. *Acta Anaesthesiol Scand* 2010;54:804-813

147. Karlsson LO, Zhou AX, Larsson E, et al. Cyclosporine does not reduce myocardial infarct size in a porcine ischemia-reperfusion model. *J Cardiovasc Pharmacol Ther* 2010;15:182-189
148. Karlsson LO, Bergh N, Grip L. Cyclosporine A, 2.5 mg/kg, Does Not Reduce Myocardial Infarct Size in a Porcine Model of Ischemia and Reperfusion. *J Cardiovasc Pharmacol Ther* 2011;[Epub ahead of print]
149. Hausenloy D, Boston-Griffiths E, Yellon D. Cyclosporin A and cardioprotection: from investigative tool to therapeutic agent. *Br J Pharmacol* 2011;[Epub ahead of print]
150. Lim WY, Messow C, Berry C. Cyclosporin variably and inconsistently reduces infarct size in experimental models of reperfused myocardial infarction: a systematic review and meta-analysis. *Br J Pharmacol* 2011;[Epub ahead of print]
151. Ruiz-Meana M, Inserte J, Fernandez-Sanz C, et al. The role of mitochondrial permeability transition in reperfusion-induced cardiomyocyte death depends on the duration of ischemia. *Basic Res Cardiol* 2011;106:1259-1268
152. Jagtap PG, Degterev A, Choi S, et al. Structure-activity relationship study of tricyclic necroptosis inhibitors. *J Med Chem* 2007;50:1886-1895
153. Teng X, Degterev A, Jagtap P, et al. Structure-activity relationship study of novel necroptosis inhibitors. *Bioorg Med Chem Lett* 2005;15:5039-5044
154. Wang K, Li J, Degterev A, et al. Structure-activity relationship analysis of a novel necroptosis inhibitor, Necrostatin-5. *Bioorg Med Chem Lett* 2007;17:1455-1465
155. Zheng W, Degterev A, Hsu E, et al. Structure-activity relationship study of a novel necroptosis inhibitor, necrostatin-7. *Bioorg Med Chem Lett* 2008;18:4932-4935
156. Cho Y, McQuade T, Zhang H, et al. RIP1-dependent and independent effects of necrostatin-1 in necrosis and T cell activation. *PLoS One* 2011;6:e23209
157. You Z, Savitz SI, Yang J, et al. Necrostatin-1 reduces histopathology and improves functional outcome after controlled cortical impact in mice. *J Cereb Blood Flow Metab* 2008;28:1564-1573
158. Rosenbaum DM, Degterev A, David J, et al. Necroptosis, a novel form of caspase-independent cell death, contributes to neuronal damage in a retinal ischemia-reperfusion injury model. *J Neurosci Res* 2010;88:1569-1576
159. Trichonas G, Murakami Y, Thanos A, et al. Receptor interacting protein kinases mediate retinal detachment-induced photoreceptor necrosis and compensate for inhibition of apoptosis. *Proc Natl Acad Sci U S A* 2010;107:21695-21700
160. Northington FJ, Chavez-Valdez R, Graham EM, et al. Necrostatin decreases oxidative damage, inflammation, and injury after neonatal HI. *J Cereb Blood Flow Metab* 2011;31:178-189
161. Xu X, Chua KW, Chua CC, et al. Synergistic protective effects of humanin and necrostatin-1 on hypoxia and ischemia/reperfusion injury. *Brain Res* 2010;1355:189-194
162. Smith CC, Davidson SM, Lim SY, et al. Necrostatin: a potentially novel cardioprotective agent? *Cardiovasc Drugs Ther* 2007;21:227-233
163. Lim SY, Davidson SM, Mocanu MM, et al. The cardioprotective effect of necrostatin requires the cyclophilin-D component of the mitochondrial permeability transition pore. *Cardiovasc Drugs Ther* 2007;21:467-469
164. Lacerda L, Somers S, Opie LH, et al. Ischaemic postconditioning protects against reperfusion injury via the SAFE pathway. *Cardiovasc Res* 2009;84:201-208
165. Liu J, van MA, Vrijssen K, et al. MicroRNA-155 prevents necrotic cell death in human cardiomyocyte progenitor cells via targeting RIP1. *J Cell Mol Med* 2010;15:1474-1482
166. Noort WA, Oerlemans MI, Rozemuller H, et al. Human versus porcine mesenchymal stromal cells: phenotype, differentiation potential, immunomodulation and cardiac improvement after transplantation. *J Cell Mol Med* 2011;[Epub ahead of print]
167. Hausenloy DJ, Yellon DM. Reperfusion injury salvage kinase signalling: taking a RISK for cardioprotection. *Heart Fail Rev* 2007;12:217-234
168. Lasley RD, Rhee JW, Van Wylen DG, et al. Adenosine A1 receptor mediated protection of the globally ischemic isolated rat heart. *J Mol Cell Cardiol* 1990;22:39-47

169. Thornton JD, Liu GS, Olsson RA, et al. Intravenous pretreatment with A1-selective adenosine analogues protects the heart against infarction. *Circulation* 1992;85:659-665
170. McIntosh VJ, Lasley RD. Adenosine Receptor-Mediated Cardioprotection: Are All 4 Subtypes Required or Redundant? *J Cardiovasc Pharmacol Ther* 2011;[Epub ahead of print]
171. Norton ED, Jackson EK, Turner MB, et al. The effects of intravenous infusions of selective adenosine A1-receptor and A2-receptor agonists on myocardial reperfusion injury. *Am Heart J* 1992;123:332-338
172. Mahaffey KW, Puma JA, Barbagelata NA, et al. Adenosine as an adjunct to thrombolytic therapy for acute myocardial infarction: results of a multicenter, randomized, placebo-controlled trial: the Acute Myocardial Infarction Study of Adenosine (AMISTAD) trial. *J Am Coll Cardiol* 1999;34:1711-1720
173. Marzilli M, Orsini E, Marraccini P, et al. Beneficial effects of intracoronary adenosine as an adjunct to primary angioplasty in acute myocardial infarction. *Circulation* 2000;101:2154-2159
174. Quintana M, Hjemdahl P, Sollevi A, et al. Left ventricular function and cardiovascular events following adjuvant therapy with adenosine in acute myocardial infarction treated with thrombolysis, results of the ATTenuation by Adenosine of Cardiac Complications (ATTACC) study. *Eur J Clin Pharmacol* 2003;59:1-9
175. Ross AM, Gibbons RJ, Stone GW, et al. A randomized, double-blinded, placebo-controlled multicenter trial of adenosine as an adjunct to reperfusion in the treatment of acute myocardial infarction (AMIS-TAD-II). *J Am Coll Cardiol* 2005;45:1775-1780
176. Fokkema ML, Vlaar PJ, Vogelzang M, et al. Effect of high-dose intracoronary adenosine administration during primary percutaneous coronary intervention in acute myocardial infarction: a randomized controlled trial. *Circ Cardiovasc Interv* 2009;2:323-329
177. Kasama S, Furuya M, Toyama T, et al. Effect of atrial natriuretic peptide on left ventricular remodelling in patients with acute myocardial infarction. *Eur Heart J* 2008;29:1485-1494
178. Takagi G, Kiuchi K, Endo T, et al. Alpha-human atrial natriuretic peptide, carperitide, reduces infarct size but not arrhythmias after coronary occlusion/reperfusion in dogs. *J Cardiovasc Pharmacol* 2000;36:22-30
179. Sangawa K, Nakanishi K, Ishino K, et al. Atrial natriuretic peptide protects against ischemia-reperfusion injury in the isolated rat heart. *Ann Thorac Surg* 2004;77:233-237
180. Yang XM, Philipp S, Downey JM, et al. Atrial natriuretic peptide administered just prior to reperfusion limits infarction in rabbit hearts. *Basic Res Cardiol* 2006;101:311-318
181. Rastegar MA, Vegh A, Papp JG, et al. Atrial natriuretic peptide reduces the severe consequences of coronary artery occlusion in anaesthetized dogs. *Cardiovasc Drugs Ther* 2000;14:471-479
182. Hough AK, McNamee RA, Kerner A, et al. Atrial natriuretic peptide increases inflammation, infarct size, and mortality after experimental coronary occlusion. *Am J Physiol Heart Circ Physiol* 2009;296:H655-H661
183. Hayashi M, Tsutamoto T, Wada A, et al. Intravenous atrial natriuretic peptide prevents left ventricular remodeling in patients with first anterior acute myocardial infarction. *J Am Coll Cardiol* 2001;37:1820-1826
184. Kuga H, Ogawa K, Oida A, et al. Administration of atrial natriuretic peptide attenuates reperfusion phenomena and preserves left ventricular regional wall motion after direct coronary angioplasty for acute myocardial infarction. *Circ J* 2003;67:443-448
185. Kasama S, Toyama T, Hatori T, et al. Effects of intravenous atrial natriuretic peptide on cardiac sympathetic nerve activity and left ventricular remodeling in patients with first anterior acute myocardial infarction. *J Am Coll Cardiol* 2007;49:667-674
186. Kitakaze M, Asakura M, Kim J, et al. Human atrial natriuretic peptide and nicorandil as adjuncts to reperfusion treatment for acute myocardial infarction (J-WIND): two randomised trials. *Lancet* 2007;370:1483-1493
187. Lonborg J, Vejstrup N, Kelbaek H, et al. Exenatide reduces reperfusion injury in patients with ST-segment elevation myocardial infarction. *Eur Heart J* 2011;[Epub ahead of print]
188. Davidson MB, Bate G, Kirkpatrick P. Exenatide. *Nat Rev Drug Discov* 2005;4:713-714
189. Davidson MH. Cardiovascular effects of glucagonlike peptide-1 agonists. *Am J Cardiol* 2011;108:33B-41B

190. Nikolaidis LA, Mankad S, Sokos GG, et al. Effects of glucagon-like peptide-1 in patients with acute myocardial infarction and left ventricular dysfunction after successful reperfusion. *Circulation* 2004;109:962-965
191. Nikolaidis LA, Elahi D, Hentosz T, et al. Recombinant glucagon-like peptide-1 increases myocardial glucose uptake and improves left ventricular performance in conscious dogs with pacing-induced dilated cardiomyopathy. *Circulation* 2004;110:955-961
192. Nikolaidis LA, Elahi D, Shen YT, et al. Active metabolite of GLP-1 mediates myocardial glucose uptake and improves left ventricular performance in conscious dogs with dilated cardiomyopathy. *Am J Physiol Heart Circ Physiol* 2005;289:H2401-H2408
193. Sokos GG, Nikolaidis LA, Mankad S, et al. Glucagon-like peptide-1 infusion improves left ventricular ejection fraction and functional status in patients with chronic heart failure. *J Card Fail* 2006;12:694-699
194. Nikolaidis LA, Doverspike A, Hentosz T, et al. Glucagon-like peptide-1 limits myocardial stunning following brief coronary occlusion and reperfusion in conscious canines. *J Pharmacol Exp Ther* 2005;312:303-308
195. Bose AK, Mocanu MM, Carr RD, et al. Glucagon-like peptide 1 can directly protect the heart against ischemia/reperfusion injury. *Diabetes* 2005;54:146-151
196. Bose AK, Mocanu MM, Carr RD, et al. Glucagon like peptide-1 is protective against myocardial ischemia/reperfusion injury when given either as a preconditioning mimetic or at reperfusion in an isolated rat heart model. *Cardiovasc Drugs Ther* 2005;19:9-11
197. Bose AK, Mocanu MM, Carr RD, et al. Myocardial ischaemia-reperfusion injury is attenuated by intact glucagon like peptide-1 (GLP-1) in the *in vitro* rat heart and may involve the p70s6K pathway. *Cardiovasc Drugs Ther* 2007;21:253-256
198. Sonne DP, Engstrom T, Treiman M. Protective effects of GLP-1 analogues exendin-4 and GLP-1(9-36) amide against ischemia-reperfusion injury in rat heart. *Regul Pept* 2008;146:243-249
199. Timmers L, Henriques JP, de Kleijn DP, et al. Exenatide reduces infarct size and improves cardiac function in a porcine model of ischemia and reperfusion injury. *J Am Coll Cardiol* 2009;53:501-510
200. Ban K, Noyan-Ashraf MH, Hoefler J, et al. Cardioprotective and vasodilatory actions of glucagon-like peptide 1 receptor are mediated through both glucagon-like peptide 1 receptor-dependent and -independent pathways. *Circulation* 2008;117:2340-2350
201. Ban K, Kim KH, Cho CK, et al. Glucagon-like peptide (GLP)-1(9-36)amide-mediated cytoprotection is blocked by exendin(9-39) yet does not require the known GLP-1 receptor. *Endocrinology* 2010;151:1520-1531
202. Scholte M, Timmers L, Bernink FJ, et al. Effect of additional treatment with EXenatide in patients with an acute myocardial infarction (EXAMI): study protocol for a randomized controlled trial. *Trials* 2011;12:240
203. Zorov DB, Juhaszova M, Sollott SJ. Mitochondrial ROS-induced ROS release: an update and review. *Biochim Biophys Acta* 2006;1757:509-517
204. Javadov S, Karmazyn M, Escobales N. Mitochondrial permeability transition pore opening as a promising therapeutic target in cardiac diseases. *J Pharmacol Exp Ther* 2009;330:670-678
205. Bell RM, Yellon DM. There is More to Life than Revascularization: Therapeutic Targeting of Myocardial Ischemia/Reperfusion Injury. *Cardiovasc Ther* 2010;29:e67-e79
206. Satoh N, Sato T, Shimada M, et al. Lusitropic effect of MCC-135 is associated with improvement of sarcoplasmic reticulum function in ventricular muscles of rats with diabetic cardiomyopathy. *J Pharmacol Exp Ther* 2001;298:1161-1166
207. Satoh N, Kitada Y. Effects of MCC-135 on Ca²⁺ uptake by sarcoplasmic reticulum and myofilament sensitivity to Ca²⁺ in isolated ventricular muscles of rats with diabetic cardiomyopathy. *Mol Cell Biochem* 2003;249:45-51
208. Yarbrough WM, Mukherjee R, Escobar GP, et al. Modulation of calcium transport improves myocardial contractility and enzyme profiles after prolonged ischemia-reperfusion. *Ann Thorac Surg* 2003;76:2054-2061

209. Satoh N, Kitada Y. Cardioprotective effect of MCC-135 is associated with inhibition of Ca²⁺ overload in ischemic/reperfused hearts. *Eur J Pharmacol* 2004;499:179-187
210. Kawasumi H, Satoh N, Kitada Y. Caldaret, an intracellular Ca²⁺ handling modulator, limits infarct size of reperfused canine heart. *J Pharmacol Sci* 2007;103:222-233
211. Bar FW, Tzivoni D, Dirksen MT, et al. Results of the first clinical study of adjunctive CALdaret (MCC-135) in patients undergoing primary percutaneous coronary intervention for ST-Elevation Myocardial Infarction: the randomized multicentre CASTEMI study. *Eur Heart J* 2006;27:2516-2523
212. Jang IK, Weissman NJ, Picard MH, et al. A randomized, double-blind, placebo-controlled study of the safety and efficacy of intravenous MCC-135 as an adjunct to primary percutaneous coronary intervention in patients with acute myocardial infarction: Evaluation of MCC-135 for left ventricular salvage in acute myocardial infarction (EVOLVE). *Am Heart J* 2008;155:113-118
213. Tzivoni D, Balkin J, Bar FW, et al. Effect of caldaret on the incidence of severe left ventricular dysfunction in patients with ST-elevation myocardial infarction undergoing primary coronary intervention. *Am J Cardiol* 2009;103:1-4
214. Arslan F, Smeets MB, O'Neill LA, et al. Myocardial ischemia/reperfusion injury is mediated by leukocytic toll-like receptor-2 and reduced by systemic administration of a novel anti-toll-like receptor-2 antibody. *Circulation* 2010;121:80-90
215. Lai RC, Arslan F, Lee MM, et al. Exosome secreted by MSC reduces myocardial ischemia/reperfusion injury. *Stem Cell Res* 2010;4:214-222.

7



Martinus I.F.J. Oerlemans¹

Jia Liu^{1,2}

Fatih Arslan¹

Krista den Ouden¹

Ben J. van Middelaar¹

Pieter A. Doevendans^{1,3}

Joost P.G. Sluijter^{1,3}

¹ Department of Cardiology, University Medical Center Utrecht, the Netherlands.

² Department of Endocrinology, Provincial Hospital affiliated to Shandong University, Jinan, China.

³ Interuniversity Cardiology Institute Netherlands (ICIN), Utrecht, the Netherlands.

Inhibition of RIP1-dependent necrosis prevents adverse cardiac remodeling after myocardial ischemia-reperfusion *in vivo*

Basic Res Cardiol. 2012; 107: 270-282

ABSTRACT

Background

Accumulating evidence indicated that programmed necrosis plays a critical role in cell death during ischemia-reperfusion. Necrostatin-1 (Nec-1), a small molecule capable of inhibiting a key regulator of programmed necrosis (RIP1), was shown to prevent necrotic cell death in experimental models including cardiac ischemia. However, no functional follow-up was performed and the action of Nec-1 remains unclear. Here, we studied whether Nec-1 inhibits RIP1-dependent necrosis and leads to long-term improvements after ischemia-reperfusion *in vivo*.

Methods and Results

Mice underwent 30 minutes of ischemia and received, 5 minutes before reperfusion, 3.3mg/kg Nec-1 or vehicle treatment, followed by reperfusion. Nec-1 administration reduced infarct size to $26.3 \pm 1.3\%$ ($P=0.001$) compared to $38.6 \pm 1.7\%$ in vehicle-treated animals. Furthermore, Nec-1 inhibited RIP1/RIP3 phosphorylation *in vivo* and significantly reduced necrotic cell death, while apoptotic cell death remained constant. By using MRI, cardiac dimensions and function were assessed before and 28 days after surgery. Nec-1-treated mice displayed less adverse remodeling (end-diastolic volume 63.5 ± 2.8 vs. $74.9 \pm 2.8 \mu\text{l}$, $P=0.031$) and preserved cardiac performance (ejection fraction 45.81 ± 2.05 vs. $36.03 \pm 2.37\%$, $P=0.016$). Nec-1 treatment significantly reduced inflammatory influx, tumor necrosis factor- α mRNA levels and oxidative stress levels. Interestingly, this was accompanied by significant changes in the expression signature of oxidative stress genes.

Conclusion

Administration of Nec-1 at the onset of reperfusion inhibits RIP1-dependent necrosis *in vivo*, leading to infarct size reduction and preservation of cardiac function. The cardioprotective effect of Nec-1 highlights the importance of necrotic cell death in the ischemic heart, thereby opening a new direction for therapy in patients with myocardial infarction.

INTRODUCTION

Acute myocardial infarction (MI) remains one of the leading causes of morbidity and mortality in the western world for which early reperfusion is currently the most effective therapy¹. Paradoxically, reperfusion itself results in additional damage, also known as myocardial ischemia-reperfusion (I/R) injury². Although the exact mechanism remains to be established, I/R injury can extent cell death in the endangered myocardium even further, in which generation of reactive oxygen species (ROS), mitochondrial dysfunction, and a rapid increase of inflammatory cells and cytokines play an important role^{3, 4} as well as coronary microembolization⁵. For many years, apoptosis was considered as the only form of regulated cell death and studies investigating myocyte cell death mainly focused on apoptosis^{6, 7}. However, it has become clear that at least some part of necrotic cell death is regulated, mediated by opening of the mitochondrial permeability transition pore (MPTP)^{8, 9}. Furthermore, emerging evidence has demonstrated that the kinase activity of receptor-interacting protein 1 (RIP1) and its interaction with RIP3 after death receptor stimulation are critically involved in programmed necrosis, also known as necroptosis¹⁰. Necrostatin-1 (Nec-1), a small molecule capable of inhibiting RIP1 kinase activity, was shown to inhibit necroptosis without affecting other RIP1-mediated processes and efficiently prevented necrotic cell death after ischemic brain injury^{11, 12}.

Although the protocol was limited to 2 hours of reperfusion only, Nec-1 also reduced myocardial infarct size^{13, 14}. Unfortunately, these data were obtained from a limited number of animals and no functional follow-up was performed. Many cardioprotective interventions, although successful in experimental studies, failed in clinical settings for which the lack of functional follow-up and difficulties in translating infarct size reduction to improved (clinical) outcome were mainly responsible^{15, 16}. Currently, it is unclear whether Nec-1 directly inhibits necrotic cell death via targeting RIP1/3 phosphorylation after cardiac I/R *in vivo*, whether apoptosis is involved and if ROS is affected. More importantly, long-term efficiency needs to be established before taking further steps towards a clinical setting.

In the present study, we show that administration of Nec-1 prior to reperfusion inhibits RIP1/3-phosphorylation and necrotic cell death *in vivo* and prevents adverse cardiac remodeling by reducing the inflammatory response and limiting oxidative stress. These results highlight the potential therapeutic value of Nec-1 in protection against I/R injury which might be translated to a novel cardioprotective strategy for patient benefit in the future.

METHODS

Approval for this study was granted by the Animal Ethical Experimentation Committee (Utrecht University) and was carried out in accordance with the *Guide for the Care and Use of Laboratory Animals*, with prior approval. A figure to illustrate the experimental design and overview of tissue collection obtained at different times of reperfusion is provided online (Supplementary Figure 1).

Murine Model of Myocardial Ischemia-Reperfusion and Drug Administration

Male C57Bl/6 mice (10-12 weeks, Harlan Laboratories) underwent left coronary artery (LCA) ligation as previously described¹⁷, followed by reperfusion. Briefly, mice were anesthetized with fentanyl (0.05 mg/kg), midazolam (5 mg/kg) and medetomidine 0.5 mg/kg through an intraperitoneal (ip) injection and ventilated with 100% oxygen, maintaining a core body temperature of 37°C. The LCA was ligated just below the left atrial appendage for 30 minutes with an 8-0 Ethilon monofil suture, including a piece of soft tubing. Reperfusion was initiated by releasing the ligature and removal of the tubing, leaving a piece of suture in place. The chest wall was closed in layers and the animals received atipamezole (2.5 mg/kg ip), flumazenil (0.5 mg/kg ip) and temgesic (0.1 mg/kg ip). After detubation, mice were kept warm until fully recovered. Mice were given either phosphate-buffered saline (PBS) or 3.5mg/kg Necrostatin-1 (Calbiochem) dissolved in PBS via a tail vein injection 5 minutes prior to reperfusion. Mice were sacrificed using a cocktail of ketamine (100mg/kg ip) and medetomidine (8mg/ml), followed by cardiac explantation.

Infarct Size

After 24 hours of reperfusion (n=8/group), infarct size (IS) was determined as a percentage of the area at risk (AAR)^{18, 19}. After re-ligating the LCA at the level marked by the suture left in place, Evans Blue dye (4%) was injected retrogradely via the thoracic aorta and hearts were explanted, rinsed and put in a -20°C freezer. After 1 hour, hearts were sliced into 1mm cross sections and incubated in 1% triphenyltetrazolium chloride (TTC, Sigma-Aldrich) at 37°C for 15 minutes, followed by formaldehyde fixation. Cardiac sections were photographed (Canon EOS 400D) and IS, AAR, and left ventricular (LV) area were measured with ImageJ software (version 1.34) and analyzed by a blinded investigator.

Immunoprecipitation and Western Blotting

Snap-frozen cardiac tissue was homogenized in 1ml of ice-cold lysis buffer and the supernatant was collected as previously described²⁰. For RIP1 immunoprecipitation, 2mg protein was pre-cleared with protein G-sepharose beads for 2 hours and incubated with anti-RIP1 antibody (BD 610459) or control IgG O/N at 4°C. For western blotting, immunoprecipitates or 20µg total lysate were run on 4%-12% SDS-polyacrylamide gel electrophoresis and transferred onto nitrocellulose membranes. After blocking with 5% bovine serum albumin (BSA), membranes were incubated with RIP1 (BD 610459), phosphoserine (Zymed 61-8100), RIP3 (SantaCruz sc-135170), MLKL (Abcam ab71399) or GAPDH (Cell Signaling 2118), followed by incubation with goat anti-rabbit secondary antibody (Dako, P0448). Signal was visualised with enhanced chemiluminescence using the ChemiDoc XRS system (Bio-Rad) and analyzed with Image Lab (Bio-Rad).

Propidium Iodide and TUNEL staining

Animals received ip injections of 10mg/kg Propidium Iodide (PI; Sigma) to label necrotic cells one hour before termination (n=6/group). After termination, hearts were explanted and snap-frozen in liquid nitrogen. Frozen sections of 7µm were cut and counterstained with Hoechst after which quantification of necrotic cells was performed. Using alternating slides, TUNEL staining (In Situ Death Detection Kit 1684795, Roche) was performed to

detect apoptotic cells. Data analysis was performed by a blinded investigator using Cell[^]P imaging software (Olympus).

Lactate Dehydrogenase Assay

After termination, blood was collected to determine total Lactate Dehydrogenase (LDH) released from the heart. After centrifugation at 1300 x g for 10 minutes, 10 μ l of plasma was used to determine LDH concentration using the Toxicology Assay Kit (Sigma) according to the manufacturer's manual and expressed as absorbance at 492nm on a multiwell plate reader (Thermo Fisher).

Magnetic Resonance Imaging

Mice underwent serial assessment of cardiac dimensions and function by magnetic resonance imaging (9.4T MRI; Bruker, Germany) under isoflurane anaesthesia before and 28 days after surgery (n=9/group). LV function and geometry was assessed by a technician, blinded to treatment as previously described^{18,19}. All MRI data were analyzed with Qmass digital imaging software (Medis, Leiden, the Netherlands).

Immunohistochemistry and Histology

After termination at 1 and 3 days post-IR, hearts were flushed with 0.9% saline, explanted, and fixed in 4% formalin. Paraffin-embedded heart sections of 5 μ m were stained for neutrophils (rat anti-mouse Ly6G, BD Pharmingen 551459) and macrophages (rat anti-mouse Mac-3, BD Pharmingen 553322). Secondary antibody used was goat anti-rat IgG (Southern Biotech, 3052-08) followed by HRPO-coupled streptavidine (Southern Biotech, 7100-05), using 3-Amino-9-ethyl carbazole (AEC) for visualisation. Quantification of scar area after 28 days of infarction was performed with picosirius red staining of 4% formalin-fixed and paraffin-embedded heart sections of 5 μ m as previously described. Analysis was done with circularly polarized light and digital image microscopy. Total scar area was determined as the percentage positive staining for picosirius red of the LV wall.

Detection of Reactive Oxygen Species

In situ ROS levels were assessed using dihydroethidium (DHE) as described previously²¹ in sections after 24 hours of reperfusion. The fluorescence reaction was carried out by incubating cardiac sections with DHE (10 μ mol/L) for 30 minutes at 37°C.

Quantitative RT-PCR

Total RNA was isolated from LV using TriPure (Roche Applied Science) after 24 hours of reperfusion (n=5/group). One μ g DNA-free RNA was used for cDNA synthesis (iScript cDNA synthesis kit, Bio-Rad), followed by quantitative real-time PCR (qRT-PCR) amplification with Sybr-Green mastermix (Bio-Rad) in a MyIQ single-colour real-time PCR system (Bio-Rad). After normalisation for P0, relative gene expression was calculated by $\Delta\Delta$ Ct.

Oxidative Stress and Antioxidant Defense Super-Array

Total DNA-free RNA was isolated as described above and cDNA of Nec-1 and vehicle-treated animals was pooled. A total of 84 genes involved in oxidative stress and antioxidant

defense (SABiosciences, PAMM-065A) were detected using a qRT-PCR profiling array, followed by analysis using online RT2 Profiler™ PCR Array Data Analysis software. Genes showing a difference of >2-fold were screened and subsequently selected if any relationship with cardiac injury was described, followed by confirmation with qRT-PCR in Nec-1 vs. vehicle-treated animals (n=5/group).

Statistical analysis

Data are presented as mean±SEM. Differences between groups were analyzed using ANOVA with Bonferroni correction or Mann–Whitney U test when appropriate. Paired T-test was used to compare individual groups at baseline and 28 days. All tests were two-sided, using a significance level of P<0.05 (SPSS Statistics v17Chicago, United States).

RESULTS

Necrostatin-1 inhibits RIP1- and RIP3-phosphorylation after myocardial I/R *in vivo*

RIP1 kinase activity and subsequent recruitment of RIP3 to RIP1 are necessary for the induction of programmed necrosis²². Therefore, we assessed the expression of RIP1 and RIP3 protein after myocardial I/R, which were significantly increased after vehicle treatment compared to baseline (Figure 1a, b). RIP3 expression was markedly increased in vehicle-treated animals but not after Nec-1 treatment, suggesting that RIP1-mediated necrosis is involved in myocyte death in the ischemic heart. In addition, we assessed the expression of RIP3 and RIP1 mRNA levels in the heart by qRT-PCR (Supplementary Figure 2a, b). RIP3 mRNA expression increased significantly after myocardial I/R in both groups (no differences between treatments), RIP1 mRNA levels increased slightly.

Next, we investigated the role of RIP1 phosphorylation and recruitment of RIP3 to RIP1 by immunoprecipitation (Supplementary Figure 2c). In the vehicle-treated animals, the amount of immuno-precipitated RIP1 protein and its phosphorylation status were clearly increased after myocardial I/R, compared to Nec-1 treatment (Figure 1c, d). Importantly, Nec-1 significantly decreased RIP1 phosphorylation *in vivo* and significantly reduced RIP3 recruitment to RIP1 as well, together with its phosphorylation status.

Very recently, MLKL (mixed lineage kinase domain-like) was identified as key component downstream of RIP3 in the execution of RIP1-mediated necrosis *in vitro*^{23, 24}. MLKL protein expression was significantly increased after myocardial I/R (Fig 1e, f). Interestingly, Nec-1 treatment significantly reduced the amount of MLKL protein recruited to RIP1 *in vivo* (Figure 1g, h). Inhibition of RIP1/3 phosphorylation and the interaction with MLKL are clearly involved in Nec-1 induced protection *in vivo*.

Necrostatin-1 prevents necrotic cell death and reduces myocardial infarct size *in vivo*

We examined whether decreased RIP1/3-phosphorylation by Nec-1 also affected the amount of necrosis after myocardial I/R. Nec-1 administration resulted in less PI-positive cells in the infarct when compared to vehicle treatment (5317±140 vs. 9754±677 cells/mm², P=0.028), suggesting a reduction of necrotic cell death with 45% (Figure 2). The presence of TUNEL-positive cells/mm² was not affected by Nec-1 (Supplementary Figure

3). Subsequently, we investigated whether Nec-1 treatment attributed to a reduction in infarct size. Twenty-four hours after reperfusion, vehicle-treated mice showed an infarct size of $38.6 \pm 1.7\%$ (Figure 3a-c) whereas Nec-1 administration reduced infarct size to

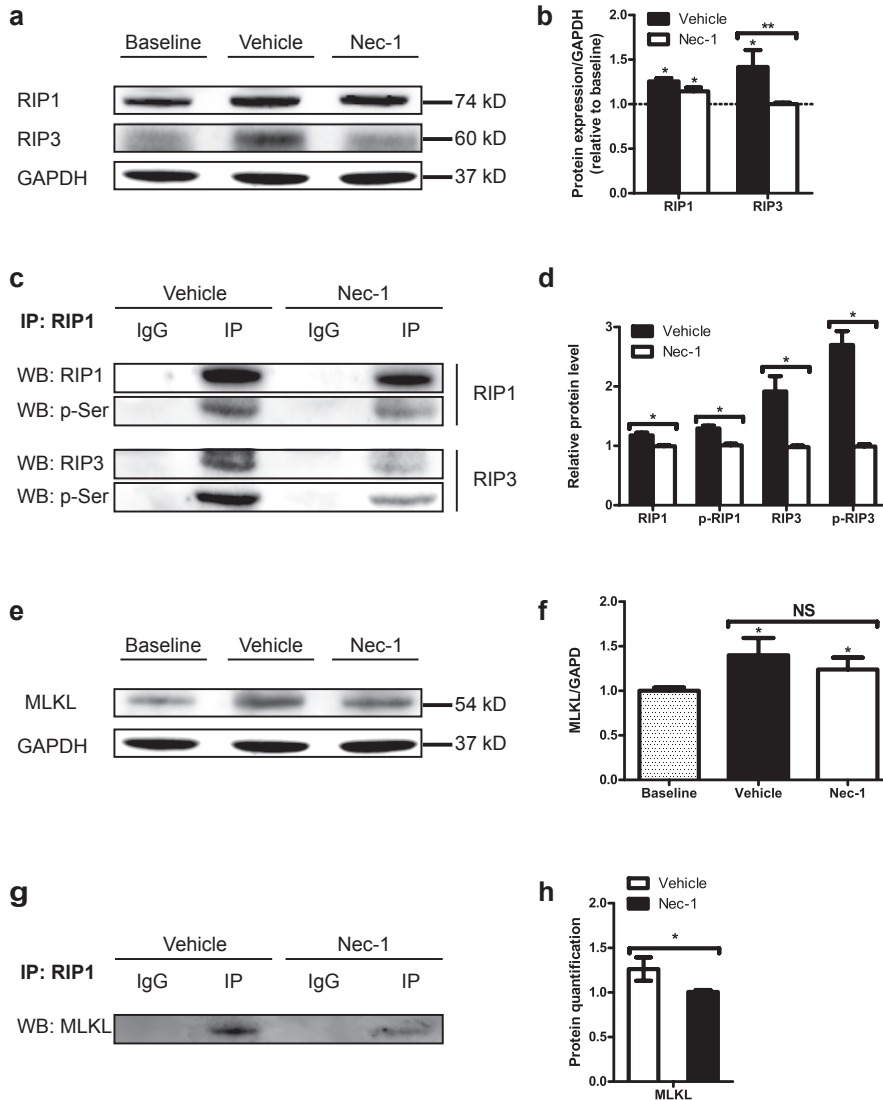


Figure 1 | Nec-1 inhibits RIP1/3-phosphorylation and MLKL recruitment after myocardial I/R *in vivo* (a, b) Western blot and quantification showing increased RIP1 and RIP3 protein expression after ischemia-reperfusion. (c, d) RIP1 phosphorylation, binding of RIP3 and RIP3 phosphorylation were significantly decreased in Nec-1 – treated animals. (e, f) Western blot and quantification showing increased MLKL protein expression after ischemia-reperfusion. (g, h) MLKL recruitment to RIP1 was significantly decreased after Nec-1 treatment. (n=5/group, (b, f) *P<0.05 vs. baseline, (b) **P<0.05 between treatments, (d, h) *P<0.05 between treatments)

26.3±1.3% (32% reduction, P=0.001), while the area at risk was similar. In line with a reduction in infarct size, relative plasma LDH levels -released by necrotic cardiomyocytes- were also decreased (Figure 3d). LDH levels in vehicle-treated animals increased four times after I/R, while Nec-1 treatment showed a 2-fold increase only (P=0.025).

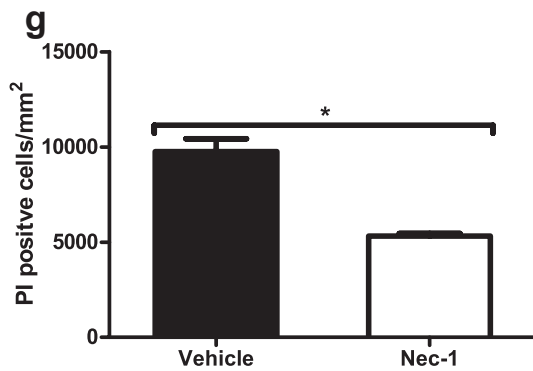
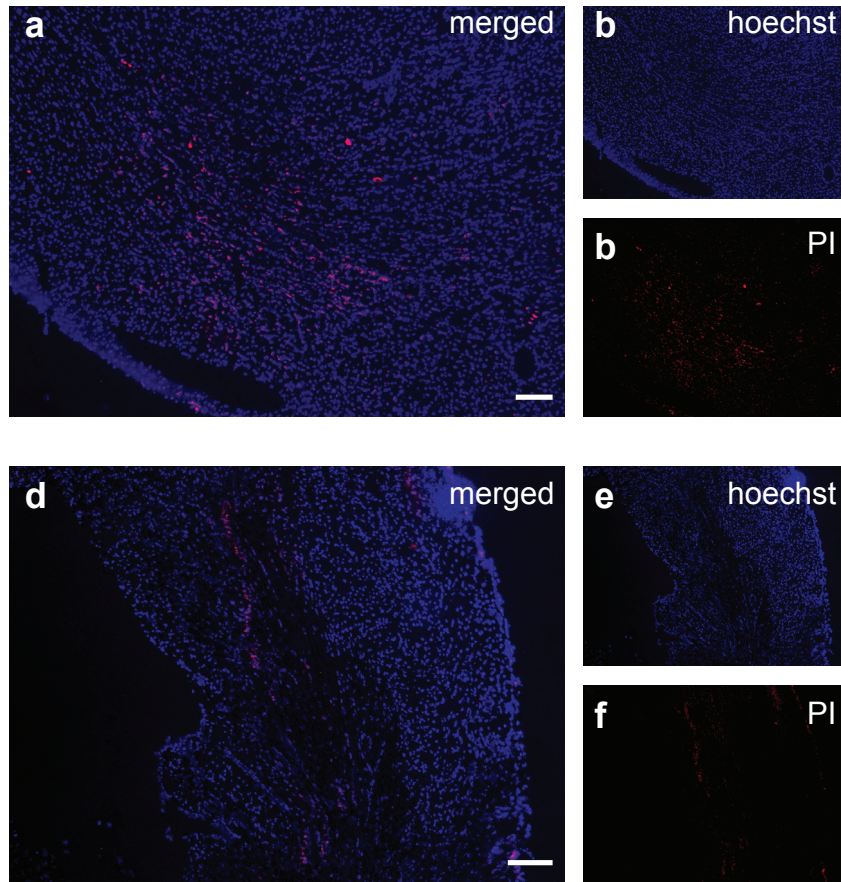


Figure 2 | Nec-1 prevents necrotic cell death in vivo after I/R

Representative pictures of propidium iodide (PI, red) and nuclear (Hoechst, blue) staining 1d after I/R. (a) Merged and separated (b-c) fluorescent pictures of vehicle-treated animals. (d) Merged and separated (e-f) fluorescent pictures after Nec-1 treatment (scale bar 200 µm). (g) Quantification of PI-positive cells representing necrotic cell death 1 day after I/R (n=6/group, *P<0.05).

Necrostatin-1 preserves cardiac function and prevents adverse cardiac remodeling after myocardial I/R injury *in vivo*

We assessed the effect of Nec-1 on long-term cardiac function and remodeling, an important step for investigating novel cardioprotective strategies¹⁵. Both end-diastolic volume (EDV) and end-systolic volume (ESV) of vehicle-treated animals increased significantly after myocardial I/R when compared to baseline (Figure 4). Nec-1 administration preserved LV volumes compared to vehicle treatment ($P < 0.05$). As shown in Table 1, ejection fraction (EF) was preserved in Nec-1-treated animals ($45.8 \pm 2.1\%$ vs. $36.0 \pm 2.4\%$, $P = 0.016$). Consistently, regional LV function (systolic wall thickening, $P = 0.012$) was maintained and LV wall thinning was significantly decreased in Nec-1-treated mice ($P = 0.020$). In line with prevention of adverse remodeling, mice treated with Nec-1 showed less fibrotic scar formation when compared to vehicle treatment (38.4 ± 2.7 vs. $22.5 \pm 2.0\%$ of LV, $P < 0.01$; Figure 4d,e).

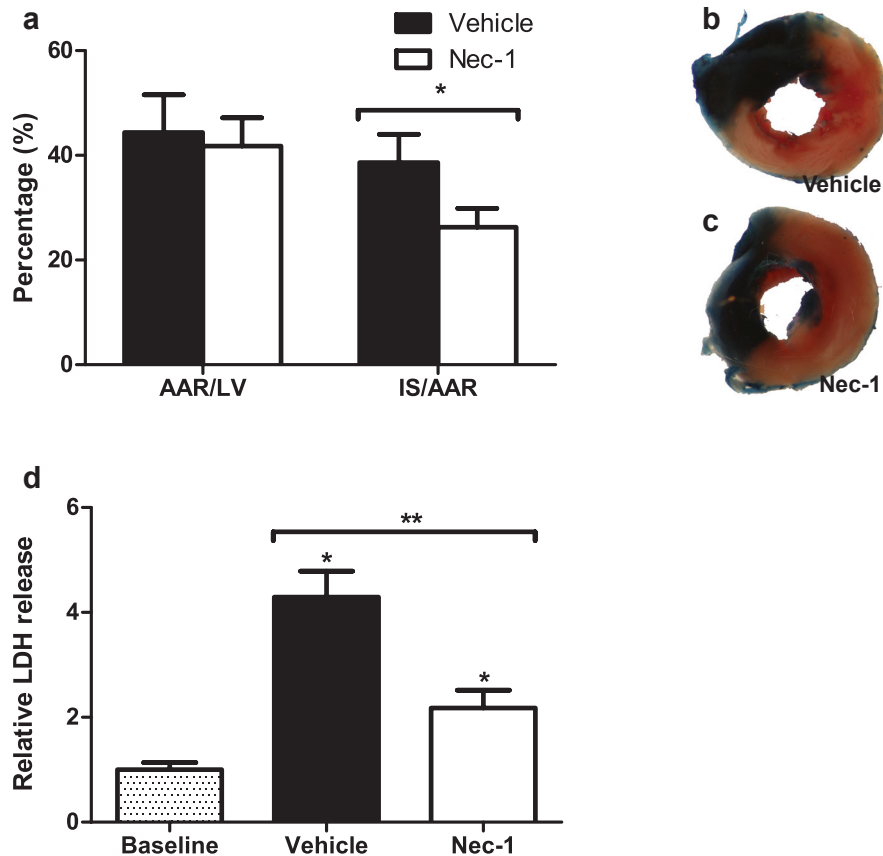


Figure 3 | Nec-1 reduces myocardial infarct size. Infarct size (IS) is expressed as %AAR (a) Nec-1 reduces IS, while AAR was equal in both groups ($n = 8/\text{group}$, $*P < 0.01$). (b-c) Representative cross sections after 24 hours of reperfusion. (d) Relative plasma LDH levels at baseline and 24 hours of reperfusion ($n = 6/\text{group}$, $*P < 0.01$ vs. control, $**P < 0.05$ between treatments).

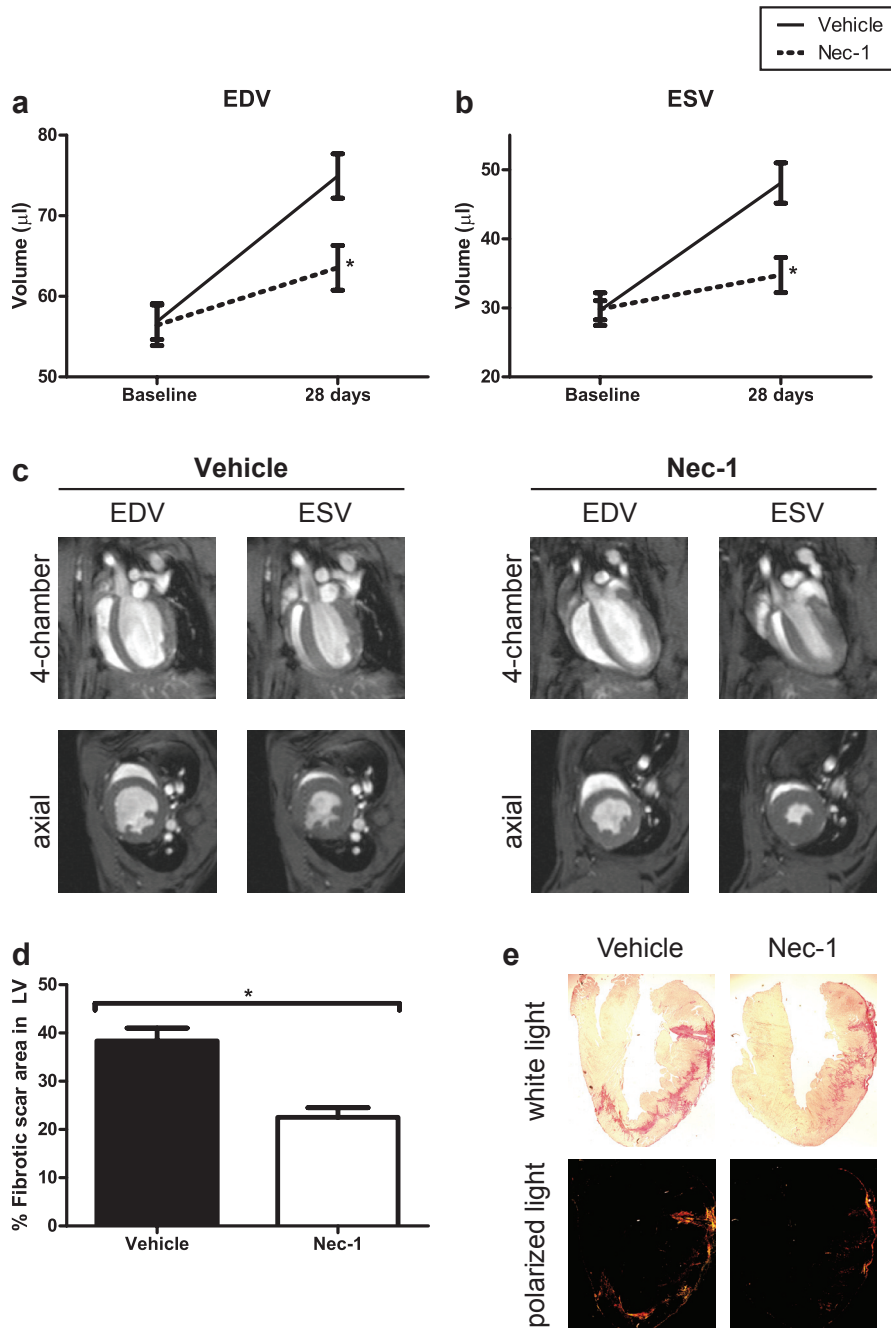


Figure 4 | Cardiac geometry and fibrosis

Nec-1 prevents cardiac remodeling after I/R. Both increase in EDV (a) and ESV (b) was significantly decreased in Nec-1-treated animals 28 days after I/R (n=9/group, *P<0.05). Representative 4-chamber and axial MRI pictures of EDV and ESV in vehicle-treated (c) and Nec-1-treated (d) animals. Quantification (e) and representative pictures (f) of scar area as percentage of the LV after 28 days of infarction (n=7/group, *P<0.01).

Table 1 | EF, Systolic Wall Thickening and Wall Thickness at baseline and 28 days after reperfusion

	Vehicle		Nec-1	
	Baseline	28 Days	Baseline	28 Days
Ejection Fraction (EF), %	48.21±0.67	36.03±2.37*	47.77±2.07	45.81±2.05†
Systolic Wall Thickening (SWT), remote, %	37.60±1.26	33.39±1.65	36.46±1.67	40.62±1.97†
Systolic Wall Thickening (SWT), infarct, %	47.76±1.88	15.41±3.02*	44.04±2.77	29.46±3.77*†
Wall Thickness (WT), remote, mm	0.81±0.01	0.83±0.02	0.83±0.02	0.85±0.02
Wall Thickness (WT), infarct, mm	0.90±0.02	0.77±0.04*	0.91±0.03	0.90±0.04†

Data are presented as mean±SEM, n=9/group. *P<0.05 vs. baseline, †P<0.05 vs. vehicle treatment.

Necrostatin-1 reduces inflammation after myocardial I/R injury *in vivo*

As circulating inflammatory cells also contribute to myocardial I/R injury, we studied the influx of neutrophils and macrophages at 1 and 3 days of reperfusion (Figure 5). Nec-1–treated animals showed a reduction of neutrophil influx at all time points compared to vehicle treatment (Figure 5a-b, P<0.05). Macrophage influx in the infarcted area was also reduced by Nec-1 treatment, especially on day 3 post-I/R (Figure 5c-d, P<0.05). In accordance with a reduction of inflammatory cells, Nec-1 treatment significantly reduced tumor necrosis factor- α (TNF α) mRNA levels after 24 hours of reperfusion (Figure 5e).

Necrostatin-1 reduces ROS generation after myocardial I/R injury *in vivo*

By interacting with several proteins including glycogen phosphorylase (PYGL), glutamate–ammonia ligase (GLUL) and glutamate dehydrogenase 1 (GLUD1), RIP1/3 kinases were reported to directly regulate ROS production²⁵. Therefore, we assessed ROS production after 24 hours of reperfusion using DHE fluorescence intensity (Supplementary Figure 4a-b). Nec-1 treatment significantly reduced fluorescent intensity (31.7±3.9 vs. 18.4±3.3, P=0.03), suggesting lower levels of ROS after I/R injury when necroptosis is inhibited (Supplementary Figure 4c). Both Nec-1–treated and vehicle-treated animals showed similar changes in PYGL, GLUL, and GLUD1 mRNA levels after 24 hours of reperfusion when compared to baseline (Supplementary Figure 4d; P<0.05).

Necrostatin-1 treatment changes the *in vivo* expression signature of oxidative stress genes after myocardial I/R injury

In order to find other potential factors that could influence ROS production, we performed a PCR array on genes involved in oxidative stress and ROS handling (Supplementary Figure 5a). The expression of 84 genes involved in oxidative stress signalling were analysed after 24 hours of reperfusion: Six genes were found to be involved in cardiac disease, of which 4 genes were upregulated and 2 genes downregulated upon Nec-1 treatment (Supplementary Figure 5b).

Validation by qRT-PCR revealed that Nec-1 treatment significantly decreased both CYBA (p22phox subunit of NADPH oxidase) and TXNIP (thioredoxin interacting protein) mRNA levels after 24 hours of I/R injury (Figure 6a-b). In contrast, NOS2 (nitric oxidase synthase 2), COX-2 (cyclo-oxygenase 2), GPX1 (glutathione peroxidase 1) and GAB1 (GRB2-associated binding protein 1) mRNA levels were significantly upregulated (Figure 6c-f).

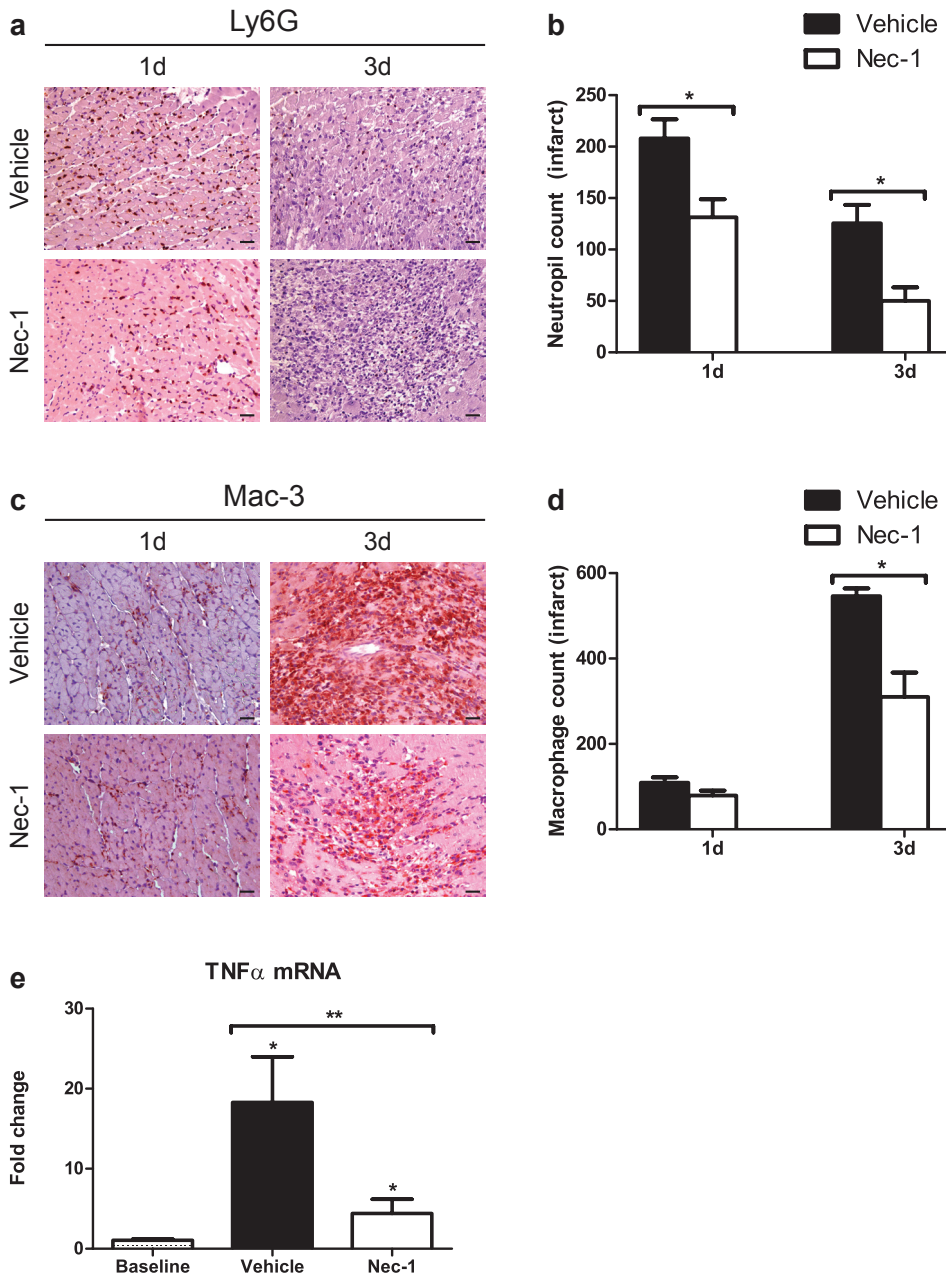


Figure 5 | Nec-1 reduces the inflammatory response after I/R
 Representative pictures (a) and quantification (b) of neutrophils (Ly6G staining, brown) 1 day and 3 days after I/R (n=6/group, *P<0.05; scale bar 20 μ m). Representative pictures (c) and quantification (d) of macrophages (Mac-3 staining, brown) 1 day and 3 days after I/R (n=6/group, *P<0.05; scale bar 20 μ m). (e) Cardiac TNF α mRNA levels at baseline and 1 day post-I/R (n=6/group, *P<0.05 vs. control, **P<0.01 between treatments).

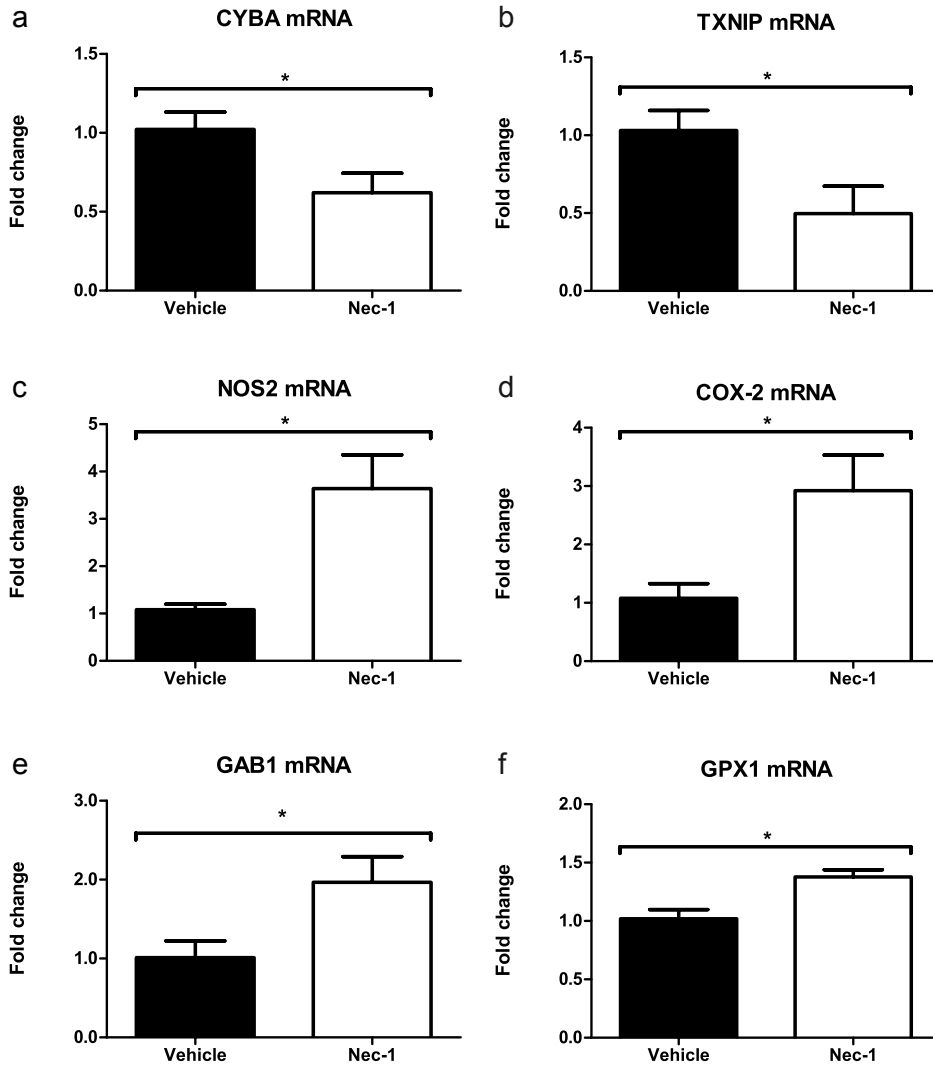


Figure 6 | Nec-1 changes the expression of oxidative stress genes after I/R
Cardiac mRNA levels of CYBA (a) and TXNIP (b) are significantly reduced in Nec-1-treated animals. NOS2 (c), COX-2 (d), GAB1 (e) and GPX1 (f) mRNA levels are significantly increased upon Nec-1 treatment (n=5/group, *P<0.05).

DISCUSSION

In this study, we have demonstrated that RIP1/3 phosphorylation is increased after myocardial I/R *in vivo*, which can be inhibited by Nec-1 administration, resulting in prevention of necrotic cell death and reduction of myocardial infarct size. Importantly, this preserved long-term cardiac function and prevented adverse cardiac remodeling. In addition, inflammatory influx and myocardial ROS generation were decreased upon Nec-1 administration, accompanied by significant changes in the expression signature of oxidative stress genes.

Cardiac I/R injury consists of, among others, both myocardial and vascular injury⁴, and salvage of endothelial cells could be an additional way of limiting ischemic injury. We and others observed that Nec-1 exerted a cytoprotective effect on neonatal mouse cardiomyocytes, endothelial cells (data not shown), neuronal cells, and other cardiac-derived lineages *in vitro* under oxidative stress^{11, 13, 26}. We investigated the effect of a single dose of Nec-1, given at reperfusion which is an important prerequisite for future clinical translation¹⁵. To our knowledge, we are the first to demonstrate that RIP1 and RIP3 and their phosphorylation are increased in the cardiac response to ischemia-reperfusion. The finding that Nec-1 administration decreased RIP1/3-phosphorylation *in vivo* after I/R, together with beneficial effect on both short- and long-term cardiac function after myocardial ischemia-reperfusion is novel. Furthermore, we focussed on a very recently *in vitro* identified downstream key protein involved in RIP1-mediated necrosis, MLKL^{23, 24}. Nec-1 treatment significantly reduced the amount of MLKL protein recruited to RIP1, suggesting that inhibition of RIP1/3 phosphorylation and the interaction with MLKL are clearly involved in Nec-1 induced protection *in vivo*. To our knowledge, the observation that Nec-1 prevents this pathway including MLKL *in vivo* in the context of ischemia-reperfusion is novel and provides additional mechanistic insights.

Importantly, infarct size was determined after 1 day of reperfusion, which was lacking in previous work that was limited to 2 hours¹³. As a consequence, inflammatory response and myocardial ROS levels were also decreased. Our results indicate that Nec-1 could be effective when administered to patients prior to reperfusion, thereby inhibiting RIP1-mediated necrotic cell death. However, of course these results were obtained in a model of young and healthy mice, without co-morbidities and use of other medication and future studies in such populations are needed.

Several mechanisms are thought to contribute to RIP1-induced cell death, including ROS production and metabolic changes or changes in cellular energetics^{10, 22}. Furthermore, RIP1-dependent necrosis via death receptor stimulation and mitochondrial (execution of) necrosis appear to be related²⁷, in which MPTP opening seems to play an important role¹⁴.

We observed *in vivo* inhibition of RIP1/3 phosphorylation upon Nec-1 treatment, which was associated with decreased myocardial ROS levels after myocardial I/R. In line with our results, RIP1/RIP3-mediated cell death was found to be largely dependent on the production of ROS and phosphorylated RIP3 was shown to increase the TNF α -driven ROS production in L929 and 3T3 cells^{25, 28}. In an attempt to find potential mediators involved in ROS handling, we observed differences in the expression of several oxidative stress genes.

CYBA and TXNIP were both downregulated, while NOS2, COX-2, GPX1 and GAB1 increased significantly. Increased NADPH oxidase activity (including CYBA, the p22phox subunit) was found to contribute to I/R-induced ROS formation and cell death and is related to heart failure^{29, 30}. Furthermore, inhibition of TXNIP, which negatively regulates the anti-oxidant protein thioredoxin, was shown to enhance survival of cardiomyocytes and attenuated cardiac hypertrophy^{31, 32}. Next, several studies clearly demonstrated that both NOS2 and COX-2 (possibly also via NOS2) are important in cardioprotection by increasing ischemia-reperfusion tolerance^{33, 34}. Lastly, GPX1 deficiency exacerbated I/R injury and GAB1, required for normal homeostasis, was reported to be involved in cell survival and exerted a protective role during left ventricular dysfunction³⁵⁻³⁸. Altogether, Nec-1 treatment seems to alter the expression of genes that are critically involved in oxidative stress regulation, thereby increasing ROS tolerance as illustrated by decreased myocardial ROS levels.

Invading inflammatory cells play an important role in I/R injury, capable of releasing degrading enzymes and producing large amounts of ROS³⁹. The inflammatory response is further enhanced by the myocardium through the release of chemoattractant factors (i.e. TNF α) and many other mediators (i.e. ROS)^{2, 4} in which necrotic cell death is known to play an important role^{40, 41}. In line with a reduction of RIP1-mediated necrosis, we observed that Nec-1 also reduced leukocyte influx, supported by similar effects seen in models of brain injury^{42, 43}. This could also contribute to the difference in ROS levels, secondary to less necrosis-induced inflammation, leading to diminished activation of detrimental enzymes responsible for superoxide generation^{40, 41, 44}.

Another mechanism of RIP1-mediated cell death is related to changes in carbohydrate metabolism. RIP1/3 kinases were reported to interact with several metabolic enzymes including glycogen phosphorylase (PYGL), glutamate–ammonia ligase (GLUL) and glutamate dehydrogenase 1 (GLUD1), which play an important role in the formation of glucose from glutamine which unfortunately is accompanied by the formation of ROS²⁵. During reperfusion, energy and substrate levels are suddenly restored to normal, increasing carbohydrate metabolism to avoid further loss of cardiomyocytes^{45, 46}. It is not unlikely that Nec-1 protects the endangered myocardium against its very own attempt to survive, as this attempt unfortunately goes along with the generation of large amounts of free radicals⁴⁷.

Furthermore, increased ROS production (either directly or via increased metabolism) may lead to MPTP opening and consecutive mitochondrial dysfunction, causing ATP depletion and cell death²⁷. MPTP opening, a critical event in lethal reperfusion injury, is also linked to increased ROS levels^{2, 48, 49}. Interestingly, RIP1 was reported to directly influence mitochondrial function by stimulating ROS production after death receptor stimulation⁵⁰. More evidence for mitochondrial involvement was shown previously in CypD knockout mice, as inhibition of MPTP opening was shown to be one of the mechanisms responsible for the cytoprotective effects of Nec-1¹⁴.

Many events may be related to the execution of RIP1-mediated necrosis, however, molecular understanding is still limited. Based on the present study, we propose a model in which Nec-1 reduces myocardial I/R injury, ultimately leading to less ROS-induced damage (Figure 7). We suggest that inhibition of RIP1-mediated necrosis not only reduces the initial loss of myocytes but possibly leads to an increased resistance to oxidative stress,

preventing additional I/R injury and spreading throughout the myocardium leading to less mitochondrial dysfunction^{9, 51}. This idea is supported by the fact that many mediators of I/R not only cause damage by itself, but may lead to a chain reaction of lethal injury and MPTP opening when ROS levels reach a certain threshold⁵². We are well aware of the fact that our proposed model is based on individual observations rather than a direct causal relation and further research is clearly indicated to validate this concept.

In conclusion, our study shows that Nec-1 inhibits RIP1-dependent necrosis after myocardial I/R *in vivo* and prevents adverse cardiac remodeling. Furthermore, Nec-1 reduces the inflammatory response and ROS generation, accompanied by significant changes in the expression level of genes involved in oxidative stress handling. Therefore, Nec-1 represents a very promising and powerful candidate for cardioprotection in patients undergoing reperfusion therapy, which should be further investigated in large-animal models of cardiac ischemia.

Acknowledgements

We thank the following persons for their excellent assistance: Maringa Emons, Sebastian Baars, Jerry Oduro, Esther van Eeuwijk, Sridevi Jaksani, Corina Metz, Chaylendra Strijder and Arjan Schoneveld (all at the University Medical Center Utrecht, the Netherlands). This work was supported by the Novartis Foundation for Cardiovascular Excellence (JS), a Bekalis price (PD), the "Wijnand M. Pon Stichting" (MO) and "Stichting Swaeneborgh" (MO).

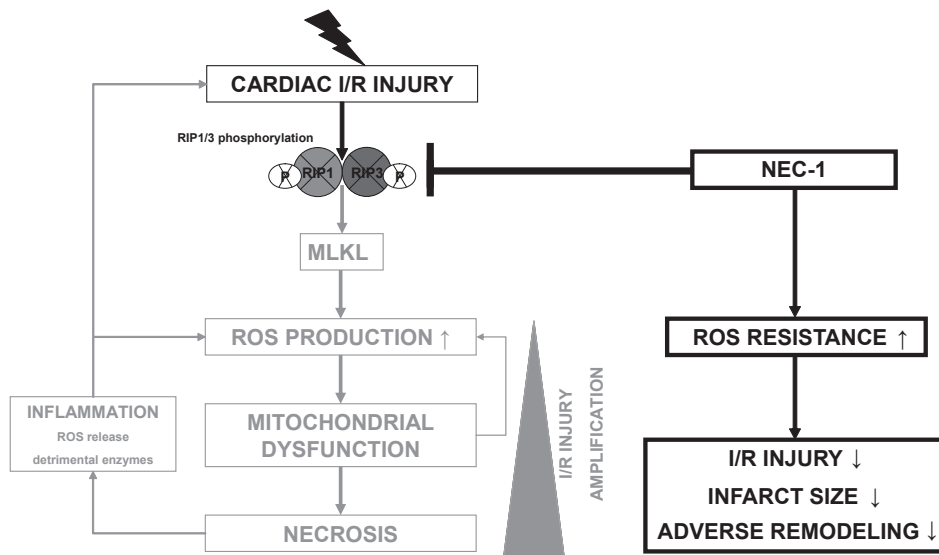


Figure 7 | Proposed mechanism by which Nec-1 exerts its cardioprotective effects

Upon cardiac I/R, RIP1/3-mediated cell death is activated, accompanied by overgeneration of ROS in which MLKL is a key component. Increased levels of ROS lead to mitochondrial dysfunction and necrosis, followed by the inflammatory response. Both mitochondrial dysfunction and inflammation cause an additional increase in ROS levels, triggering a chain reaction of I/R injury. Nec-1 inhibits RIP1/3 phosphorylation, thereby limiting necrotic cell death in which increased resistance to ROS seems to play an important role. Spreading of I/R injury is prevented, leading to IS reduction and preservation of LV function.

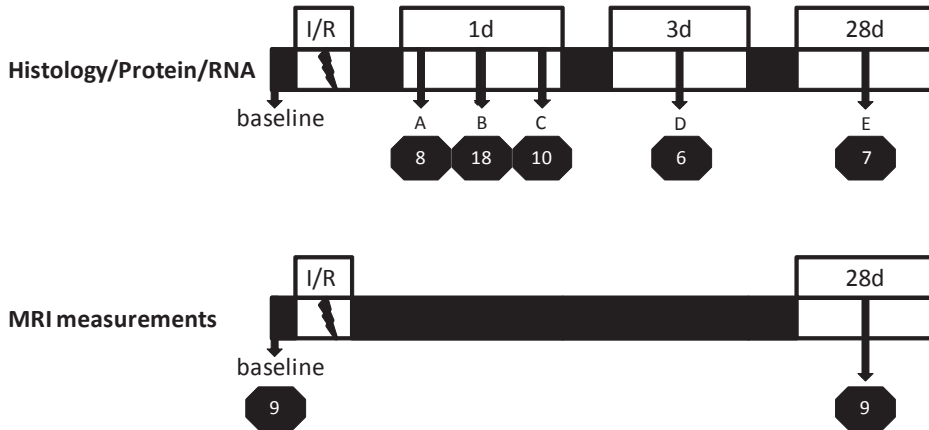
REFERENCES

1. Lloyd-Jones D, Adams RJ, Brown TM, et al. Heart disease and stroke statistics–2010 update: a report from the American Heart Association. *Circulation* 2010;121:e46-e215.
2. Yellon DM, Hausenloy DJ. Myocardial reperfusion injury. *N Engl J Med* 2007;357:1121-1135.
3. Baines CP. The mitochondrial permeability transition pore and ischemia-reperfusion injury. *Basic Res Cardiol* 2009;104:181-188.
4. Prasad A, Stone GW, Holmes DR, et al. Reperfusion injury, microvascular dysfunction, and cardioprotection: the “dark side” of reperfusion. *Circulation* 2009;120:2105-2112.
5. Heusch G, Kleinbongard P, Bose D, et al. Coronary microembolization: from bedside to bench and back to bedside. *Circulation* 2009;120:1822-1836.
6. Gottlieb RA. Mitochondrial signaling in apoptosis: mitochondrial daggers to the breaking heart. *Basic Res Cardiol* 2003;98:242-249.
7. Whelan RS, Kaplinskiy V, Kitsis RN. Cell death in the pathogenesis of heart disease: mechanisms and significance. *Annu Rev Physiol* 2010;72:19-44.
8. Hausenloy DJ, Ong SB, Yellon DM. The mitochondrial permeability transition pore as a target for preconditioning and postconditioning. *Basic Res Cardiol* 2009;104:189-202.
9. Heusch G, Boengler K, Schulz R. Inhibition of mitochondrial permeability transition pore opening: the Holy Grail of cardioprotection. *Basic Res Cardiol* 2010;105:151-154.
10. Vandenabeele P, Galluzzi L, Vanden BT, et al. Molecular mechanisms of necroptosis: an ordered cellular explosion. *Nat Rev Mol Cell Biol* 2010;11:700-714.
11. Degtarev A, Huang Z, Boyce M, et al. Chemical inhibitor of nonapoptotic cell death with therapeutic potential for ischemic brain injury. *Nat Chem Biol* 2005;1:112-119.
12. Degtarev A, Hitomi J, Germscheid M, et al. Identification of RIP1 kinase as a specific cellular target of necrostatins. *Nat Chem Biol* 2008;4:313-321.
13. Smith CC, Davidson SM, Lim SY, et al. Necrostatin: a potentially novel cardioprotective agent? *Cardiovasc Drugs Ther* 2007;21:227-233.
14. Lim SY, Davidson SM, Mocanu MM, et al. The cardioprotective effect of necrostatin requires the cyclophilin-D component of the mitochondrial permeability transition pore. *Cardiovasc Drugs Ther* 2007;21:467-469.
15. Hausenloy DJ, Baxter G, Bell R, et al. Translating novel strategies for cardioprotection: the Hatter Workshop Recommendations. *Basic Res Cardiol* 2010;105:677-686.
16. Oerlemans MI, Koudstaal S, Chamuleau SA, et al. Targeting cell death in the reperfused heart: Pharmacological approaches for cardioprotection. *Int J Cardiol* 2012.
17. Oerlemans MI, Goumans MJ, van MB, et al. Active Wnt signaling in response to cardiac injury. *Basic Res Cardiol* 2010;105:631-641.
18. Arslan F, Smeets MB, O'Neill LA, et al. Myocardial ischemia/reperfusion injury is mediated by leukocytic toll-like receptor-2 and reduced by systemic administration of a novel anti-toll-like receptor-2 antibody. *Circulation* 2010;121:80-90.
19. Noort WA, Oerlemans MI, Rozemuller H, et al. Human versus porcine mesenchymal stromal cells: phenotype, differentiation potential, immunomodulation and cardiac improvement after transplantation. *J Cell Mol Med* 2012;16:1827-1839.
20. He S, Wang L, Miao L, et al. Receptor interacting protein kinase-3 determines cellular necrotic response to TNF-alpha. *Cell* 2009;137:1100-1111.
21. Liu X, Gai Y, Liu F, et al. Trimetazidine inhibits pressure overload-induced cardiac fibrosis through NADPH oxidase-ROS-CTGF pathway. *Cardiovasc Res* 2010;88:150-158.
22. Vandenabeele P, Declercq W, Van Herreweghe F, et al. The role of the kinases RIP1 and RIP3 in TNF-induced necrosis. *Sci Signal* 2010;3:re4.
23. Sun L, Wang H, Wang Z, et al. Mixed lineage kinase domain-like protein mediates necrosis signaling downstream of RIP3 kinase. *Cell* 2012;148:213-227.
24. Zhao J, Jitkaew S, Cai Z, et al. Mixed lineage kinase domain-like is a key receptor interacting protein 3

- downstream component of TNF-induced necrosis. *Proc Natl Acad Sci U S A* 2012.
25. Zhang DW, Shao J, Lin J, et al. RIP3, an energy metabolism regulator that switches TNF-induced cell death from apoptosis to necrosis. *Science* 2009;325:332-336.
 26. Liu J, van MA, Vrijksen K, et al. MicroRNA-155 prevents necrotic cell death in human cardiomyocyte progenitor cells via targeting RIP1. *J Cell Mol Med* 2011;15:1474-1482.
 27. Kung G, Konstantinidis K, Kitsis RN. Programmed necrosis, not apoptosis, in the heart. *Circ Res* 2011;108:1017-1036.
 28. Cho YS, Challa S, Moquin D, et al. Phosphorylation-driven assembly of the RIP1-RIP3 complex regulates programmed necrosis and virus-induced inflammation. *Cell* 2009;137:1112-1123.
 29. Borchi E, Parri M, Papucci L, et al. Role of NADPH oxidase in H9c2 cardiac muscle cells exposed to simulated ischaemia-reperfusion. *J Cell Mol Med* 2009;13:2724-2735.
 30. Heymes C, Bendall JK, Ratajczak P, et al. Increased myocardial NADPH oxidase activity in human heart failure. *J Am Coll Cardiol* 2003;41:2164-2171.
 31. Xiang G, Seki T, Schuster MD, et al. Catalytic degradation of vitamin D up-regulated protein 1 mRNA enhances cardiomyocyte survival and prevents left ventricular remodeling after myocardial ischemia. *J Biol Chem* 2005;280:39394-39402.
 32. Yoshioka J, Imahashi K, Gabel SA, et al. Targeted deletion of thioredoxin-interacting protein regulates cardiac dysfunction in response to pressure overload. *Circ Res* 2007;101:1328-1338.
 33. Insete J, Molla B, Aguilar R, et al. Constitutive COX-2 activity in cardiomyocytes confers permanent cardioprotection: Constitutive COX-2 expression and cardioprotection. *J Mol Cell Cardiol* 2009;46:160-168.
 34. Li Q, Guo Y, Tan W, et al. Cardioprotection afforded by inducible nitric oxide synthase gene therapy is mediated by cyclooxygenase-2 via a nuclear factor-kappaB dependent pathway. *Circulation* 2007;116:1577-1584.
 35. Ardanaz N, Yang XP, Cifuentes ME, et al. Lack of glutathione peroxidase 1 accelerates cardiac-specific hypertrophy and dysfunction in angiotensin II hypertension. *Hypertension* 2010;55:116-123.
 36. Cao C, Huang X, Han Y, et al. Galpha(i1) and Galpha(i3) are required for epidermal growth factor-mediated activation of the Akt-mTORC1 pathway. *Sci Signal* 2009;2:ra17.
 37. Nakaoka Y, Nishida K, Narimatsu M, et al. Gab family proteins are essential for postnatal maintenance of cardiac function via neuregulin-1/ErbB signaling. *J Clin Invest* 2007;117:1771-1781.
 38. Shiomi T, Tsutsui H, Matsusaka H, et al. Overexpression of glutathione peroxidase prevents left ventricular remodeling and failure after myocardial infarction in mice. *Circulation* 2004;109:544-549.
 39. Vinten-Johansen J. Involvement of neutrophils in the pathogenesis of lethal myocardial reperfusion injury. *Cardiovasc Res* 2004;61:481-497.
 40. Morgan MJ, Kim YS, Liu ZG. TNFalpha and reactive oxygen species in necrotic cell death. *Cell Res* 2008;18:343-349.
 41. Zhang C, Wu J, Xu X, et al. Direct relationship between levels of TNF-alpha expression and endothelial dysfunction in reperfusion injury. *Basic Res Cardiol* 2010;105:453-464.
 42. You Z, Savitz SI, Yang J, et al. Necrostatin-1 reduces histopathology and improves functional outcome after controlled cortical impact in mice. *J Cereb Blood Flow Metab* 2008;28:1564-1573.
 43. Northington FJ, Chavez-Valdez R, Graham EM, et al. Necrostatin decreases oxidative damage, inflammation, and injury after neonatal HI. *J Cereb Blood Flow Metab* 2011;31:178-189.
 44. Kleinbongard P, Heusch G, Schulz R. TNFalpha in atherosclerosis, myocardial ischemia/reperfusion and heart failure. *Pharmacol Ther* 2010;127:295-314.
 45. Li C, Jackson RM. Reactive species mechanisms of cellular hypoxia-reoxygenation injury. *Am J Physiol Cell Physiol* 2002;282:C227-C241.
 46. Turrens JF. Mitochondrial formation of reactive oxygen species. *J Physiol* 2003;552:335-344.
 47. Nishida H, Matsumoto A, Tomono N, et al. Biochemistry and physiology of mitochondrial ion channels involved in cardioprotection. *FEBS Lett* 2010;584:2161-2166.
 48. Hausenloy DJ, Yellon DM. The mitochondrial permeability transition pore: its fundamental role in mediating cell death during ischaemia and reperfusion. *J Mol Cell Cardiol* 2003;35:339-341.
 49. Heusch G, Boengler K, Schulz R. Cardioprotection: nitric oxide, protein kinases, and mitochondria. *Cir-*

- ulation 2008;118:1915-1919.
50. Temkin V, Huang Q, Liu H, et al. Inhibition of ADP/ATP exchange in receptor-interacting protein-mediated necrosis. *Mol Cell Biol* 2006;26:2215-2225.
 51. Steenbergen C, Das S, Su J, et al. Cardioprotection and altered mitochondrial adenine nucleotide transport. *Basic Res Cardiol* 2009;104:149-156.
 52. Zorov DB, Juhaszova M, Sollott SJ. Mitochondrial ROS-induced ROS release: an update and review. *Biochim Biophys Acta* 2006;1757:509-517.

Overview of experimental design and used animals at over time (both treatment groups)

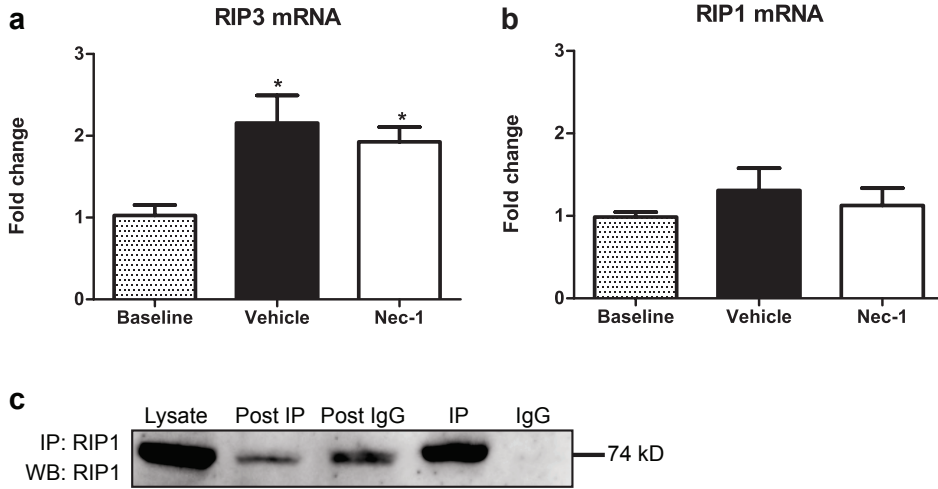


- A = Infarct Size (TTC)/LDH assay (n=8)
- B = Histology: Necrosis (n=6), Apoptosis/DHE (n=6), Ly6g/Mac-3 staining (n=6)
- C = Protein for WB/IP (n=5), RNA for PCR/Oxidative Stress Array (n=5)
- D = Ly6g/Mac-3 staining (n=6)
- E = Picrosirius Red Staining (n=7)
- MRI measurements: baseline and 28days post-I/R (n=9)

7

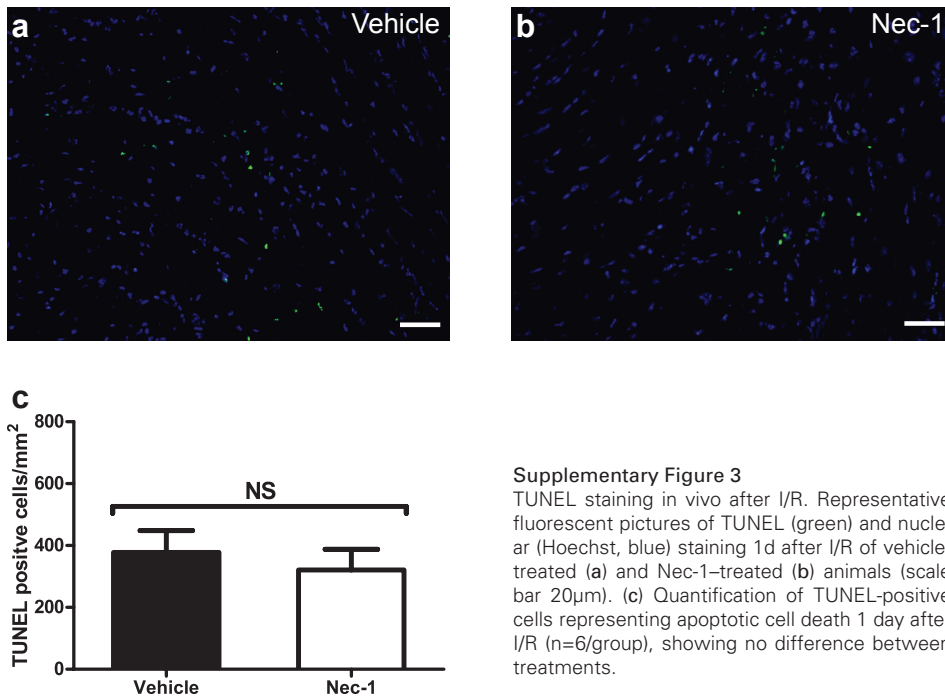
Supplementary Figure 1

Overview of the experimental design and tissue collection obtained at different times of reperfusion, including MRI measurements. For both vehicle- and Nec-1 – treated animals, a similar design was used.



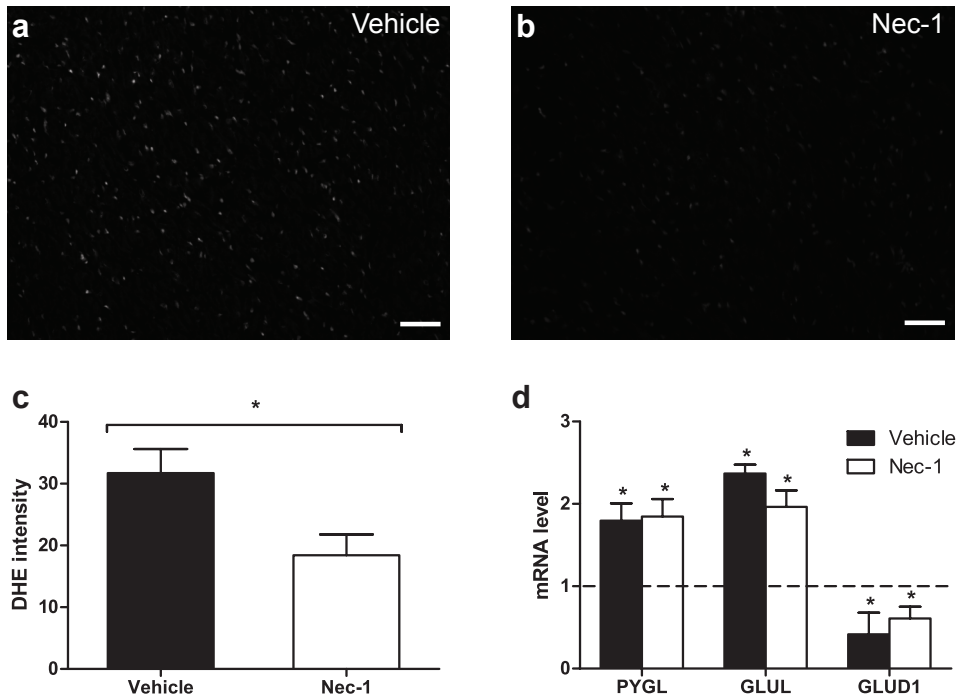
Supplementary Figure 2

Cardiac mRNA levels of RIP3 and RIP1 at 1 day after I/R. (a) RIP3 mRNA levels increased significantly after I/R in both groups when compared to baseline. (b) RIP1 mRNA levels increased slightly after I/R, which was similar in both groups. N=6/group, *P<0.05 vs. baseline. (c) Control western blot showing a strong depletion of RIP1 after immunoprecipitation (post IP), while RIP1 was not present in the negative control (IgG). n=5/group.



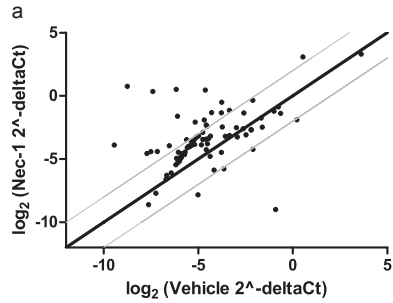
Supplementary Figure 3

TUNEL staining in vivo after I/R. Representative fluorescent pictures of TUNEL (green) and nuclear (Hoechst, blue) staining 1d after I/R of vehicle-treated (a) and Nec-1-treated (b) animals (scale bar 20µm). (c) Quantification of TUNEL-positive cells representing apoptotic cell death 1 day after I/R (n=6/group), showing no difference between treatments.



Supplementary Figure 4

Nec-1 reduces reactive oxygen species *in vivo* after I/R. Representative fluorescent pictures of ROS detection using dihydroethidium (DHE) of vehicle-treated (a) and Nec-1-treated (b) animals (scale bar 20 μ m). (c) Quantification of DHE intensity, showing a significant decrease after Nec-1 treatment 1 day after reperfusion (n=6/group, *P<0.05). (d) Cardiac mRNA levels of PYGL and GLUL increased significantly in both groups after I/R, while GLUD1 mRNA levels decreased significantly when compared to baseline (n=6/group, *P<0.05 vs. baseline).



b

Gene	Description	Fold change	Possible effect (Reference)
COX-2	PTGS2, prostaglandin-endoperoxide synthase 2	upregulated	Cardioprotective (18, 22)
CYBA	cytochrome b-245, NADPH oxidase P22	downregulated	ROS-induced cell death, Adverse remodeling (4, 17)
GAB1	GRB2-associated binding protein 1	upregulated	Cell survival, Adverse remodeling (5, 35)
GPX1	glutathione peroxidase 1	upregulated	Prevention of I/R injury (1, 28)
NOS2	nitric oxide synthase 2, iNOS	upregulated	Cardioprotective (18, 22)
TXNIP	thioredoxin interacting protein, TBP-2, VDUP1	downregulated	Myocardial cell death, Hypertrophy (45, 47)

Supplementary Figure 5

Nec-1 changes the expression of oxidative stress genes after I/R. (a) Scatter plot showing the relative gene expression of 84 genes involved in oxidative stress in Nec-1 vs. vehicle treatment after 1 day of reperfusion. Lines on both sides mark a 2-fold difference. (b) List of differentially expressed genes (>2-fold difference when compared to vehicle treatment) related to cardiac injury with representative references.

8



Martinus I.F.J. Oerlemans¹
Stefan Koudstaal^{1,2}
Tycho I.G. Van der Spoel¹
Aafke W.F. Janssen
Gerard Pasterkamp^{1,2}
Pieter A. Doevendans¹
Joost P.G. Sluijter^{1,2}
Steven A.J. Chamuleau^{1,2}

¹ Department of Cardiology, Division Heart and Lungs, University Medical Center
Utrecht, Utrecht, the Netherlands.

² Interuniversity Cardiology Institute of the Netherlands (ICIN), Utrecht, the Netherlands.

Necrostatin-1 reduces myocardial ischemia/reperfusion injury in pigs

Submitted

ABSTRACT

Purpose

Receptor-interacting protein 1 (RIP1) plays an important role during programmed necrosis upon myocardial ischemia/reperfusion-induced cell death. Previously, we have demonstrated that administration of Necrostatin-1 (Nec-1), thereby inhibiting the kinase activity of RIP1, protected cardiomyocytes from necrotic cell death after ischemia/reperfusion (I/R) in small rodents and subsequently improved long-term cardiac performance. The purpose of this study was to investigate the ability of Nec-1 to inhibit programmed necrosis through a clinically feasible intravenous delivery in a large-animal model of myocardial ischemia/reperfusion.

Methods

In a preclinical porcine model, acute I/R injury was induced by a 75 min surgical ligation of the LCX followed by 24 hours of reperfusion. Ten minutes prior to reperfusion, pigs were allocated to receive intravenously either two different doses of Nec-1 (1 mg/kg and 3.3 mg/kg, respectively) or vehicle treatment. Infarct size (IS), expressed as a percentage of the area at risk (AAR), and global and regional cardiac function was assessed using echocardiography and pressure volume-loop analysis, prior to the occlusion and after 24 hours of reperfusion.

Results

Administration of the high dose Nec-1 (3.3 mg/kg) resulted in an infarct size reduction of 57% compared to vehicle treatment (19.4 ± 10.7 vs. 44.2 ± 22.1 , $p=0.027$). Furthermore, Nec-1 significantly reduced neutrophil influx in the infarcted area. Both global systolic function (ejection fraction, stroke work, and preload recruitable stroke work) and regional systolic function (systolic wall thickening) were preserved in a dose-dependent manner upon Nec-1 treatment. After 24 hours of reperfusion, systolic wall thickening was preserved in animals treated with Nec-1 3.3 mg/kg compared to vehicle treatment ($17.9 \pm 2.4\%$ vs. $-1.7 \pm -3.4\%$; $p < 0.01$).

Conclusions

In a preclinical porcine model of myocardial ischemia/reperfusion injury relevant to human disease, Nec-1 administration significantly reduced infarct size and preserved left ventricular systolic function after 24 hours of reperfusion. Given the need for new cardioprotective options next to reperfusion, Nec-1 is a promising adjunctive therapeutic for patients with acute myocardial infarction.

INTRODUCTION

Acute myocardial infarction (MI) remains one of the leading causes of morbidity and mortality in the western world for which early reperfusion is currently the most effective therapy.¹ Unfortunately, reperfusion itself results in additional damage, also known as myocardial ischemia/reperfusion (I/R) injury, enhancing cell death in the endangered myocardium even further, mainly mediated by reactive oxygen species (ROS) and proinflammatory cytokines.²⁻⁴ Unfortunately, many interventions to increase cardiomyocyte survival, although successful in experimental studies, failed in the clinical setting. Here, the lack of functional follow-up and difficulties in translating infarct size reduction to improved (clinical) outcome were probably the main factors.⁵ Moreover, promising rodent findings should be reproduced in large animals as they have greater physiological relevance than murine models of MI⁶. According to the current guidelines on novel cardioprotective strategies, especially infarct size (IS) reduction should be one of the main endpoints in follow-up studies in large-animal.

For many years, apoptosis was considered as the only form of regulated cell death in the ischemic heart in contrast to necrosis, its non-regulated counterpart^{7, 8}. Emerging evidence has demonstrated that at least some part of necrotic cell death is regulated, in which the kinase activity of receptor-interacting protein 1 (RIP1) and its interaction with RIP3 are critically involved.⁹ Very recently, several reports have shown that inhibition of this signaling pathway prevents necrosis execution at the mitochondrial level^{10, 11}. Necrostatin-1 (Nec-1), a small molecule capable of inhibiting RIP1 kinase activity, was shown to inhibit programmed necrosis without affecting other RIP1-mediated processes and efficiently prevented necrotic cell death after ischemic brain injury^{12, 13}. The concept of programmed necrosis and the possibility to inhibit this in the ischemic heart gives rise to new therapeutic options to prevent myocardial cell death¹⁴.

We previously demonstrated that Nec-1 administration, just prior to reperfusion, reduced infarct size and improved cardiac function in a mouse model of ischemia/reperfusion¹⁵. Additionally, Nec-1 significantly reduced inflammation and formation of reactive oxygen species, probably by prevention of the RIP1/RIP3/MLKL signaling axis, thereby extending our knowledge on the role of programmed necrosis in the ischemic heart which was missing from previous studies^{16, 17}. However, it is still unclear whether Nec-1 administration will be effective in a large-animal model with relevance to the human situation. In the present study, we demonstrate that administration of Nec-1 in the ischemic period before reperfusion reduces infarct size and improves left ventricular systolic function in a clinically relevant porcine model.

METHODS

Animals and Experimental Study Design

All animals received humane care in compliance with the national guidelines on animal care and prior approval by the Animal Experimentation Committee of the Faculty of Medicine, Utrecht University, the Netherlands.

Anesthetized open-chest pigs (female Dutch landrace, weighing ± 70 kg) were subjected to 75 minutes of regional ischemia by temporal ligation of the proximal circumflex coronary artery and 24 hours of reperfusion. The animals were randomly assigned in a 2:1 ratio to Nec-1 treatment (1.0 mg/kg (n=4) or 3.3 mg/kg (n=5) in PBS) or vehicle (n=6), which was administered intravenously 10 minutes prior to reperfusion. Following 24 hours of reperfusion, functional endpoints were measured and animals were euthanized by exsanguination under general anaesthesia.

Anesthesia

The pigs were sedated with ketamine (10mg/kg), midazolam (0.5mg/kg), and atropine (0.04 mg/kg) and subsequently induced with thiopental (4 mg/kg) before they were intubated and connected to positive pressure ventilatory support with a mixture of oxygen and air (FiO₂ of 0.50). The ear vein was cannulated and used for continuous admission of saline and anesthesia. Anesthesia was maintained by continuous infusion of midazolam (0.7mg/kg/h), whereas analgesia was preserved by continuous infusion of sufentanil citrate (6 μ g/kg/h) and finally muscle relaxation via pancurorium bromide (0.1mg/kg/h). Prior to infarction, 300 mg of amiodarone was infused intravenously in 45 minutes to minimize onset of cardiac arrhythmias.

Echocardiography

The echocardiographic examination was performed with the animals under general anaesthesia, lying in the right lateral position. Ultrasound data were acquired using a Philips iE33 scanner (Philips Healthcare, Eindhoven, the Netherlands) with a S5-1 phased array transducer (1-5 MHz) and a X3 transducer. Standard parasternal long and short axis views were obtained. Left ventricular dimensions and wall thickness were measured in accordance with the standards of the American Society of Echocardiography¹⁸.

Pressure Volume loop analysis

Pressure-volume (PV) loops were assessed using a 7-F conductance catheter. Briefly, LV pressure and volumes were measured and stored using a Leycom CFL-512 (CD-Leycom, Zoetermeer, the Netherlands). After correct placement in the LV, checked by the individual segmental conductance signals, the conductance signals were calibrated by cardiac output based on transonic flow probe measurements (Transonic Systems Inc, Ithaca, NY, USA). All data were collected while mechanical ventilation was paused. Regarding data recorded under different preload conditions, temporal inferior caval vein ligation was used. Data analysis and calculations were performed off-line using custom-made software (CD Leycom, Zoetermeer, the Netherlands). Systolic LV function was quantified by end systolic pressure, end systolic volume of 100ml (V100), LV ejection fraction, stroke work and preload recruitable stroke work.

Infarct size

After 24 hours of reperfusion, IS was determined as a percentage of the area at risk (AAR). After re-ligating the proximal circumflex coronary artery, Evans Blue dye (4%) was injected and hearts were explanted, rinsed and incubated for 30 minutes in 1% triphenyltetrazolium

chloride (TTC, Sigma-Aldrich) at 37°C. Cardiac sections were photographed (Canon EOS 400D) and IS, AAR, and left ventricular (LV) area were measured with ImageJ software (version 1.34) and analyzed by a blinded investigator. The ratio IS/AAR (%) was the primary end point of this study to assess the efficacy of Nec-1 treatment according to the current guidelines on novel cardioprotective strategies⁶.

Immunohistochemical staining

Snap-frozen tissue samples from the infarct zone and remote area were embedded in Tissue-Tek (Sakura) and 5 µm cryosections were prepared on a microtome (Leika). Sections were dried for 30 min at room temperature (RT) and fixed in acetone. For the staining of neutrophils, endogenous biotin was blocked with Biotin blocking system (X0590, Dako), followed by incubation with 10% normal horse serum for 30 minutes and mouse anti-pig neutrophils (1:100, Ls-c58180, LifeSpan BioSciences Inc.). Development was performed using biotin-labelled horse anti-mouse (1:200, BA-2000, Vector Laboratories), followed by streptavidin-horseradish peroxidase (1:1000, 7100-05, Southern Biotech), and subsequent visualization using the chromogen 3-amino-9-ethyl carbazole (AEC).

Macrophages and neutrophils were counted in 15 random fields divided over 2 standardized regions (infarct area) in all included animals. The macrophages and neutrophils were counted per field (40x) by an investigator blinded to the treatment allocation.

Statistics

Data are presented as mean ± SEM. Functional data, area at risk, and infarct size were analysed by one-way ANOVA. When a significant difference was found, post hoc Dunnet t test was performed with vehicle treatment as control. Differences were regarded as significant at the $p < 0.05$ level.

RESULTS

Necrostatin-1 reduces infarct size in a dose dependent manner

We investigated whether Nec-1 treatment attributed to a reduction in infarct size compared to vehicle treatment. For this, we used a Nec-1 dose that was previously effective in rodents (3.3mg/kg) and a lower dose to see if the compound could be down scaled. Infarct size (IS) between three groups was significantly different by ANOVA ($p = 0.038$). Post-hoc analysis revealed that the infarct size was comparable between the control group and the low dose group, 1.0mg/kg (Figure 1A; $44.2 \pm 22.1\%$ vs. 48.7 ± 11.4 , $p = 0.909$). High Nec-1 dose, 3.3mg/kg significantly reduced IS by 57% compared to the control group (19.4 ± 10.7 vs. 44.2 ± 22.1 , $p = 0.027$). AAR was similar between all groups (Figure 1B, $p = 0.81$)

Next, we assessed the level of myocardial necrosis markers, lactic dehydrogenase (LDH) and creatinin kinase (CK) at multiple time points after the I/R injury. At 24 hours, LDH levels increased in the control group (Figure 1C; 2143 ± 725 IU/L), compared to 545 ± 247 IU/L in the high dose group. In contrast, treatment with low dose Nec-1 resulted in similar levels compared to the vehicle treatment (Figure 1C; 2821 ± 1159 IU/L). As depicted in Figure 1D, a similar trend was found for CK levels after 24 hours of I/R injury.

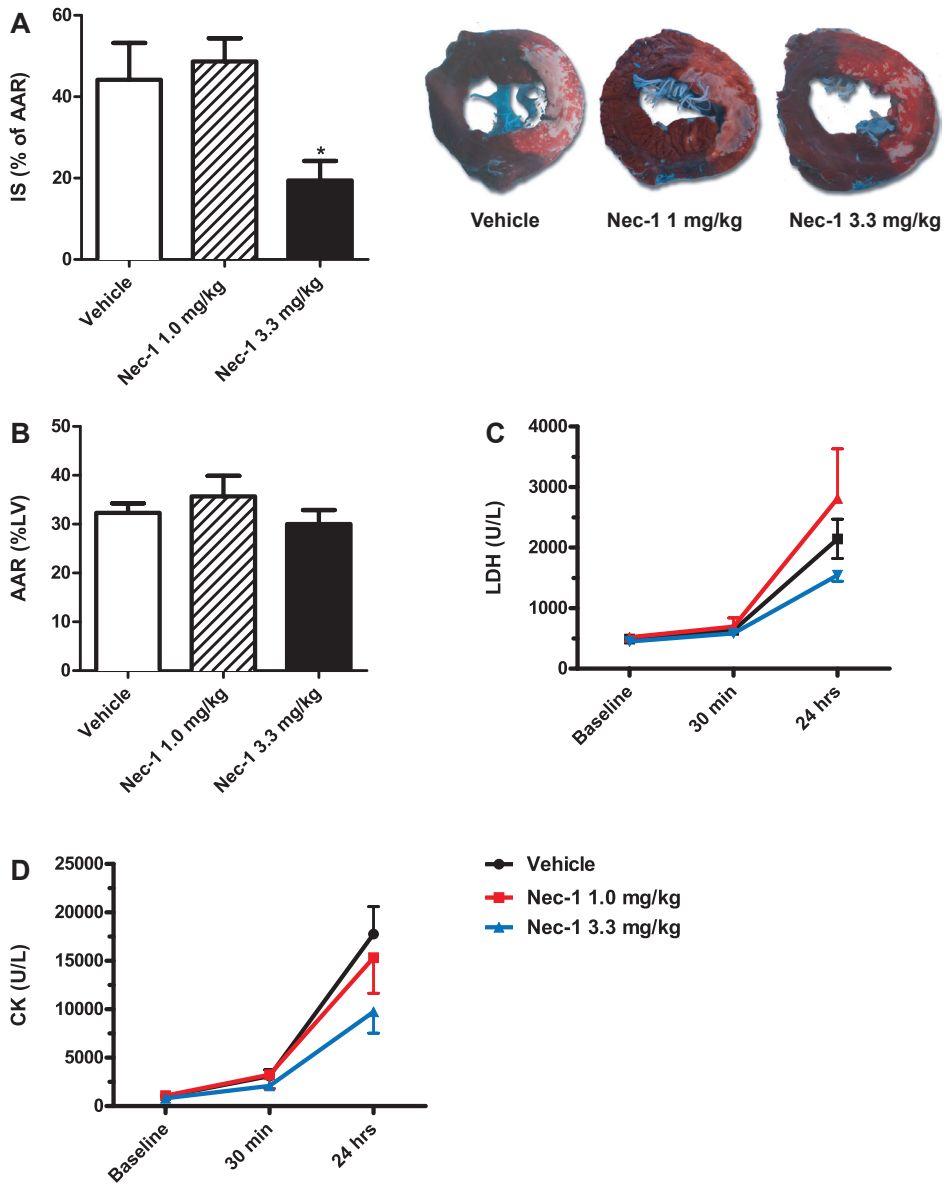


Figure 1
 Nec-1 reduces myocardial infarct size. (A) Representative TTC staining and quantification showing that high-dose Nec-1 significantly reduces IS compared to vehicle treatment (* $p = 0.027$), while the area at risk (AAR) was similar between the groups (B). Nec-1 treatment resulted in lower levels of both LDH (C) and CK-MB (D) after 24 hours of reperfusion.

Necrostatin-1 reduces inflammation after myocardial I/R injury

As circulating inflammatory cells also contribute to myocardial I/R injury, we studied the influx of neutrophils, the first responders after cardiac injury has occurred¹⁹. After 24 hours of reperfusion, neutrophil influx in animal receiving a high dose of Nec-1 was significantly reduced compared to vehicle treatment (Figure 2D, $p=0.02$). The number of neutrophils in the infarcted area after low dose Nec-1 treatment was comparable with vehicle-treated animals.

Necrostatin-1 preserves systolic function after myocardial I/R injury

To test the effect of Nec-1 on global cardiac function and hemodynamics, PV loop analysis was performed prior to and 24 hrs after myocardial I/R. At baseline, no differences in global and regional systolic function were observed. Measurement of LV ejection fraction (LVEF) 24 hours post-IR showed that Nec-1 treatment resulted in a dose-dependent preservation, with LVEF of $52.5\pm 3.4\%$ (Nec-1 3.3mg/kg) vs. $42.5\pm 4.3\%$ (vehicle). Preload recruitable

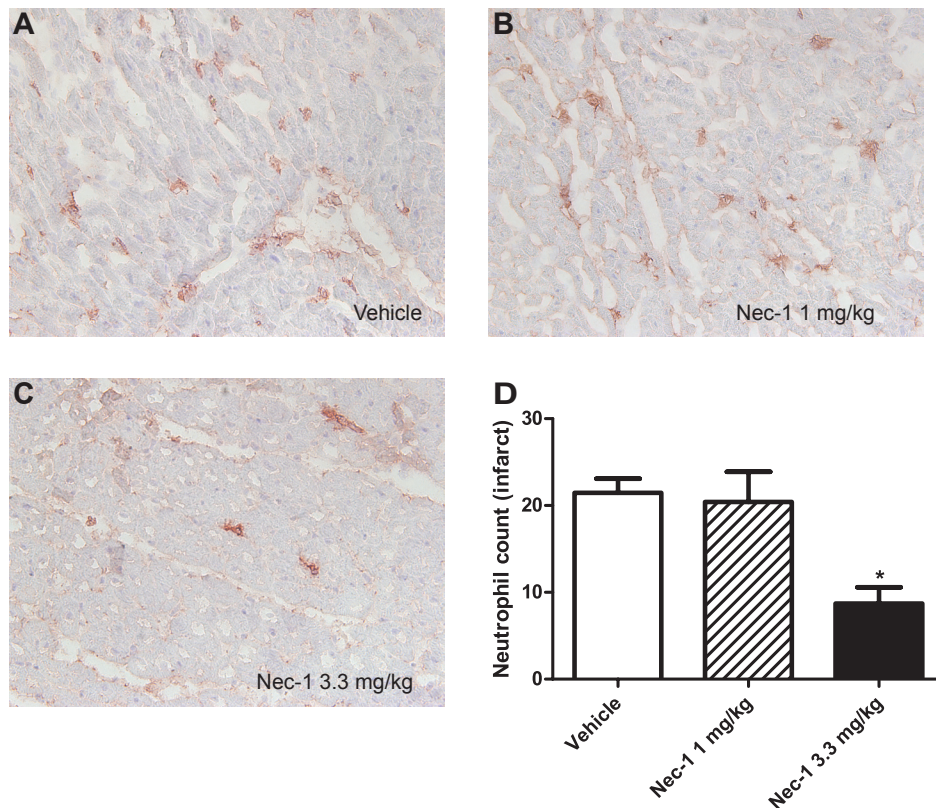


Figure 2

Nec-1 reduces the inflammatory response after I/R. Representative pictures (A-C) and quantification (D) of neutrophils (Ly6G staining, brown) 1 day after I/R, showing a significantly less infiltration in the infarcted area of Nec-1 treated animals.

stroke work (PRSW), another measure for left ventricular systolic function, was preserved in a dose dependent manner as well (Figure 3B). Furthermore, high dose Nec-1 treatment prevented rapid deterioration in LV stroke work compared to vehicle-treated and low dose of Nec-1 animals (Figure 3C). Finally, to measure regional systolic function, systolic wall thickening (SWT) of the infarct was assessed using echocardiography (Figure 3D). In vehicle-treated animals, contraction in the infarcted area was lost as indicated by a negative SWT. In line with improved LVEF, high dose Nec-1 treatment significantly preserved SWT compared to vehicle treatment ($17.9 \pm 2.4\%$ vs. $-1.7 \pm 3.4\%$; $p < 0.01$). Low dose of Nec-1, although less pronounced, also improved SWT compared to vehicle treatment.

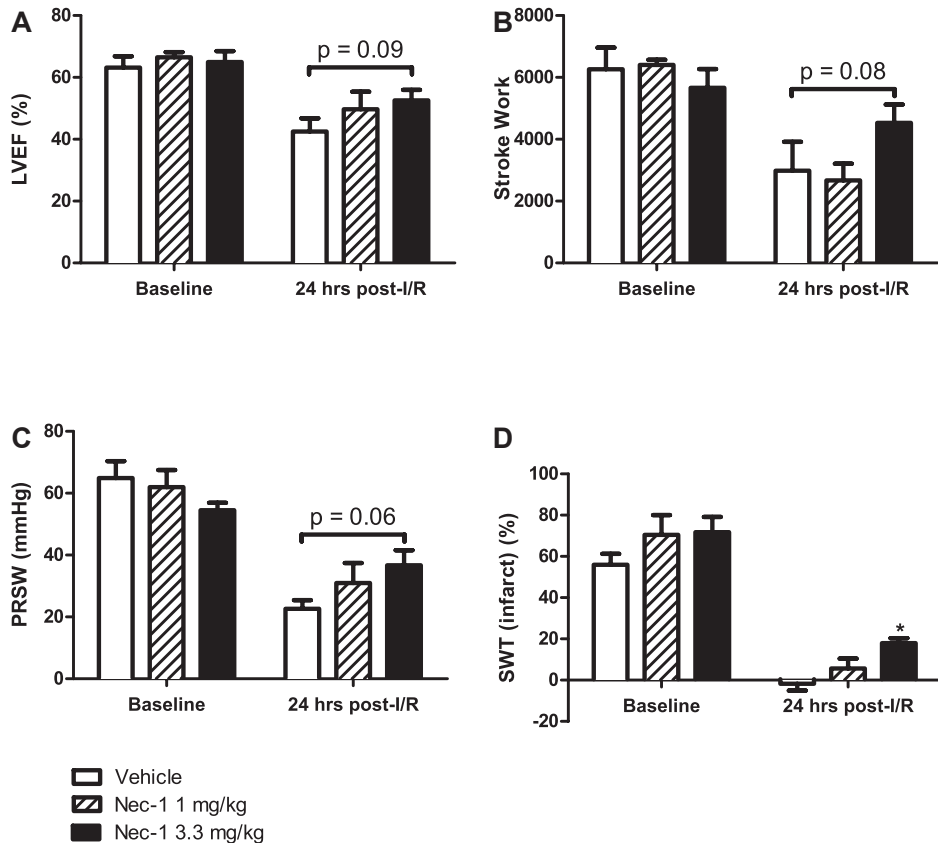


Figure 3
 Nec-1 preserves global and regional cardiac function. LVEF (A), stroke work (B) and PRSW (C) showed a dose-dependent preservation upon Nec-1 treatment. In vehicle-treated animals, contraction in the infarcted area was lost as indicated by a negative SWT, whereas high dose Nec-1 treatment significantly preserved SWT ($p < 0.01$).

DISCUSSION

Technical and pharmacological advances have improved patient outcome and prognosis, especially in terms of infarct-related deaths¹. However, the incidence of heart failure has increased, which has led to numerous studies attempting to reduce myocardial apoptosis and, to a lesser extent, necrosis^{5, 14}. Unfortunately, many interventions to increase cardiomyocyte survival, although successful in experimental studies, were not properly reproduced in large animals before entering the clinical arena and failed in the clinical setting⁶. As soon as Nec-1 and the concept of inhibition of programmed necrosis appeared^{12, 13}, it was demonstrated in a somewhat limited model of cardiac ischemia that Nec-1 reduced infarct size^{16, 17}. More importantly, very recently we demonstrated that Nec-1 administration just prior to reperfusion reduced IS and preserved cardiac function in mice, mediated by inhibition of RIP1/RIP3/MLKL signalling¹⁵. As a next step, using a physiologically more relevant porcine model of I/R injury better resembling the clinical patient and setting, we determined the therapeutic efficacy of Nec-1 administration prior to reperfusion.

To our knowledge, we are the first reporting IS reduction after 24 hours of reperfusion in a preclinical porcine model. Compared to vehicle treatment, IS was reduced with 57%. Surprisingly, the observed effect of Nec-1 (3.3mg/kg) seems to be higher in the current study compared to our previous observations in rodents (32% IS reduction)¹⁵ and is also large compared to other studies on cardioprotection in large animals⁶. One possible explanation could be that Nec-1 was administered 10 minutes (instead of 5 minutes) prior to reperfusion, eventually leading to a higher concentration at reperfusion in the ischemic myocardium. Nevertheless, being the primary end-point of this preclinical study, we were able to demonstrate the therapeutic efficacy of Nec-1 on IS reduction.

In line with IS reduction, although not reaching statistical significance, several markers of myocardial necrosis (LDH, CK-MB) showed a dose-dependent reduction in circulating levels after I/R injury. Furthermore, this was accompanied by a significant reduction in neutrophil influx in the infarcted area. As necrosis, not apoptosis, is known to evoke an inflammatory response, this suggests that administration of Nec-1 indeed limited the amount of necrotic cardiomyocytes after I/R injury¹⁹. This is also in line with our earlier report on Nec-1 administration in a mouse model of myocardial I/R, leading to less influx of inflammatory cells as well as a reduction of necrotic cell death demonstrated by propidium iodide staining¹⁵.

Finally, Nec-1 significantly improved cardiac systolic performance after myocardial I/R injury. Global systolic parameters (LVEF, stroke work, PRSW) showed a strong trend with increasing concentrations of Nec-1, leading to improved global systolic function compared to vehicle treatment. Importantly, systolic wall thickening (the percentage increase of myocardial thickening during contraction), a regional measure of systolic performance, was significantly higher in Nec-1-treated pigs compared with vehicle treatment having a dose-dependent effect. This was in sharp contrast with the negative SWT observed in vehicle treated animals, demonstrating a complete loss of systolic function in the affected area. Already at this early time-point after 24 hours of reperfusion, Nec-1 administration seems to attenuate a decline in myocardial function.

Although a positive trend was observed, we were not able to show a significant improvement in global systolic function, a limitation mostly caused by the fact that this study was slightly underpowered. Furthermore, a second limitation is the fact that our follow-up period was 24 hours, which is too short to demonstrate any effects on long-term cardiac remodeling and performance. Lastly, future studies will need to focus on pharmacokinetics and dynamics in order to start a first-in-man (FIM) study as soon as possible, as knowledge in this area are currently unknown.

In conclusion, Nec-1 administration before reperfusion significantly reduces myocardial IS and preserves global and regional systolic function in a model of porcine I/R. As novel cardioprotective therapies are needed, these findings may have great clinical impact. Nec-1 represents a very promising candidate to limit reperfusion injury in patients with acute MI.

REFERENCES

1. Lloyd-Jones D, Adams RJ, Brown TM, et al. Heart disease and stroke statistics—2010 update: a report from the American Heart Association. *Circulation* 2010;121:e46-e215.
2. Yellon DM, Hausenloy DJ. Myocardial reperfusion injury. *N Engl J Med* 2007;357:1121-1135.
3. Baines CP. The mitochondrial permeability transition pore and ischemia-reperfusion injury. *Basic Res Cardiol* 2009;104:181-188.
4. Prasad A, Stone GW, Holmes DR, et al. Reperfusion injury, microvascular dysfunction, and cardioprotection: the “dark side” of reperfusion. *Circulation* 2009;120:2105-2112.
5. Oerlemans MI, Koudstaal S, Chamuleau SA, et al. Targeting cell death in the reperfused heart: Pharmacological approaches for cardioprotection. *Int J Cardiol* 2012.
6. Hausenloy DJ, Baxter G, Bell R, et al. Translating novel strategies for cardioprotection: the Hatter Workshop Recommendations. *Basic Res Cardiol* 2010;105:677-686.
7. Gottlieb RA. Mitochondrial signaling in apoptosis: mitochondrial daggers to the breaking heart. *Basic Res Cardiol* 2003;98:242-249.
8. Whelan RS, Kaplinskiy V, Kitsis RN. Cell death in the pathogenesis of heart disease: mechanisms and significance. *Annu Rev Physiol* 2010;72:19-44.
9. Vandenabeele P, Galluzzi L, Vanden BT, et al. Molecular mechanisms of necroptosis: an ordered cellular explosion. *Nat Rev Mol Cell Biol* 2010;11:700-714.
10. Sun L, Wang H, Wang Z, et al. Mixed lineage kinase domain-like protein mediates necrosis signaling downstream of RIP3 kinase. *Cell* 2012;148:213-227.
11. Wang Z, Jiang H, Chen S, et al. The mitochondrial phosphatase PGAM5 functions at the convergence point of multiple necrotic death pathways. *Cell* 2012;148:228-243.
12. Degtarev A, Huang Z, Boyce M, et al. Chemical inhibitor of nonapoptotic cell death with therapeutic potential for ischemic brain injury. *Nat Chem Biol* 2005;1:112-119.
13. Degtarev A, Hitomi J, Gernscheid M, et al. Identification of RIP1 kinase as a specific cellular target of necrostatins. *Nat Chem Biol* 2008;4:313-321.
14. Kung G, Konstantinidis K, Kitsis RN. Programmed necrosis, not apoptosis, in the heart. *Circ Res* 2011;108:1017-1036.
15. Oerlemans MI, Liu J, Arslan F, et al. Inhibition of RIP1-dependent necrosis prevents adverse cardiac remodeling after myocardial ischemia-reperfusion in vivo. *Basic Res Cardiol* 2012;270-282.
16. Smith CC, Davidson SM, Lim SY, et al. Necrostatin: a potentially novel cardioprotective agent? *Cardiovasc Drugs Ther* 2007;21:227-233.
17. Lim SY, Davidson SM, Mocanu MM, et al. The cardioprotective effect of necrostatin requires the cyclophilin-D component of the mitochondrial permeability transition pore. *Cardiovasc Drugs Ther* 2007;21:467-469.
18. Lang RM, Bierig M, Devereux RB, et al. Recommendations for chamber quantification: a report from the American Society of Echocardiography’s Guidelines and Standards Committee and the Chamber Quantification Writing Group, developed in conjunction with the European Association of Echocardiography, a branch of the European Society of Cardiology. *J Am Soc Echocardiogr* 2005;18:1440-1463.
19. Frantz S, Bauersachs J, Ertl G. Post-infarct remodelling: contribution of wound healing and inflammation. *Cardiovasc Res* 2009;81:474-481.

9



Summary, General discussion and Future perspectives

Acute myocardial infarction (MI) remains one of the leading causes of morbidity and mortality in the western world¹. Starting in the early 70s, much effort has been put in the modulation of cell death since infarct size, due to irreversible loss of cardiomyocytes, is the major determinant of prognosis after MI^{2,3}. After initial reports demonstrated that part of the ischemic damage could be reversed either pharmacologically or by early reperfusion^{4,6}, reduction of infarct size has been a major subject for studies in cardiovascular research. As a consequence, reperfusion therapy has become the most effective therapy for patients suffering from acute MI⁷. Unfortunately, experimental data clearly demonstrated that reperfusion itself increases myocardial cell death as well, which has changed the research focus the last decades more towards adjunctive therapy to reduce this lethal reperfusion injury^{8,9}. Although several cardioprotective strategies seemed promising on the experimental level, translation to the clinical setting has failed dramatically^{10,11}.

Although infarct-related deaths are significantly reduced due to reperfusion therapy, the incidence of chronic heart failure is rising. Also in the Netherlands, hospital admission due to cardiovascular disease is still increasing¹². With increasing aging of the population and the increasing incidence of cardiovascular risk factors, one can expect an even further increase in the near future. Next to understanding and intervening on the limitation of reperfusion injury, new insights in the process of infarct healing, inflammation and adverse remodelling might lead to novel therapeutic strategies as well. Additionally, earlier diagnosis of acute MI could be another important strategy, thereby reducing myocyte loss by limiting the time of ischemia in the heart. Next to the patient benefit, this will greatly reduce time and money consumption, as delays in 'ruling out' acute MI is associated with raising health care costs¹³. Taken together, the ongoing quest for new diagnostic and therapeutic strategies is therefore essential to deal with this growing problem.

As summarized earlier in this thesis (**Chapter 1, Figure 1**), several important events take place after acute coronary occlusion. Interference in this negative chain reaction could greatly reduce patient morbidity and mortality following MI. In this thesis, we focussed on improving early diagnosis (**Part I**) and on increasing the basic understanding of cardiac wound healing, cell transplantation and cell death, in order to find novel cardioprotective strategies (**Part II**). The findings of these studies will be discussed below.

EARLY DIAGNOSIS (PART ONE)

The current clinical biomarker of choice for detection of myocardial damage, cardiac-specific troponin (cTn), can be detected in the circulation after ³⁻⁴ hours¹⁴. Even with the state-of-the-art high-sensitive assays, troponin cannot be detected consistently within the first hours after symptom onset, moreover, ST segment elevation on the ECG only pertains to a minority of patients presenting to the emergency department (ED). One of the major challenges for daily clinical practise, is the identification of reliable biomarkers that can be measured routinely in easily accessible samples, using a rapid, accurate and inexpensive method. Because of their stability in the circulation, miRNAs are currently being explored for their potential as novel biomarkers for cardiovascular disease, including MI.

The diagnostic value of circulating miRNAs

In Chapter 2, the diagnostic value of circulating miRNAs in a large group of patients (n=332) presenting with chest pain to the emergency department was investigated. Circulating microRNAs were measured in serum, collected immediately upon presentation. Main advantage of the presented study is the population, as previous studies on miRNAs focused on patients already known to have an acute MI, using healthy controls, or failed to address the added diagnostic value of miRNAs¹⁵. Circulating microRNA levels (miR-1, -208a, -499, -21 and -146a) were higher in ACS patients. Even when initial troponin levels were negative. It is this particular population (i.e. troponin levels below threshold at presentation), which will normally require repetitive measurements of troponin to safely rule out an acute MI¹⁶. Our results indicate that circulating miRNAs hold great promise as novel early biomarkers, which might lead to better management of suspected ACS patients, in particular those with unstable angina pectoris and NSTEMI in whom diagnostic uncertainty is high. An unanswered question, however, is where these circulating miRNAs come from and how they maintain their remarkable stability in the circulation. Several binding partners have been identified, including lipid-like or vesicle-like structures called microparticles¹⁷. Depending on their size and origin, this group of particles includes exosomes (50-100nm) and microvesicles (0.1-1µm), both released from cells¹⁸. Furthermore, apoptotic bodies released during programmed cell death (0.5-2µm) were also found to contain microRNAs¹⁹. Next to microparticles, miRNAs were also found to be associated with circulating protein complexes (i.e. Ago2) and HDL cholesterol^{20, 21}. Given their stability in the circulation, it seems very likely that microRNAs participate in cell-to-cell communication. Alternatively, shedding of miRNAs in the circulation might also be a more passive process, similar to troponin leakage upon cardiac injury.

CARDIOPROTECTIVE STRATEGIES (PART TWO)

The role of inflammatory miRNA-223 after ischemia-reperfusion

In Chapter 3, the role of miR-223 was investigated during ischemia-reperfusion(I/R) by its modulation *in vivo* using antagomirs²². MiR-223 was chosen because of its interesting profile after I/R, demonstrating a very early rise peaking at 1 to 3 days, corresponding with the early inflammatory phase after cardiac injury²³. We demonstrated that this microRNA is highly expressed in the border zone after 3 days post-I/R. Surprisingly, miR-223 is predominantly expressed in myocytes, not in non-myocytes (i.e. inflammatory cells), which was confirmed by *in vitro* experiments showing increased miR-223 expression in myocytes after oxidative stress stimulation. *In vivo* inhibition of miR-223 reduced the influx of inflammatory cells after I/R without any effect on long term cardiac function, raising the question whether inhibition is beneficial or not. As with many other attempts to positively modulate inflammation after MI, time- and cell-dependency is crucial²⁴. In our model, antagomirs were administered at 3 days post-I/R. It is possible that the long-lasting inhibitory effect (up till 28 days after the initial injury) reversed the potentially beneficial effects of temporal inhibition in the early inflammatory phase. Furthermore, miR-223 was suggested to increase GLUT4 expression in diabetic hearts²⁵. Increased myocardial miR-223 levels

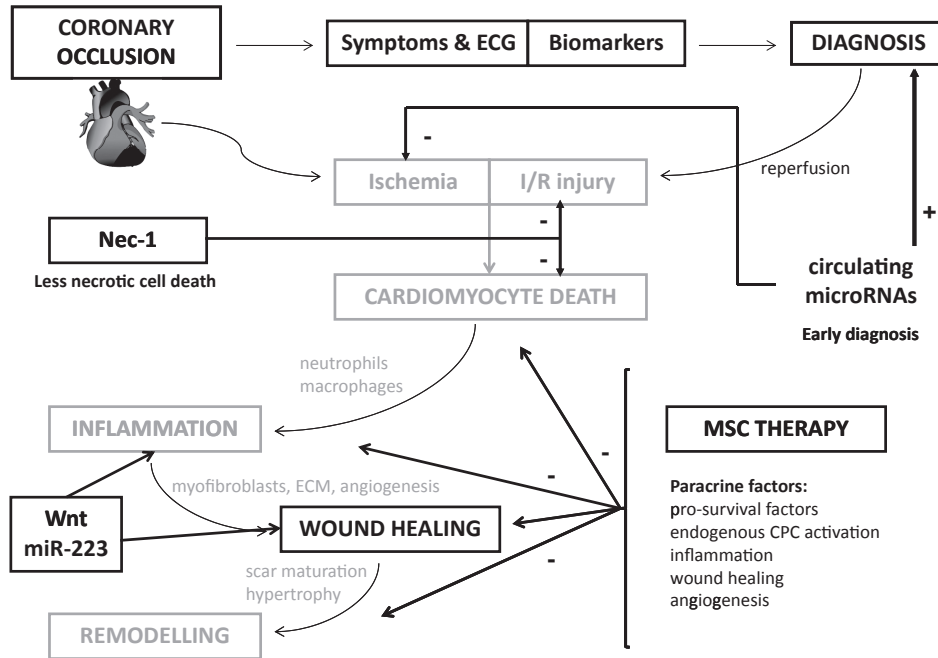


Figure 1 | Overview of diagnostic and cardioprotective strategies provided in this thesis

After coronary occlusion, earlier diagnosis of acute MI using circulating microRNAs could reduce the duration of ischemia. Together with the limitation of lethal reperfusion injury by administration of Nec-1 prior to reperfusion, this will lead to a reduction of myocyte death and infarct size. Cell-specific and time-dependent modulation of microRNA-223 and Wnt signalling might also offer clinical benefit, attenuating the inflammatory response and cardiac wound healing after MI. Application of MSCs, merely by their paracrine factors, also contributes to optimal infarct healing. Overall, the combination of these diagnostic and cardioprotective strategies will improve patient prognosis and reduce mortality and morbidity after MI.

might therefore be beneficial leading to increased glucose uptake, thereby promoting cell survival. On the other hand, it was reported very recently that mice with a total miR-223 knock-out developed a more pro-inflammatory macrophage programme, increasing M1 subtype macrophages and leading to an increased inflammatory response²⁶. Therefore, it is possible that the effect of miR-223 modulation on cardiomyocytes (i.e. increased cell survival) is opposing the effect on inflammatory cells (i.e. inhibition leading to a more pro-inflammatory subset). General miR-223 inhibition after ischemia-reperfusion, involving many cell types in a period that exceeds the inflammatory phase, might therefore not lead to a net beneficial effect on the long term.

Wnt signalling after cardiac injury

Wnt/ β -catenin is regarded as an important regulator of wound healing after MI^{27, 28}. However, to what extent active Wnt signalling is present, what cell types are involved, and at what time point this is occurring, has never been adequately documented. In **Chapter 4**, we used Axin2^{+/LacZ} reporter mice to reliably detect Wnt activity by visualizing LacZ-reporter positive cells²⁹. We demonstrated that active Wnt signalling is significantly upregulated in cell

populations that are considered to play a role in cardiac wound healing. This was not limited to a specific cell type, as next to cardiac progenitor cells and endothelial cells, also leukocytes, fibroblasts and myocytes demonstrated LacZ positivity, and therefore active Wnt signalling.

Considering the significant increase of Wnt signalling in Sca+/CD31- progenitor cells starting from day 7 post-MI, one important question is whether Wnt modulates their differentiation *in vivo* as this was demonstrated *in vitro* before^{27,30}. Interestingly, transplantation of Sca+/CD31- progenitors after MI was shown to contribute to infarct healing³¹. In contrast, cardiac specific inhibition of β -catenin lead to enhanced differentiation of Sca+ progenitor cells *in vivo*³². However, the potential effects of β -catenin on other processes including cell survival and MPTP opening were largely neglected^{33,34} and a model of permanent LAD ligation was used. Inhibition of Frizzled proteins, one of the receptors involved in Wnt signalling, prevented adverse cardiac remodelling by increasing fibroblast influx in the infarcted area³⁵. In line with this study, we also observed increased Wnt activity in fibroblasts. Alternatively, Wnt signalling was crucial to evoke a pro-fibrotic response enabling epicardial-mediated cardiac repair³⁶. Taken together, the effect of therapeutic modulation of Wnt signalling will greatly depend on a temporal targeting of specific cell types.

Cardioprotective properties of human *versus* porcine MSCs

Stem cell engraftment and the number of newly generated cardiomyocytes upon stem cell therapy were too low in many experimental studies to explain the significant cardiac improvements, the focus shifted towards their paracrine factors secreted in the damaged myocardium³⁷. Although many different stem cells were used, MSCs seem to be an attractive source: they can be acquired autologously, expand easily and have been used in the clinical setting for many years already and seem to improve cardiac function after MI³⁸⁻⁴¹. However, several issues still need to be addressed including proper cell characterization and optimal expansion *in vitro*, arrhythmogenesis, and optimal delivery and timing^{42, 43}, requiring the use of porcine cells to prevent immune rejection in a pre-clinical porcine model.

In **Chapter 5**, we compared the characteristics and therapeutic efficacy of human *versus* porcine MSC in a mouse model of MI according to the International Society of Cell Therapy (ISCT) criteria for MSC⁴⁴. Cell surface markers showed similar expression between hMSC and pMSC. However, for several markers we did not find cross-reactivity (CD105, CD73, CD19, CD49b, ALP and SSEA4) and porcine-reactive antibodies were not available for these epitopes. We demonstrated for the first time that selecting CD271+ cells from porcine BM resulted in enrichment of MSC. It is this marker, CD271 or Low-Affinity Nerve Growth Factor Receptor (LNGFR), which is more and more used to identify the true MSC population⁴⁵. Importantly, both the immunosuppressive capacity *in vitro* as well as the improvement on cardiac function after transplantation *in vivo* for pMSC was similar to hMSC. These findings suggest that the minimal criteria for MSC might need further refinement and demonstrate that pMSCs have comparable characteristics and functionality with hMSCs, making reliable extrapolation of future pre-clinical pMSC studies into a clinical setting very well possible.

Myocardial infarct size

During acute myocardial infarction and in the reperfused heart, loss of cardiomyocytes is mostly caused by apoptosis and necrosis. As apoptosis was seen as the only regulated form of cell death for many years, genetic and pharmacological approaches targeting necrosis are relatively rare⁴⁶. However, it has become clear that at least some part of necrotic cell death can be regulated, in which opening of the mitochondrial permeability transition pore (MPTP) plays an important role^{47,48}. In **Chapter 6**, an extensive overview of cell death in the reperfused heart was presented and pharmacological approaches to reduce cell death were discussed. Although the list of potential cardioprotective compounds seems promising, it remains to be seen whether these compounds can reduce myocardial infarct size in patients. Many promising results on cardioprotection at the experimental level could not be translated successfully to the clinical setting^{10,11}.

A rather novel compound is Necrostatin-1 (Nec-1), a small molecule capable of inhibiting the kinase activity of receptor interacting protein-1 (RIP1) and its interaction with RIP3, two key molecules involved in the execution of programmed necrosis^{49,50}. In **Chapter 7**, we demonstrated for the first time that Nec-1 administration decreased RIP1/3-phosphorylation *in vivo* after I/R in mice, together with beneficial effect on both short- and long-term cardiac function after myocardial I/R. Nec-1 reduced infarct size by 32% compared to vehicle-treatment by significantly reducing necrotic cell death after I/R. Furthermore, Nec-1 also reduced the amount of MLKL protein recruited to RIP1, a downstream key protein involved in RIP1-mediated necrosis^{51,52}. Using a physiologically more relevant model better resembling the clinical situation, we determined the therapeutic efficacy of Nec-1 administration prior to reperfusion in a model of porcine I/R injury in **Chapter 8**. The ratio IS/AAR (%) was the primary end point of this study according to the current guidelines on novel cardioprotective strategies¹¹. Similar as in mice, Nec-1 reduced infarct size and improved left ventricular systolic function, findings which may have great clinical impact. Therefore, Nec-1 represents a very promising candidate to limit reperfusion injury in patients with acute MI. Future studies will need to focus on pharmacokinetics and dynamics in order to start a first-in-man (FIM) study, as knowledge on these particular aspects are currently unknown.

FUTURE PERSPECTIVES

The ongoing quest for new diagnostic and therapeutic strategies is essential to deal with the growing burden of cardiovascular disease worldwide. Unfortunately, many cardioprotective strategies, although successful in experimental studies, failed in the clinical settings^{7,11,53}. Several factors are responsible for this failure, including the absence of large animal testing and lack of basic and mechanistic understanding. The current thesis provides new insights on diagnostic, mechanistic and therapeutic level, which may contribute to improved patient outcome following MI (summarized in Figure 1).

The use of circulating microRNAs as biomarkers for acute MI seems promising: they are stable, can be detected in a sensitive and specific way (real-time PCR) and discriminate ACS from non-ACS patients when hs-troponin levels are still below threshold detection

(Chapter 2). Future studies should be aiming for more rapid and cheaper detection methods as well as more mechanistic insights on a cellular level to explain the differential expression of miRNAs after myocardial injury. As more basic insights on the process of cardiac wound healing and inflammation seems necessary, future studies should focus on new genes and factors which might provide novel therapeutic approaches to attenuate cardiac remodelling. Considering the role of miR-223 and Wnt signalling after MI (Chapter 3 and 4), future studies aiming for temporal modulation targeting specific cells (i.e. myocytes or inflammatory cells) seem necessary to unravel their beneficial or detrimental effects after MI. Mesenchymal stem cells (MSCs) hold great potential as they can be acquired autologously, expand easily and have been used in the clinical setting for many years. As we have demonstrated that pMSCs are comparable to hMSCS (Chapter 5), pMSC studies can be extrapolated safely to the human situation. Future studies should focus on MSC yield, pre-conditioning *in vitro*, optimal delivery and engraftment as well as the effect of repetitive injections or packaging in scaffolds, knowledge that is currently still lacking. Prevention of lethal reperfusion injury (i.e. 'damage control') as adjuvant therapy next to reperfusion using Necrostatin-1 (Chapter 7 and 8), seems to be a promising novel strategy which offers important clinical benefit. As we could reproduce our results in a large animal model sharing a similar cardiac physiology and anatomy with humans, future studies will need to focus on pharmacokinetics and dynamics in order to start a first-in-man (FIM) study. Special attention to adverse reactions and toxicology will be of major importance.

Taken together, interference in the negative chain of events taking place following MI could greatly reduce patient morbidity and mortality (Figure 1). Ideally, this will be an approach directed towards several processes at the same time including earlier diagnosis, modulation of inflammation or wound healing and limitation of infarct size and remodelling. However, as we still cannot predict when a plaque ruptures and how many cardiomyocytes will die, the ongoing quest for new diagnostic and therapeutic strategies should continue.

REFERENCES

1. Lloyd-Jones D, Adams RJ, Brown TM, et al. Heart disease and stroke statistics—2010 update: a report from the American Heart Association. *Circulation* 2010;121:e46-e215.
2. Sobel BE, Bresnahan GF, Shell WE, et al. Estimation of infarct size in man and its relation to prognosis. *Circulation* 1972;46:640-648.
3. McKay RG, Pfeffer MA, Pasternak RC, et al. Left ventricular remodeling after myocardial infarction: a corollary to infarct expansion. *Circulation* 1986;74:693-702.
4. Jennings RB, Sommers HM, Smyth GA, et al. Myocardial necrosis induced by temporary occlusion of a coronary artery in the dog. *Arch Pathol* 1960;70:68-78.
5. Maroko PR, Libby P, Braunwald E. Effect of pharmacologic agents on the function of the ischemic heart. *Am J Cardiol* 1973;32:930-936.
6. Braunwald E, Maroko PR, Libby P. Reduction of infarct size following coronary occlusion. *Circ Res* 1974;35 Suppl 3:192-201.
7. Oerlemans MI, Koudstaal S, Chamuleau SA, et al. Targeting cell death in the reperfused heart: Pharmacological approaches for cardioprotection. *Int J Cardiol* 2012;[Epub ahead of print].
8. Yellon DM, Hausenloy DJ. Myocardial reperfusion injury. *N Engl J Med* 2007;357:1121-1135.
9. Prasad A, Stone GW, Holmes DR, et al. Reperfusion injury, microvascular dysfunction, and cardioprotection: the “dark side” of reperfusion. *Circulation* 2009;120:2105-2112.
10. Garcia-Dorado D, Ruiz-Meana M, Piper HM. Lethal reperfusion injury in acute myocardial infarction: facts and unresolved issues. *Cardiovascular research* 2009;83:165-168.
11. Hausenloy DJ, Baxter G, Bell R, et al. Translating novel strategies for cardioprotection: the Hatter Workshop Recommendations. *Basic Res Cardiol* 2010;105:677-686.
12. Vaartjes I, van Dis I, Visseren FLJ, et al. Hart- en vaatziekten in Nederland 2011, cijfers over leefstijl- en risicofactoren, ziekte en sterfte. Den Haag: Hartstichting; 2011.
13. Forberg JL, Henriksen LS, Edenbrandt L, et al. Direct hospital costs of chest pain patients attending the emergency department: a retrospective study. *BMC Emerg Med* 2006;6:6.
14. Thygesen K, Alpert JS, White HD, et al. Universal definition of myocardial infarction. *Circulation* 2007;116:2634-2653.
15. Engelhardt S. Small RNA biomarkers come of age. *J Am Coll Cardiol* 2012;60:300-303.
16. Twerenbold R, Jaffe A, Reichlin T, et al. High-sensitive troponin T measurements: what do we gain and what are the challenges? *Eur Heart J* 2012;33:579-586.
17. Zampetaki A, Willeit P, Drozdov I, et al. Profiling of circulating microRNAs: from single biomarkers to re-wired networks. *Cardiovasc Res* 2012;93:555-562.
18. Gupta SK, Bang C, Thum T. Circulating microRNAs as biomarkers and potential paracrine mediators of cardiovascular disease. *Circ Cardiovasc Genet* 2010;3:484-488.
19. Zernecke A, Bidzhekov K, Noels H, et al. Delivery of microRNA-126 by apoptotic bodies induces CX-CL12-dependent vascular protection. *Sci Signal* 2009;2:ra81.
20. Arroyo JD, Chevillet JR, Kroh EM, et al. Argonaute2 complexes carry a population of circulating microRNAs independent of vesicles in human plasma. *Proc Natl Acad Sci U S A* 2011;108:5003-5008.
21. Vickers KC, Palmisano BT, Shoucri BM, et al. MicroRNAs are transported in plasma and delivered to recipient cells by high-density lipoproteins. *Nat Cell Biol* 2011;13:423-433.
22. Thum T. MicroRNA therapeutics in cardiovascular medicine. *EMBO Mol Med* 2012;4:3-14.
23. Cleutjens JP, Blankesteyn WM, Daemen MJ, et al. The infarcted myocardium: simply dead tissue, or a lively target for therapeutic interventions. *Cardiovasc Res* 1999;44:232-241.
24. Frangogiannis NG. Targeting the inflammatory response in healing myocardial infarcts. *Curr Med Chem* 2006;13:1877-1893.
25. Lu H, Buchan RJ, Cook SA. MicroRNA-223 regulates Glut4 expression and cardiomyocyte glucose metabolism. *Cardiovasc Res* 2010;86:410-420.
26. Zhuang G, Meng C, Guo X, et al. A Novel Regulator of Macrophage Activation: miR-223 in Obesity Associated Adipose Tissue Inflammation. *Circulation* 2012.

27. Cohen ED, Tian Y, Morrisey EE. Wnt signaling: an essential regulator of cardiovascular differentiation, morphogenesis and progenitor self-renewal. *Development* 2008;135:789-798.
28. Brade T, Manner J, Kuhl M. The role of Wnt signalling in cardiac development and tissue remodelling in the mature heart. *Cardiovasc Res* 2006;72:198-209.
29. Lustig B, Jerchow B, Sachs M, et al. Negative feedback loop of Wnt signaling through upregulation of conductin/axin2 in colorectal and liver tumors. *Mol Cell Biol* 2002;22:1184-1193.
30. Kwon C, Arnold J, Hsiao EC, et al. Canonical Wnt signaling is a positive regulator of mammalian cardiac progenitors. *Proc Natl Acad Sci U S A* 2007;104:10894-10899.
31. Wang X, Hu Q, Nakamura Y, et al. The Role of the Sca-1/CD31 Cardiac Progenitor Cell Population in Postinfarction Left Ventricular Remodeling. *Stem Cells* 2006;24:1779-1788.
32. Zelarayan LC, Noack C, Sekkali B, et al. Beta-Catenin downregulation attenuates ischemic cardiac remodeling through enhanced resident precursor cell differentiation. *Proc Natl Acad Sci U S A* 2008;105:19762-19767.
33. Kaga S, Zhan L, Altaf E, et al. Glycogen synthase kinase-3beta/beta-catenin promotes angiogenic and anti-apoptotic signaling through the induction of VEGF, Bcl-2 and survivin expression in rat ischemic preconditioned myocardium. *J Mol Cell Cardiol* 2006;40:138-147.
34. Juhaszova M, Zorov DB, Yaniv Y, et al. Role of glycogen synthase kinase-3beta in cardioprotection. *Circ Res* 2009;104:1240-1252.
35. Laeremans H, Hackeng TM, van Zandvoort MA, et al. Blocking of frizzled signaling with a homologous peptide fragment of wnt3a/wnt5a reduces infarct expansion and prevents the development of heart failure after myocardial infarction. *Circulation* 2011;124:1626-1635.
36. Duan J, Gherghe C, Liu D, et al. Wnt1/betacatenin injury response activates the epicardium and cardiac fibroblasts to promote cardiac repair. *EMBO J* 2012;31:429-442.
37. Gneocchi M, Zhang Z, Ni A, et al. Paracrine mechanisms in adult stem cell signaling and therapy. *Circ Res* 2008;103:1204-1219.
38. Nesselmann C, Ma N, Bieback K, et al. Mesenchymal stem cells and cardiac repair. *J Cell Mol Med* 2008;12:1795-1810.
39. Satija NK, Singh VK, Verma YK, et al. Mesenchymal stem cell-based therapy: a new paradigm in regenerative medicine. *J Cell Mol Med* 2009;13:4385-4402.
40. Williams AR, Hare JM. Mesenchymal stem cells: biology, pathophysiology, translational findings, and therapeutic implications for cardiac disease. *Circ Res* 2011;109:923-940.
41. Gneocchi M, Danieli P, Cervio E. Mesenchymal stem cell therapy for heart disease. *Vascul Pharmacol* 2012;57:48-55.
42. Richardson JD, Nelson AJ, Zannettino AC, et al. Optimization of the Cardiovascular Therapeutic Properties of Mesenchymal Stromal/Stem Cells-Taking the Next Step. *Stem Cell Rev* 2012.
43. Ranganath SH, Levy O, Inamdar MS, et al. Harnessing the mesenchymal stem cell secretome for the treatment of cardiovascular disease. *Cell Stem Cell* 2012;10:244-258.
44. Dominici M, Le BK, Mueller I, et al. Minimal criteria for defining multipotent mesenchymal stromal cells. The International Society for Cellular Therapy position statement. *Cytotherapy* 2006;8:315-317.
45. Flores-Torales E, Orozco-Barocio A, Gonzalez-Ramella OR, et al. The CD271 expression could be alone for establisher phenotypic marker in Bone Marrow derived mesenchymal stem cells. *Folia Histochem Cytobiol* 2010;48:682-686.
46. Whelan RS, Kaplinskiy V, Kitsis RN. Cell death in the pathogenesis of heart disease: mechanisms and significance. *Annu Rev Physiol* 2010;72:19-44.
47. Baines CP, Kaiser RA, Purcell NH, et al. Loss of cyclophilin D reveals a critical role for mitochondrial permeability transition in cell death. *Nature* 2005;434:658-662.
48. Nakagawa T, Shimizu S, Watanabe T, et al. Cyclophilin D-dependent mitochondrial permeability transition regulates some necrotic but not apoptotic cell death. *Nature* 2005;434:652-658.
49. Vanlangenakker N, Vanden BT, Krysko DV, et al. Molecular mechanisms and pathophysiology of necrotic cell death. *Curr Mol Med* 2008;8:207-220.
50. Vandenabeele P, Galluzzi L, Vanden Berghe T, et al. Molecular mechanisms of necroptosis: an ordered cellular explosion. *Nat Rev Mol Cell Biol* 2010;11:700-714.

51. Sun L, Wang H, Wang Z, et al. Mixed lineage kinase domain-like protein mediates necrosis signaling downstream of RIP3 kinase. *Cell* 2012;148:213-227.
52. Zhao J, Jitkaew S, Cai Z, et al. Mixed lineage kinase domain-like is a key receptor interacting protein 3 downstream component of TNF-induced necrosis. *Proc Natl Acad Sci U S A* 2012.
53. Bolli R, Becker L, Gross G, et al. Myocardial protection at a crossroads: the need for translation into clinical therapy. *Circ Res* 2004;95:125-134.

10



Nederlandse samenvatting

Een acuut myocardinfarct (MI) en de gevolgen hiervan vormt nog steeds één van de belangrijkste oorzaken van sterfte wereldwijd¹. De acute afsluiting van een coronair arterie veroorzaakt zuurstoftekort (ischemie) aan de hartspier wat tot het afsterven van hartspiercellen leidt. Al sinds de jaren '70 is veel onderzoek gedaan naar het beïnvloeden van celdood na een myocardinfarct. De grootte van het infarct is een bepalende factor voor de prognose van de patiënt^{2,3}, het is daarom niet verwonderlijk dat het verminderen van de infarctgrootte een uitgebreid thema binnen het cardiovasculair onderzoek is geweest de afgelopen decennia^{4,6}. Als gevolg hiervan is het herstellen van de circulatie (reperfusie) bij patiënten met een acuut MI tegenwoordig de meest effectieve behandeling⁷. Het laatste decennium is echter duidelijk geworden dat reperfusie zelf ook tot extra celdood kan leiden, een fenomeen dat "reperfusieschade" wordt genoemd^{8,9}. Helaas hebben veel experimentele studies die onderzochten hoe het hart tegen reperfusie schade kon worden beschermd (cardioprotectie), niet geleid tot therapeutische opties in de dagelijkse praktijk^{10,11}.

Ondanks het feit dat het infarct-gerelateerde sterfterisico aanzienlijk is afgenomen door o.a. vroege revascularisatie, is het aantal patiënten dat te maken krijgt met hartfalen en aanverwante aandoeningen ten gevolge van een acuut MI groeiende¹². Met de toenemende vergrijzing en toename van het voorkomen van cardiovasculaire risicofactoren als hypertensie en diabetes, is de verwachting dat dit aantal nog verder zal stijgen in de toekomst. Nieuwe mogelijkheden om dit groeiende probleem aan te pakken zijn daarom noodzakelijk. Naast het tegengaan van reperfusieschade, is het van groot belang om meer inzicht te krijgen in de gebeurtenissen die plaatsvinden na een MI (**Figuur 1, Introductie**). Hieronder vallen het proces van genezing, inflammatie en de aanpassingen van het hart op langere termijn na een infarct, remodellering genoemd. Het onderbreken van deze keten van opeenvolgende gebeurtenissen is belangrijk, aangezien dit grote invloed kan hebben op de prognose van de patiënt. Daarnaast valt ook winst te behalen in de diagnostische fase, aangezien de schade aan de hartspier beperkt kan blijven als reperfusie zo spoedig mogelijk plaatsvindt.

In **Deel I** van dit proefschrift beschrijven we een manier om sneller tot de diagnose acuut myocardinfarct te komen. In **Deel II** richten we ons op nieuwe cardioprotectieve strategieën om herstel van de hartspier na een myocardinfarct te bevorderen door het vergroten van de basiskennis van cardiale wondgenezing, de toepassing celtransplantatie en het remmen van celdood.

VROEGE DIAGNOSE (DEEL ÉÉN)

De huidige biomarker om schade aan de hartspier te meten in het bloed van patiënten is cardiaal-specifieke troponine (cTn), wat kan worden gemeten drie tot vier uur na het ontstaan van een myocardinfarct¹³. Ook in het geval van nieuwere en meer gevoelige troponine bepalingen (high-sensitief assays) is de detectie van schade aan de hartspier in de eerste uren na aanvang van klachten niet direct mogelijk. Identificatie van betrouwbare biomarkers die bovendien eenvoudig, snel, nauwkeurig en goedkoop zijn vormt een grote uitdaging. Door hun stabiliteit in de circulatie, worden microRNAs momenteel onderzocht als nieuwe biomarkers voor hart- en vaatziekten. MicroRNAs zijn korte niet-coderende

RNAs die, naast veranderde expressie in het hart na myocardinfarct, ook verschillen in expressie laten zien in het bloed van patiënten met o.a. diabetes en hart- en vaatziekten. In **Hoofdstuk 2** bepalen we de diagnostische waarde van circulerende microRNAs in een grote groep patiënten (n=332) die zich presenteren met pijn op de borst op de afdeling spoedeisende hulp (SEH). Het grootste voordeel van deze studie is de populatie, aangezien eerdere studies zich hebben gericht op patiënten die al een bewezen MI hadden, geen goede controlegroep gebruikten of niet keken wat microRNAs toevoegden aan de huidige biomarkers zoals troponine. Circulerende microRNA-niveaus (miR-1,-208A, -499, -21 en -146a) waren hoger bij patiënten met MI. Interessant genoeg was dit ook het geval bij patiënten waar de troponineswaarde onder de detectiedrempel zat op moment van presentatie. Bovendien was de diagnostische waarde van deze microRNAs hoger dan die van troponine. Onze resultaten laten zien dat circulerende microRNAs grote potentie hebben als nieuwe biomarkers, in het bijzonder bij patiënten waarbij geen sprake is van duidelijke ECG-afwijkingen die het direct stellen van de diagnose acuut myocardinfarct mogelijk zouden maken. Met de vroegdiagnostiek van een acuut MI kan veel tijd en geld worden bespaard omdat er geen herhaaldelijke metingen meer nodig zijn. Verder profiteert de patiënt door het eerder beginnen met de juiste behandeling als de diagnose is gesteld.

CARDIOPROTECTIEVE STRATEGIËN (DEEL TWEE)

De rol van microRNA-223 na een myocardinfarct

In **Hoofdstuk 3** beschrijven we de rol van miR-223 na een myocardinfarct en onderzoeken we wat het effect is als we deze microRNA blokkeren met behulp van antagomirs in de muis¹⁴. De reden dat we specifiek naar miR-223 hebben gekeken is dat de veranderingen in expressie - toename in het hart na één en drie dagen post-MI - sterk overeenkomt met de fase waarin de ontstekingsreactie op gang komt¹⁵. Opvallend genoeg hebben we gezien dat microRNA-223 toeneemt in het gebied rondom het infarct, met name in de hartspiercellen zelf en in mindere mate in andere cellen (o.a. inflammatoire cellen). Remming van microRNA-223 na infarct ging gepaard met minder invasie van inflammatoire cellen in het hart. Dit had echter geen effect op de lange termijn, aangezien de hartfunctie in muizen niet verschilde tussen wel of geen behandeling met de microRNA-223-remmer. Net als bij andere pogingen om het ontstekingsproces positief te beïnvloeden na MI, zijn timing en specifiek effect op een bepaald soort type cel van groot belang¹⁶. Het is mogelijk dat het langdurige remmend effect (tot 28 dagen na de initiële verwonding) wat in onze studie werd waargenomen, de mogelijk gunstige effecten van de tijdelijke remming in de vroege inflammatoire fase teniet heeft gedaan. Totale miR-223 remming na een infarct zonder onderscheid in celtype, in een periode die langer duurt dan alleen de inflammatoire fase, lijkt geen netto positief effect op de lange termijn te hebben. Tijd- en celspecifieke remming zou misschien wel een gunstig resultaat kunnen opleveren.

Wnt-signalering na een myocardinfarct

Wnt is een signaleringsmolecuul dat een belangrijke rol speelt in wondgenezig na een MI^{17, 18}. Het is echter onduidelijk in welke celtypes en op welk tijdstip activatie

van Wnt plaatsvindt na een infarct. In **Hoofdstuk 4** maken we gebruik van een speciale muis ($Axin2^{+/LacZ}$ reporter muis) om Wnt-activiteit op een betrouwbare manier te visualiseren¹⁹. We laten zien dat Wnt-activatie plaatsvindt in de celpopulaties die een cruciale rol spelen in cardiale wondgenezing, inclusief cardiale voorlopercellen, endotheelcellen, inflammatoire cellen, fibroblasten en hartspiercellen. Interessant is de observatie dat Wnt ook hoog tot expressie komt in $Sca+/CD31$ -cardiale voorlopercellen, omdat deze cellen *in vitro* kunnen uitgroeien tot een volwassen hartspiercel en *in vivo* betrokken zijn bij infarctgenezing^{17, 20, 21}. In de literatuur worden zowel positieve als negatieve resultaten beschreven na remming van Wnt in geval van een myocardinfarct²²⁻²⁴. Ook hier lijkt het effect van Wnt-modulatie af te hangen van celtype en moment van ingrijpen.

Cardioprotectieve eigenschappen van humane- versus varkensMSCs

De afgelopen decennia is veel onderzoek gedaan naar het effect van stamcelinjecties na MI, wat heeft geleid tot nieuwe aangrijpingspunten. De belangrijkste is misschien wel de observatie dat de positieve effecten niet in relatie stonden tot het beperkte aantal cellen

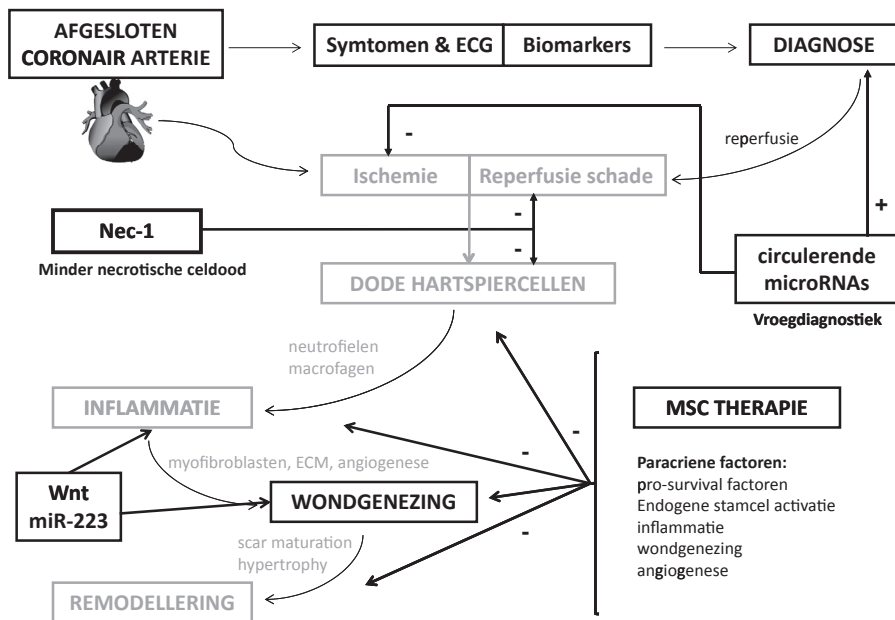


Figure 1. Overzicht van de diagnostische and cardioprotective strategiën uit dit proefschrift

Na een acute afsluiting van een coronair arterie, kan vroegdiagnostiek met behulp van circulerende microRNAs de ischemie-tijd verkorten. Samen met het verminderen van reperfusieschade door toediening van Nec-1, zullen er minder hartspiercellen verloren gaan en zal de infarctgrootte beperkt blijven. Cel-specifieke modulatie van microRNA-223 and Wnt in een afgebakende periode na een infarct kan ook een gunstig effect hebben, door de ontstekingsreactie en het proces van cardiale wondgenezing positief te beïnvloeden na MI. Toediening van MSCs, in het bijzonder door de factoren die ze uitscheiden, draagt ook bij aan optimale genezing na een infarct. De combinatie van deze diagnostische en cardioprotectieve strategiën zal de prognose van de individuele patiënt verbeteren en daarnaast infarctgerelateerde mortaliteit en morbiditeit aanzienlijk verminderen.

dat kon worden teruggevonden na injectie. Ten gevolge daarvan is de idee ontstaan dat niet de geïnjecteerde cellen zelf, maar de factoren die door deze cellen worden uitgescheiden, verantwoordelijk zijn voor de effecten die worden waargenomen²⁵. Er is tegenwoordig een veelheid aan stamcelsoorten beschikbaar, maar mesenchymale stamcellen (MSCs) vormen een aantrekkelijke bron: ze kunnen relatief makkelijk worden verzameld uit het beenmerg, vermeerderen zich snel in celweek, met deze cellen is al geruime tijd klinische ervaring opgedaan en experimentele studies laten gunstige effecten zien na een MI²⁶⁻²⁹. Toch zijn er nog zaken die goed moeten worden onderzocht, onder meer betrouwbare identificatie van deze cellen, optimale uitgroei, optimale injectie en timing na infarct^{30, 31}. Om dit te onderzoeken in een klinisch relevant model, lijkt het varken de meest voor de hand liggende optie, waarvoor dan ook MSCs uit varkens nodig zullen zijn. Een directe vergelijking tussen humane en varkens MSCs was tot op heden niet uitgevoerd. In **Hoofdstuk 5** vergelijken we de celkarakteristieken en het therapeutisch effect van humane- versus varkensMSC in een myocardinfarct-model in de muis. Humane- en varkensMSCs lieten een vergelijkbaar patroon zien van oppervlaktemarkers die kunnen worden gebruikt voor identificatie. Ook tonen we aan dat varkensMSCs met behulp van de marker CD271 zeer goed een efficiënt uit beenmerg kunnen worden geïsoleerd³². Daarnaast was er geen verschil in functionaliteit tussen beide soorten en was er een vergelijkbaar positief effect op het hart na transplantatie in de muis. Deze resultaten laten zien dat resultaten uit pre-klinische varkensstudies met MSCs op betrouwbare wijze kunnen worden geëxtrapoleerd naar de humane situatie.

Grootte van het myocardinfarct

Tijdens een acuut MI tredt celdood op van hartspiercellen, waarvoor twee verschillende vormen van celdood verantwoordelijk zijn, te weten apoptose and necrose. Lange tijd werd apoptose gezien als de enige vorm van celdood die kon worden gereguleerd, waardoor mogelijkheden om necrose te bestrijden na een hartinfarct nauwelijks werden onderzocht³³. Het laatste decennium is echter duidelijk geworden dat er ook een vorm van necrotische celdood bestaat die wel kan worden gereguleerd^{34, 35}. In **Hoofdstuk 6** wordt een uitgebreid overzicht gegeven van celdood in het hart tijdens ischemie en reperfusie, samen met de pogingen die er zijn gedaan om celdood te remmen tijdens een acuut MI. Lange tijd werd apoptose gezien als enige vorm van celdood, de mogelijkheden om necrose te bestrijden werden nauwelijks onderzocht. Zoals eerder gezegd slagen veelbelovende cardioprotectieve middelen er helaas niet in om ook in de klinische praktijk een significante verkleining van de infarctgrootte teweeg te brengen^{10, 11}.

Necrostatin-1 (Nec-1) is een relatief nieuw middel dat in staat is om gereguleerde necrose te remmen^{36, 37}. In **Hoofdstuk 7** laten we zien dat Nec-1, wanneer toegediend net voor het moment van reperfusie in een muizenmodel van ischemie-reperfusie, een positief effect laat zien op zowel de korte als de lange termijn. Nec-1 geeft een verkleining van de infarctgrootte van 32% vergeleken met de controlegroep, veroorzaakt door een aanzienlijke vermindering van necrotische celdood. Bovendien verminderd Nec-1 ook de activatie van MLKL, een eiwit dat een belangrijke rol speelt in gereguleerde necrose^{38, 39}. Tenslotte bepalen we het effect van Nec-1 in een pre-klinisch varkensmodel van ischemie-reperfusie in **Hoofdstuk 8**. Net als in de muizenstudie zorgt Nec-1 voor een afname van de

infarctgrootte met daarnaast een verbetering van de systolische hartfunctie, resultaten die van grote waarde kunnen zijn voor de klinische praktijk. Vervolgstudies met speciale aandacht voor farmacokinetiek en dynamiek zullen nodig zijn om zo snel mogelijk een studie bij de mens te kunnen starten.

TOEKOMSTPERSPECTIEF

Kort samengevat worden in dit proefschrift nieuwe inzichten op diagnostisch, mechanistisch en therapeutisch niveau beschreven, die tot een betere prognose van de patiënt kunnen leiden in geval van een acuut MI (samengevat in Figuur 1). Het gebruik van circulerende MicroRNAs als biomarkers voor acuut MI lijkt veelbelovend: ze zijn stabiel, kunnen worden gedetecteerd op een gevoelige en specifieke manier (real-time PCR) en onderscheiden zelfs MI van niet-MI wanneer troponine nog onder de detectiedrempel is (Hoofdstuk 2). Toekomstige studies zullen moeten streven naar snellere en goedkopere detectiemethoden, zodat er echt van vroegdiagnostiek kan worden gesproken. Omdat er meer inzicht in het proces van wondgenezing post-MI nodig is, moet toekomstig onderzoek zich richten op nieuwe genen en factoren die nieuwe therapeutische opties kunnen zijn om cardiale remodelling gunstig te beïnvloeden. Gezien de rol van miR-223 en de Wnt-signalering na MI (Hoofdstuk 3 en 4), zullen toekomstige studies moeten streven naar modulatie gericht op specifieke cellen in een bepaalde tijdsframe (bv. myocyten, ontstekingscellen) om hun positieve of negatieve gevolgen te ontrafelen na MI. Mesenchymale stamcellen (MSCs) zijn een potentieel interessante therapeutische optie aangezien ze makkelijk kunnen worden verkregen, snel kunnen uitgroeien en al jarenlang worden gebruikt in de klinische setting. Aangezien we hebben aangetoond dat varkensMSCs te vergelijken zijn met humane MSCs (Hoofdstuk 5), kunnen resultaten van toekomstige pre-klinische varkensstudies met MSCs veilig worden geëxtrapoleerd naar de menselijke situatie. Toekomstig onderzoek zal zich met name moeten richten op MSC-opbrengst, optimale aflevering en instelling en het effect van herhaalde injecties. Preventie van celdood ten gevolge van reperfusieschade ('damage control') als adjuvante therapie naast reperfusie met Necrostatine-1 (Hoofdstuk 7 en 8), lijkt een veelbelovende strategie die een belangrijk klinisch voordeel biedt. Aangezien we deze resultaten konden reproduceren in een groot diermodel met een vergelijkbare cardiale fysiologie en anatomie als de mens, zal toekomstig onderzoek zich moeten richten op de farmacokinetiek en dynamiek om een first-in-man(FIM)-onderzoek te starten. Speciale aandacht voor bijwerkingen en toxicologie zal hierbij van groot zijn belang.

Al met al is onderbreking van de negatieve reeks van gebeurtenissen die plaatsvindt na MI van groot belang (Figuur 1). Idealiter is dit een benadering gericht op verschillende processen tegelijk: vroegdiagnostiek, modulatie van het proces van ontsteking en wondgenezing en beperking van infarctgrootte en remodelling. Aangezien we nog steeds niet kunnen voorspellen wanneer een hartinfarct precies plaatsvindt en hoeveel hartspiercellen er dan zullen sterven, zal de zoektocht naar nieuwe diagnostische en therapeutische strategieën voortgezet moeten worden.

REFERENCES

1. Lloyd-Jones D, Adams RJ, Brown TM, et al. Heart disease and stroke statistics--2010 update: a report from the American Heart Association. *Circulation* 2010;121:e46-e215.
2. Sobel BE, Bresnahan GF, Shell WE, et al. Estimation of infarct size in man and its relation to prognosis. *Circulation* 1972;46:640-648.
3. McKay RG, Pfeffer MA, Pasternak RC, et al. Left ventricular remodeling after myocardial infarction: a corollary to infarct expansion. *Circulation* 1986;74:693-702.
4. Jennings RB, Sommers HM, Smyth GA, et al. Myocardial necrosis induced by temporary occlusion of a coronary artery in the dog. *Arch Pathol* 1960;70:68-78.
5. Maroko PR, Libby P, Braunwald E. Effect of pharmacologic agents on the function of the ischemic heart. *Am J Cardiol* 1973;32:930-936.
6. Braunwald E, Maroko PR, Libby P. Reduction of infarct size following coronary occlusion. *Circ Res* 1974;35 Suppl 3:192-201.
7. Oerlemans MI, Koudstaal S, Chamuleau SA, et al. Targeting cell death in the reperfused heart: Pharmacological approaches for cardioprotection. *Int J Cardiol* 2012.
8. Yellon DM, Hausenloy DJ. Myocardial reperfusion injury. *N Engl J Med* 2007;357:1121-1135.
9. Prasad A, Stone GW, Holmes DR, et al. Reperfusion injury, microvascular dysfunction, and cardioprotection: the "dark side" of reperfusion. *Circulation* 2009;120:2105-2112.
10. Garcia-Dorado D, Ruiz-Meana M, Piper HM. Lethal reperfusion injury in acute myocardial infarction: facts and unresolved issues. *Cardiovascular research* 2009;83:165-168.
11. Hausenloy DJ, Baxter G, Bell R, et al. Translating novel strategies for cardioprotection: the Hatter Workshop Recommendations. *Basic Res Cardiol* 2010;105:677-686.
12. Vaartjes I, van Dis I, Visseren FLJ, et al. Hart- en vaatziekten in Nederland 2011, cijfers over leefstijl- en risicofactoren, ziekte en sterfte. Den Haag: Hartstichting; 2011.
13. Thygesen K, Alpert JS, White HD, et al. Universal definition of myocardial infarction. *Circulation* 2007;116:2634-2653.
14. Thum T. MicroRNA therapeutics in cardiovascular medicine. *EMBO Mol Med* 2012;4:3-14.
15. Cleutjens JP, Blankesteyn WM, Daemen MJ, et al. The infarcted myocardium: simply dead tissue, or a lively target for therapeutic interventions. *Cardiovasc Res* 1999;44:232-241.
16. Frangogiannis NG. Targeting the inflammatory response in healing myocardial infarcts. *Curr Med Chem* 2006;13:1877-1893.
17. Cohen ED, Tian Y, Morrisey EE. Wnt signaling: an essential regulator of cardiovascular differentiation, morphogenesis and progenitor self-renewal. *Development* 2008;135:789-798.
18. Brade T, Manner J, Kuhl M. The role of Wnt signalling in cardiac development and tissue remodelling in the mature heart. *Cardiovasc Res* 2006;72:198-209.
19. Lustig B, Jerchow B, Sachs M, et al. Negative feedback loop of Wnt signaling through upregulation of conductin/axin2 in colorectal and liver tumors. *Mol Cell Biol* 2002;22:1184-1193.
20. Kwon C, Arnold J, Hsiao EC, et al. Canonical Wnt signaling is a positive regulator of mammalian cardiac progenitors. *Proc Natl Acad Sci U S A* 2007;104:10894-10899.
21. Wang X, Hu Q, Nakamura Y, et al. The Role of the Sca-1/CD31 Cardiac Progenitor Cell Population in Postinfarction Left Ventricular Remodeling. *Stem Cells* 2006;24:1779-1788.
22. Barandon L, Couffignal T, Ezan J, et al. Reduction of infarct size and prevention of cardiac rupture in transgenic mice overexpressing FrzA. *Circulation* 2003;108:2282-2289.
23. Laeremans H, Hackeng TM, van Zandvoort MA, et al. Blocking of frizzled signaling with a homologous peptide fragment of wnt3a/wnt5a reduces infarct expansion and prevents the development of heart failure after myocardial infarction. *Circulation* 2011;124:1626-1635.
24. Duan J, Gherghc C, Liu D, et al. Wnt1/betacatenin injury response activates the epicardium and cardiac fibroblasts to promote cardiac repair. *EMBO J* 2012;31:429-442.
25. Gnechchi M, Zhang Z, Ni A, et al. Paracrine mechanisms in adult stem cell signaling and therapy. *Circ Res* 2008;103:1204-1219.

26. Nesselmann C, Ma N, Bieback K, et al. Mesenchymal stem cells and cardiac repair. *J Cell Mol Med* 2008;12:1795-1810.
27. Satija NK, Singh VK, Verma YK, et al. Mesenchymal stem cell-based therapy: a new paradigm in regenerative medicine. *J Cell Mol Med* 2009;13:4385-4402.
28. Williams AR, Hare JM. Mesenchymal stem cells: biology, pathophysiology, translational findings, and therapeutic implications for cardiac disease. *Circ Res* 2011;109:923-940.
29. Gneocchi M, Danieli P, Cervio E. Mesenchymal stem cell therapy for heart disease. *Vascul Pharmacol* 2012;57:48-55.
30. Richardson JD, Nelson AJ, Zannettino AC, et al. Optimization of the Cardiovascular Therapeutic Properties of Mesenchymal Stromal/Stem Cells-Taking the Next Step. *Stem Cell Rev* 2012.
31. Ranganath SH, Levy O, Inamdar MS, et al. Harnessing the mesenchymal stem cell secretome for the treatment of cardiovascular disease. *Cell Stem Cell* 2012;10:244-258.
32. Flores-Torales E, Orozco-Barocio A, Gonzalez-Ramella OR, et al. The CD271 expression could be alone for establisher phenotypic marker in Bone Marrow derived mesenchymal stem cells. *Folia Histochem Cytobiol* 2010;48:682-686.
33. Whelan RS, Kaplinskiy V, Kitsis RN. Cell death in the pathogenesis of heart disease: mechanisms and significance. *Annu Rev Physiol* 2010;72:19-44.
34. Baines CP, Kaiser RA, Purcell NH, et al. Loss of cyclophilin D reveals a critical role for mitochondrial permeability transition in cell death. *Nature* 2005;434:658-662.
35. Nakagawa T, Shimizu S, Watanabe T, et al. Cyclophilin D-dependent mitochondrial permeability transition regulates some necrotic but not apoptotic cell death. *Nature* 2005;434:652-658.
36. Vanlangenakker N, Vanden BT, Krysko DV, et al. Molecular mechanisms and pathophysiology of necrotic cell death. *Curr Mol Med* 2008;8:207-220.
37. Vandenabeele P, Galluzzi L, Vanden Berghe T, et al. Molecular mechanisms of necroptosis: an ordered cellular explosion. *Nat Rev Mol Cell Biol* 2010;11:700-714.
38. Sun L, Wang H, Wang Z, et al. Mixed lineage kinase domain-like protein mediates necrosis signaling downstream of RIP3 kinase. *Cell* 2012;148:213-227.
39. Zhao J, Jitkaew S, Cai Z, et al. Mixed lineage kinase domain-like is a key receptor interacting protein 3 downstream component of TNF-induced necrosis. *Proc Natl Acad Sci U S A* 2012.

ADDENDUM

A



Dankwoord
List of publications
Curriculum vitae

DANKWOORD

Dit proefschrift zou niet tot stand zijn gekomen zonder hulp van een heleboel mensen die voor kortere dan wel langere tijd bij mijn promotie betrokken zijn geweest. Langs deze weg wil ik daar graag een aantal mensen voor bedanken.

Prof. dr. P.A. Doevendans, beste Pieter. Ik kan me ons eerste gesprek over een eventuele wetenschappelijke stage nog goed herinneren: jij liet een mooi filmpje zien over kloppende cardiomyocyten, je belde Joost Sluijter en voor ik het wist was ik bezig met een onderwerp (Wnt signalling) wat voor een medisch student - en later arts-onderzoeker - misschien niet direct het meest logische onderwerp is. Na een half jaar had ik in ieder geval voldoende kennis gemaakt met de moleculaire cardiologie en het labwerk om "ja" te kunnen zeggen tegen een promotietraject en maakte ik deel uit van de stamcel groep. Ik heb je leren kennen als een betrokken persoon en heb veel geleerd van je doelgerichtheid. Bedankt voor de kritische vragen en stimulerende gesprekken, waarmee je me wist te prikkelen om de juiste weg in te slaan. Bij voor mij persoonlijke "mijlpalen" (bijv. mijn eerste presentatie op de AHA), wilde je ook echt weten hoe ik het had ervaren, daarbij refererend aan hoe dit ooit voor jou is geweest. Deze open en eerlijke benadering, zowel op het gebied van werk als privé, heb ik zeer gewaardeerd. Pieter, nogmaals bedankt, ik hoop onze prettige samenwerking nog vele jaren voort te kunnen zetten.

Dr. J.P.G. Sluijter, beste Joost. Alhoewel je me niet aan kon steken met jouw liefde voor de celkweek en wat daar uit voort kan komen, pakte de zoektocht naar alternatieven goed uit: *in vivo* werk met levende organismen (muizen en later varkens). Als niet primair stamcel-gerichte MD in jouw groep "eerstelingen" heb ik een mooie tijd met je gehad. Naast de labgrapjes over dokters die er niets van kunnen, had je ook een serieuzere kant. Met veel plezier denk ik terug aan de vele momenten waarop we hebben kunnen sparren over bijna alles wat met het leven (en eventueel daarna) te maken heeft. Tijdens autoritten, op hotelkamers of het lab, je schuwde het niet om een laag dieper te gaan. Het siert je dat je daarin ook duidelijk vragen aan jezelf durfde te stellen, ik beschouw het als een eer daar bij te hebben mogen zijn. En onder het genot van een drankje kwam de Brabantse gezelligheid altijd weer boven, alhoewel ik dit nooit heb meegemaakt tijdens de periode van het jaar waarin een bepaald deel van Nederland het het lab op zijn gat ligt. Ik herinner me ook goed de situaties - die zijn namelijk op één hand te tellen - dat ik het echt niet meer wist. Bedankt dat ik dan binnen kon lopen, we de situatie misschien wel 10x analyseerden en ik toch met een positieve twist weer de deur uit kon gaan. Je moleculaire inzicht en hoe dat toe te passen gaf meerdere keren de doorslag. Ik ben er trots op dat de IP toch is gelukt! Ondanks de drukte, hield je altijd je gezin voor ogen, waar ik met veel plezier op de jaarlijkse BBQ weer even mee kon bijpraten. Kortom, Joost, bedankt voor alles. Ik ben blij dat ik jou als co-promotor mocht meemaken en ik zie uit naar nog vele mooie en succesvolle momenten in de toekomst.

Prof. dr. G. Pasterkamp, beste Gerard, allereerst dank voor de tijd die je hebt genomen om mijn proefschrift te beoordelen. Als nieuwe aanwinst in het lab weet ik nog goed dat ik bij

het labuitje prompt door je werd aangewezen om dit het jaar erop te organiseren. Je “drive” die bovenkomt wanneer basale resultaten klinisch relevant worden werkte aanstekelijk. Bedankt voor de tijd in het lab en het GDL, het potje tennis met voor mij een mooie uitkomst zal ik nooit vergeten.

Prof. dr. D.P.V. de Kleijn, beste Dominique. Jouw kenmerkende lach die ik af en toe om de hoek van de kamer hoorde komen in de periode dat ik je buurman was, werkte aanstekelijk. Hoewel ik slechts enkele malen bij je heb aangeklopt, heb ik de gesprekken die we hadden als erg nuttig ervaren. Ook onze Skype sessie met S’pore over circulerende microRNAs kan ik me nog goed herinneren. Waar ter wereld dan ook, als Joost en ik je weer eens ergens tegenkwamen, werd het vaak laat en gezellig.

Leden van de leescommissie, Prof. dr. A.W. Hoes, Prof.dr. A. de Bruin en Prof.dr. D. Duncker, hartelijk dank voor uw tijd en kritische beoordeling van mijn proefschrift.

Mannen van het eerste uur: Tycho, Krijn en Alain. Alain, jij komt later in dit hoofdstuk aan bod! Beste Krijn, bedankt voor je gezelligheid en de momenten dat je me hebt geholpen met ingewikkelde technieken of celkweek. Je was altijd bereid om te helpen, ook als het al laat was en ik nog heel veel RNA samples moest isoleren. De ‘ESC Summer School’, voetbal kijken op je binnenplaats, bierproeverijen op de vrijdag, wijn drinken in Varenna en het spotten van muizen in je oude woonkamer, allemaal mooie momenten. Heel veel succes met het afronden van je promotie, veel woongenot in je nieuwe huis en ik wens je alle geluk van de wereld samen met Dominique! En dan dokter van der Spoel: onze eerste ontmoeting was tijdens de proefdiercursus, wat was ik blij dat ik die had gehaald (en jij ook). Tycho, jongen, of ik je nu op het lab, op de gang in het UMCU, in een groen pakje in het GDL of op straat tegenkwam, je had altijd weer een mooi verhaal waar je uitgebreid over kon vertellen! Je moest niets van muizen weten, maar toen ik me uiteindelijk met piggies ging bemoeien kon ik op je rekenen. Bedankt voor je hulp, voor de gezelligheid tijdens een hapje eten of wat drinken in de stad, pauzeermomentjes op je kamer in het UMC of gewoon even lekker mopperen. Zet jou in een club in Parijs of München en je hebt een mooie avond :) Goed dat je ook in het Diak bent begonnen, het wordt een mooie tijd, ook daarna nog! We gaan nog steeds een keer een balletje slaan.

Stamcel collega’s: Dries, good luck with your experiments and finishing your PhD, it was nice working with you. Roberto, I really enjoyed your love for food and wine, keep up the good work! Zhiyong, I liked your Chinese style of working, thanks for all the nice food in our room. Stefan, bedankt voor je inzet voor ons gezamenlijke Nerello project en daarbuiten. Ik heb genoten van de potjes squash incl. afterparty. Succes met de verdere afronding van je promotie en tot ziens in de kliniek. En denk eraan: *hati-hati!* Steven, bedankt voor je positieve kijk en voortdurende drang om dingen vlot te regelen. Frebus, jouw out-of-the-box denken was verassend en verfrissend, bedankt voor de gezelligheid. Paul, bedankt voor je kritische vragen en je hulp, veel succes met je verdere carrière. Sailay, we hebben elkaar maar heel kort in het lab meegemaakt, maar succes met je vele dromen in de toekomst. Jan Willem, je zit nu aan de overkant van de oceaan, maar de tijd op onze krappe en

lawaaierige kamer was top. Het was mooi om elkaars data en denken af en toe eens lekker ondersteboven te halen. Esther en Corina, bedankt voor jullie inzet, geduld en hulp. Zonder jullie isoleer-, snij- en bewerkkracht was mijn promotie nog steeds niet af geweest! Krista, bedankt voor de vele MRI sessies inclusief uitwerkingen daarvan, die je altijd zeer nauwkeurig hebt gedaan. Hamid, mooi dat je erbij bent gekomen, veel succes met je onderzoekslijn. Peter Paul, tot ziens in het lab dan wel in de kliniek. Oud-collegas Willy, Sridevi, Marie-José, Anke, Piet, Martha, bedankt voor jullie expertise en hulp.

Met veel plezier denk ik terug aan de kamergenoten van mijn eerste werkplek, waar ik als "vreemde eend" in de bijt begon aan de overkant van het lab. Beste Fatih, jouw gesmeerde boterhammetjes waren om jaloers op te worden. Bedankt voor je tips and tricks voor de muizenmodellen. Mooi dat ik je nu weer in de kliniek tegenkom en zal blijven tegenkomen! Beste Daphne, de cabrio tour naar Cape Canaveral was er één om in te lijsten. Bedankt voor al je hulp en de koffie die jij op heerlijke wijze uit dat miezerige apparaatje wist te krijgen. Beste René, het was een enorm gezellige tijd met je, binnen en buiten het lab en tussendoor onder het genot van een Gutenberg. Inmiddels zit jouw promotie er al weer een tijdje op, succes met de nieuwe tak van sport waar je volgens mij heel goed in bent. Beste Mihaela, ik heb het laatste stukje van je promotie mogen meemaken, succes met je verdere loopbaan bij de Pathologie. Ook mijn nieuwe kamergenoten van de long dan wel traumatologie, Vera, Sacha en Okan, bedankt voor jullie aanwezigheid.

Ik was tijdens mijn promotie regelmatig te vinden in het GDL, waarbij het muizenwerk mij het meest bezig heeft gehouden. Beste Ben, jij stond aan de wieg van mijn muizencarrière! Jouw ervaring met de OK's, de fijne kneepjes en je geduld waren onmisbaar. Hele dagen zij aan zij achter de microscoop, terwijl ik net terug was van huwelijksreis, dat was me wat. Bedankt voor alles en succes op de weg die je bent ingeslagen, iets heel anders dan je altijd hebt gedaan. Beste Evelyn, bedankt voor je hulp en het plannen van de experimenten, je collegialiteit en de bereidheid om altijd mee te denken als de dingen net even wat anders liepen dan ik had verwacht. Beste Marcel, Eissa, Sandra, Maringa, Cees, Merel, Joyce en Marlijn, hartelijk dank voor jullie samenwerking en inzet bij de vele experimenten.

Daarnaast gaat veel dank en waardering uit naar mijn mede-collega's en promovendi op het lab en daarbuiten. Beste Arjan, bedankt voor je bijdrage aan mijn experimenten. Naast het feit dat jij zorgde dat alles er op tijd was - en anders wist je wel een oplossing - wil ik je bedanken voor de talloze technische tips die je me hebt gegeven. Mirjam, ik kwam als buurman naast je op het lab terecht. Bedankt dat ik altijd een beroep kon doen op jouw enorme ervaring. Loes, bedankt voor al je hulp en je gezelligheid, zowel binnen als buiten het lab. Imo, bedankt voor je hulp met het opzetten van diverse FACS experimenten en de gezellige avondjes waarbij we elkaar konden *abknallen*. Sander vd W, bedankt voor je bereidheid om mee te denken met diverse experimenten. Ellen, in Parijs leerde ik je pas echt goed kennen, van de opera is het helaas niet meer gekomen. Sanne, succes met het afronden van je promotie en bedankt voor de goede gesprekken. Guus, bedankt voor de

mooie avondjes eten en drinken, ik vond het beregezellig met jou. Rob, ik denk met veel plezier terug aan onze squahspartijen, bedankt. Ineke, Marjolein en Tamara, hartelijk dank voor jullie ondersteuning en hulp. Karlijn, Leo, Vince, Pleunie, Sander vd L, Louise, Vincent, Dave, Herman, Wouter P, Geert, Marten, Joost F, Noortje, Martin, Bas, Arianne en iedereen die ik nog ben vergeten, bedankt voor de gezellige tijd.

Stafleden Cardiologie Meander Medisch Centrum Amersfoort, in het bijzonder Arend Mosterd. Dank voor de prettige samenwerking, wat heeft geleid tot een prachtige publicatie. Ik zie uit naar onze samenwerking in de toekomst.

Bachelor- en masterstudenten Nancy, Sebastian en Jerry, dank voor jullie inzet en veel succes in de toekomst gewenst.

Stafleden en arts-assistenten Cardiologie Jeroen Bosch Ziekenhuis Den Bosch, de vier maanden bij jullie waren leerzaam en leuk. Dank voor jullie belangstelling tijdens de drukke periode van het afronden van mijn promotie.

Stafleden en arts-assistenten Interne Geneeskunde Diakonessenhuis Utrecht, dank voor jullie collegialiteit en begrip. Ik werk met veel plezier met jullie samen, dit kan alleen maar beter worden.

Stafleden en arts-assistenten Cardiologie UMCU, dank voor jullie belangstelling en tot ziens in de kliniek.

Vrienden, zonder jullie relativeringsvermogen, ondersteuning en avondjes ontspanning was ik niet zo ver gekomen. Ontzettend bedankt (in willekeurige volgorde): Paul, Mathijs, Huib, Ruben, Peter, Taco, Benjamin, Hans, Arjan, Jelte, Willard en Samuel.

Beste Alain, je bent een wetenschapper van wereldformaat. Vanaf de eerste dag in het lab heb je me met raad en daad terzijde gestaan. Ik heb je leren kennen als iemand op wie je kunt bouwen en met wie je enorm veel lol kunt beleven. Met veel plezier denk ik terug aan de vele activiteiten die we samen hebben afgelopen, variërend van Pitch&Putt op Papendal en het labuitje tot en met het heen en weer scheuren naar Noordwijk in je Alpha en een prijs winnen zonder bij de uitreiking te zijn geweest. Bedankt ook voor de gezelligheid buiten het lab incl. etentjes, biertjes, koffie op je dakterras, visavonturen en een goed gesprek. Ik ben er trots op dat je mijn paranimf bent en ik heb er alle vertrouwen in dat je een succesvolle toekomst als wetenschapper tegemoet gaat!

Beste Taco, wat zijn de laatste 3 jaar hard gegaan! Toen ik begon met mijn promotie zat je nog in het laatste jaar van geneeskunde. Inmiddels zijn we beiden getrouwd en zelfs trotse vader van een dochter dan wel een zoon. Bedankt voor alle steun de afgelopen jaren, ook al is de tijd die we voor elkaar kunnen reserveren beduidend minder geworden. Desondanks heeft onze vriendschap daar niet onder te lijden gehad, iets wat ik als een groot goed beschouw. Bedankt dat ik ook altijd bij jou (en Inge) kon aanschuiven als ik weer eens wat

later dan gepland van het lab terugkwam of als het zo uitkwam, Jamie Oliver is er niets bij! Ik ben er trots op dat je tijdens de 45 minuten naast me staat. Succes met je verdere medische carrière en ik kijk uit naar onze volgende wintersport!

Lieve papa en mama, dank voor jullie steun al die jaren ook al was het inhoudelijk niet altijd even goed te volgen. Bedankt dat ik bij jullie altijd weer even kon bijkomen en kon genieten van een heerlijke Indonesische maaltijd. Lieve Pris, ik ben er trots op dat je mijn zus(je) bent en ik ben dankbaar voor de goede band die we hebben! Bedankt voor wie je bent en succes met je verdere loopbaan. Lieve Herman en Margreet, bedankt voor jullie betrokkenheid en vele praktische hulp. Lieve Simme & Cara, Joeri en Sarah, dank voor jullie interesse en begrip.

Lieve Mary, de afgelopen drie jaren waren zeker niet altijd even makkelijk, want onze tijd samen schoot er vaak bij in. Terugkijkend hebben we de afgelopen jaren veel meegemaakt. Trouwen, een nieuw (eigen) huis en een pracht van een zoon. Bedankt voor al je geduld en je onvoorwaardelijke steun, zonder jou was dit alles nooit gelukt. Met jou ben ik gelukkig en ik weet dat ik altijd op je kan rekenen. Ik kan me geen betere vrouw wensen, ik houd van je, heel veel! Lieve Lucas, mijn zoon! Jouw komst heeft op een wonderlijke manier mijn leven op zijn kop gezet, je bezorgt me elke dag vele vreugdevolle momenten. Ik houd van je!

LIST OF PUBLICATIONS

Oerlemans MI*, Koudstaal S*, van der Spoel TI, Janssen AQ, Doevendans PA, Sluijter JP, Chamuleau SA. Necrostatin-1 reduces myocardial ischemia/reperfusion injury in pigs.

Submitted *Authors contributed equally

Oerlemans MI, van Mil A, Liu J, van Eeuwijk E, den Ouden K, Doevendans PA, Sluijter JP. Inhibition of miR-223 reduces inflammation but not adverse cardiac remodelling after myocardial ischemia-reperfusion *in vivo*.

Accepted for publication in Discovery Biology and Medicine. 2012

Oerlemans MI, Mosterd A, Dekker MS, de Vrey EA, van Mil A, Pasterkamp G, Doevendans PA, Hoes AW, Sluijter JP. Early assessment of acute coronary syndromes in the emergency department: the potential diagnostic value of circulating microRNAs.

EMBO Mol Med. 2012 Oct 1. Epub ahead of print

Oerlemans MI, Liu J, Arslan F, den Ouden K, van Middelaar BJ, Doevendans PA, Sluijter JP. Inhibition of RIP1-dependent necrosis prevents adverse cardiac remodeling after myocardial ischemia-reperfusion *in vivo*.

Basic Res Cardiol. 2012;107(4):270-82

Oerlemans MI, Koudstaal S, Chamuleau SA, de Kleijn DP, Doevendans PA, Sluijter JP. Targeting cell death in the reperfused heart: Pharmacological approaches for cardioprotection.

Int J Cardiol. 2012 Mar 27. Epub ahead of print

van Mil A, Grundmann S, Goumans MJ, Lei Z, **Oerlemans MI**, Jaksani S, Doevendans PA, Sluijter JP. MicroRNA-214 inhibits angiogenesis by targeting Quaking and reducing angiogenic growth factor release.

Cardiovasc Res. 2012;93(4):655-65

Noort WA*, **Oerlemans MI***, Rozemuller H, Feyen D, Jaksani S, Stecher D, Naaijken B, Martens AC, Bühring HJ, Doevendans PA, Sluijter JP. Human *versus* porcine mesenchymal stromal cells: phenotype, differentiation potential, immunomodulation and cardiac improvement after transplantation.

J Cell Mol Med. 2012;16(8):1827-39 *Authors contributed equally

Oerlemans MI, Goumans MJ, van Middelaar B, Clevers H, Doevendans PA, Sluijter JP. Active Wnt signaling in response to cardiac injury.

Basic Res Cardiol. 2010;105(5):631-41

Oerlemans MI, Lok DJ, Cornel JH, Mosterd A. One-year mortality after a first visit to a cardiology outpatient clinic: a useful performance indicator?

Neth Heart J. 2009;17(2):52-55

CURRICULUM VITAE

Martinus Ishak Flavius Jan (Marish) Oerlemans was born on September 25th 1983 in Rotterdam (the Netherlands). After graduating from secondary school (Dr. W.A. Visser 't Hooft Lyceum, Leiden) in 2002, he studied medicine at the Utrecht University from 2002 to 2008. During his study he became interested in translational research and in the last year of his study he performed an internship under supervision of Prof. Dr. P.A. Doevendans (Head of the Department of Cardiology) and Dr. J.P.G. Sluijter (associate professor) in the Laboratory of Experimental Cardiology, University Medical Center Utrecht. After graduation in 2008 he started his PhD research at the same department. During this period, his research focussed on the role of new biomarkers in early diagnosis of acute myocardial infarction and novel cardioprotective strategies which led to the formation of this thesis. In November 2011 he finished his PhD research and worked as a non-training resident at the Department of Cardiology in the Jeroen Bosch Hospital, 's Hertogenbosch, under supervision of Dr. M.C.G. Daniëls. In April 2012 he started his residency in Cardiology and is currently working at the Department of Internal Medicine of the Diaconessenhuis, Utrecht, supervised by Dr. A.F. Muller. Marish is married to Marie-Louise Oerlemans-Willemsen (September 2009) and has a son called Lucas.